# Marginal Detonation

# in

# Hydrocarbon - Oxygen Mixtures.

Thesis

submitted for the degree of

Doctor of Philosophy

in the

Faculty of Science

of the

University of London

by

Henricus Josephus Michels, Drs.

Department of Chemical Engineering
and Chemical Technology,
Imperial College of Science and Technology,
London.

June 1967.

## ABSTRACT.

Detonation velocities and detonation limits have been established for gaseous mixtures of oxygen with : hydrogen; with saturated aliphatic hydrocarbons in the series methane, n-propane, n-butane and neo-pentane; and with propylene. For ambient pressure and temperature and with initiating impact from detonating stoichiometric hydrogen - oxygen, the following limits in mole % have been observed in a 1-inch diameter tube :

| | | | |
|---|---|---|---|
| Hydrogen | 15.8 | and | 92.9% |
| Methane | 8.25 | and | 55.8% |
| n-Propane | 2.50 | and | 42.50% |
| n-Butane | 2.05 | and | 37.95% |
| neo-Pentane | 1.50 | and | 33.00% |
| Propylene | 2.50 | and | 50.0% |

Comparable results for the systems oxygen-ethane and oxygen-ethylene, collected from other reliable sources, have been included.

For the complete composition region aspects of detonation propagation have been related to shock strength. Results for the hydrocarbon containing systems have been normalised on the basis of homologous similarity of the fuel molecules, leading to extensive correlation of the results obtained for the different systems.

For the hydrodynamic stable regimes, comparison of results calculated for homologous related initial mixtures reveals a striking correspondence in the state parameters and composition of the C-J condition and of the final state of the reaction products behind the rarefaction wave.

For conditions marginal to detonation propagation, normalisation of results on the basis of homology extends to the actual limit compositions for the various systems. It is shown that, especially at the fuel-lean limits, marginal conditions can be correlated to a critical temperature rise of about 1300°K - 1200°K. For low-molecular weight aliphatic hydrocarbons a somewhat higher temperature rise is required. The possibility is discussed that this requirement is related to the critical rate of a cracking mechanism in the overall bond rearrangement which releases the energy necessary for continued propagation of the detonation wave.

For the fuel-rich limits it appears more likely that stability factors, related to modes of solid condensation, determine the remarkable uniform limit composition observed for the normalised systems of oxygen with higher saturated hydrocarbons and with propylene.

Suggestions for further investigation of the subject are made.

TO MY PARENTS AND TO MY WIFE.

ACKNOWLEDGEMENTS.

At the completion of this thesis I should like to thank Professor A.R.Ubbelohde, F.R.S. for the opportunity of working at Imperial College and for his encouragement and patient guidance during the past years. I consider myself fortunate to have enjoyed the benefit of his extensive knowledge and look forward to his continued interest in my future work.

I am particularly indebted to Dr.G.Munday for his untiring assistance and valuable advice in the execution of the experiments and the compilation of this thesis. In addition I have greatly appreciated the many tokens of his helpful friendship.

The experiments would have been impossible without the assistance of the technical services of the Department. I am therefore grateful to Mr A.Alger and Mr L.Tyley for their co-operation in solving the practical problems involved and for the quality of the equipment that has been produced by the members of their staff. Similarly I would like to thank Mr A.Jones and Mr L.Moulder for the proofs of their craftsmanship.

Finally I want to express my gratitude for the help and friendship of all others from whose presence in the Department I have benefited during these years.

I am greatly indebted to Imperial Chemical Industries Limited for making available the funds that have supported my family during this study. I also acknowledge my thanks to the Trustees of the Van Rhijn Trust, for relieving me of the financial problems involved in the production of this thesis.

In thanking furthermore all others who at some stage have contributed to my scientific education and training, I am fortunately able to mention in particular my father, Professor A.Michels. In addition to everything I owe him as his son, I thank him for all I have learned from him and from his work up to date. With all my admiration for his capacities and knowledge, the greatest lesson he has given as a scientist and teacher remains his own example of indefatigable energy in pursuing the interest of his family and his work.

# E R R A T A

| | | | | | |
|---|---|---|---|---|---|
| page | 1, | line | 8: | mole % | - mole % fuel |
| ,, | 40, | ,, | 18: | recording | - routine |
| ,, | 43, | ,, | 7: | mixing | - mixture |
| ,, | 44, | ,, | 2: | deviation of | - deviation from |
| ,, | 83, | ,, | 21: | high | - wide |
| ,, | 151, | ,, | 2: | comparison | - compression |
| ,, | 153, | ,, | 14: | higher | - wider |
| ,, | 177, | ,, | 10: | considering | - considering equations IV, 11 and 24, |

INDEX.


| | | Page |
|---|---|---|
| Chapter I. | Introduction. | 11 |
| I.1. | Detonation. | 11 |
| 2. | Detonation research. | 13 |
| 3. | Marginal detonation. | 18 |
| 4. | Marginal detonation of homologous series. | 21 |
| Chapter II. | The experimental investigation of detonation propagation in gaseous mixtures. | 27 |
| 1. | Considerations of design and instrumentation. | 27 |
| | a. Detonation tubes. | 27 |
| | b. Velocity measurements. | 38 |
| | c. Preparation of gas mixtures. | 41 |
| 2. | The equipment. | 46 |
| | a. The detonation train. | 48 |
| | b. Recording equipment. | 52 |
| | c. The gas mixing equipment. | 64 |
| | d. Additional sources of information. | 67 |
| | Evaluation of final pressures. | 67 |
| | Analysis of gaseous reaction products. | 68 |
| | Study of condensation products. | 74 |
| 3. | Experimental procedure. | 74 |
| 4. | Further instrumental development. | 81 |
| | a. Review of possible improvements. | 81 |
| | b. The circular probe. | 86 |
| | c. The 2-inch detonation tube. | 90 |
| Chapter III. | Experimental Results. | 97 |
| 1. | Instrument performance. | 97 |
| | a. The accuracy of mixture compositions. | 97 |
| | b. Experimental conditions. | 103 |
| | c. The accuracy of recorded results. | 105 |

Page

III. 2. Gas purity. 109

3. The hydrogen-oxygen system. 110

4. Systems of saturated aliphatic hydrocarbons and oxygen. 116

5. Systems of ethylenic hydrocarbons and oxygen. 133

Chapter IV. Elements of detonation theory. 139

1. The detonation wave. 139

a. The co-ordinate system. 139

b. The conservation equations. 142

c. Detonation with infinite reaction rate.

d. The Chapman-Jouguet point. 144

e. Calculation of the parameters of state at the Chapman-Jouguet point. 146

f. The influence of turbulence on the C-J condition. 148

g. The Mach-product. 149

2. The detonation front. 150

a. Shock conditions. 150

b. Energy relaxation in a shock front. 152

c. Shock temperatures calculated from measured detonation velocities. 154

3. Detonations with finite reaction rate. 157

Chapter V. Discussion. 165

1. Introduction. 165

2. The hydrogen-oxygen system. 166

a. Velocity data. 166

b. Detonation limits. 168

c. Shock front temperatures for composition limits. 170

d. The Mach-product as function of composition. 177

3. Detonation limits for systems of saturated aliphatic hydrocarbons and oxygen. 178

4. Homologous aspects of hydrocarbon-oxygen detonations. 184

a. The detonation velocity data. 184

V.4. b. Mach-product data. 189
c. Shock front temperatures for composition limits. 200
d. Homologous correlation of initial mixture compositions and Mach-product data. 206
e. Homologous correlation of C-J condition. 224
f. Homologous correlation of final states. 232
g. Homologous correlation of composition limits. 238
a. Fuel-lean limits. 238
b. Fuel-rich limits. 240
5. The results for systems of ethylenic hydrocarbons and oxygen. 248
a. Steady-state conditions. 249
b. Composition limits. 253
c. Shock front temperatures at the detonation limits. 257
d. The final state. 257
6. Conclusion. 258
7. Suggestions for further investigations. 265

Appendix A. The non-additivity of partial pressures in mixing two gases with dissimilar molecules. 271
B. The accuracy of calculated mixture compositions. 287
C. The time-dependence of detonation initiation by spark ignition. 299
D. Calculation of final test mixture pressures. 309
E. Condensation products from detonation of fuel-rich n-butane-oxygen mixtures. 318
F. Calculation of the ratio of condensation energy and net reaction energy. 318
G. Results for ethane-oxygen and ethylene-oxygen mixtures. 321
H Determination of detonation velocities with the electronic counter. 324

References. 341

## LIST OF FIGURES.


| | | | Page |
|---|---|---|---|
| Fig. II. | 1. | Equipment lay-out. | 47 |
| | 2. | Detonation train and block diagram. | 49 |
| | 3. | Sparking plug mounting. | 51 |
| | 4. | Line filter unit. | 51 |
| | 5. | Timing probe and probe body. | 58 |
| | 6. | Timing probe circuit. | 58 |
| | 7. | Trigger probe circuit. | 62 |
| | 8. | Schematic diagram of gas mixing equipment. | 65 |
| | 9. | Schematic diagram of sampling apparatus for gaseous reaction products. | 70 |
| | 10. | Schematic flow diagram for gas chromatographic analysis of reaction products. | 72 |
| | 11. | Circular probe elements. | 87 |
| | 12. | Circular probe holder. | 89 |
| | 13.a. | 2-inch detonation tube. | 91 |
| | b. | idem. | 92 |
| Fig.III. | 1. | Correction for test mixture composition. | 102 |
| | 2. | Detonation velocity along tube. | 104 |
| | 3. | Time dependence of detonation initiation. | 104 |
| | 4. | Relative uncertainty of pressure data. | 107 |
| | 5. | Detonation velocities for system $H_2$-$O_2$. | 113 |
| | 6. | Overall pressure change for system $H_2$-$O_2$. | 114 |
| | 7. | Detonation velocities for systems of oxygen with saturated aliphatic hydrocarbons. | 121 |
| | 8. | Idem; fuel-lean limits. | 122 |
| | 9. | Idem; fuel-rich limits. | 123 |
| | 10. | Overall pressure change for systems of oxygen with saturated aliphatic hydrocarbons. | 126 |

| | | | Page |
|---|---|---|---|
| III. | 11. | Electron micrographs and electron diffraction patterns of solid reaction products. | 130 |
| | 12. | Detonation velocities for systems of oxygen with unsaturated aliphatic hydrocarbons. | 135 |
| | 13. | Overall pressure change for the system oxygen-propylene. | 137 |
| Fig. IV. | 1. | Detonation co-ordinates. | 141 |
| | 2. | Hugoniot curve. | 141 |
| | 3. | Family of Hugoniot curves indicating gas state in detonation wave. | 159 |
| | 4. | Mass flow model. | 161 |
| Fig. V. | 1. | Mach product for the system $H_2$-$O_2$. | 173 |
| | 2. | Stoichiometric mixture ratios and detonation limits for systems of oxygen and saturated aliphatic hydrocarbons. | 186 |
| | 3. | Mach product for systems of oxygen with saturated aliphatic hydrocarbons. | 194 |
| | 4. | Relative Mach product vs. composition as fraction of mixtures with maximum $\gamma M^2$. | 199 |
| | 5. | Relative Mach product vs. composition on homology element basis for systems $C_nH_{2n+2}$-$O_2$. | 216 |
| | 6a. | Computed C-J composition for $C_3H_8$-$O_2$ | 227 |
| | b. | and $C_6H_{14}$-$O_2$. | 228 |
| | 7. | Mean molecular weight of reaction products at C-J plane. | 231 |
| | 8. | Normalised overall pressure change for $C_nH_{2n+2}$ - $O_2$ systems. | 235 |
| | 9. | Variation of mean Mach-product with formation of solid reaction products. | 245 |
| | 10. | Relative Mach product vs. composition on homology element basis for systems $C_nH_{2n}$ - $O_2$. | 253 |

| | | | Page |
|---|---|---|---|
| Fig. A. | 1. | Conversion curve for evaluation of non-additivity of partial properties in binary mixtures from data for the equimolar mixture. | 274 |
| | 2. | Force parameters of the intermolecular potential field. | 274 |
| C. | 1. | Time dependence of propagation of spark-ignited detonation in $2H_2 + O_2$. | 302 |
| | 2. | Initiation of spark ignited detonation in $2H_2 + O_2$. | 304 |
| | 3. | Relative positions of the detonation front and possible acoustic precursors. | 307 |
| D. | 1. | Dimensions of 1-inch detonation tube. | 312 |
| H. | 1. | System logic for counter operation. | 325 |
| | 2. | Block schematic of 1 channel counter. | 327 |
| | 3a. | Counter circuits block diagrams. | 334 |
| | b. | Idem. | 335 |
| | c. | Idem. | 336 |

# Chapter I. INTRODUCTION.

## I.1. Detonation.

As is well known, detonation is essentially a shock wave, closely followed by a combustion zone.

The undeniable simplicity of this concept is in striking contrast to the almost inextricable tangle of theoretical and experimental problems to which all searching investigation into the nature of these very fast combustion processes seems to lead. At the same time it does not convey to us the laborious studies and vast differences of opinion that preceded the formulation of this now generally accepted description.

Originally a detonation was thought to be a single homogeneous shock wave in which the adiabatic combustion of the gas maintained an abrupt pressure rise in the vicinity of the wave front [Vieille, 1889]. For almost half a century after French scientists [Berthelot and Vieille, 1881; Mallard and le Chatelier, 1881], laid down the first empirical rules on detonation propagation, numerous theoretical and experimental investigations were undertaken on the basis of this common understanding. Results of this work, though often modified in their interpretation, are still part of the present day knowledge in this field. However, with the increase of information it became also

more difficult to accomodate all the essentials of a satisfactory propagation mechanism within the boundaries of a single shock wave. One of the main questions that resulted from this, was whether the observed pulse of compression, instead of being itself the detonation wave, could possibly be travelling slightly ahead [Garner, 1926].

There can be no doubt that the present concept for the basic structure of a detonation wave has resulted from the series of well known experiments on aspects of detonation initiation and spin effects, performed by Professor Bone and his colleagues at Imperial College around 1930 [Bone, Fraser (and Wheeler), 1929, 1931, 1936]. Under certain conditions they observed that the shock and combustion phenomena, although ultimately dependent on each other for their continued existence, could for short lengths of time proceed separated, without inevitably causing breakdown of detonation propagation. The photographic evidence of this work suggested that these two aspects of a detonation wave exist as a separate and separable association between an "intensively radiating flame front and an invisible shock wave immediately ahead of it". From this information the investigators drew the still generally acceptable conclusion that "a detonation in an explosive gaseous medium is the propagation through it as a wave, of a condition of intensive combustion; initiated and maintained in a shock wave by (radiation from) an associated flame front".

## I. 2. Detonation research.

Apart from the already mentioned interests in detonation initiation and spin effects, many other aspects of detonation have been studied, like ignition, propagation and stability of detonation, marginal effects and critical influences, and energy and kinetic problems. All of these have been studied in a variety of ways and excellent comprehensive discussions of these can be found in modern literature [e.g. Lewis and von Elbe, 1961; Gaydon and Hurle, 1963; Wagner, 1961; Zeldovich, 1960; Shchelkin and Troshin, 1965]. Through these theoretical and experimental studies, different fields of physics and chemistry have made their characteristic contributions to the compilation of facts and presumptions that represent our present day insight into the details of this complicated phenomenon.

Considering the various starting points of the different investigations of the subject, one could perhaps distinguish three main lines of approach.

The hydrodynamic analysis, which concentrates initially on the macroscopical shock similarity of a detonation, became first established. In this it is characteristic for the period of the first experiments, when considerable interest had already been paid to the theory of shock waves [Hugoniot, 1887, 1888]. Before

the end of the nineteenth century, Mikhelsen [1893] and Chapman [1899], apparently independent from each other, adapted the existing mathematical treatment to the hydrodynamic model of a shock wave in which complete chemical reaction takes place, and only a few years later, Jouguet [1905, 1906] proved some of the still doubtful assumptions in their work to be right.

If one concentrates rather on the combustion character of the process, studies will primarily become involved with aspects of physical chemistry and consider factors like reaction mechanisms and reaction rates and problems concerned with the liberation and dissipation of energy.

Alternatively again, with the growing understanding of structural and thermodynamic aspects of detonation propagation, investigation on the basis of molecular physics has become increasingly important. This is, no doubt, a very intriguing development, as it tends towards an ultimate description of detonation waves by statistical evaluation of the influence of numerous, understood patterns in molecular behaviour.

Whatever the nature of the investigation, results must be equally valid in any of these possible studies. In fact, such transfer of information will only catalyse

further progress. An example of this is the first of the repeated renewals and improvements of the hydrodynamic theory of detonation through information from structural and kinetic studies. In its original form the Chapman - Jouguet theory is incapable of dealing with developments, taking place between the shock front and the Chapman-Jouguet point, which is the limit of energy feed-back to the detonation front. For stable detonations combustion is assumed to be complete at this point. Hydrodynamics, like thermodynamics, concerns itself with relations of states. Starting from a specified initial condition, it can produce functional expressions for parameters of any state that can be attained, irrespective of path, as long as the rules that are laid down for the individual case, are not violated. For a detonation wave these rules are the continuity principles, which require a "closed" system. Provided some characteristic information on the "final" state is available, the corresponding parameters can be evaluated. Before the structure of a detonation became understood, little could be said about conditions inside the wave and it was therefore not possible to consider in detail any state ahead of the C-J point. However, after Bone et al. [1936] had shown that chemical reaction starts only some distance behind the shock front, Zeldovich [1940], von Neumann [1942] and Döring [1943] improved the hydrodynamic treatment considerably by

including in their considerations the intermediate stages of a combustion zone with finite reaction rate.

Despite its being grafted on the structure of a detonation wave, the theory of Zeldovich et al. remains essentially a hydrodynamic treatment. As such it has, with all its further improvements, become the common basis for most contemporary work in this field. One of the main reasons for this is probably its simple basis, which consists conveniently of a few mathematical laws that must in principle always be obeyed. A simple check on this is often obtained by calculating detonation velocities from assumed equilibrium conditions at the C-J point and comparing these with experimental data. This convenient method has however two characteristic restrictions, which have been observed experimentally and can easily be understood in a qualitative way.

Calculated detonation velocities depend only on the initial conditions of the unburned gas and on the situation at the C-J point. Consequently the result will in principle be independent from the assumed structure and identical for all mechanisms that lead to the same final situation. Only variations in the C-J products, as can for instance be considered by introducing the effect of dissociation [comp.: Lewis and Friauf, 1930 and: Berets,

Greene and Kistiakowsky, 1950], can lead to a difference of second order, which has to be judged against experimental velocity data.

The second limitation can be observed under circumstances where the shock front receives hardly sufficient support from the combustion zone to maintain detonation propagation. Experimentally this causes marginal effects, like pulsating and spinning detonation, followed by steep velocity decline for compositions at the limits of the detonation regime [Wendlandt, 1924, 1925].

Despite these superficial explanations, the critical details are hardly understood, not mentioning the still remote possibility of realising a quantitative justification of limit phenomena in detonations. In attempts to disclose the real cause of marginal behaviour, modern research has produced a variety of results, leading to opinions that range between two extreme points of view. The first of these states that detonation limits depend on hydrodynamic factors, in which case the existing theory is, at best, incomplete and in need of further extension. The opposite view is that limits cannot be explained correctly on hydrodynamic principles, as they depend on other factors, concerned with structure, reaction mechanisms or kinetics of the shock and combustion wave. Both theories have their protagonists and estimating the validity and consequences of

various interpretations of results or combining these into one explanation, is still extremely difficult.

## I.3. Marginal detonation.

The fluctuating and rapidly changing character of many of the phenomena that can be observed in marginal detonation of gaseous mixtures, does not in itself seem to favour investigation into fundamental aspects of these very fast combustion processes. Nonetheless, the combined interest of science and industry to understand and control the critical conditions for this rapid energy conversion, has resulted in a varied, if somewhat incoherent collection of information on the subject. Composition limits to detonation propagation have been determined for a number of gaseous systems and some of these have been collected in table I.1. As can be seen, the variety in details of the experimental methods is as wide as the choice of systems and the implications of this will be discussed at a later stage.

Some authors have tried to draw generally valid conclusions on marginal detonation from the results of their work. Pusch and Wagner [1962, 1965] studied extensively the dependence of detonation limits on the tube diameter and concluded from their final results that limits must be governed by kinetic and hydrodynamic factors. Wagner [1955]

Table I.1. Composition limits for detonation of binary gaseous systems containing oxygen, at ambient pressure and room temperature.

| Reference | Fuel | Limits (mole %) Lean | Rich | Tube Length [mtr.] | Bore [cm.] | Initiation and tube separation. |
|---|---|---|---|---|---|---|
| Payman e.a. [1923] | $CH_4$ | 11.1 | 53.3 | 100 (coil) | 0.9<br>2.5 | spark in test mixture |
| Wendlandt [1924] | CO | 39.2 | 65.6+ | 9 | 2.1 | spark in $2H_2 + O_2$; membrane. |
| Bone e.a. [1931] | CO | 40.0 | 82 | 63 (coil) | 1.3 | spark in test mixture. |
| Laffitte e.a. [1936] | $C_3H_8$ | 3.1 | 37.0 | 5 | 1.4 | mercury-fulminate detonator in test mixture. |
| | $C_4H_{10}$ | 2.8 | 31.4 | | | |
| | $C_2H_2$ | 3.5 | 93 | | | |
| | $NH_3$ | 25.0 | 76 | | | |
| | $(C_2H_5)_2O$ | 2.6 | eq.pr. | | | |
| | $H_2$ | 15 | 90.4 | | | |
| Schuller [1954] | $H_2$ | 15 | 91 | 10 (coil) | 1.5 | Spark in $2H_2 + O_2$; membrane |
| | $C_2H_6$ | 4.0 | 46 | | | |
| | $C_2H_4$ | 4.5 | 60 | | | |
| Harper e.a. [1959] | $O_3$ | 9 | 100 | 7 | 2.5 | spark in $2H_2 + O_2$; membrane. |
| Miles e.a. [1962] [1966] | $H_2$ | 16 | 90.5 | 6 | 2.5 | spark in $2H_2 + O_2$; valve. |
| | $C_4H_4O$ | 4 | 57 | | | |
| | $(CH_3)_4Si$ | 3.5 | 48 | | | |
| Pusch e.a. [1965] | $H_2$ | 17 | 90.7 | 22 | 1.6 | spark in $CH_4 + 2\ O_2$; membrane. |
| | $CH_4$ | 8.5 | 51.5 | | | |
| | $C_2H_4$ | 3.5 | 59 | | | |

also investigated the thickness of the reaction zone of $CO - O_2$ detonations under steady-state and marginal conditions. His observations of pulsating and spinning effects under the latter circumstances are in accordance with the hydrodynamic-kinetic description given by Brinkley and Richardson [1953] for these near-limit phenomena. Data obtained for three component systems by Jost and Schuller [1953] strongly indicate kinetic influences. Belles [1959] recently made a purely theoretical contribution, in which he attempted, with moderate success, to predict the limits of the hydrogen - oxygen system by combining kinetic reaction data with observed hydrodynamic behaviour.

Gordon, Mooradian and Harper [1959] investigated the influence of water vapour and pressure variation on composition limits. Like Wendlandt [1925] thirty-four years earlier, they concluded that the temperature rise in the shock front influences the duration of the reaction initiation period and that the minimum temperature rise required for detonation, is comparable to the normal temperature explosion limit of the system. Although evaluation of shock temperatures for this purpose is still problematic, mainly because of the uncertain values for specific heats under these conditions, experimental evidence obtained by Miles, Munday and Ubbelohde [1962] suggests the

requirement of a similar temperature rise in the shock front as a condition for detonation propagation.

Indisputable confirmation of this indication will have important consequences for the interpretation of the mechanism of a detonation wave. Consequently, continued investigation of marginal detonation conditions of other gaseous systems has become desirable.

## I.4. MARGINAL DETONATION OF HOMOLOGOUS SERIES.

The research described in this thesis deals in principle with factors that limit propagation of detonation in gaseous mixtures. The purpose of this is to obtain information that might lead to a better understanding of some of the fundamental steps involved in these rapid combustion processes. The principal method on which the experimental part of the investigation is based, is the determination and study of characteristic detonation velocities and modes of propagation, as function of mixture compositions.

Previous departmental studies on marginal detonations in gaseous mixtures were concerned with the effects of additives [Miles et al., 1962]. The investigations dealt with the binary systems hydrogen - oxygen and furan - oxygen and three component systems of

hydrogen and oxygen with various additives. These systems were selected with particular reference to processes of energy relaxation of internal degrees of freedom in the shock front and to distinctive mechanisms of energy release and feedback in the reaction zone behind it. From careful analysis of the results, some cautious conclusions were drawn.

First of all, it was concluded that, whenever the temperature of the shock front drops below critical, experimental values, the rate of energy release in the reaction zone becomes insufficient to sustain detonation. These temperatures are calculated from measured detonation velocities by classical hydrodynamic shock wave theory, with assumed values for the specific heats; temperature data obtained in this way are comparable with the results of Gordon et al. [1959].

To investigate aspects of energy relaxation behind the shock front, data obtained for various ternary systems were compared with results for similar mixtures containing an inert gas as third component. From this study it became apparent that the initiation of chemical reaction follows the enthalpy changes in the shock front so rapidly that even at the limits, randomisation of internal energy for diluent molecules cannot take place.

Shock temperatures, calculated by Miles et al. for the complete composition range of the detonation regime,

clearly indicate another minimum value somewhere around the middle of the region of stable detonations. It is presumed that these minima occur for the mixture ratio that is most favourable for rapid liberation and feed-back of energy. For the hydrogen - oxygen system this situation coincides with the stoichiometric ratio for complete conversion to water vapour. However, for the furan - oxygen system selection on this understanding indicates optimal conditions for such a fuel-rich mixture as permits only oxidation to carbon monoxide and hydrogen molecules.

Although the facts, formulated in these tentative statements, are so intimately related to the detonation process that research into details of one of these will almost inevitably supply information on the other aspects, the work described in this thesis was started with the intention to continue investigation into the first of the carefully drawn conclusions. Calculation of temperature variations in the still unburned gas immediately behind the front of the detonation wave, is one of the most obvious possibilities that result from measuring detonation velocities for known mixture compositions. It was considered useful to try next to find more information and confirmation on the conclusion of the limiting temperature rise and - if possible - on the unrelaxed energy state of the mixture components at the onset of combustion. To this end the information on

detonation velocities and detonation limits, that is available from literature, has been studied. Most of this information, however, appeared to be unsuitable for a straightforward comparative study. Results, some obtained many years ago and with varying accuracy, are often restricted to a few composition points of the detonation regime and contrary to practice in the work by Miles et al., initial pressures were in many cases well below one atmosphere. Where the velocity versus composition curve is complete and determined at ambient pressure, the influence of variable conditions, such as detonation initiation methods, tube diameters and velocity recording techniques, are still to be evaluated. Because of these influences, results may differ appreciably for otherwise comparable experiments. It has therefore been concluded from the survey of literature that reliable and comparable information for a continued study on these aspects of marginal detonation could only be obtained by further experiments.

In selecting suitable systems, it was decided to concentrate for the time being on a group of consecutive members of a homologous series, hoping that this choice would lead to some revelations on how small differences in structural, thermodynamic and chemical properties of comparable molecules will cause changes like a shift in the

mole ratio of fuel and oxygen at the detonation limits. There are a number of reasons why the saturated aliphatic hydrocarbons appeared a good choice for the first sequence of such experiments. At the start of the series of these alkanes there are a reasonable number of members that can conveniently be handled as gases at room temperature and ambient pressure; the saturated molecular structure is relatively simple and it is formed on single bonds only. Fundamental information is extensive; in particular mechanisms of internal energy distribution have been studied in some detail in recent years. Furtnermore, these gases can easily be obtained in a high purity grade.

In the present context these hydrocarbons have still another attraction. Detonated with deficit of oxygen, they are likely to produce solid combustion products for both stable and marginal conditions of detonation. These phenomena have already been observed on systems containing excessive amounts of furan [Miles et al., 1962] and have also been studied in more detail for detonations in mixtures containing tetramethylsilane and oxygen [Miles, Munday and Ubbelohde, 1966]. In such systems the total energy that sustains the detonation front is released at a relatively slow rate, part of it being supplied through condensation of some of the reaction products. This phase

in energy release seems to take place behind the combustion reaction and in general greatly increases the duration of the total enthalpy liberation. Under such circumstances the actual reaction zone from which energy is fed back to the shock front, becomes considerably extended and, although the total mechanism is somewhat different from that in a normal detonation wave, the chemical and physical changes can be studied in much greater detail. In view of these attractions it is also reasonable to expect further information on developments taking place between the shock front and the combustion zone.

On account of these considerations and possibilities, it has been decided to examine detonation regimes for mixtures of saturated aliphatic hydrocarbons and oxygen with special attention to the marginal conditions. At a later stage the study has been extended to include some aspects of olefinic detonation. As a start, marginal detonations have once more been studied for the hydrogen - oxygen system, to form a reference for the following study and to clarify some details, concerned with the location of the detonation limits.

# Chapter II. THE EXPERIMENTAL INVESTIGATION OF DETONATION PROPAGATION IN GASEOUS MIXTURES.

## II. 1. Considerations of design and instrumentation.

Experimental investigation of detonation propagation in gaseous mixtures involves four essential operations. Detonations are to be initiated and stabilised; their propagation is to be studied and gas mixtures of selected composition must be prepared. The first two operations are usually executed in a detonation train; in addition the use of recording instruments is needed for observation and the gases are, as a rule, mixed in separate apparatus.

This section deals with various possibilities for the experimental provisions; these are discussed with special reference to the nature and requirements of the present study.

### a. Detonation tubes.

As with shock waves, detonations are normally studied during their propagation in long tubes. One reason for this is that, after initiation, these waves require time to reach steady-state conditions. For detonation this

becomes particularly important under marginal conditions, where quasi-stable states may persist over relatively long distances [Wagner, 1955]. In many cases, the use of long tubes also allows for a convenient description of detonation waves as one-dimensional processes, featuring planar zones normal to the axis of the tube. It must however be realised that this is an approximation which can easily cause misleading conclusions, especially in macroscopical or microscopical considerations of near-limit effects.

Initiation of detonation is concerned with all developments in the tube between the initial conditions and the first occurrence of detonation. This can be realised in a number of ways.

In many cases it is possible to achieve detonation propagation by spark or hot-wire ignition of the test mixture. As the flame spreads out, it sends compression waves ahead into the unburned gas, preheating it and causing in turn gradual acceleration of the flame, until shock waves are formed, leading to detonation ahead of the still subsonic flame; [Bone et al., 1936; Zeldovich, 1960, page 196]. The process is accelerated by turbulence and coalescence of shocks reflected from the wall of the tube. This implies the existence of a wall effect. Normal figures for the distance between the spark and the first occurrence of detonation, in readily detonable mixtures at ambient pressure,

are about 60 times the diameter of the tube [Lewis and Von Elbe, 1961, page 547].

Under marginal conditions, however, energy liberation caused by spark igrition is relatively slow and the essential shock waves will consequently require a long time and a very long tube section to be formed. Mixtures for which this energy release is so slow, that they just fail to lead to detonation, irrespective of the length of the tube, can be regarded as representing the limits of spark-ignited detonation. These limits are in fact the normal explosion limits. In practice these composition limits are always well inside the detonation limits, obtained after other modes of detonation initiation [Manson and Ferrié, 1953], although, as a rule, detonation will not occur outside the normal inflammability limits (exceptions: ozone- and acetylene-oxygen systems). As it is commonly accepted that the determination of detonation limits should not depend on the initiation method, but rather on the readiness of a test mixture to continue propagation of existing detonation, initiation for limit studies should in principle be suitable for a wider composition range than is covered by the detonation regime. For this reason and because of the requirement for tubes with extremely long initiation sections, spark ignition is less suitable for investigation of marginal detonation.

A convenient alternative for detonation initiation is the impact method, which can for instance be applied by detonating a strong solid explosive in the test mixture or bursting a diaphragm, which separates the test mixture from a reservoir with "driver"-gas at higher pressure. In the latter case, the strength of the impact is controlled by the initial pressure ratio across the diaphragm. Objections to the application of such techniques in detonation research are that they achieve combustion by processes only partly related to the true nature of detonation. In addition, pressure drivers may influence the self propagating detonation wave. The initial pressure ratio required to start detonation, determines the minimum propagation velocity of the driver gas into the reaction products of the test mixture. Around limiting compositions for detonation, the combustion wave will decelerate in the stabilisation section. Consequently it may be overtaken by the pressure pulse of the driver gas. This will lead to continuation of detonation-like combustion, but in the form of a shock wave which is only in part sustained by energy from chemical reaction. Phenomena of this type are hard to distinguish from true behaviour in marginal detonation and the technique tends therefore to cause definition of too widely separated limits.

A most satisfactory impact can be obtained from spark ignited detonation of a highly explosive standard mixture. As the initial pressure of this "primer" can be the same as the pressure in the test mixture, the diaphragm can be replaced by a straight-bore valve, which is to be opened prior to ignition. The impact is similar to that of the combustion driven shock, which is to be initiated in the test mixture, and detonation propagation is realised without contamination of the products by "foreign" driver gas.

After initiation has been achieved, detonation in the stabilisation section can either settle down to a stable velocity, characteristic for the mixture composition, propagate in the pulsating manner, which is inherent to the nature of marginal detonation, or degenerate to a much slower moving front. The last situation does not necessarily correspond to propagation of a normal explosion [Wagner, 1955] and is sometimes reached after considerable time. The delay depends partly on the exact mixture composition, partly on the diameter of the tube. For accurate limit studies the length of the stabilisation section should be at least one hundred times the diameter of the tube.

With respect to the length of the stabilisation section, special precaution should be taken with spark-ignited impact methods that do not require a diaphragm in

the tube. During initiation and stabilisation of detonation, acoustic disturbances, generated by the spark, are moving ahead into the undisturbed gas mixture. Although the influence of these waves is probably small, the length of the stabilisation section should be sufficient to allow the detonation front to catch up and overtake all disturbances, before it reaches the observation section of the tube.

The design of the observation section depends largely on the nature and aim of the experiments. Some investigations require only short sections, with stations for spectral work, temperature measurements or structural studies. For analysis of reaction products or studies of equilibrium conditions, expansion chambers are sometimes fitted to the end of the tube. For velocity studies the most common methods are the optical recording of detonation wave propagation on a rotating film or the measurement of time intervals between the passage of the detonation wave over consecutive timing stations in the tube wall. The former technique provides a continuous speed record but is quite complicated and requires very careful adjustment. The measurement of time intervals allows only calculation of mean velocities, but the method is very simple and reliable. Probes, to be used as timing stations in detonation trains, are usually situated in one line along the tube wall and should be sensitive to one of the rapid

physical changes that are caused in their environment by the passing detonation front. Scientific literature reports on a number of designs for these probes, the most common being pressure transducers, temperature-dependent resistance elements, light probes, such as photodiodes, and ionisation gauges. These detectors are part of an electronic circuit, which produces an output signal in response to changes at the sensing element of the probe.

The number of probes should be sufficiently large to permit calculation of a representative mean detonation velocity. The probes must be equally spaced and far enough apart to give realistic results, even for pulsating and spinning detonation waves as can be observed under marginal conditions. Since the pitch of a spinning detonation is about three times the length of the tube diameter [Bone et al., 1936; Gordon et al., 1959], the probes should be at least some multiple of this ratio apart. On the other hand, the distance between probes must be sufficiently small to prevent obscuration of meaningful oscillations in propagation velocity. An acceptable figure is 10 to 15 tube diameters.

Beyond the last probe a short length of tube should be provided to separate the signals from the first passage of combustion from those of the detonation-like waves that travel back through the tube after reflection of the original wave on the end plate of the tube. These phenomena are particularly strong in mixtures of limiting composition.

Reviewing the minimum requirements for complete execution of the specific functions in all three sections of the detonation train, a combined estimate indicates that for investigation of detonation limits, tubes should have a length of at least two-hundred times their diameter. Such lengths may be difficult to accommodate, especially with wider tubes. Detonation trains which have been designed to overcome this problem, often include a stabilisation section wound and stacked into large diameter loops. This method has, for example, been used by Dixon [1893], Payman and Walls [1923] and Jost and Schüller [1953, 1954]. It is claimed that, for a sufficiently long ratio of the bending radius to the tube diameter, boundary effects absorb the influence of the tube curvature on detonation propagation. However, boundary layer effects play a decisive role in detonation behaviour under marginal conditions, which constitutes the present field of interest. Consequently it must be considered imprudent to jeopardize the outcome of these critical experiments by the use of such equipment. Furthermore, studies involving gaseous systems which produce condensation products, require thorough cleaning of the tube after each detonation and this will be extremely difficult with a coiled stabilisation section.

As will be appreciated from the preceding discussion, the diameter of the tube is a very important

factor in design of detonation trains. For steady state detonations the influence of the tube diameter has been the subject of theoretical studies by Manson and Guénoche [1955], Fay [1952] and Döring and Schön [1950]. Manson [1957], Peck and Thrap [1957], Kistiakowsky, Knight and Malin [1952] and Kistiakowsky and Zinmann [1955] report also on experimental investigations. The experimental results indicate a linear relation between the detonation velocity and the reciprocal of the tube diameter. As has already been mentioned, tube diameter effects on detonation limits have been studied extensively by Pusch and Wagner [1962, 1965], who observed a similar relation between the limiting concentration of the combustion gas and the reciprocal of the limiting tube diameter. The two types of experiments are not performed for the same range of diameters, but, assuming that extrapolation of these functions is allowed, wider tubes are more important for limit studies than for velocity measurements. For example, comparison of results calculated for a 1 cm. bore tube with those found on this basis for a tube with "infinite" diameter, shows a difference in velocity of about 1 percent, but a shift in limit composition of a few percent of the complete composition range. This information stresses the need to minimise boundary layer effects by the use of tubes with larger

diameters, but this in turn is unfavourable with respect to the requirement for one-dimensional conditions in the detonation wave. Moreover, experiments involving large quantities of explosive gaseous mixtures are to be avoided. Depending on circumstances and the type of experiments, most detonation tubes have a bore between 1.5 and 7.5 centimeters

Usually, tubes have circular cross-sections. The use of other shapes has been investigated [Bone et al., 1936], but even for spinning detonations the differences in results were negligible. As flat walls are an advantage in optical studies, rectangular cross-sections have found some application or, as a compromise with the advantages of cylindrical tubes, hexagonal sections. Everything considered, circular cross-sections are however to be preferred for most purposes; tubes can be bought from stock and in wide selection, their sections are easily machined and assembled, and their shape is most favourable for experiments asscciated with the development of a theoretical axially-symmetrical model.

Numerous materials have been used in the construction of detonation tubes. With care, glass sections can be incorporated when visual observation or optical study is being considered. Otherwise metal tubes are most

regularly employed, copper mainly being favoured for spectroscopical work because of the simple pattern of its spectral lines, and iron or steel in situations where strength is more important. Chromium-plated or stainless steel tubes are used in the presence of corrosive mixture components. Results of not yet published research in the department have indicated that wall material can have a pronounced effect on the marginal behaviour of detonating gas mixtures. In circumstances where all requirements cannot be met by any of the readily available materials, coating of the tube may provide a suitable solution. This can also be helpful when the nature of the experiments puts the most stringent demands on the surface finish at the inside of the detonation tube. Non-metallic materials have been used in studies on the influence of E.M. fields on detonation propagation.

Little is known about the influence of pressure and temperature on the detonation limits. Wagner [1961] gives a short survey of information available on the influence of these parameters on the detonation velocity. The effect is small. For convenience, experiments are most readily performed at ambient pressure and room temperature.

b. Velocity measurements.

Evaluation of detonation velocities requires determination of the distance between the probes and of the time intervals between their consecutive signals.

Time intervals are measured by means of electronic counters or by photographic recording of oscilloscope traces. The application of either of these methods must be considered in relation to the requirements of the work. For studies on steady state detonations a much higher accuracy is needed than for investigation of marginal behaviour. With the most readily detonating mixtures of a system, the fluctuations in propagation velocity are usually not much larger than 1 m/sec., [Miles et al., 1962]. To detect these oscillations, the accuracy of the recording equipment should be better than 0.05% or 0.05 μsec. absolute. Such accurate data can be useful in comparing calculated and measured detonation velocities.

Close to the detonation limits, fluctuations in detonation velocity due to spin, are of the order of 20 to 100 m/sec or 2 to 10%. Fluctuations caused by pulsating propagation can be a multiple of this. Under these circumstances, measuring techniques allowing accuracies of 1% or approximately 2 μsec. are quite sufficient.

Electronic counters register the number of cycles

from a standard frequency, that occur between the consecutive signals from two different probe circuits. Their accuracy is therefore ± 1 count. The absolute accuracy depends on the standard frequency of the crystal in the oscillator unit and the range of the counter recording. A 1 MHz. oscillator will give accuracies of ± 1 μsec., which corresponds to 1.0 to 0.5%.

Oscilloscopes are often more flexible in use, as their range does not depend on the standard frequency of a crystal. On the other hand, accurate time intervals can only be evaluated from photographic records of traces, after developing and measuring with a travelling microscope. The accuracy depends on the sharpness of the trace, the stability of the calibrated display and the quality of the pictures. Much depends on the experimenter's experience, but with three or four probe signals on one trace, the maximum accuracy of measured peak distances is about 1%.

As can be seen, both of these standard methods are adequate for investigation of marginal behaviour in detonation, but for pure steady state research other recording methods are required. Counter frequencies for this field will have to be very high. Sometimes oscilloscope records can be made by using a raster display, for which single horizontal sweeps are successively triggered from a steadily decreasing voltage, applied to the vertical

plates of the oscilloscope tube. An extremely accurate measurement of time intervals can be obtained from the spiral display developed by Munday and Tyley, the principles of which are described in the paper by Miles [1962] or in the book by Gaydon and Hurle [1963]. Accuracies of $\pm$ 0.02% can be realised.

For calculation of detonation velocities from the measured time intervals, the inter probe distances must be known. For a relatively narrow tube of, for instance, 2 cm. diameter, the distance should be at least 20 cm. (see II, 1.a). With a travelling microscope probe-to-probe distances can be determined with great accuracy, but taking into account the width of the detecting element in the probe, figures must be insignificant below approximately 0.2 mm. Distances are therefore known with an accuracy of about 0.1% or better and the uncertainty in the evaluated velocities will consequently be entirely due to that of the time recording, as long as only the recording techniques are used for this.

In this it has been taken for granted that the response time of the probes and the probe circuits will be small compared with the accuracy limits and that transfer times of signals from the circuits to the recording instruments can be neglected or made comparable.

c. Preparation of gas mixtures.

The accuracy to which gas mixtures for investigation of detonation limits must conform with selected composition values, should be at least as good as the accuracy required for the determination of the limits. The uncertainty in values for the limit compositions should in turn be smaller than the influence of the experimental conditions on these results and than the spread in limit values that have been calculated on theoretical considerations for various assumptions. These different requirements with respect to accuracy, are necessary to permit a satisfactory interpretation of the experimental results.

As can be observed from limit data that are available in literature (cf. table I.1) or from the discussed influence of tube diameters on detonation limits, (see II.1.a), the variation in limit values for various experimental conditions, is between a half to a few percent. The spread in limit data, calculated from theory for various assumptions, is of the same order of magnitude [Belles, 1959], although absolute values may differ more from the experimental results. However, in a comparative study of detonation limits for consecutive members of a homologous series, smaller variations will be significant. This applies particularly at the oxygen rich limits, where Laffitte and

Breton [1936] observed a difference in the fuel - oxygen ratio for propane and butane systems of 0.3 to 0.4%. On this basis, determination of the composition limits should be attempted with an accuracy of 0.1 to 0.05% of composition, to reveal significant differences between limits of the various systems. It follows, in turn, that careful examination of the limit regime, requires preparation of mixtures to within 0.05 to 0.01% of the selected composition ratios.

The two alternative systems, most commonly applied for the preparation of gaseous mixtures, are the flow method, by which gas can be mixed and supplied to the tube in the same operation, and the static method, which allows for the successive introduction of measured amounts of gas into a storage system and requires satisfactory mixing by other means, before the detonation experiments can be carried out.

The first technique is based on adjusting two separate flows of the component gases in such a way that their combined supply delivers a mixture of constant selected composition. This system is in principle very attractive: the equipment is small, mixtures can be supplied immediately when required and for any composition ratio, and results should consequently be obtained at a relatively high rate. Experience has however shown that the initial flow adjustment can be extremely tedious and often results in

loss of gas; this is particularly uneconomical when expensive, rare or high purity samples have to be used. Apart from this, the main disadvantage is the limited accuracy, which is not better than approximately 0.1% of mixture composition.

In the alternative method, gas quantities for mixing can be determined either by partial volume or by partial pressure. As mixing compositions are the same as mole ratios, mixing by volume should in principle be preferred. For this, two adjustable and calibrated volumes are filled to the same pressure with the respective components and subsequently brought together. The technical disadvantages of the calibration and the design of the mixing arrangement are however considerable.

These disadvantages can in part be overcome by mixing two components to the ratio of their partial pressures, after the quantities of gas have been measured at selected pressures in two separate, but fixed, calibrated volumes. The design problems concerned with the mixing operation, are however not solved in this way.

Technically it is most simple to mix the components by their successive admission to a vessel, assuming that the respective pressure alterations are numerically representative for the mixture composition. For accurate composition determination, the non-additivity of partial pressures in

mixtures of dissimilar molecules, should be considered. This deviation of the behaviour of ideal gases depends on the nature of the components and their ratio in the mixture. As the non-additivity is generally not larger than 0.1% for mixtures containing equal amounts of a gaseous component and oxygen or nitrogen [Michels and Boerboom, 1953], the simplest method is to ignore this factor for steady state conditions, but to evaluate the corrections for the individual composition ratios of the detonation limits.

Apart from the correction for the volume change on mixing the separate components, the accuracy of this method depends on the influence and control of factors like temperature variation during mixing and its effect on manometer indication. Further errors of this type are introduced as temperature fluctuations inside the vessels, resulting from compression changes on the gases. Proper evaluation of these errors is most important, as the normally used mercury manometers can be read accurately enough by means of a kathetometer, to enable reproducibility of 0.01% of composition in mixture preparation.

Apparatus of this type is rather large and extensive safety precautions are required. With regard to explosion dangers, the installation should be assembled behind a safety screen and be operated by remote control. It must remain leak-proof over long periods and removal of

surrounding atmosphere must constantly be guaranteed. The apparatus should also be designed in such a way that explosion in the detonation train cannot penetrate back into the storage system.

Adavantages of this type of gas mixing apparatus are, that systems with any number of components can be prepared and that sufficient gas mixture can be stored for several runs. This is particularly useful for repetitive experiments and for ample storage of the primer mixture. The only restrictions to this are the safety objections against large quantities or high pressures for stores of readily detonating gas mixtures.

As the detonation train is usually filled by bleeding the mixtures from the storage vessels into the tube, gaseous remnants in the vessels will at least be at ambient pressure. To minimise loss of mixture containing expensive samples, the volume of the storage vessels should not be too large. Alternatively, arrangements could be made to utilise this remnant for the preparation of further mixtures. For the same reasons of safety and economy, it is recommended to reduce volumes of lines to such limits as is still compatible with specifications for evacuation speed and purity.

Materials, applied in the construction of gas mixing equipment, vary. However, as extreme vacua and

purities are seldom required, glass can be used in most circumstances, especially as the safety screen can be relied on for protection. When high explosion pressures are likely, metal vessels are even more dangerous as fragmentation of such materials will occur at much higher pressures than for glass. Other important advantages of glass are the possibility for any required shape and the ease of inspection. Leak tests are easily carried out; stirring facilities can quickly be installed. Finally, objections on the ground of lack of flexibility have been largely overcome, since standard glass fittings, like taps and couplings, were introduced on the market.

## II. 2. The equipment.

Basically, the equipment used for most of the experimental work described in this thesis, is similar to the arrangement from which the results for detonation of tetramethylsilane mixtures were produced [Miles et al., 1966]. A number of alterations has been made and in this section the system is discussed in its present form.

For these experiments an explosion bay was available which was approximately 21 feet long and 6 ft wide. In this bay the detonation train has been built. It is positioned along the closed wall and mounted on a channel beam,

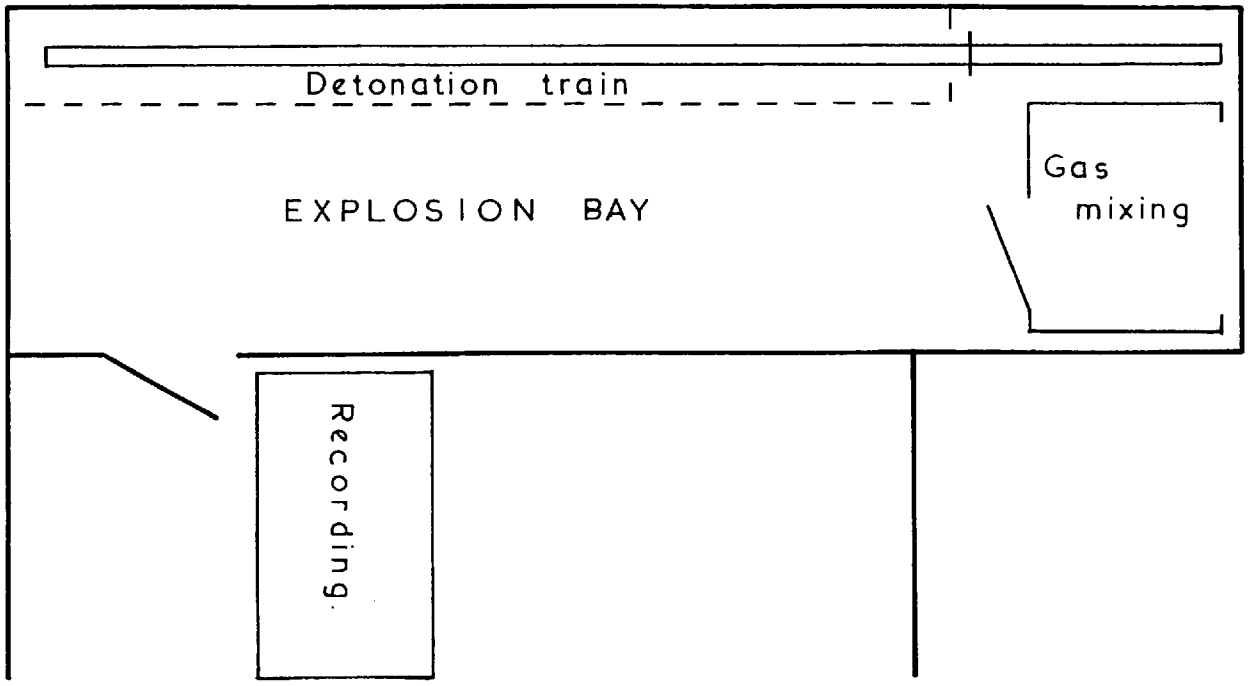



Fig. II. 1. Equipment lay-out.

which is supported by a rigid, tubular frame; see figure II.1. Units of the recording equipment that have to be close to the probes, are mounted on a stand above the observation section of the tube. All other recording instruments are placed on a steel angle frame outside the explosion bay. The firing of the ignition can also be effected from this position. The gas mixing equipment has been set up at the far end of the explosion bay, in front of the exhaust ducts of the ventilation system.

a. The detonation train.

In view of the various interrelated requirements, which have been dealt with in the previous section, the detonation train has been made from a 1 inch bore, stainless steel tube with 10 s.w.g. walls. It is shown schematically in figure II, 2. For convenience, experiments are carried out at ambient pressure and room temperature.

Spark ignition of stoichiometric hydrogen-oxygen mixtures has been selected as standard method of detonation initiation. To this end, an initiation or priming section has been provided, which is approximately 5 feet long and at one end sealed off by a removeable plate. In the centre of this plate, the sparking plug has been mounted. To prevent electromagnetic signals from the plug influencing the

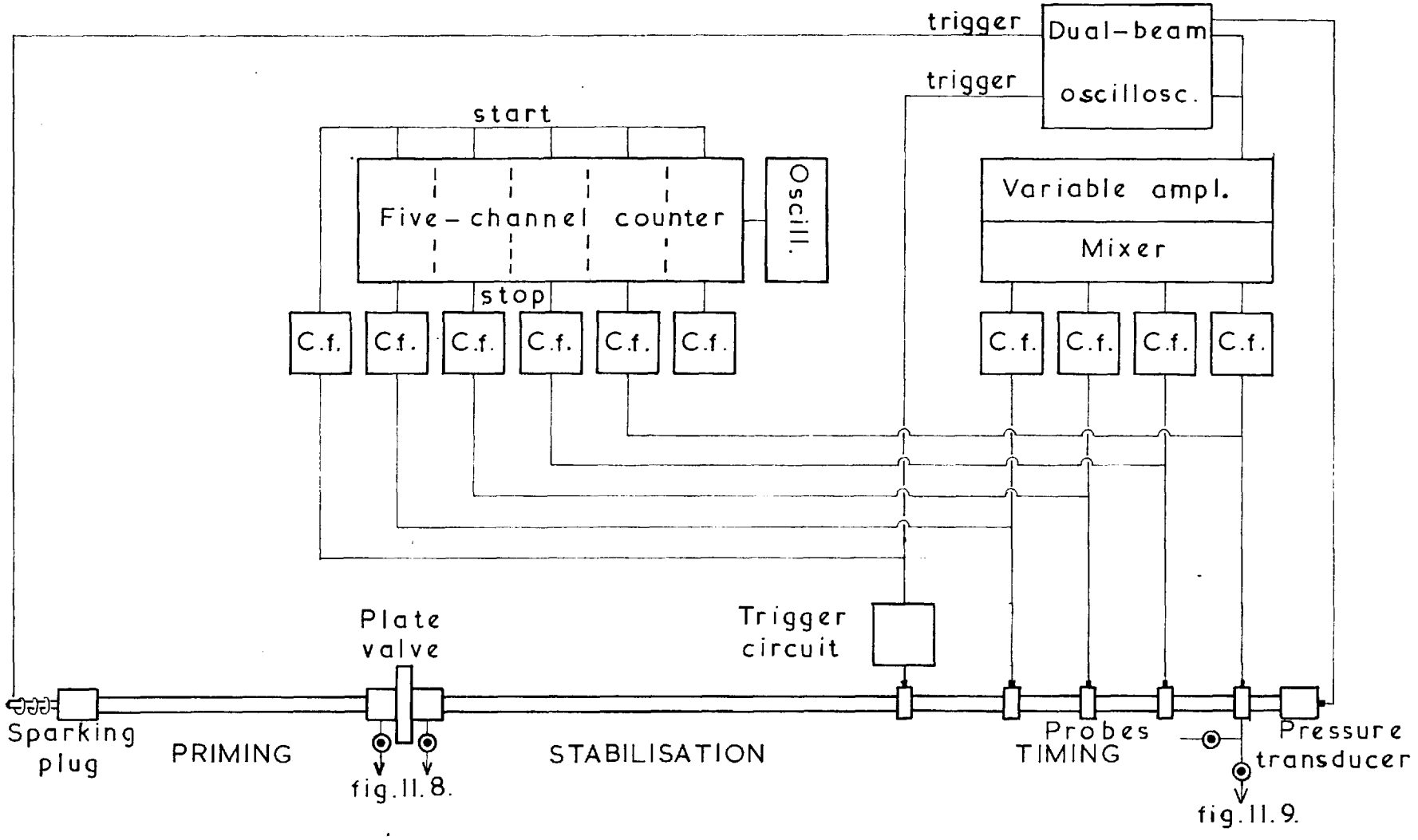



Fig.11.2. Detonation train and block diagram.

sensitive recording equipment at the other end of the tube, the end plate is insulated from the tube by nylon rings, as is shown in figure II.3.

At the other end of the priming section, the detonation tube extends, first of all, through the body of a plate valve, which can be operated by rotation of an outer ring and has been described in detail by the designer [Munday, 1963]. When the valve is closed, gas samples can be pumped from or let into the tube through connections on each side of the plate valve. Flow through these connections is controlled by needle valves.

The stabilisation section, which is connected to the other side of the plate valve, is 9 feet long. It continues into the 5 feet long observation section, which can more accurately be described as "timing section" for these experiments. Four brass collars are used as mounting points for the timing probes. These rings are hard soldered to the tube at intervals of 12 inches. A special collar is provided for a trigger probe at the beginning of the timing section. Beyond the last collar the tube extends another 6 inches before it is sealed off by another removeable plate, which is mounted in a brass block. This end is connected to a vacuum line, served by an oil rotary pump, capable of reaching $10^{-3}$ mm. mercury, and to a mercury manometer, which can be sealed off from the tube by needle valves.

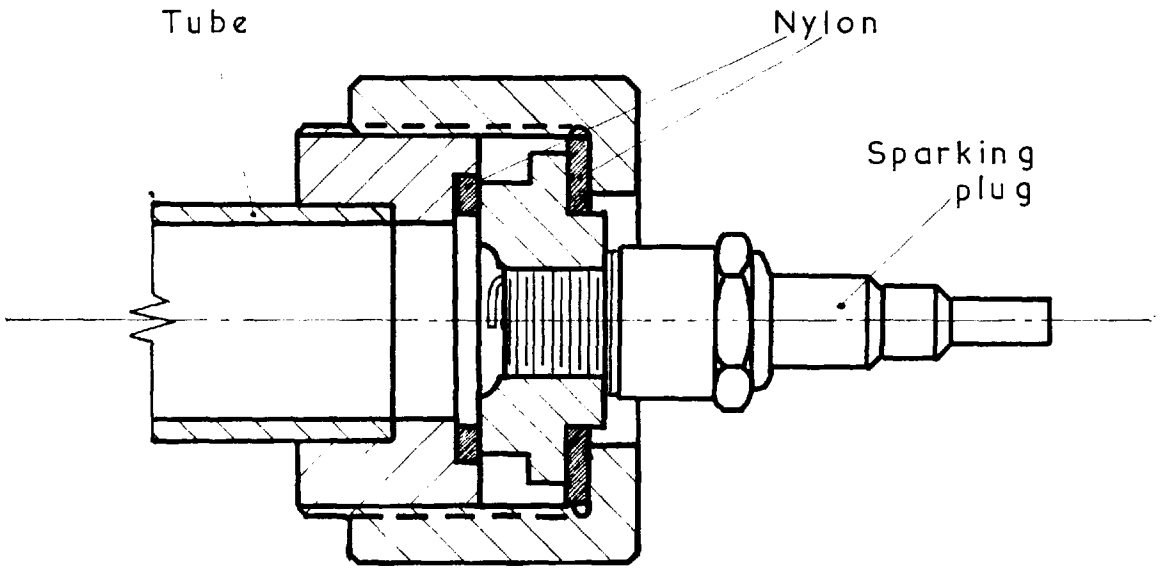



Fig.II.3. Sparking plug mounting.
scale: 1 : 1

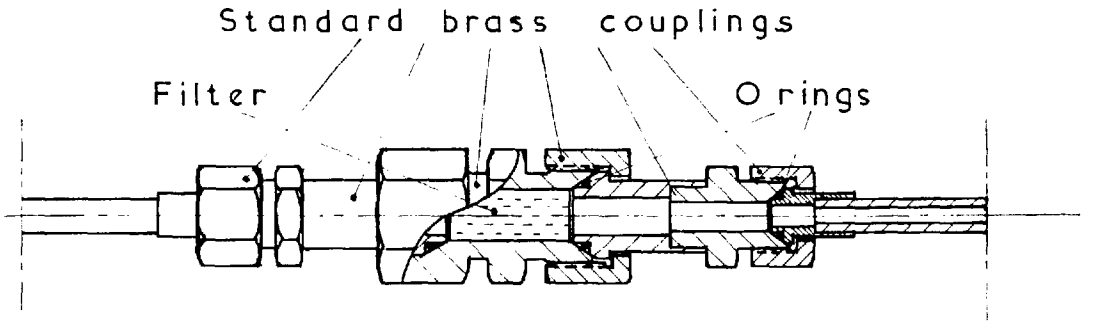



Fig.II.4. Line filter unit.
scale: 1 : 1

As it has been found that condensation products, as formed under fuel-rich detonation conditions, gradually contaminate the lines and the equipment connected to the detonation tube, various protecting filter devices have been tried out. The most satisfactory device consists of standard brass coupling units, enclosing a cigarette filter, which is renewed after each run, see figure II.4. These filters are placed immediately beyond the needle valves which seal off the detonation tube from the other equipment and whose satisfactory operation has been found to be insensitive to contamination by solid reaction products.

b Recording equipment.

Most of the characteristic properties of detonation which can be utilised for detector design, decay strongly at the detonation limits. This complicates the selection of a suitable system for velocity measurements under marginal conditions.

In the present research, ionisation probes are used for the stations in the timing section of the tube. These detectors are basically a simple break in an electric circuit, which is momentarily closed by the free charges that are known to be present in the detonation front. The selection of these probes is based on their simple design,

which is relatively easily adapted to suit the small extent of conductivity that can still be found in the detonation front under marginal conditions. Furthermore, these probes are reliable in operation and readily cleaned, which is particularly useful when condensation products from detonation can be expected.

A scheme of the general arrangement for the recording equipment is enclosed in figure II.2. Registration of time intervals is, in the first place, effected by photographic records of oscilloscope traces. Subsidiary information is obtained from counter readings. The choice has resulted from the investigation into the hydrogen-oxygen detonation limits. From these it is found that at the limits the conductivity of the detonation front is so much reduced, that, despite the use of very sensitive ionisation probes, it becomes almost impossible to produce sufficiently strong output signals to operate counter valves. By using an oscilloscope arrangement, these problems have been met in the following way.

At the beginning of the timing section of the tube, a special sensitive arrangement of probe and probe circuit has been installed as a trigger unit. With proper adjustment, all but the most marginal explosions inside the detonation regime, will produce a sufficiently strong output signal to trigger an oscilloscope trace. The time base for

this single sweep has been selected to cover the time interval ending with the impact of the detonation on the end plate of the tube. Output signals from the four timing probe circuits are fed through cathode followers, a mixer and a variable amplifier and applied to the vertical plates of the oscilloscope tube. With sufficient amplification even very weak signals can be detected on the records and their positions can be measured with a travelling microscope.

However, accurate determination of detonation limits requires velocity measurements on both sides of the critical composition. Attempts to do this with the described arrangement have shown that the conductivity of combustion processes outside the detonation regime, is insufficient to disturb even the very sensitive balance of the trigger probe circuit. This problem has been overcome by the use of a second single oscilloscope sweep, for which the trigger line runs from a solenoid, placed around the high tension line to the sparking plug. The voltage pulse which is induced in the coil when the sparking plug is charged, starts the sweep of the oscilloscope trace. The time base is selected to cover propagation of trans limit combustion to the end of the tube. In practice, the duration of the former sweep is 2 milliseconds in most cases and the duration of the latter sweep 20 milliseconds.

Detonations are best studied from the first trace and slower modes of combustion propagation from the other trace.

When marginal behaviour of the detonation wave is very strong or when detonation fails to establish itself in the stabilisation section of the tube, re-ignition of detonation is likely to occur as the primary wave hits the end plate of the detonation train. This leads to propagation of a "reflected" detonation wave, travelling in the opposite direction. Probe signals resulting from this second passage, are sometimes comparable with the primary signals or even stronger than these. On oscilliscope records they may be hard to distinguish from the original peaks, especially as signals from different probes can only be recognized by their sequence. To avoid confusion, the system has been further modified by mounting a pressure transducer in the end plate of the tube. The signal which results from the impact of the primary combustion wave, is used to suppress temporarily the sweep of the slower oscilloscope trace. For indistinct records of limit detonation propagation, the break in the trace helps to distinguish between the primary and secondary probe signals.

For sufficiently strong detonation, additional records to time intervals are obtained with the counter, to which all signals are fed through separate cathode

followers. A pulse from the trigger circuit starts all the channels of the counter, which are then successively stopped by pulses from the timing probes, fed to the counter along cables of identical length. The strength of the pulses, required to stop the counter, is however too great to allow for the use of the counter within approximately one percent of composition difference from the limiting condition.

Various types of ionisation probes have been used in these experiments. Each of these probes is enclosed in a probe body, which is shaped as a 4BA screw (diameter 0.142 inch) with a specially designed head. The body fits into a 4BA hole that is drilled and tapped radially through the brass rings around the timing section and the tube wall. In position the end of the probe body must be flush with the inside wall of the detonation train to minimise shock disturbances. Through the stem one or more insulated conductors are fitted and these constitute the ionisation gap, either with the tube wall or between each other, at the probe tip.

All timing probes contain a single conductor. For this a 0.040 inch standard metal rod is generally used. Originally the conductor was surrounded by a plastic body [Miles et al., 1966], which formed a gap to the tube wall of approximately 0.05 inch. However, in the present

research these probes have been found to be unsatisfactory, partly because of their poor sensitivity. A more practical objection to their use has risen from the fact that the head of the plastic screw does not give a durable vacuum seal. This problem can be solved by application of a varnish coating across the outside of the seal, but this prevents regular unscrewing of the probe for cleaning purposes. In detonation experiments involving formation of condensation products, cleaning of the probes after each run is unavoidable and different designs are therefore required.

The present design of the timing probes, as shown in figure II,5, consists of a brass rod sealed with araldite into a brass body. These probes are made in the following way. The probe body is turned to the required shape on a lathe and a hole of 0.055 inch diameter is drilled through its axis. Inside the head of the probe body, this capillary hole is bored out to 1/4 inch cross section. The 0.04 inch standard brass rod is coated with a uniform layer of "Araldite" - epoxy resin. To do this, a die has to be made by drilling a 0.051 inch hole, countersunk to a sharp edge through a metal plate which is clamped to the table of a pedestal drill. The standard brass rod is then secured in the rotating head and pushed down far enough through the hole in the plate to permit coating of at least one inch of the rod protruding from the underside of the

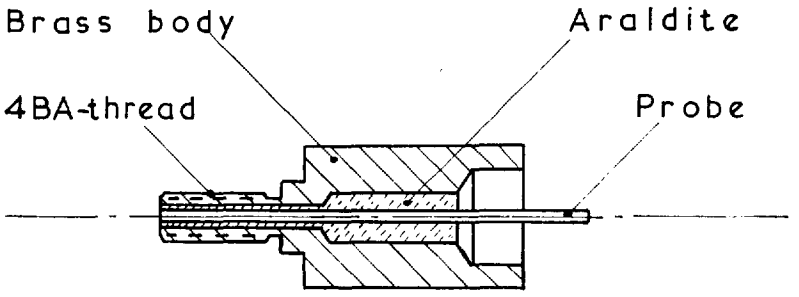



Fig.11.5. Timing probe and probe body.
scale: 2 : 1

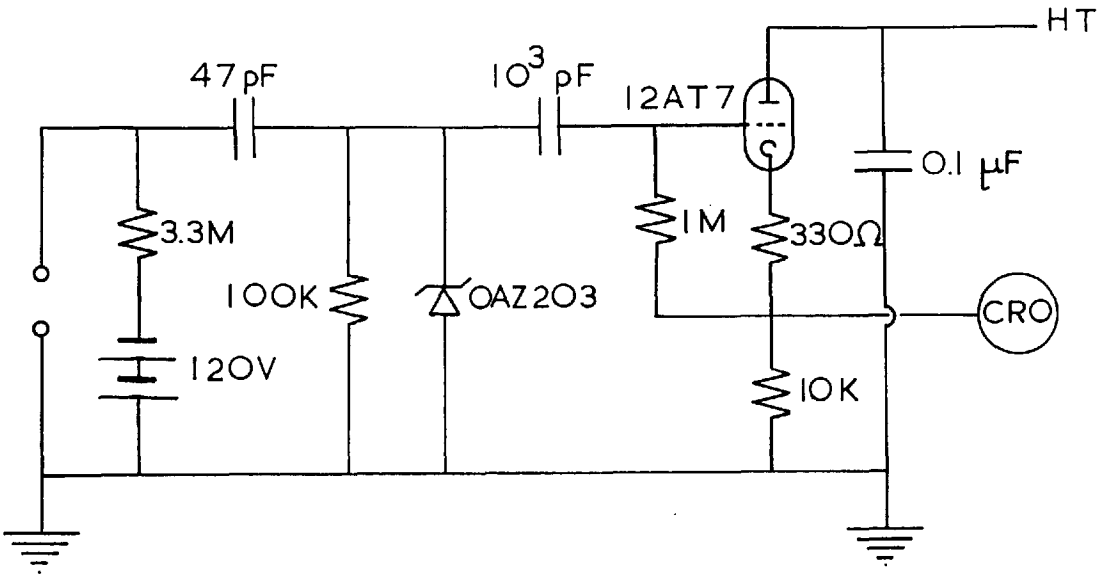



Fig.11.6. Timing probe circuit.

table. To promote proper flow properties, a warm mixture of Araldite epoxy resin and hardener must be used. A uniform layer is then obtained by pulling the coated end of the rod through the centre of the die hole. After hardening of this Araldite layer, the lower half of the 1/4 inch hole in the probe body is filled with a similar warm Araldite mixture and through this the coated end of the brass rod is pushed down the capillary hole unitl it appears at the other end. Excess Araldite is removed from the protruding tip of the rod, which is then rotated until more Araldite appears through the narrow gap between the coated rod and the probe body. The rod is secured in the body by hardening of the Araldite for half an hour at 120°C. Finally the stem of the probe is turned down to the required length and the uncoated rod protruding from the head of the probe body is cut off approximately 1/8 inch above the top of the probe body. In probes of this type the Araldite layer between the central conductor and the probe body is approximately 0.007 inch thick and has been found to give improved results in studies of detonation limits. Sealing requirements are met by an O-ring, fitted over a collar at the top of the probe stem. The ring is compressed when the probe body is screwed into the wall of the detonation train.

Probe circuits are shown in figure II,6., together with the cathode follower circuit, through which signals are

fed to the recording units. As a probe becomes conductive, the condenser discharges and the resulting voltage drop over the 100 kilo-ohm resistor gives the output signal. The 3.3 mega-ohm resistor in the positive tension line retards recharging of the condenser from the 120 volt battery sufficiently to prevent repetitive discharge by the same detonation front. The diode is included in the circuit to limit the output signal to a maximum amplitude of 6.2 volts.

Probe circuits of this type have been built on a frame which will slide into insulated tubes of 3/8 inch internal diameter. The ends of such a tube can be push fitted over the head of a probe body. A mini-plug inside this tube will then slip into the 1/4 inch clearance hole in the head of the probe body and plug over the free end of the conductor pin. In this arrangement the earth connection to the probe does not use the probe body but a common earth for all probes, fixed to the end of the tube. Shielding from outside E.M. influences is realised by covering the outside of the tube around the circuit with conductive paint, which is in contact with the shield of the coaxial cables used throughout the recording system.

The circuit used for the main start trigger-line requires a probe with two conductors. Originally two

parallel enamelled copper wires were used. However, the actual position of the core ends of the fitted probe with respect to the axis of the detonation tube influences the sensitivity of the probe and the nature of the signal. To combine the necessity of the two conductors with the advantages of sensitivity and orientation independence of the circular timing probes, the two conductors have been fitted inside each other by much the same techniques as used for the construction of the timing probes. The result is a brass probe body with an axial 0.070 inch diameter hole, in which has been fitted a copper capillary tube of 0.064 inch outside diameter and a wall thickness of 0.007 inch. Inside this capillary a standard brass rod of 0.040 inch diameter has been fixed. Consequently the Araldite layers between the conductors and the probe body are approximately 0.004 inch thick, which gives excellent sensitivity for limit investigation, but sometimes causes unintended discharge of the probe. This depends in part on the quality of the Araldite, which has reasonable wear properties but tends to absorb water vapour. Due to this probes will gradually age and lose sensitivity, but they can be reconditioned to some extent by a heat treatment in an oven at 100 - 120°C for about an hour.

The trigger circuit is shown in figure II,7. The variable resistor is to be adjusted to keep the grid voltage

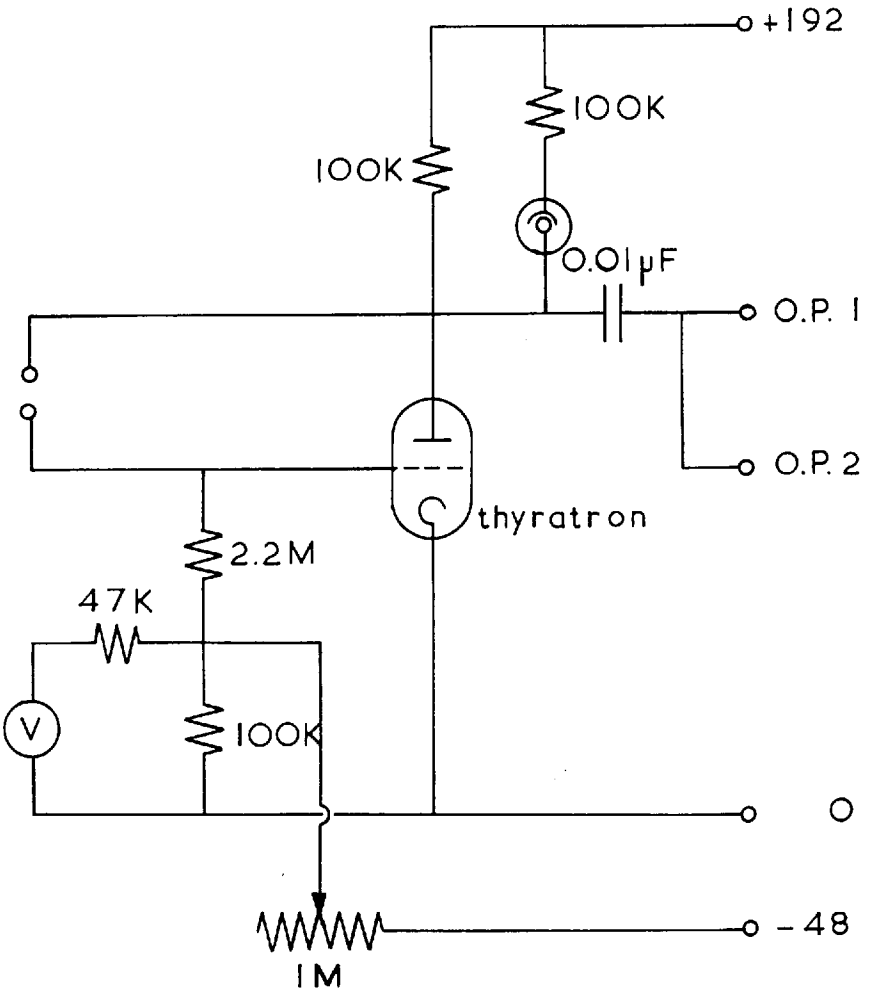



Fig. 11. 7. Trigger probe circuit.

of the thyratron just below cut-off value. Disturbance of this balance, even by very small diminishing of the resistance of the probe, will make the valve conductive and produce a negative voltage change from+240 to+48 volts on the output.

Recording of the oscilloscope traces has been considerably simplified in this study by the use of a Tektronix 555 Dual-Beam Oscilloscope, which has independent time base arrangements for the two traces. This has made it possible to use a single camera, and to obtain photographic records showing the two traces, one above the other.

The counter, used in measuring the time intervals between sufficiently strong signals from successive stations, has already been described in short by Miles et al. [1966]. Details of the electronics are shown in appendix H. As can be seen from figure II,2, it consists essentially of a counter with five channels, which register microsecond pulses from an oscillator unit. All channels become operative by a signal from the trigger probe and each channel can only be stopped by a signal from one particular timing probe. The accuracy with which the time intervals are recorded is $\pm$ 1 microsecond.

c. The gas mixing equipment.

Preparation of gas mixtures for limit investigation by the flow method has been disregarded because of the limited accuracy and reproducibility; the instrumental difficulties of the other techniques have favoured the choice of mixture preparations with respect to pressure alterations due to successive addition of various components.

The apparatus is schematically shown in figure II.8. Its centre is the manifold, which is attached to a closed mercury manometer. The manifold is separated from the other parts of the system by metal needle valves or high-vacuum spring-loaded stopcocks. These other parts are: a vacuum line for gas removal; a supply line for the introduction of pure gaseous mixture components; a 5 litre mixing and storage vessel for the primer mixture and a 10 litre vessel for the test mixture, each provided with an open mercury manometer to check on mixing proceedings; finally two outlet lines to supply the mixtures from the storage vessels, through the manifold to the two parts of the detonation train.

The manometer of the test mixture storage vessel can be closed off from the vessel and independently connected to the manifold and the vacuum line. This makes it possible to determine pressures of remnant test mixtures with respect to barometric pressures and consequently to use such gases

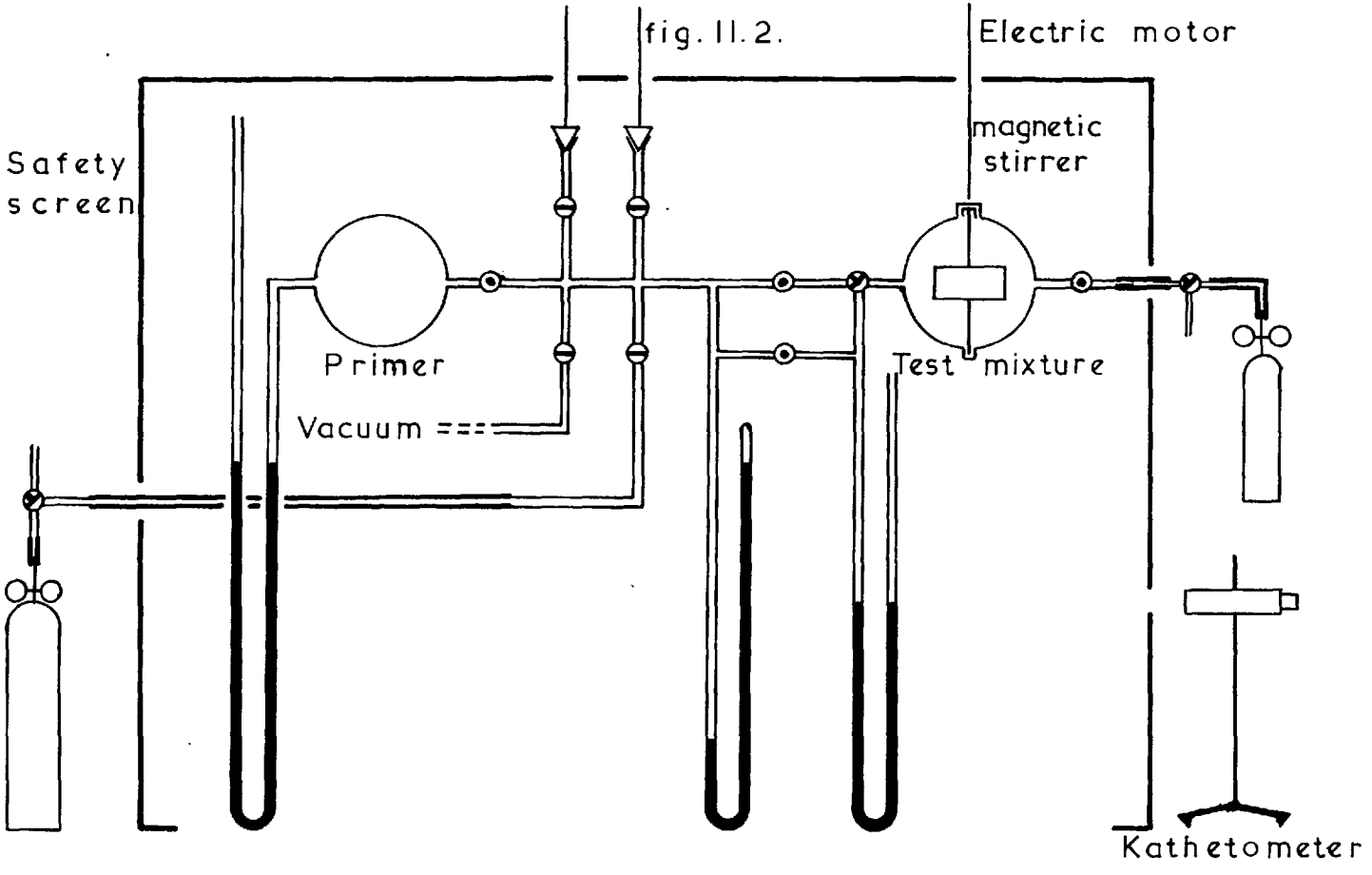



Fig. 11.8. Schematic diagram of gas mixing equipment. For symbols see figure 11.9.

for further preparation of mixtures containing expensive components. For such samples an extra capillary inlet to the vessel has been provided. This vessel also has a magnetic stirrer, rotated by a variable speed electric motor.

Vacuum is supplied by an oil rotary pump, which will attain inlet pressures of $10^{-3}$ mm. mercury in a few minutes. This pump can also be used to supply backing pressure to an oil diffusion pump, capable of reaching $10^{-5}$ mm. mercury. However, the nature of the research dealt with in this thesis, does not require maximum exclusion of common impurities. Furthermore, with regard to marginal conditions, previous experiments in the laboratory [Miles et al., 1962] have not confirmed the necessity for extreme exclusion of water, mentioned by Gordon et al. [1959]. For these reasons the diffusion pump has only been used for leak testing of the system.

The apparatus has predominantly been made of glass. Cone and socket connections have been used throughout; for glass to metal joints a metal cone has been used. Taps in the system were originally lubricated with Apiezon M grease, but in the latter stages of experiments KEL-F90 grease has been used because of its better sealing properties for long term storage of gas mixtures containing higher members of the paraffin series. Except for blow-out safety devices, all static seals against pressures above ambient have been

made with picein wax or, when possible, with Araldite epoxy resin.

The system has been built on a tubular frame behind a safety screen made from 1/4 inch thick plates of mild steel and screened on top by a 3/8 inch mesh gauze of steel wire. The front of the screen has a man-high access door and a control panel, from which all operations can be performed with knobs, connected to the taps and valves by flexible shafts. Viewing slits, covered with perspex, allow for inspection of the apparatus and the reading of the manometer of the 10 litre vessel by means of a kathetometer, installed outside the screen.

d. Additional sources of information.

This study of detonation propagation and detonation limits of hydrocarbon-oxygen mixtures has been supplemented in three ways. In all experiments additional information was obtained by recording the final preasure. In some cases analysis of gaseous reaction products has also been undertaken. Finally condensation products have always been collected when formed and stored for possible further study.

Evaluation of final pressures.

From the first results of the hydrogen-oxygen detonations, it appeared that the final pressures in the

detonation train depend very strongly on the initial mixture composition. In particular it seemed that near the limits final pressures have a similar relation to mixture composition as the rapidly changing detonation velocity. Final pressures have been recorded as it was hoped that evaluation of such data would reveal something about the nature of the reaction mechanism in detonation waves. Particularly interesting is the change of this mechanism with composition variation and breakdown of the supporting reaction at the detonation limits.

The final pressure over the whole of the detonation train is recorded on the manometer fitted to the end of the timing section of the tube. To calculate from these figures the final pressure of the test mixture, a number of corrections have to be applied, since the true final pressures in the priming and test sections of the tube are averaged over the volume of the detonation train. These corrections have been calculated and a formula has been derived to evaluate the proper final pressure for various circumstances. Details of this are given in appendix D.

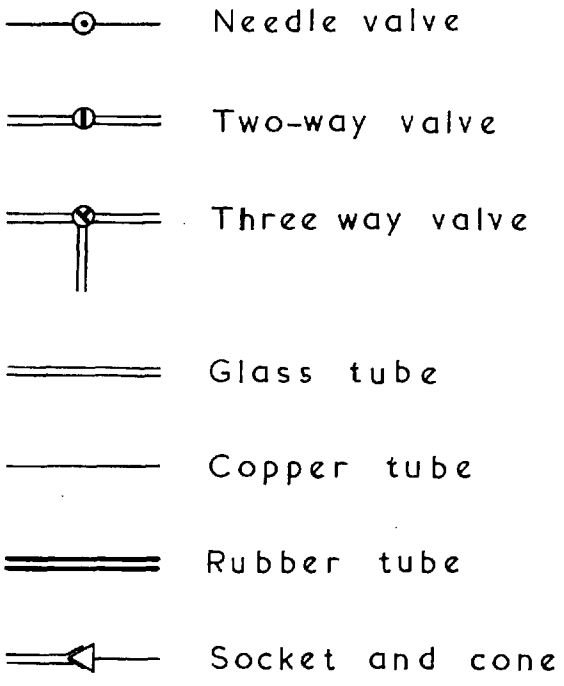
Analysis of gaseous reaction products.

A Perkin-Elmer gas chromatograph was used for the analysis of gaseous reaction products. After final pressures had been recorded, samples for analysis were collected in an

evacuated glass ampoule fitted with two three-way valves. One of these could be joined to a connection on the manometer at the end of the timing section. Through this connection samples were admitted to the ampoule. As the analysis was carried out at ambient pressure, samples had to be supplied at more than one atmosphere. Low pressure reaction products were therefore supplemented with recorded quantities of helium, which is used as carrier gas in the analysis.

Such samples can be prepared by means of the arrangement shown in figure II.9. The three-way valve which is joined to the manometer, is also connected to the vacuum line via another three-way valve on top of a helium cylinder. When gas has been sampled from the tube, through the manometer line, into the ampoule, all valves are closed and the manometer is evacuated through the two three-way valves. Helium is then let into the manometer to the required final sample pressure and subsequently also admitted to the sample. The actual final pressure of the sample is recorded for calculation of the correction factor for the concentrations found by the subsequent gas analysis.

Chromatographic gas analysis is carried out at 30° centigrade and flow rates of approximately 50 cc/sec. In all cases columns are used which have been filled with 100 - 120 mesh PORapak -Q, as supplied by Waters Associates Ltd., Stockport. Calibration has shown that these beads will




Symbols.

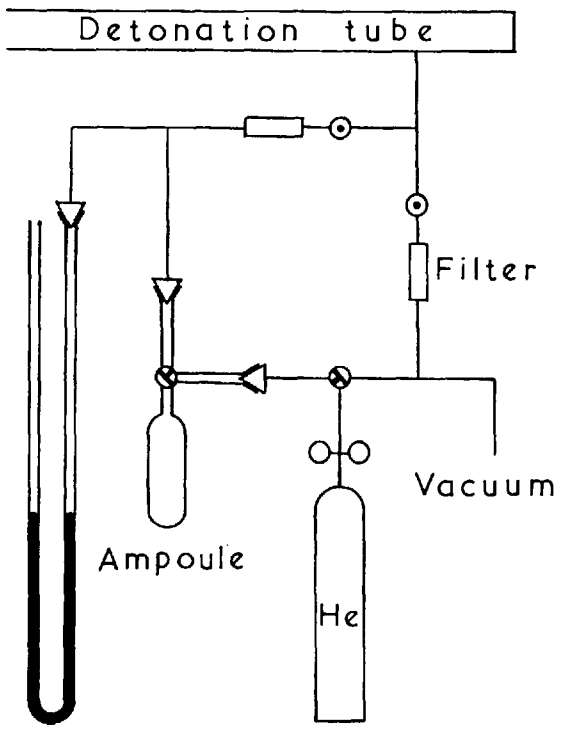



Fig. II.9. Schematic diagram of sampling apparatus for gaseous reaction products

separate all important components that are likely to be present in hydrocarbon oxidation, except carbon monoxide and oxygen. These components can be separated by a molecular sieve column, which however absorbs carbon dioxide and water irreversibly.

For routine analysis the gas samples were injected into a stabilised helium flow, which carried them through a two metres long column filled with POR-Q. This column separates samples by specific retardation into a sequence of components, related to the molecular weights. After leaving the column, the carrier gas took the components through a thermal conductivity cell. Time records of the varying output of this cell were analysed in the usual way for identification and concentration measurements of the different components. Calibration of this arrangement for normal flow conditions indicated a difference in retardation between carbon monoxide - oxygen mixtures and carbon dioxide of approximately three minutes, the carbon dioxide having the longest residential period in the two metre column.

This difference made it possible to check on the presence of either carbon monoxide or oxygen by inserting a parallel arrangement of a one-metre POR-Q column and a two-metre molecular sieve (Perkin-Elmer, DN-003), between the standard POR-Q column and the conductivity cell, as shown

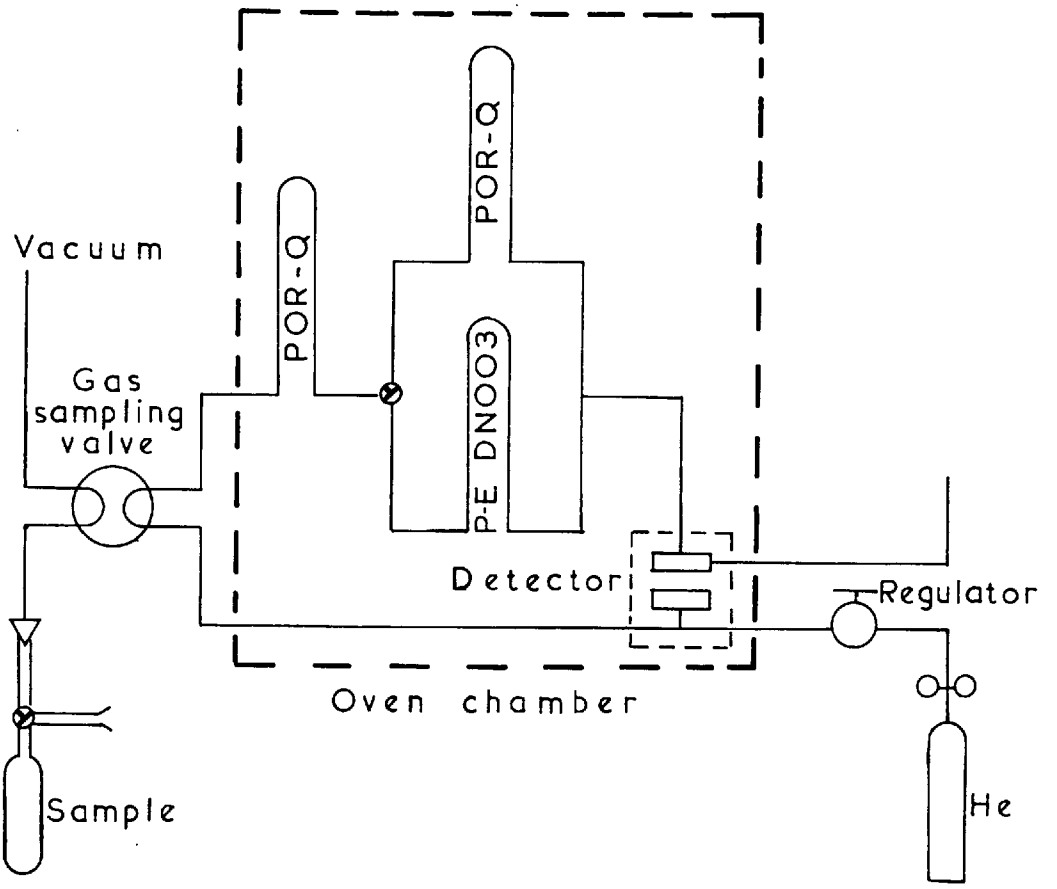



Fig. II. IO. Schematic flow diagram for gas chromatographic analysis of reaction products.

in figure II.10. Gas flow from the standard column enters this arrangement through a three-way valve. The outlets of these additional columns were connected by a T junction, leading to the conductivity cell. Before analysis, conditions in the chromatograph were stabilised with helium passing through the three-way valve into both of the two additional columns. Flow of the carrier gas was then directed from the standard column into the molecular sieve column only and after renewed stabilisation the gas sample was introduced into the carrier stream. Calibration had shown that for standard flow conditions any carbon monoxide or oxygen in the sample passed through the standard column in approximately two minutes and should within another two minutes have left the molecular sieve column and be detected by the conductivity cell. After such length of time flow through the three-way valve was quickly admitted to the second POR-Q column too, after which the molecular sieve column was closed off. The recording equipment was adjusted to compensate for changed flow conditions, while separation proceeded through the two POR-Q columns and approximately six and a half minutes after introduction of the sample, any carbon dioxide present was detected by the conductivity cell.

In practice it has been found that in the analyses carried out, oxygen and carbon monoxide did not occur simultaneously in detectable quantities.

Study of condensation products.

Detailed study of solid reaction products, formed in or behind a detonation wave, can sometimes reveal information on the nature and sequence of processes that have resulted in their formation. For this reason the occurrence and appearance of condensation products has been recorded with the other results and samples of each run were collected from the detonation train with a cotton wool swab and stored in a glass ampoule. These were marked with a label to facilitate selection of samples that might become of interest for further study after a preliminary evaluation of all other results.

On this basis some samples were selected as possible representatives for different modes of solid formation from detonation processes and electron micrographs and electron diffraction patterns have been made through facilities that are available in the department.

## II. 3. Experimental procedure.

In the general procedure for preparation of the gas mixtures, the mixing of the stoichiometric hydrogen-oxygen primer followed a standard routine. Atmospheric pressure was read from the calibrated manometer of the vessel under vacuum and the needle valve to the manifold was closed.

The oxygen cylinder was connected to the extension of the manifold inlet, outside the safety screen and some gas was flushed through into the vacuum line to remove impurities. After the vacuum line had been closed off, oxygen was admitted to the manifold and subsequently to the vessel until stable ambient pressure had been attained, as indicated by equal mercury levels in the manometer. The oxygen cylinder was then replaced by a hydrogen cylinder, the manifold and lines were evacuated and purged with hydrogen. For above-ambient pressures vessels were always filled by a two stage process for safety reasons: first the pressure in the manifold was increased from the cylinder which was then temporarily shut off; subsequently the gas in the manifold was admitted to the vessel. In this way hydrogen was added to the priming vessel until twice the absolute pressure of oxygen was achieved. The final pressure was adjusted against a scale, until the total pressure was stable at 3 atms. The gases were then left to mix by diffusion for at least two hours. The total quantity in the vessel proved sufficient for eight to nine experiments.

Pressures to be recorded in the preparation of test mixtures were obtained more accurately by means of the kathetometer. Pressures of components for a selected mixture composition were calculated for the prevailing conditions of ambient pressure and temperature. Approximate

corresponding kathetometer readings were found from a calibration curve. The first component, usually the fuel, was then admitted to the vessel and left to settle for five minutes before pressures and temperatures were recorded. The total fuel pressure was then used to calculate to within 0.01% the pressure contribution required from the oxygen addition to reach the selected composition ratio. This calculation did not take into account the non-additivity of the partial pressures. Oxygen was subsequently admitted accordingly until a satisfactory stable pressure reading was attained. Usually about ten minutes were required before final pressures and temperatures could be recorded. From the respective pressure contributions a mixture composition quoting figures to 0.01% was then calculated. The total pressure of test mixture was usually about $2\frac{1}{4}$ atm., which was adequate for four test runs. The mixing process was accelerated by the magnetic stirrer and mixtures could be used after one hour.

Cylinders containing expensive fuel samples were connected to the capillary inlet of the test mixture vessel, before starting investigation of another gaseous system. This connection needed to be purged only once, as the cylinder could ~~not~~ remain joined to the system until experiments had been completed. Before mixtures were made, the line from the vessel to the cylinder was evacuated,

together with the vessel for about half an hour.

Also in preparation of test mixtures containing expensive fuel samples, remnants of mixtures made for other composition values were sometimes utilised in ccnsequent mixtures. Further additions of components were calculated from the known and absolute pressure of the remnant gas. To obtain the absolute pressure value, a vacuum reading was taken on the manometer of the test mixture vessel by evacuating it independently through the side connection to the manifold, see figure II.8. The absolute pressure of the remnant was the difference betweer this value and that indicated by the manometer when it was subsequently connected with the vessel.

This method was never repeated more than once for consecutive mixtures and the last mixture prepared in this way was always one in the regime of steady-state detonation. where the usual accuracy for composition is not required. For investigation of oxygen-rich detonation limits, application of this method for mixture preparation implies that fuel is added to the oxygen. The method is then not self-consistent with respect to systematical errors in the mixture composition due to the non-additivity of the partial pressures. However, as mixtures for limit investigation were, as a rule, not prepared in this way, the influence on

considerations concerning the accuracy of the determination of limits is negligibly small.

Ambient pressure readings on the manometer of the 10 litre storage vessel, independently from any gas mixture in the vessel, was also of some use when the preparation of such test mixtures required a relatively long time. Delays in operation could be caused by slow dissipation of thermal effects or by temporary condensation of fuel components on the mercury of the manometer after admission of oxygen to the vessel. If, due to such retarding influences, mixture preparation required more than half an hour, a second reading of barometric pressure at the end of mixing proceedings became necessary. Evacuation of the manometer independently from the storage vessel still removes so much of the test mixture as was contained between the three-way valve on top of the manometer and the mercury level. Such independent readings from the manometer could therefore not be made within at least half an hour of admission of the last component to the vessel. Evacuation of the manometer before the end of that period would almost certainly remove a disproportionate amount of each of the two components. In practice, the barometric pressure recorded at the beginning of mixing proceedings, was always used in calculations and the second vacuum reading was only taken to estimate how accurate the last pressure readings in preparing the mixture had been.

In the preparation of the equipment for detonation of a test mixture, the train was first thoroughly cleaned with a cotton wool plug pulled through the tube with the end plates removed. New filters were placed in the appropriate holders and probes were cleaned with alcohol and checked for resistance requirements of better than about $10^7$ ohms. Probes were then screwed into position in the wall of the tube and tested again, using the electronic equipment. The train was subsequently closed and the gate valve shut.

The vacuum pump associated with the gas mixing equipment was used to evacuate the manifold, the supply line to the priming section of the tube and the priming section. The pump at the other end of the detonation train was used to evacuate the stabilisation section and the timing section of the tube, the supply line up to the manifold, the gas sampling equipment and the manometer used for reading the final pressures. After a check on leaks had been made, pumping was continued for twenty minutes. The camera was checked for unexposed film and mounted in front of the oscilloscope screen. The hood was then closed and, as the screen of the Tektronix 555 is fluorescent, care was taken not to trigger a sweep for the last few minutes before the detonation run.

Room temperature was recorded and atmospheric

pressure was measured with the open-end manometer at the end of the timing section. All valves were then closed and, through the manifold, the gas mixtures were admitted successively to the two parts of the detonation train, adjusting the final pressure to ambient conditions by means of a short calibration scale on the closed-end manometer of the manifold. After the needle valves on the inlets to the tube had been closed, the supply lines from the manifold to the tube were evacuated as additional protection against propagation of detonation from the tube to the gas mixing and storage apparatus. The vacuum pumps and the electric motor for the stirrer in the test mixture were switched off to avoid unnecessary interference during recording.

Probe circuits were charged and the counter, oscilloscope and pressure transducer set for triggering. The plate valve was then opened, the ignition coil connected to a 12 volt battery, the door to the explosion bay was closed and the camera shutter was then opened. The sparking plug could then be fired.

After the detonation, the final pressure in the tube was measured, counter readings - if obtained - were recorded and the picture of the oscilloscope traces was developed and measured. If required, gas samples were taken for gas chromatographic analysis. Any condensation products found in the tube were collected and stored.

It is obvious that it will still be necessary to consider in detail to what extent the equipment and the experimental procedure will achieve the various requirements for accuracy and performance. These achievements will be discussed in section III.1.

## II.4. Further instrumental development.

### a. Review of possible improvements.

As can be expected, the experimental work described in this thesis has revealed a number of shortcomings of the equipment concerning the quality of its performance or efficiency. Some of these imperfections have been changed or improved between experiments and such alterations have been discussed in section 2 of this chapter as part of the present equipment. This section deals with developments, originating from experience gained in this study, but used for newer designs.

Deficiencies of the present equipment that prevent investigation of a wider or different field of detonation research will not be discussed. Alterations allowing for such development are not in the strictest sense part of this investigation. However, discussion of changes in design that would aim at improving the quality of the present

work, can be a useful contribution, even only as a critical reflection on the value of the work.

Possible alterations to the detonation train can be classified into three categories:

a. Alterations directly aimed at improvement of the reliability of information on detonation propagation, in particular in the limiting condition.

b. Alterations in the experimental conditions which will indirectly lead to more significant results.

c. Alterations that do not influence the final results, but simplify the operations and thereby improve the efficiency.

In the first category, a study of the work by Wagner [1955] and Pusch and Wagner [1962, 1965], discussed in some detail in section 1 of this chapter, shows that the influence on limits of tube diameters greater than 16 mm. is experimentally still an unknown factor and that determination of limit mixture compositions can be influenced by the length of the tube.

Another fundamental doubt concerns the use of a single line of ionisation probes for accurate velocity measurements of marginal detonation. It is known that

spinning detonation occurs near the limits and involves a rotating head and an axial tail. The wave thus describes a helical path along the tube wall and time intervals measured between two probes depend on which part of the front plane passes each probe. If two consecutive probes are both in the helix described by the spinning head, the time interval is shorter than if the second probe is only fired by the tail of the spinning wave. Basically the problem arises because a normal ionisation probe records only changes on one point of the circumference of the tube, instead of changes anywhere on that circumference.

In the present 1 inch detonation tube the fundamental requirement for a smooth bore of the detonation train is also not well fulfilled. Many investigators [e.g. Bone et al., 1936] have shown that irregularities of the tube wall promote turbulence. This favours detonation propagation and should consequently be avoided, especially in limit investigation. When the fear for disturbances supports the use of small diameters for supply and evacuation lines, the need for high pumping speeds and rapid attainment of pump inlet vacua requires high bore connections, but puts in turn high demands on valve strength.

As has been explained, high vacuum performance is not a first necessity for the present research. This is

however different from the requirement of good vacuum sealing. It has been found difficult to avoid a certain amount of leakage, which could reach rates of vacuum loss of 10 mm. mercury per hour. This problem arises from the large number of lines and seals that are part of the present system; in practice it is difficult to check all these thoroughly when vacuum loss is observed. A number of connections have been hard-soldered, which avoids a demountable joint, but might lead to cracks after a great number of test runs. These hard-soldered connections also diminish the flexibility of the system, which reduces the ease of fitting replacements or making alterations. Finally, hard-soldered joints on the inside of the tube are eroded in the long run and consequently start to cause more and more turbulence.

Wear and cavitation also affect the ionisation probes. As the number of test runs increases, the probe tips too are eroded, especially the thin Araldite insulator, which also tends to absorb water vapour. As probe performance becomes less satisfactory, the tendency is to polish up the tip of the probe with "wet and dry". If not enough is taken off, metal dust tends to fill up the araldite cavity and the probe becomes permanently conductive. If more is taken off, the probe will soon no longer be flush with the inner wall of the tube and the only solution to

extend its practical life is then to machine the body as well. This will require accurate machining of the new stem and O-ring collar, to provide the correct length and proper vacuum seal.

Some final, more practical objections against the 1-inch detonation train concern the unavoidable contamination of the tubes, lines and valves by solid condensation products and the extensive operations required to collect the deposits and to clean the detonation train for the next experiment.

In view of such considerations, attempts have been made to eliminate a number of these shortcomings and to try the improvements out in practice. For this, two designs have been made and executed.

The first design is aimed at obtaining better results from ionisation probes, especially under conditions of marginal and pulsating detonation. In line with the previous discussion of this problem, a probe has been developed which will in principle respond to changes in conductivity anywhere on the circumference of a cross-section of the tube. As this implies an increased sensitivity compared with the potential performance of the present design, the new probe, which has been built for use in a 1 inch detonation train, has been tested as trigger probe in the limit studies.

The second development is a 2 inch detonation train, made to check experimentally the influence of greater tube diameters on the position of detonation limits. For a true comparison over the range between one and two inch, the length of various tube sections and the location of probes have been made identical with the dimensions of the 1 inch tube. However, a number of alterations in detail have been made to try and improve the design with respect to some of the above mentioned shortcomings.

A detailed survey of these new designs follows below.

b. The circular probe.

Details of this probe can be seen from figure II.11. Essentially the probe consists of two separate conductors with a potential difference between them. The wires, constituting the ionisation gap in a conventional probe circuit, are wound into a tight bifiliar spiral, which lies in a circle around the inside wall of the detonation tube. Passage of a conductive explosion front anywhere across the inside of the circular spiral should in principle result in short-circuiting of the two wires.

The spiral has a diameter of 0.10 inch and is made from 28 gauge enamelled copper wire. With the aid of a

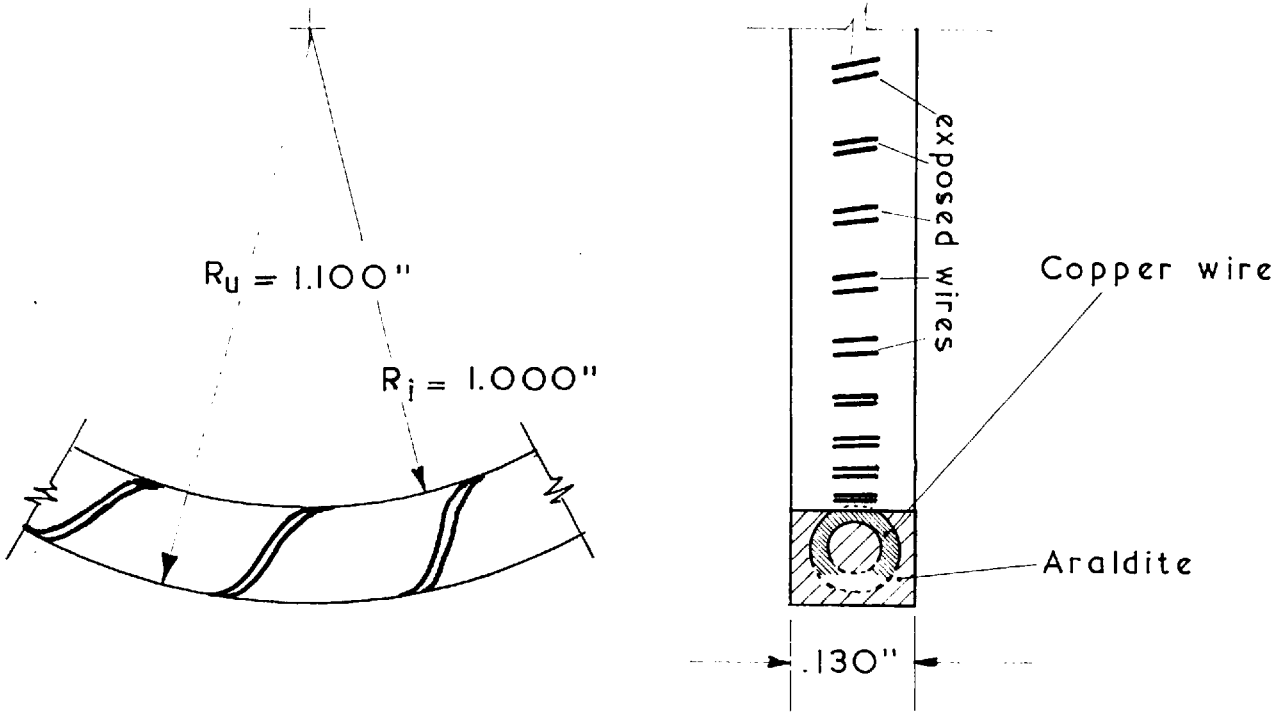
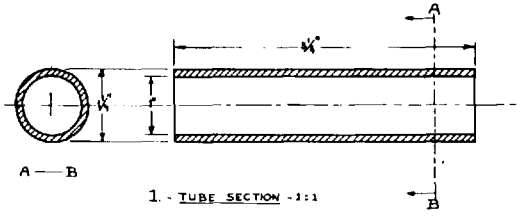



Fig. II.11. Circular probe elements

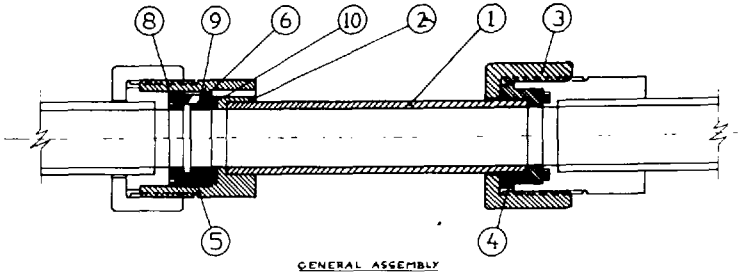
polythene mould, the spiral was embedded in a ring of araldite epoxy resin with an internal diameter of 0.99 inch. After the araldite had hardened, the width of the ring was polished down to 0.13 inch and its inside diameter was increased to 1.00 inch, which exposed numerous pairs of two short parallel lengths of bare copper wire. Care was taken not to disrupt the two wires anywhere on the inside of the ring, from which they extended to the outside.

The circular probe fits into a ring-holder, which has a 1.00 inch bore and a radial groove for passage of the probe wire ends, see figure II.12. The holder, in turn, is sealed in a cylindrical groove in the probe holder body, which is part of a short length of 1 inch tube, that fits between the stabilisation and the timing section of the 1 inch detonation train. An exit for the probe wires is provided outside the circumference of the O-rings ensuring a vacuum seal between the ring holder and the existing detonation tube.

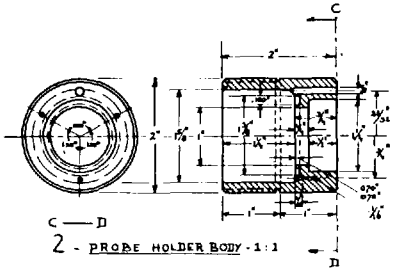
In testing this model, it was found at first try to be as sensitive as the coaxial probe used for trigger purposes in the experiments. However, the vacuum seal around the wires needed improving.



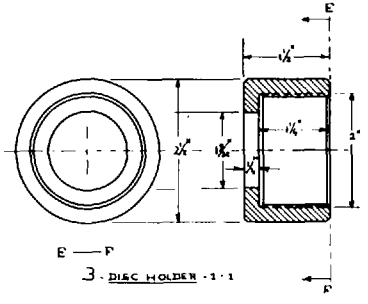

1. - TUBE SECTION - 1:1



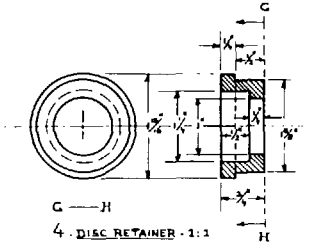

GENERAL ASSEMBLY



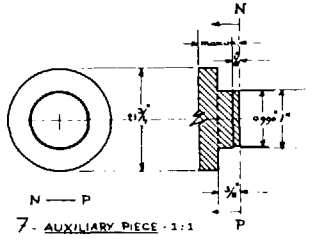

2 - PROBE HOLDER BODY - 1:1



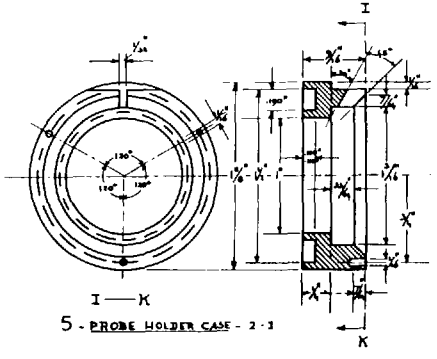

3 - DISC HOLDER - 1:1



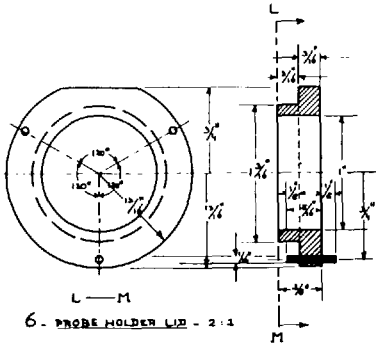

4 - DISC RETAINER - 1:1




7 - AUXILIARY PIECE - 1:1




5 - PROBE HOLDER CASE - 2:1




6 - PROBE HOLDER LID - 2:1

| Nº | Material | Remarks |
|---|---|---|
| 1 | Stainless Steel | |
| 2 | Brass | |
| 3 | " | |
| 4 | " | |
| 5 | " | |
| 6 | " | |
| 7 | Polythene | |
| 8 | Neoprene O Ring | SP 900/23 - 1¼ - 1⅞ - 1⅜ |
| 9 | " | SP 913/14 - 1⅜ - 1¼ - 8⅜ |
| 10 | " | GD 1454/7 - 1⅜ - 1⅝ - 1⅜ |

CIRCULAR IONISATION PROBE

THE HOUSE

SEPTEMBER 44

HM-IC1

AR Uttley

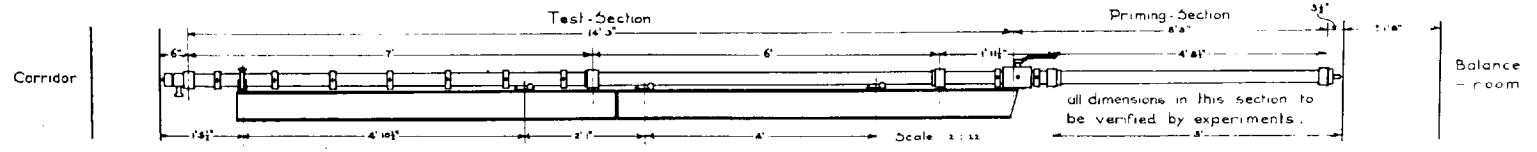
F. 11.12.

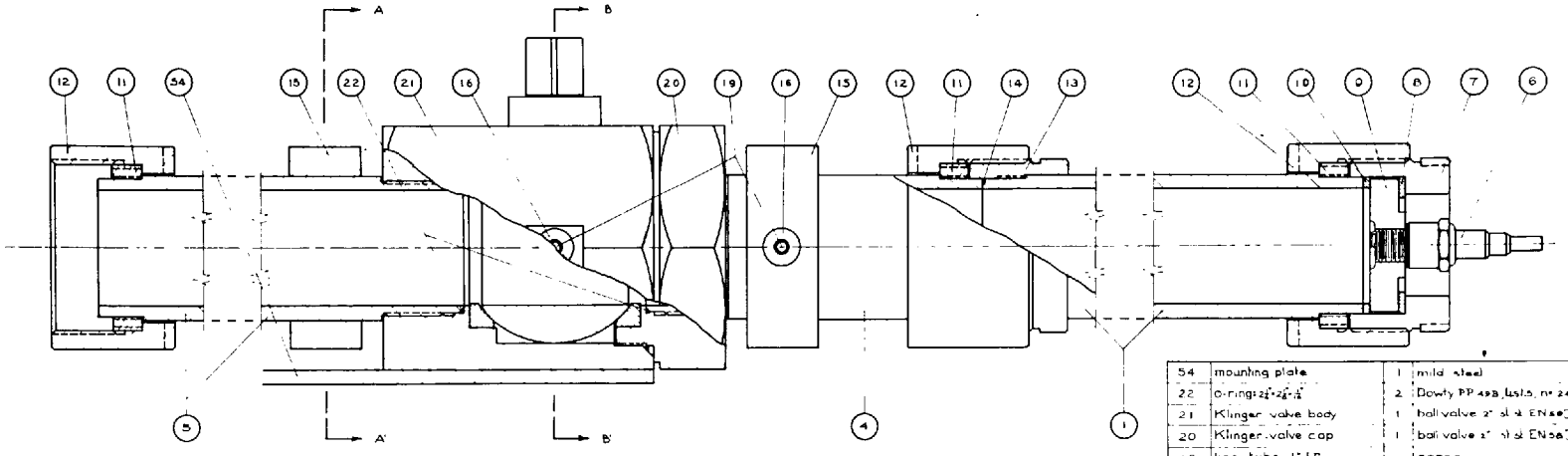
c. The 2 inch detonation tube.

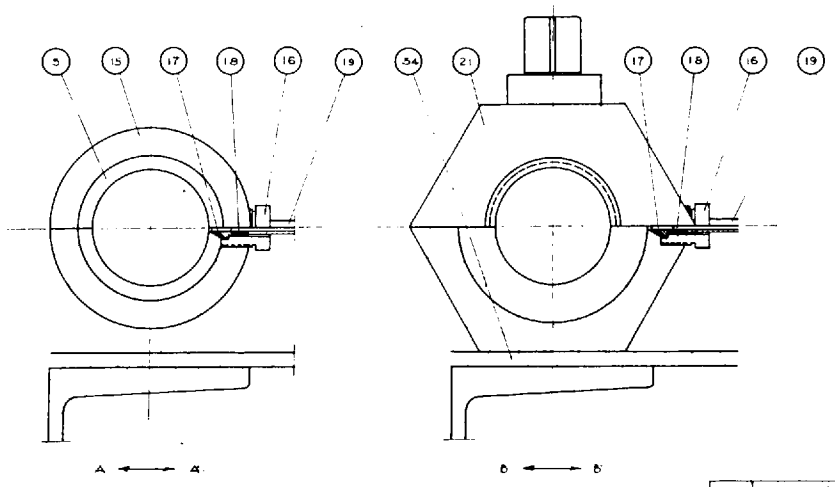
As has been pointed out, this tube has not in the first place been developed as a test bed for new designs of various details, but to obtain experimental information on diameter effects on detonation limits.

Apart from the tube diameter, the dimensions of the new train, which is shown in detail in figure II.13, a and b, are in principle identical to those of the 1 inch tube. The two tubes are installed parallel with each other; the sparking plug, valve, gas inlets, probes and vacuum connection are almost in identical positions and all the auxiliary equipment can be used for either of the two detonation tubes. However, the new train is in a more accessible position, as it is mounted on top of the channel beam, which houses the 1 inch tube between its flanges.

Although the plate valve, described by Munday [1963], has so far been most satisfactory for separation of the priming and test sections of the tube, much workshop time would have been required to make a similar valve for the new tube. For convenience a 2-inch, stainless steel Klinger ball valve was chosen instead. Short tube extensions have been fitted to the end of this valve, providing connection holes for the gas supply lines. A similar connection has been made to the valve body to allow the volume inside the ball to be




| Nº | PART NAME | REQD | MATERIAL/CHOICE | REF |
|---|---|---|---|---|
| 54 | mounting plate | 1 | mild steel | |
| 22 | o-ring: $2\frac{1}{4}$"-$2\frac{1}{8}$"-$\frac{1}{16}$" | 2 | Dowty PP 49B, list 5, nº 24 | |
| 21 | Klinger valve body | 1 | ball valve 2" st st EN58J | |
| 20 | Klinger valve cap | 1 | ball valve 2" st st EN58J | |
| 19 | line tube, $\frac{1}{4}$" ID | | copper | |
| 18 | sealing nipple | 3 | brass | |
| 17 | o-ring: $\frac{11}{16}$"-$\frac{7}{16}$"-$\frac{1}{8}$" | 10 | Dowty PP 51B list 1, nº 4 | |
| 16 | line retaining nut | 3 | brass | |
| 15 | collar | 9 | brass | |
| 14 | o-ring $2\frac{1}{8}$"-$2\frac{1}{4}$"-$\frac{1}{16}$" | 4 | Dowty PP 49B, list 5, nº 25 | |
| 13 | tube connector (male) | 3 | brass | |
| 12 | tube connector (female) | 5 | brass | |
| 11 | retaining ring | 5 | brass | |
| 10 | sealing ring | 1 | PTFE | |
| 9 | end plate | 1 | stainless steel | |
| 8 | insulating ring | 1 | PTFE | |
| 7 | end plate retainer | 1 | brass | |
| 6 | sparking plug | 1 | Champion L7 (14mm) | |
| 5 | valve extension (test side) | 1 | stainless steel EN58J | |
| 4 | valve extension (priming side) | 1 | stainless steel EN58J | |
| 1 | priming tube | 1 | stainless steel EN58J | |

Part numbers 23 till 53 incl. see HM 1C5B

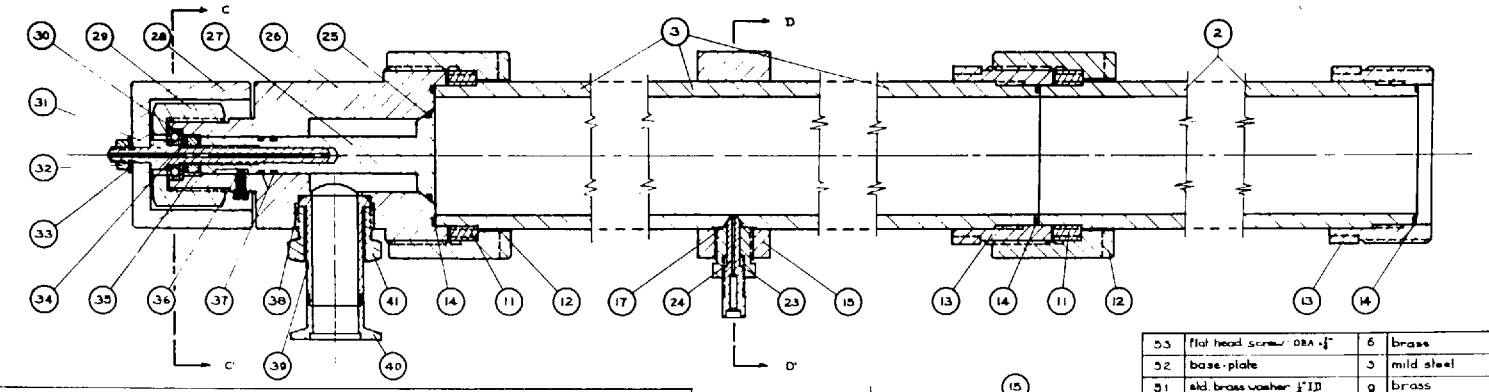
| | | | |
|---|---|---|---|
| 3 | measuring tube | 1 | stainless steel, EN 58J |
| 2 | stabilizing tube | 1 | stainless steel, EN 58J |

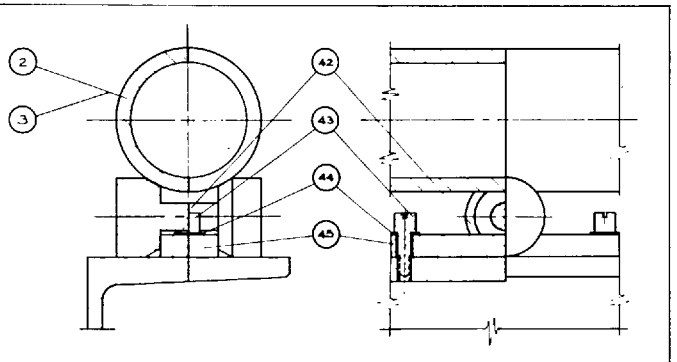
2-INCH DETONATION TRAIN
GENERAL OUTLAY
AND
PRIMING SECTION AND VALVE ASSEMBLY

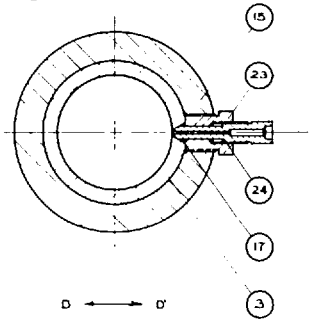
F.11.13.a.

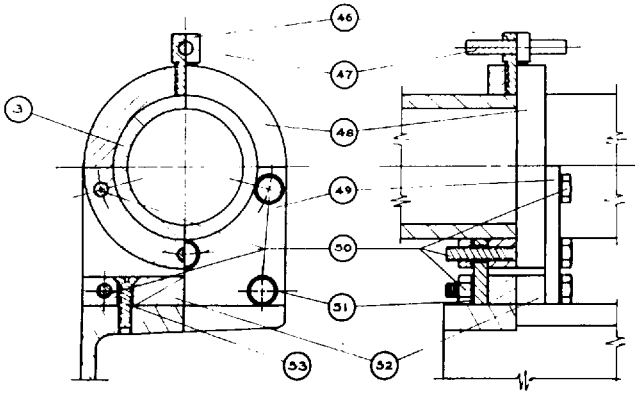
DRAWN
APPR
DATE DEC 1965
SCALE 1 : 12
1 : 1

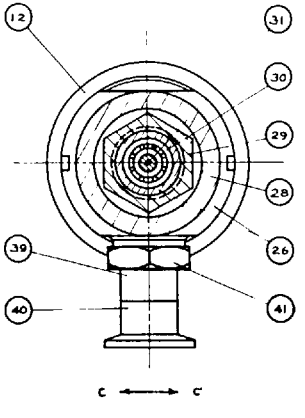
HM-1C5A




| | | | | |
|---|---|---|---|---|
| 53 | flat head screw BBA x ½" | 6 | brass | |
| 52 | base-plate | 3 | mild steel | |
| 51 | std. brass washer ¼" ID | 9 | brass | |
| 50 | bolt and nut: BSF ¼"x¾" | 9 | steel | |
| 49 | clamping support | 4 | mild steel | |
| 48 | clamping collar | 2 | brass | |
| 47 | toggle-bar | 2 | mild steel | |
| 46 | clamping screw: BSF ⅜" | 2 | mild steel | |
| 45 | rail | 3 | mild steel | |
| 44 | std brass washer: ¼" ID | 6 | brass | |
| 43 | stop screw 6BA | 6 | mild steel | |
| 42 | diabolo roller | 3 | tufnol | |
| 41 | vacuum line securing nut | 1 | brass | |
| 40 | Leybold flange connector | 1 | mild steel | |
| 39 | vacuum line connector | 1 | mild steel | |
| 38 | o-ring: ¼" x ⅛" x 1/16" | 1 | Dowty PP48B, list 3, no 12 | |
| 37 | o-ring: ⅜" x ¼" x ⅛" | 2 | Dowty PP48B, list 3, no 2 | |
| 36 | key-screw: 3BA | 1 | silver steel (hard. + temp) | |
| 35 | nut: BSF ⅜" | 1 | steel | |
| 34 | std steel washer: ⅜" ID | 1 | steel | |
| 33 | std steel washer: ¼" ID. | 1 | steel | |
| 32 | nut: Whitworth ¼" | 1 | steel | |
| 31 | valve spindle | 1 | mild steel | |
| 30 | ball-bearing 22mm OD x 8mm ID | 1 | Hoffmann, LS, MS, no 108 | |
| 29 | spindle retainer | 1 | brass | |
| 28 | valve-wheel | 1 | aluminium alloy | |
| 27 | plate-valve | 1 | stainless steel | |
| 26 | end-valve body | 1 | stainless steel | |
| 25 | o-ring: ⅜" x ⅛" x ¼" | 1 | Dowty PP 70B, list 4, no 7 | |
| 24 | probe holder | 7 | brass | |
| 23 | probe retaining nut | 7 | brass | |
| Nº | PART NAME | REQD | MATERIAL/CHOICE | REF. |

Part numbers 1 till 22 incl. and 54 ... see HM1C5A

2-INCH DETONATION TRAIN
TEST SECTION
AND
MOUNTINGS ASSEMBLY

DRAWN
APPR.
DATE : DEC 1965
SCALE 1 1

F.11.13.b.

HM-1C5B

evacuated and filled, when the valve is closed during filling procedure of the detonation tube. The valve has been fitted to a 1/4 inch mild steel plate. This plate has been screwed on top of the channel beam and constitutes the main fixing point of the new detonation train, which is also convenient in view of the stresses that might result from operating the valve.

The different sections of the tube are connected to the valve extensions. The priming section is again supported at its sealed end by a wall fixture. The stabilisation section and the timing section of the train are supported by diabolo-shaped rollers and held in position by a ring stand with a securing screw. The valve separating the vacuum line from the tube has been screwed to the end of the tube.

One of the advantages of this arrangement is the simplified procedure for cleaning the tube, as is for instance necessary when solid condensation products are formed. Handling the various tube sections in the same way as before will be quite laborious with the new equipment. The simplified procedure is to detach the sparking plug and the vacuum valve, to unscrew the connections between the tube sections and to release the clamping device on the timing section, which can then be rolled along the beam and clamped again. The stabilisation section can then be transferred

to a stand immediately in front of the beam and all three sections can be cleaned in these positions.

In other respects, too, convenience of handling has been pursued as far as possible. Fixed joints have been avoided. All connections of parts can be dismantled and vacuum seals are only provided by screw tightened O-rings. Seals in the tube wall have been reduced to a minimum number and the O ring placed as near to the inside of the tube as possible.

Flexibility is supported by standardisation of parts and threads. All dismantable couplings have been machined to within .005 inch of specified dimensions and to .002 inch of individual variations. As a result of this standardisation similar parts are interchangeable. The stabilisation section and the timing section are both an integer number of feet long and the timing section has its first and last probe at six inches distance from the ends of the tube section. Therefore, exchange of position of the timing section, which has seven probe holes at intervals of twelve inches, with the stabilisation section will allow for study of stabilisation patterns in detonation in the same way as when probes had been fitted at twelve inch intervals over the complete length of both sections. By fitting the sparking plug to the timing section, detonation

initiation can also be investigated. This is further simplified by the identical attachment to the tubes of gas inlets and probes, which are held in position by a hollow nut, screwed into a free collar around the tube.

Adequate vacuum facilities for tubes of the new dimension require much wider pumping lines than provided in the 1 inch tube and a suitable piston valve has been designed, which also acts as end plate of the detonation train. The piston is locked by a screw, running in a groove in the piston stem. The piston is driven by a spindle which can be operated by a wheel valve. Seals are provided by O rings. In the open position free passage through the valve has an area of 1.0 square inch and the straight connection line from the valve to the pump has a cross section of 0.7 square inch. The connection to the pump is made with an easily demountable Leybold fitting.

Probes have been redesigned with the purpose of obtaining a reliable model with a long lifetime, which can easily be reconditioned. The probe body consists of a long brass pin of 7/32 inch diameter with a wider head and the usual conductors down the middle. The end of the probe body is shaped like a pencil with an angle of $60^{\circ}$ and a flat tip of 3/32 inch diameter. This tip fits accurately into a 3/32 inch hole in the 1/4 inch thick wall of the detonation

tube. This hole is countersunk at 60° to a sharp edge; the outer surface of the detonation tube is machined flat at this point. In position the tip of the probe and probe body is flush with the inside wall of the tube. Probes are held in position by the thread on the other end, which is screwed into the centre of a retaining nut. As described earlier, this nut is screwed through the side of a free collar around the tube. In the fitting of a probe, the probe body must first be screwed a little way into the retaining nut and a 7/32"I.D. O-ring has to be slid over the pencil shaped end. This assembly is loosely turned into the collar, until the probe tip is in position. Then the retaining nut is loosely tightened on to the flat area around the hole, compressing the O-ring into the groove between the top of the 60° hole in the tube and the stem of the probe body which must be kept stationary. Finally the probe body and the retaining nut are both tightened at the same time.

# Chapter III. EXPERIMENTAL RESULTS.

## III.1. Instrument performance.

In the previous chapter design aspects of the equipment have been discussed in detail. Particular attention has been paid to the requirements that have led to the choice and construction of the equipment described. Before the experimental results are presented and discussed a critical survey will be made of the extent to which these requirements are achieved. For this survey it will be necessary to refer to some of the experimental results that are presented later in this chapter.

### a. The accuracy of the mixture compositions.

Compositions of gas mixtures are calculated from the individual pressure increases indicated by the manometer after admission of each mixture component. It is assumed that the ratio of each of these pressure increases to the total pressure of the gas mixture represents the fraction of each component in the gas mixture.

In view of the requirements to prepare test mixtures with a reproducibility of 0.05 - 0.01% (cf. section II.1.c) possible errors in the standard method of composition calculation must be carefully investigated.

In the first place the extent of non-additivity of partial pressures in gas mixtures should at least be evaluated for the important limit compositions to detonation as have been found in this study for various gaseous systems. The systematical errors connected with the preparation of gas mixtures in the apparatus described are also to be considered. Finally the influence of accidental disturbances during mixing operations should be estimated.

The deviation from the behaviour of ideal gases in mixtures of dissimilar molecules under conditions where only two-body interaction is to be considered, is given by

$$\frac{\Delta PV}{PV} = x_1 x_2 \, (2B_{12} - B_{11} - B_{22})$$

PV is the pressure-volume product for a mole of gas mixture, evaluated from the component properties under the assumption of ideal gas behaviour; $x_1$ and $x_2$ are the mole fractions of the two gases and the B values are the second virial coefficients for the gas mixture and its components. For values of x, the uncorrected experimental composition fractions of the gas mixtures can be used. Second virial coefficients are available for many pure gases, for which they have been evaluated from isotherm measurements. However, extremely little information is as yet available on B values for gaseous mixtures. Under the present

circumstances only two approximation methods can be used to obtain at least some estimate for the extent of the corrections that are to be applied to the present composition values.

For the first method, the systems that are investigated in this work are compared with the few systems for which experimental information is available in the literature. Michels and Boerboom [1953] measured the volume change on mixing equal amounts of two different components under constant pressure for a small number of gases. In appendix A , part 1, the comparison is worked out in some detail and estimates are made for corrections to be applied to the detonation limit compositions of the hydrogen-oxygen system and hydrocarbon-oxygen systems. The estimates are also plotted for the complete composition ranges and indicate corrections in percentage of mixture for respectively the hydrogen-rich and the hydrogen-poor limit of $-0.5 \times 10^{-3}\%$ and $-10^{-2}\%$ hydrogen. For the hydrocarbon-oxygen detonation limits the corresponding figures are approximately $+5 \times 10^{-2}\%$ and $+1.5 \times 10^{-2}\%$ hydrocarbon. The difference in sign of the corrections is not due to dissimilar behaviour of hydrogen compared with the hydrocarbons, but results from the reversed order in which fuel and oxygen were admitted to the mixing vessel in the two cases.

A second and more reliable method is to consider the compressibility behaviour of the gas mixture on the principle of the corresponding states and to calculate values for $B_{12}$ from fundamental data for the components. The principle of this method is described in appendix A , part 2.

Other systematical errors to be considered for the standard procedure in mixture preparation are concerned with the change of volume of the storage vessel. This is caused by displacement of the mercury in the manometer and the expansion of the storage vessel with increase of gas mixture pressure. A non-systematic cause for vessel expansion is the change of temperature, which has also a much more pronounced effect on the volume of the gas and, to a smaller extent, on the volume of the mercury. Finally the accuracy must be considered which is attainable when determining mercury levels in the manometer with the use of the kathetometer. All these factors are considered in detail in appendix B , part 1, and the results of these calculations are expressed as a correction to the fuel percentage.

Comparison of all correction factors with the requirement of mixture reproducibility of 0.05 - 0.01% of total composition, reveals that only three types of possible errors should be taken into account. These are : the non-additivity of partial pressures in mixing, the volume increase

of the vessel due to mercury displacement in the manometer and the expansion of the gas mixture by a temperature increase of 0.3°C, due to compression of the mixture on addition of the second component. The corrections for the first admitted component as function of the percentage in the final mixture are shown in figure III.1. It should be noted that the correction for the hydrogen-oxygen system gives a negative correction for hydrogen percentages below 50%, as it was admitted to the vessel as second component. Also shown are the overall corrections for both the hydrogen-oxygen system and the hydrocarbon-oxygen system. As can be seen the overall correction for all detonable mixtures is never greater than 0.06% of total composition under the present assumptions for the extent of non-additivity of partial pressures. It is also shown that dissipation of compression heat to final gas temperatures less than 0.3°C from the temperature of the first component will reduce the overall error considerably as the combined error contributions from other sources tend to cancel out.

A similar error calculation has been carried out for the stoichiometric hydrogen-oxygen primer. Details of this estimate can be found in appendix B, part 2. A consistent error of +0.16% of hydrogen has been evaluated, and the real priming mixture is therefore (66.8% $H_2$ + 33.2% $O_2$).

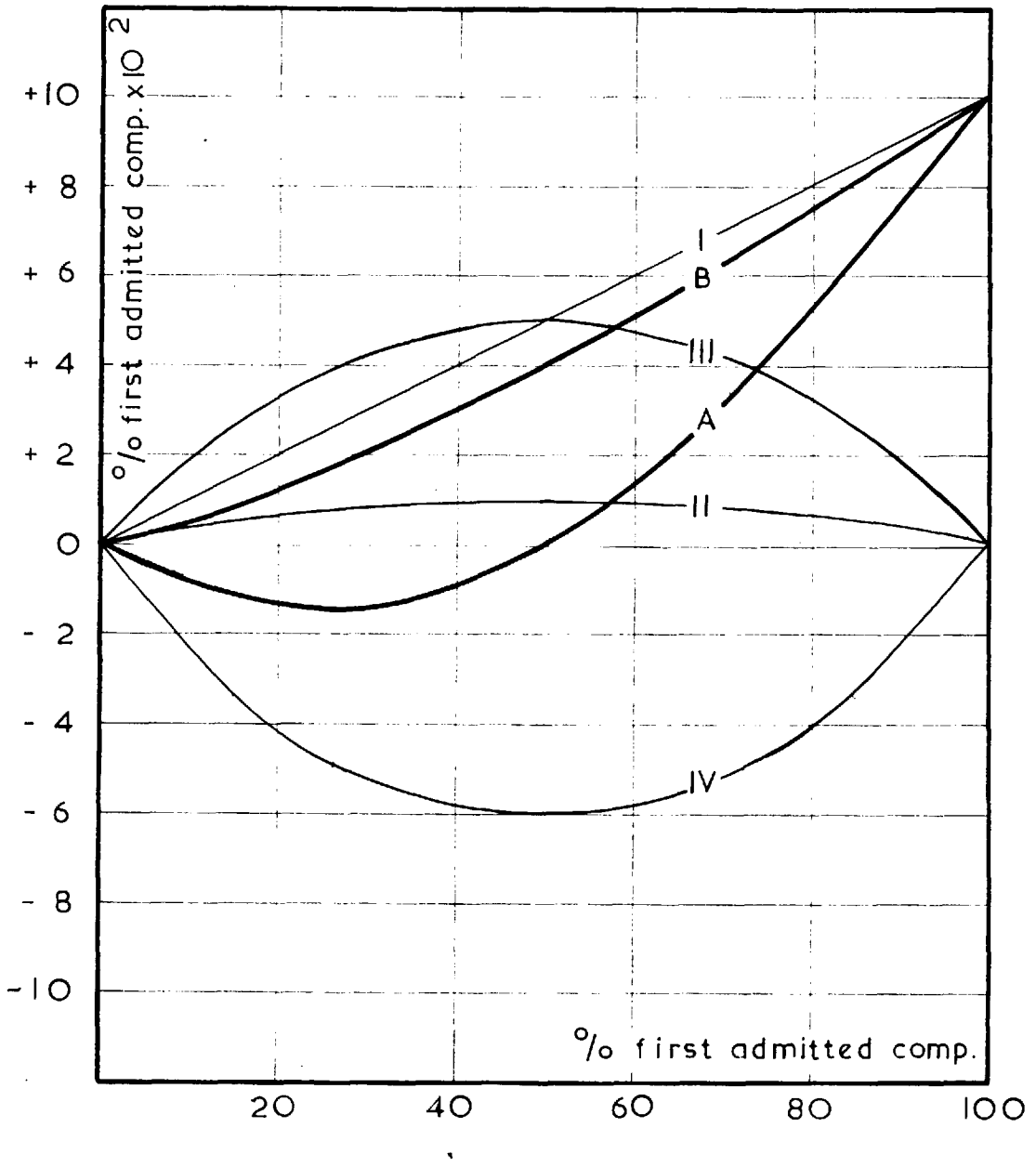



Fig.III.1. The correction for the first admitted test mixture component in percentage of mixture as function of mixture composition. (A) for $H_2 - O_2$; (B) for $C_nH_m - O_2$. (I) for thermal expansion, $\Delta T = 0.3^{\circ}C$; (II) for non additivity of partial pressures in $H_2 - O_2$; (III) id. for $C_nH_m - O_2$; (IV) for mercury displacement in manometer.

b. Experimental conditions.

Verification of the existence of proper experimental conditions in the detonation train is possible through information from two experimental investigations, only partly related to the present study.

The first reference concerns an experiment carried out by Miles et al. [1962] and is useful for ascertainment of proper stabilisation of detonation, prior to velocity recording. A 1-inch detonation tube of identical length to the present detonation train was fitted with timing probes at 12-inch intervals over the full length of the stabilisation section. In figure III.2.a record is shown, obtained for a detonation propagating from stoichiometric hydrogen-oxygen into a test mixture of 83.17% hydrogen and 16.83% oxygen. As can be observed, stabilisation to a propagation velocity of (3511 $\pm$ 2) metres per second from an impact velocity of approximately 2850 metres per second was in this case achieved within a distance of five feet. In the present arrangement this situation leaves another six feet to the first timing probe.

The second confirmation of proper experimental conditions results from investigations into the time dependence of detonation initiation by spark ignition. In

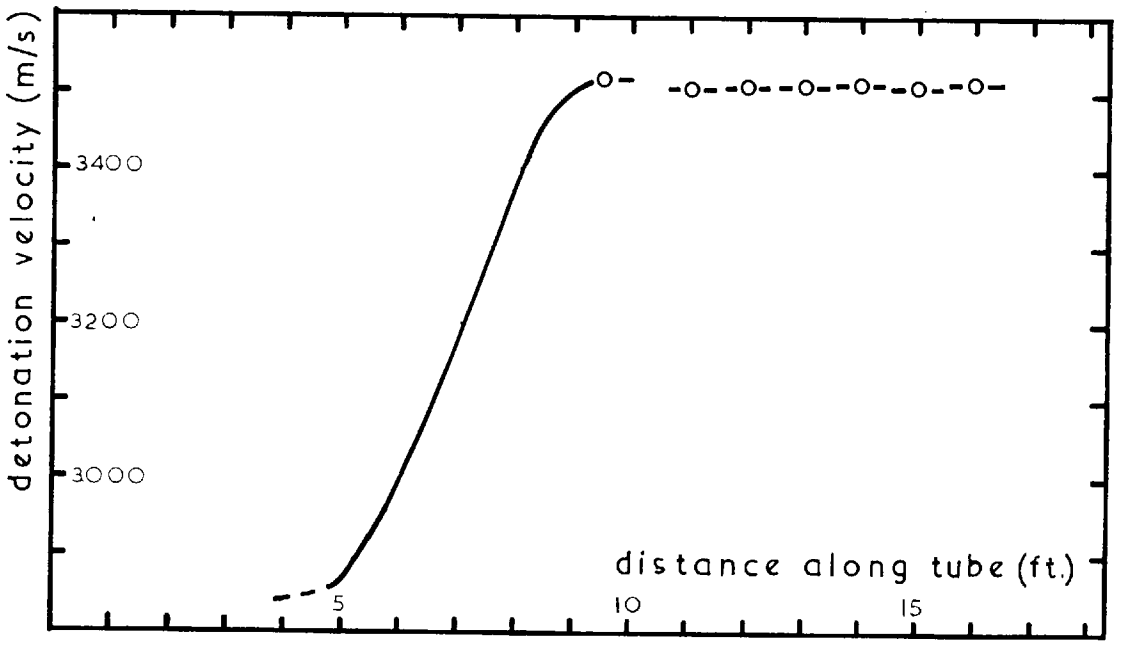



Fig. III. 2. Measured velocity for 83.17 $H_2$ + 16.87 $O_2$.

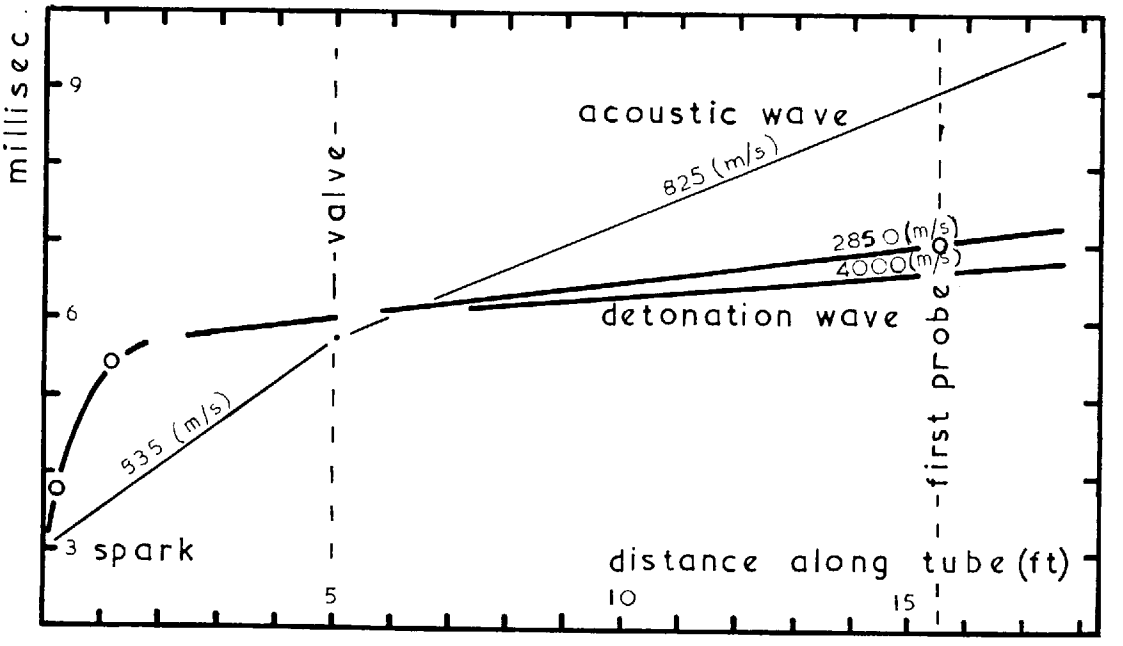



Fig. III. 3. Time dependance of detonation initiation.

the course of these experiments, which are discussed in some detail in appendix C , some of the results have been used to evaluate the relative positions of precursing disturbances and the accelerating or stabilised detonation front. A characteristic result of an evaluation of the situation in the 1-inch detonation tube is shown in figure III.3. As can be seen, the detonation train is apparently sufficiently long to guarantee that the detonation wave propagates through an initially undisturbed medium in the timing section of the tube.

c. The accuracy of recorded results.

Tables of results, presented later in this chapter, record the mixture composition, the overall pressure change in the test mixture due to detonation and the detonation velocity. The accuracy of the quoted mixture composition has been dealt with in section III.1.a; accuracies of the other data are discussed here.

In appendix D , part 1, the formula for the calculation of the final pressure of the test mixture has been derived. At the same time the propagation of errors through the calculation has been considered, resulting in a calculated uncertainty in evaluated final pressures of $\pm 1.8\%$. This percentage, however, is certainly too high as it

represents the integral sum of the values of all possible errors; reductions by application of the standard deviation rule has not been incorporated.

To test the accuracy of the formula for the calculation of the true final pressure, calibration experiments have been performed for final test mixture pressures of 0, 1 and 2 atmospheres. The investigation, which is discussed in part 2 of appendix D , shows that the mean practical error over eight experiments was $\pm$ 1.4 mm. mercury and over seven out of eight experiments $\pm$ 1.1 mm. mercury.

As the pressure change is expressed as the ratio of the true final pressure over the initial pressure of the test mixture

$$p_u = \frac{P_u}{P_i}$$

the uncertainty in p is the sum of the relative errors. The error in $P_i$ has been shown to be $1.3 \times 10^{-3}$ (appendix B , part 1). For $P_u$ the relative uncertainty depends on the value of $P_u$. For 1 atmosphere, the relative uncertainty is

$$\Delta = \frac{1.4}{760} \approx 1.8 \times 10^{-3}$$

For respectively 14, 140 and 1400 mm. mercury the uncertainty is $10^{-1}$, $10^{-2}$ and $10^{-3}$. The relative uncertainties of both pressures for various values of $P_u$ are shown in figure III.4, together with the resulting uncertainty in the pressure change $p_u$.

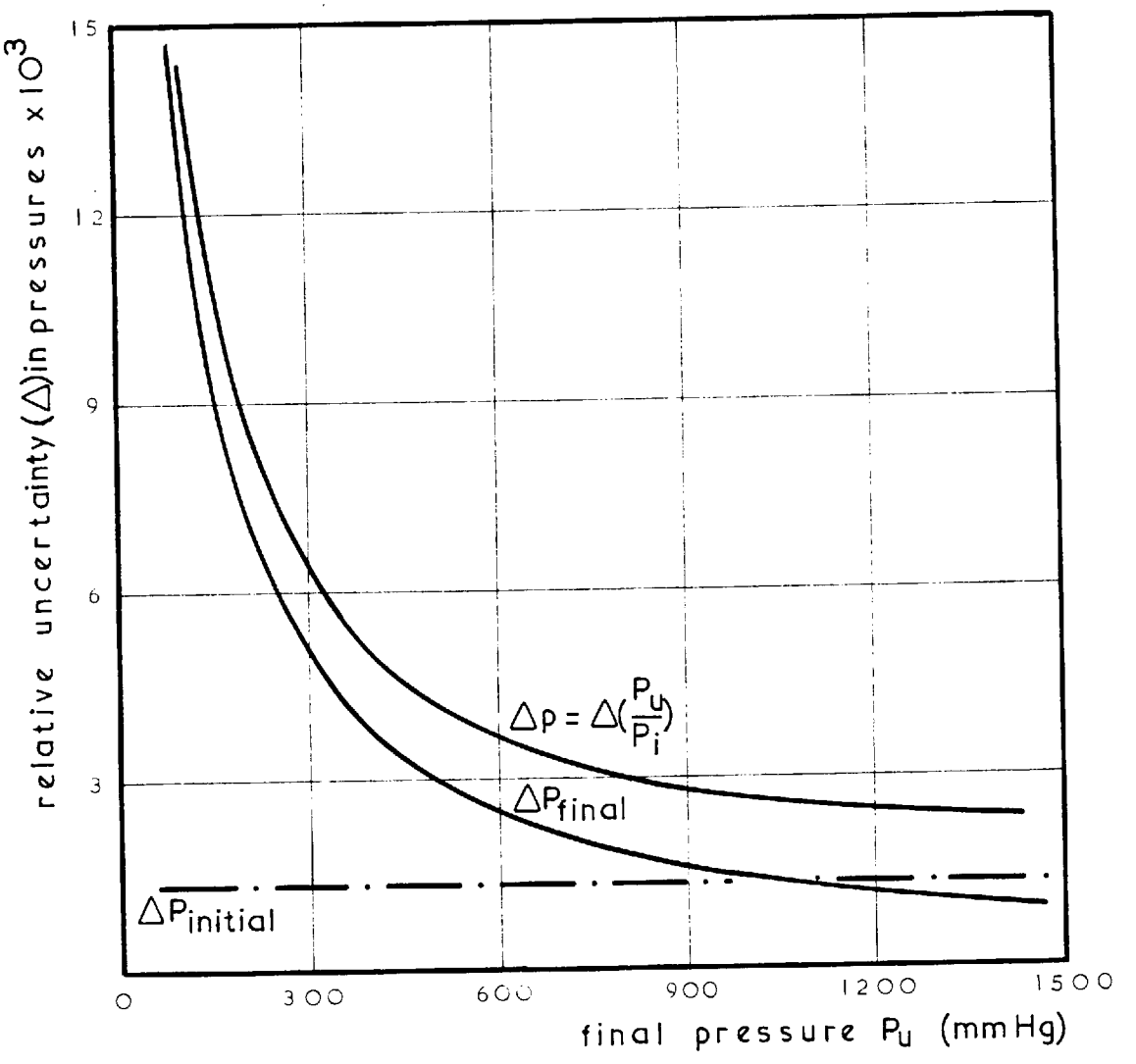



Fig. III.4. Relative uncertainty of pressure data.

In the determination of detonation velocities, time intervals measured with the counter can be shown to have an accuracy of ± 1 microsecond. For measurements of detonation propagation over fixed distances, the absolute uncertainty in the evaluated velocities increases with the speed of the detonation front. For probe intervals of twelve inches, as used in the present investigation, actual uncertainties in velocities, rounded off to integer metres per second, are tabulated in appendix H. part 2.b.

Under steady-state conditions of detonation propagation, fluctuations in detonation velocities should not be greater than approximately one metre per second. In the tables in sections III, 3,4 and 5, the fluctuations are recorded only so far as they extend outside the systematic error of measurement, which for detonation velocities between 1 and 4 km/sec. ranges from 5 to 50 m/sec. (cf. table in appendix H ). Consequently, under steady state conditions, fluctuations should be quoted as ± 0 m/sec., unless other disturbing factors occur. As can be observed this requirement is generally satisfied in all the tables concerned.

Finally the accuracy of the gas chromatographic analysis must be considered briefly. Gas samples have been measured by means of the manometer at the end of the

detonation tube. It follows from the various discussions on the accuracy obtainable with this arrangement, that sample composition can be evaluated more accurately than is required for attainment of the optimal analysis of 0.1% of composition, quoted for the gas chromatograph.

III. 2. Gas purity.

Gases used in the experiments are normally of 99% purity or better.

Hydrogen and oxygen are supplied in commercial cylinders and respectively of 99.9% and 99.5% purity. Impurities are CO, $CO_2$, $N_2$, A and Ne; water vapour content in hydrogen is not higher than $200/10^6$ to $1000/10^6$.

Hydrocarbons for the test mixtures have been obtained through Cambrian Chemicals Ltd., London, from stock of The Matheson Company, Inc., New Jersey, U.S.A., in "Instrument Grade". For methane, ethane and neo-pentane (2.2-dimethylpropane) this is specified as 99% purity, for propane and n-butane as 99.5%. Main impurities in these samples are other hydrocarbons; amounts of hydrogen impurities are stated as "negligible".

Natural Grade propane, as obtained from Shell and used for studying the effect of impurities, is approximately of 96% purity, with up to 3% ethane and/or ethylene and up to 1% methane. Hydrogen impurity is not known.

## III. 3. The hydrogen - oxygen system.

Representative data on recorded values for mixture composition, detonation velocities and overall pressure changes are given in table III.1. All measurements have been repeated at least twice. Whenever appreciably different results have been obtained for identical mixture compositions, the extremes are quoted. The results have been supplemented with some data of previous work in a 1-inch detonation tube on this system. [Miles et al. 1962]. The relevant information is marked with (+).

Mixture compositions are indicated by percentage of hydrogen. These percentages are calculated without the application of the various corrections, discussed in section III.1.a.

Velocities are expressed as the mean of values calculated from time intervals between consecutive signals from the four timing probes, as recorded by the counter or analysed from photographic records of the oscilloscope display. Fluctuations are given as maximum deviations outside the error of measurement, as explained in section III.1.c. For steady-state conditions these fluctuations can be neglected, but they become significant in approaching the composition regions of marginal detonation.

Table III.1. Detonation velocity and overall pressure change for the system hydrogen - oxygen.
(+ : results by Miles et al., [1962]).

| % $H_2$ | Mean velocity and fluctuations (m/s) | Pressure change | Notes (see foot-note) |
|---|---|---|---|
| 15.89 | 691(+40,-52) | 0.792 | |
| | 1431(+22,-52) | 0.785 | |
| 16.97 | 1455(+19, -9) | 0.775 | |
| | 1782(+67,-123) | 0.772 | |
| 17.73 | 1467(+22,-14) | 0.768 | |
| 18.66 | 1512(±38) | 0.749 | |
| | 1466(+60,-27) | 0.750 | |
| 19.17 | 1507(±0) | 0.745 | |
| | 1524(+83,-56) | 0.743 | |
| 19.67 | 1533 | 0.753 | |
| | 1600(+79,-193) | 0.741 | |
| 20.47 | 1538(±12) | 0.725 | |
| | 1572 | | |
| 24.89 | 1720(±0) | | (+) |
| 25.42 | 1738(±0) | 0.654 | |
| 30.54 | 1871(±0) | 0.569 | |
| 31.13 | 1871(±0) | | (+) |
| 38.29 | 2067(±0) | | (+) |
| 44.18 | 2177(±0) | | (+) |
| 51.61 | 2357(±0) | | (+) |
| 60.35 | 2625(±0) | | (+) |
| 66.67 | 2845(±0) | | (+) |
| 68.47 | 2889(±0) | | (+) |
| 76.20 | 3158(±0) | | (+) |
| 83.17 | 3511(±0) | | (+) |
| 84.82 | 3589(±0) | | (+) |
| 86.75 | 3660(±0) | 0.573 | |
| 87.30 | 3675(±1) | 0.633 | |
| 88.95 | 3707(+63,-31) | 0.691 | |

contd.

| % $H_2$ | Mean velocity and fluctuations(m/s) | Pressure change | Notes |
|---|---|---|---|
| 89.96 | 3768(±46) | 0.727 | |
| | 3721(±0) | 0.728 | |
| 90.43 | 3690(±0) | 0.729 | |
| | 3768(±46) | 0.735 | |
| 90.62 | 3785(+129,-63) | 0.722 | |
| | 3633(+139,-273) | 0.730 | |
| 90.77 | 3683(+340,-287) | 0.731 | |
| | 3783(+80,-16) | 0.732 | |
| 91.13 | 2630(+72,-166) | 0.754 | |
| 91.19 | 2405(±324) | 0.756 | |
| | 2608(±420) | 0.754 | |
| 91.45 | 2856(+167,-244) | 0.767 | |
| | 3655(±22) | 0.771 | |
| 91.83 | 3590(±43) | 0.590 | |
| 92.00 | 2825(±740) | 0.783 | |
| 92.46 | 3336(±55) | 0.794 | |
| 92.84 | 1930(±75) | 0.809 | |
| 93.06 | 1205(+310,-270) | 0.929 | |
| | - | 0.918 | F |

Notes: Velocity fluctuations are quoted as maximum deviations about the mean, outside the error of measurement.

The following notations have been used :

(+) : see table heading.

* : soot cloud, no collectable quantity deposit.

** : up to 1 cc. deposit per litre initial gas mixture.

*** : up to 4 cc. deposit per litre initial gas mixture.

**** : over 4 cc. deposit per litre initial gas mixture.

R : secondary detonation wave propagating backwards after reflection of primary wave from end plate of the tube.

F : recording failed.

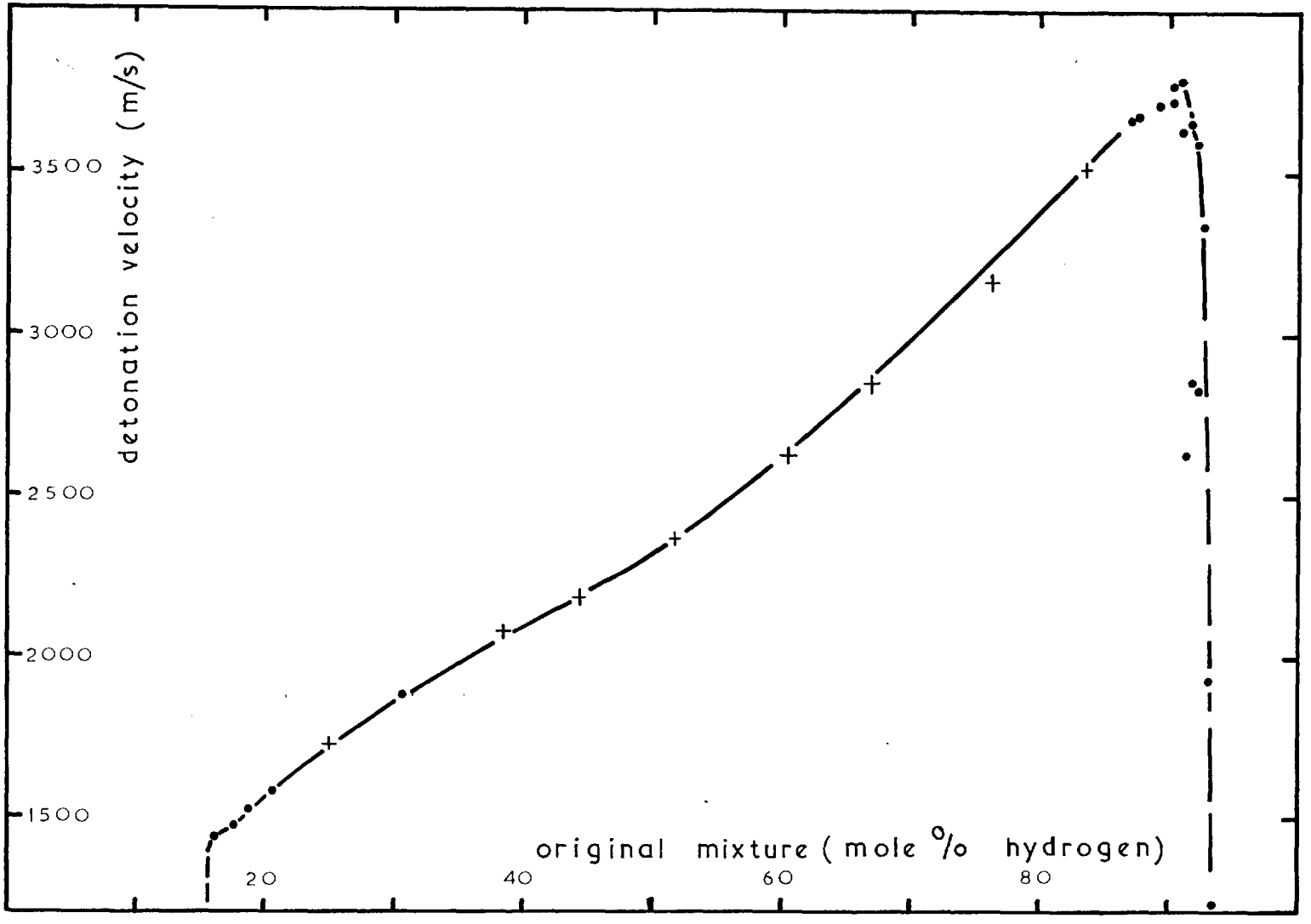



Fig. III.5. Detonation velocities for the system hydrogen-oxygen. (•), (+).

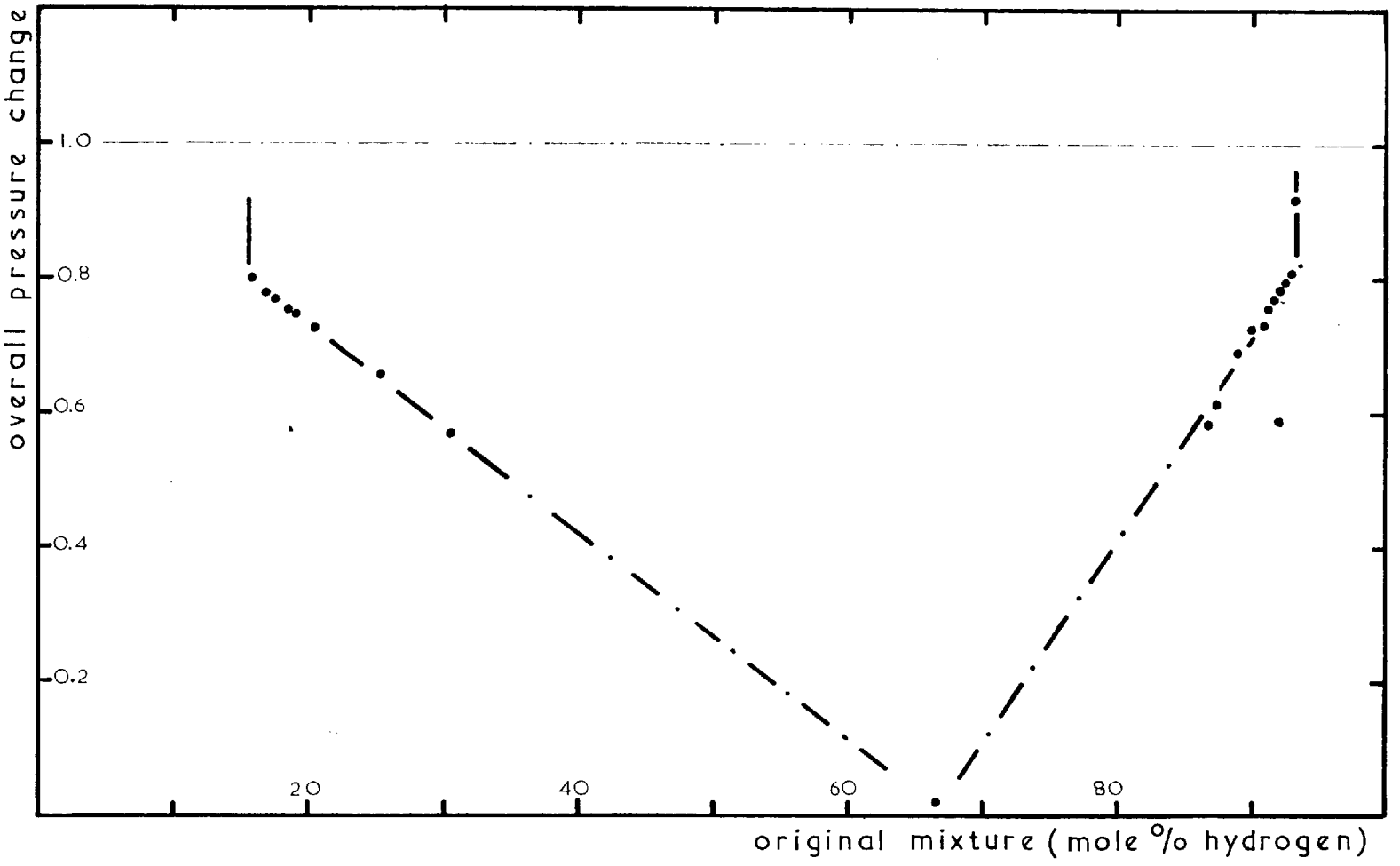



Fig. III.6. Overall pressure change in detonation of the system $H_2 - O_2$.

The experimental relation between detonation velocity and mixture composition is also shown by the curve in figure III.5. As can be seen, the correlation between the results of Miles and those of the present study is satisfactory.

Near both composition limits of detonation in hydrogen-oxygen mixtures, systematic deviations from the regularly inclined slope in the velocity curve occur. These deviations extend over approximately three percent of the total composition range inside the limit. Deviations are particularly strong near the hydrogen-rich limit, where velocity variations of almost one thousand metres per second or 25% have been recorded.

Calculated final pressures are also shown in figure III.6. Linear extrapolation of the values on both sides of the detonation regime shows a sharp intersection of the two lines at 66 - 67% hydrogen, indicating a minimum final pressure at the stoichiometric mixture composition. For this intersection the value of

$$p_u = \frac{P_u}{P_i} \approx 0.025.$$

If $P_i$ = 760 mm. mercury, $P_u$ equals approximately 19 mm mercury column, which is the vapour pressure of water at 21.3°C and would confirm the complete conversion of the gaseous mixture to water.

## III. 4. Systems of saturated aliphatic hydrocarbons and oxygen.

Results from the investigation of detonation in mixtures of oxygen and respectively methane, n-propane, n-butane and neo-pentane are given in tables III.2 to III.5. The method of recording is identical to the procedure for the hydrogen-oxygen system. For propane-oxygen detonations (table III.3) additional experiments have been performed near the fuel-rich limit with propane, containing 4% impurities. n-Pentane-oxygen detonations have also been undertaken near the oxygen-rich limit with vapour from a 99.98% pure sample of liquid n-pentane; results of these experiments are included in table III.5. Data from these additional investigations are again marked with (+) in the tables.

The detonation velocities for all hydrocarbon-oxygen mixtures investigated are also recorded in figure III.7. For comparison the results of similar investigations by W.Schuller [1954] on ethane-oxygen mixtures have been added. Values for the velocities from these experiments have been collected in appendix G, table 1, for further comparative study.

The remarkable character of the detonation velocity curves near the composition limits is as pronounced in these hydrocarbon-oxygen curves as in those for hydrogen-oxygen

Table III.2. Detonation velocity and overall pressure change for the system methane - oxygen.

| $\%CH_4$ | Mean velocity and fluctuations(m/s) | Pressure change | Notes (see table III.1) |
|---|---|---|---|
| 8.20 | 1359(+407,-200) | 0.866 | * (grey); R |
| 8.25 | 1583(+145,-299) | 0.862 | * (grey); R |
| | 1447(+23,-52) | 0.862 | * (grey); R |
| 8.34 | 1818(+77,-54) | 0.861 | |
| | 1663(±90) | 0.859 | |
| 8.65 | 1716(+254,-122) | 0.856 | |
| | 1613(+27, -7) | 0.853 | |
| 9.72 | 1682(+13,-24) | 0.839 | |
| 13.31 | 1837(+11, -0) | 0.764 | |
| 16.81 | 1968(±0) | 0.703 | |
| 26.77 | 2226(±0) | 0.509 | |
| 33.31 | 2402(±0) | 0.387 | |
| 45.12 | 2607(±0) | 0.842 | |
| 50.00 | 2640(±0) | 1.079 | |
| 53.31 | 2592(+15,-7) | 1.270 | |
| 54.92 | 2535(+7,-14) | 1.358 | |
| 55.64 | 2501(+21,-0) | 1.397 | |
| 55.96 | - | 1.109 | F |

Table III.3. Detonation velocity and overall pressure change for the system propane - oxygen.

| $\%C_3H_8$ | Mean velocity and fluctuations (m/s) | Pressure change | Notes (see table III.1) |
|---|---|---|---|
| 2.42 | - | 0.985 | + ; F |
| 2.56 | 1454(+49,-28) | 0.930 | + |
| 2.70 | 1503(+70,-84) | 0.929 | + |
| 3.03 | 1598(+70,-95) | 0.928 | + |
| 3.24 | 1613(+18, -7) | 0.921 | + |
| 3.46 | 1617(+23,-11) | 0.918 | + |
| 3.61 | 1646(+21,-15) | 0.908 | + |
| 4.16 | 1723(±0) | 0.895 | + |
| 5.17 | 1815(±0) | 0.866 | + |

contd.

| %$C_3H_8$ | Mean velocity and fluctuations(m/s) | Pressure change | Notes |
|---|---|---|---|
| 10.14 | 2108(± 0) | 0.724 | + |
| 15.14 | 2328(± 0) | 0.582 | + |
| 20.21 | 2494(+7,-14) | 0.752 | + |
| 25.00 | 2602(± 0) | 1.220 | + |
| 29.07 | 2618(± 0) | 1.672 | * |
| 30.06 | 2608(± 0) | 1.688 | + * |
| 30.97 | 2607(± 0) | 1.884 | * |
| 33.97 | 2532(± 0) | 2.189 | ** |
| 35.03 | 2480(± 0) | 2.271 | + ** |
| 35.16 | 2480(± 0) | 2.339 | ** |
| 36.55 | 2389(+13,-6) | 2.355 | + ** |
| 37.02 | 2346(± 0) | 2.366 | + ** |
| 37.55 | 2299(+12,-6) | 2.377 | + *** |
| 37.96 | 2265(± 0) | 2.330 | + *** |
| 38.89 | 2194(± 0) | 2.377 | + *** |
| 39.26 | 2163(+32,-8) | 2.365 | *** |
| 40.02 | 2111(± 0) | 2.321 | *** |
| | 2071(+18,-50) | 2.331 | *** |
| 40.11 | 2144(+35,-40) | 2.488 | + *** |
| | 2109(+24,-33) | | + *** |
| 40.71 | 2087(+78,-66) | 2.288 | + *** |
| | 2075(+0,-14) | 2.286 | + *** |
| 40.97 | 2095(+54,-34) | 2.253 | *** |
| | 2028(± 33) | 2.256 | *** |
| 41.03 | 2054(± 7) | 2.252 | + *** |
| 42.07 | 1988(± 7) | 2.232 | *** |
| 42.49 | 1857(+160,-179) | 2.238 | **** |
| 42.76 | 1173(+197,-309) | 2.048 | **** |
| 42.85 | - | 1.454 | ** ; F |

Table III.4. Detonation velocity and overall pressure change for the system n-butane - oxygen.

| % $C_4H_{10}$ | Mean velocity and fluctuations(m/s) | Pressure change | Notes (see table III.1) |
|---|---|---|---|
| 1.90 | - | 0.983 | F |
| 2.10 | 1449(± 85) | 0.945 | |
| 2.39 | 1564(+25,-16) | 0.935 | |
| 3.01 | 1661(+ 0,-3) | 0.919 | |
| 3.61 | 1713(± 10) | 0.907 | |
| 7.20 | 2047(± 0) | 0.783 | |
| 13.43 | 2370(± 0) | 0.616 | |
| 20.85 | 2592(+15,-7) | 1.303 | |
| 27.01 | 2578(± 0) | 2.140 | * |
| 31.04 | 2389(± 0) | 2.661 | ** |
| 32.64 | 2212(± 64) | 2.835 | ** |
| 34.07 | 2118(± 0) | 2.578 | ** |
| 35.34 | 2000(±20) | 2.571 | ** |
| 36.47 | 1972(+29,-43) | 2.414 | ** |
| 36.95 | 1952(+100,-122) | 2.447 | ** |
| 37.01 | 1883(+79,-141) | 2.407 | ** |
| 37.18 | 1883(+71,-80) | 2.383 | *** |
| 37.35 | 1880(+45,-38) | 2.416 | *** |
| 37.54 | 1931(+47,-68) | 2.391 | *** |
| 37.75 | 2181(±309) | 2.411 | **** |
| 37.93 | 1786(+89,-132) | 2.471 | **** ; R |
| 38.17 | 968(± 44) | 2.388 | **** ; R |
| 38.34 | 894 | 1.525 | ** |
| 38.68 | 844(+42,-27) | 2.443 | **** ; R |
| 39.09 | 551(± 22) | 1.466 | ** |

Table III.5. Detonation velocity and overall pressure change for the system neo-pentane - oxygen (+ : n-pentane).

| % $C_5H_{12}$ | Mean velocity and fluctuations (m/s) | Pressure change | Notes (see table III.1) |
|---|---|---|---|
| 1.00 | 648(± 19) | 1.003 | |
| 1.45 | 672(± 26) | 0.987 | |
| 1.50 | 1380(+37,-31) | 0.969 | |
| 1.62 | 1989(+292,-230) | 0.980 | |
| 1.65 | 1449(+124,-59) | 0.967 | |
| | 1454(+96,-80) | 0.974 | + |
| 1.75 | 1491(+91,-134) | 0.965 | |
| 1.80 | 1518(± 14) | 0.972 | + |
| 1.90 | 1516(+32,-27) | 0.955 | |
| 2.20 | 1608(+6, -3) | 0.945 | |
| 4.00 | 1875(+7, -3) | 0.872 | |
| 8.00 | 2179(+0,-15) | 0.728 | |
| 12.39 | 2415(± 0) | 0.757 | |
| 16.75 | 2570(± 0) | 1.296 | |
| 18.99 | 2600(+7,-15) | 1.676 | * |
| 21.19 | 2593(+37,-29) | 2.015 | ** |
| 23.04 | 2535(± 0) | 2.365 | ** |
| 25.04 | 2460(± 0) | 2.631 | ** |
| 26.48 | 2353(+12,-30) | 2.841 | ** |
| 27.99 | 2169(+42,-51) | 2.817 | *** |
| 29.99 | 2035(± 114) | 2.715 | *** |
| 30.96 | 2002(+46,-121) | 2.646 | *** |
| 32.20 | 2164(± 544) | 2.624 | **** |
| 32.60 | 2179 | 2.593 | **** |
| | 1898 | 2.596 | **** |
| 32.90 | 1925(+37,-87) | 2.563 | **** |
| | 1817(+656,-474) | 2.588 | **** |
| 33.04 | 1800(± 10) | 2.530 | ** |
| | 710 | 1.745 | ** |

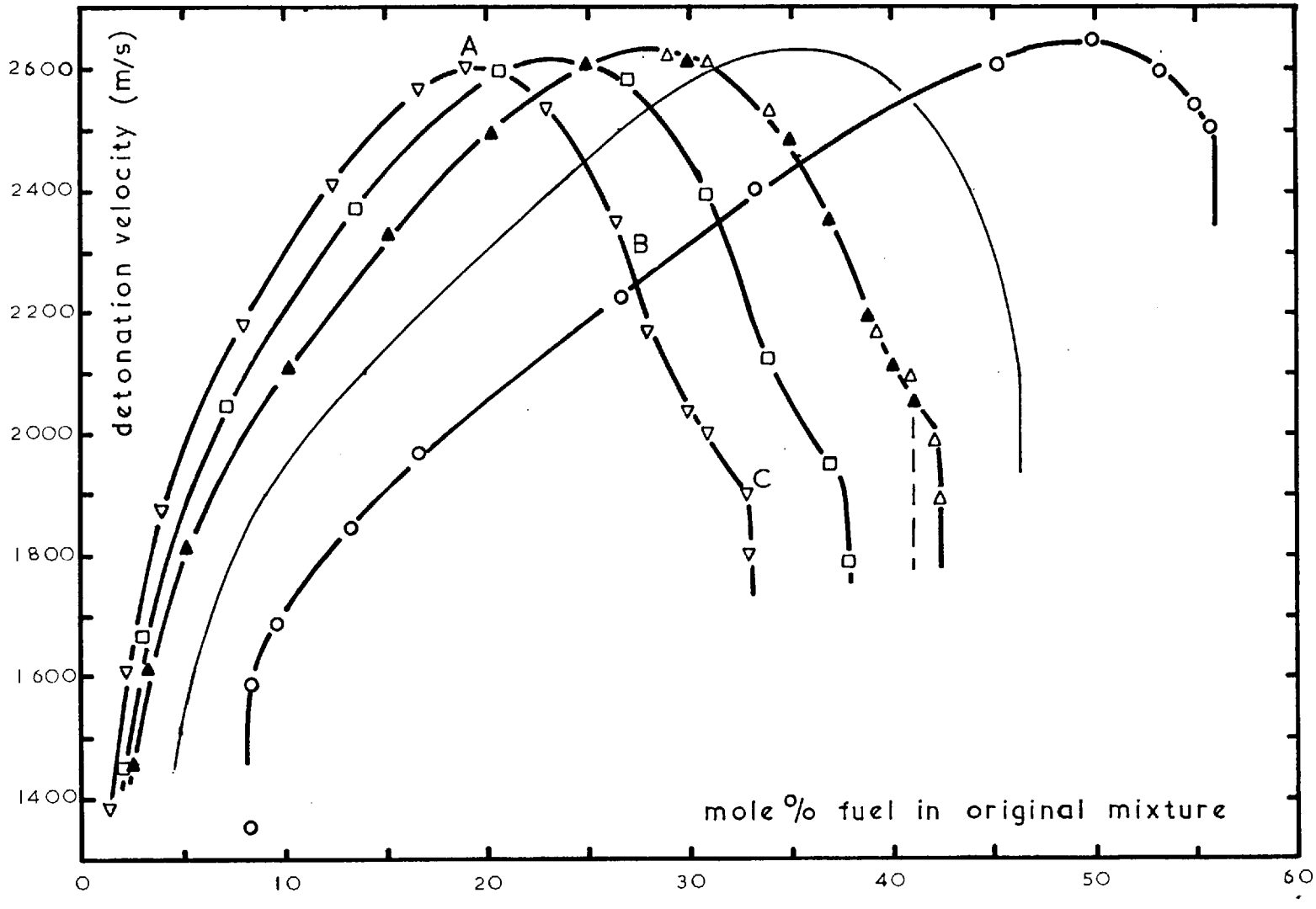



Fig. III.7. Detonation velocities for binary systems of oxygen with methane(o), ethane (SCHULLER, [1954]), n-propane(Δ), n butane(□) and neo pentane(▽).

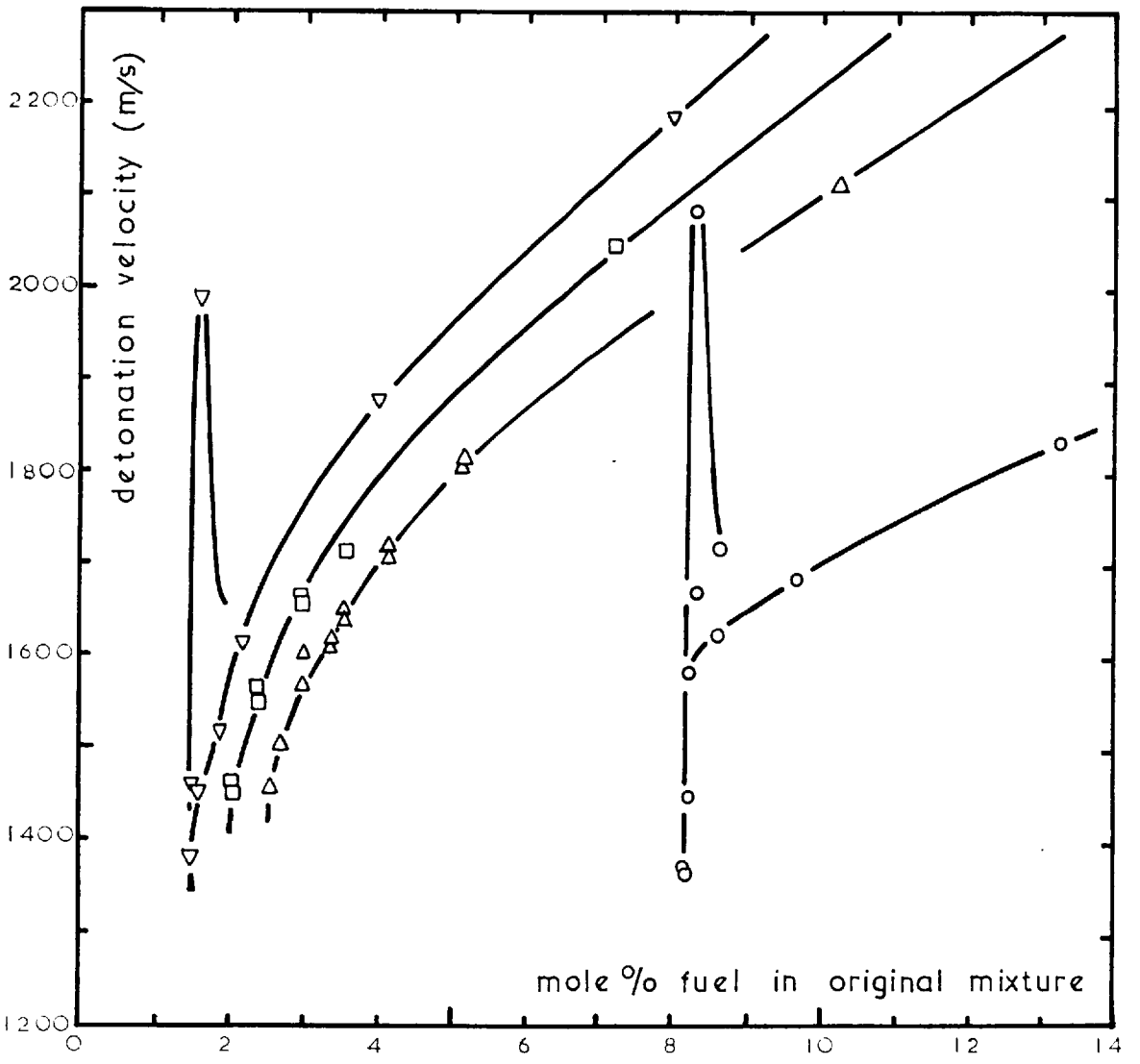



Fig. III. 8. Detonation velocities in fuel-lean mixtures for binary systems of oxygen with methane (o), n propane (Δ), n butane (□) and neo pentane (▽).

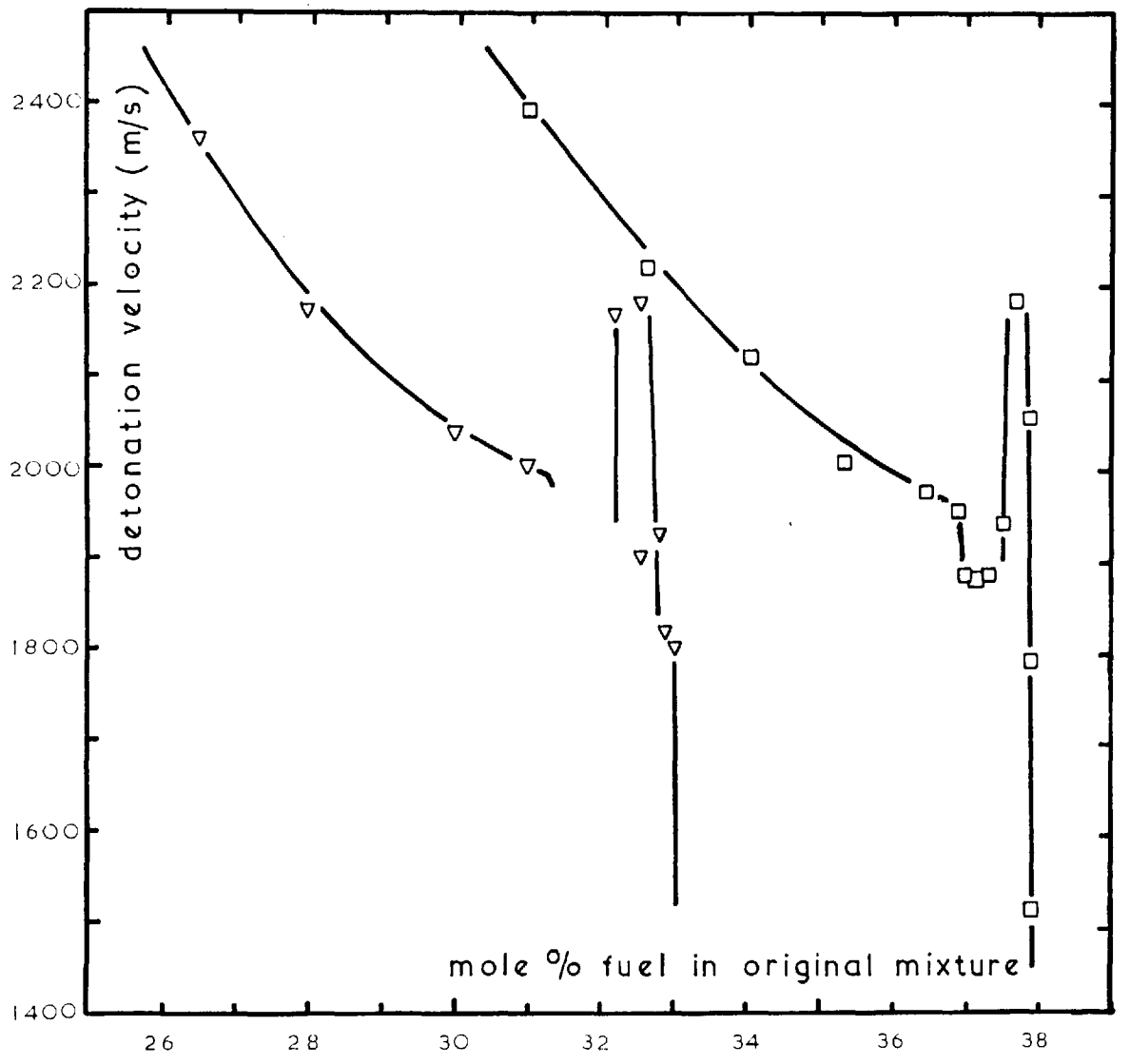



Fig. III.9. Detonation velocities in fuel-rich mixtures for binary systems of oxygen with n-~~propane~~ butane (□) and neo-pentane (▽).

detonations. Details are recorded in figure III.8 and III.9. Comparison suggests that near the oxygen-rich limits the deviations from a continuously increasing slope of the velocity curve towards lower velocities do not extend over as wide a range as near the fuel-rich limits of these mixtures. It can furthermore be said that in approaching a detonation limit from inside the detonation regime the gradient of the detonation velocity versus composition curve has two maxima and two minima and that the last minimum of the gradient before the limit is strongly negative. The velocity peak corresponding to this minimum may be several hundred metres per second higher than the value of the velocities on the smooth extrapolation of the detonation velocity curve for steady state conditions.

Considering the overall aspects of these phenomena in less detail, it can in general be said that in most cases the velocity curves appear to attain a minimum value less than one percent of mixture composition from the actual limit. On further dilution the composition limit is subsequently reached after a steep rise of detonation velocity to an intermediate maximum, several hundred metres per second higher than the previous minimum.

As in the case of detonation propagation through hydrogen-oxygen mixtures, velocity fluctuations are in the first place associated with marginal conditions. For soot-

producing hydrocarbon-oxygen mixtures additional disturbance of stability can be observed, which seems to be related to the formation of condensation products. Mixtures of oxygen and n-propane, n-butane and neo-pentane all produce velocity fluctuations of up to thirty metres per second outside the possible error of measurement, for compositions in the region of stable detonation where first signs of solid formation can be observed. For higher fuel ratios these fluctuations disappear at first, despite further increase of condensation, but they return again in the marginal region, where they are much stronger than before. At near-limit compositions the velocity fluctuations become as large as several hundred metres per second, being highest for the larger fuel molecules and apparently somehow related to the amount of produced deposits.

The overall pressure changes, given in tables III.2 to III.5, are also recorded as function of the mixture composition in figure III.10. These pressure-curves indicate again how the final pressures reach their lowest values for the classical stoichiometric mixture compositions, although, in contrast to experience with hydrogen-oxygen detonations, these values will be shown not to agree with complete conversion of the mixture into carbon dioxide and water. For the time being, the actual values of these pressure changes and the step-like change in the curves near

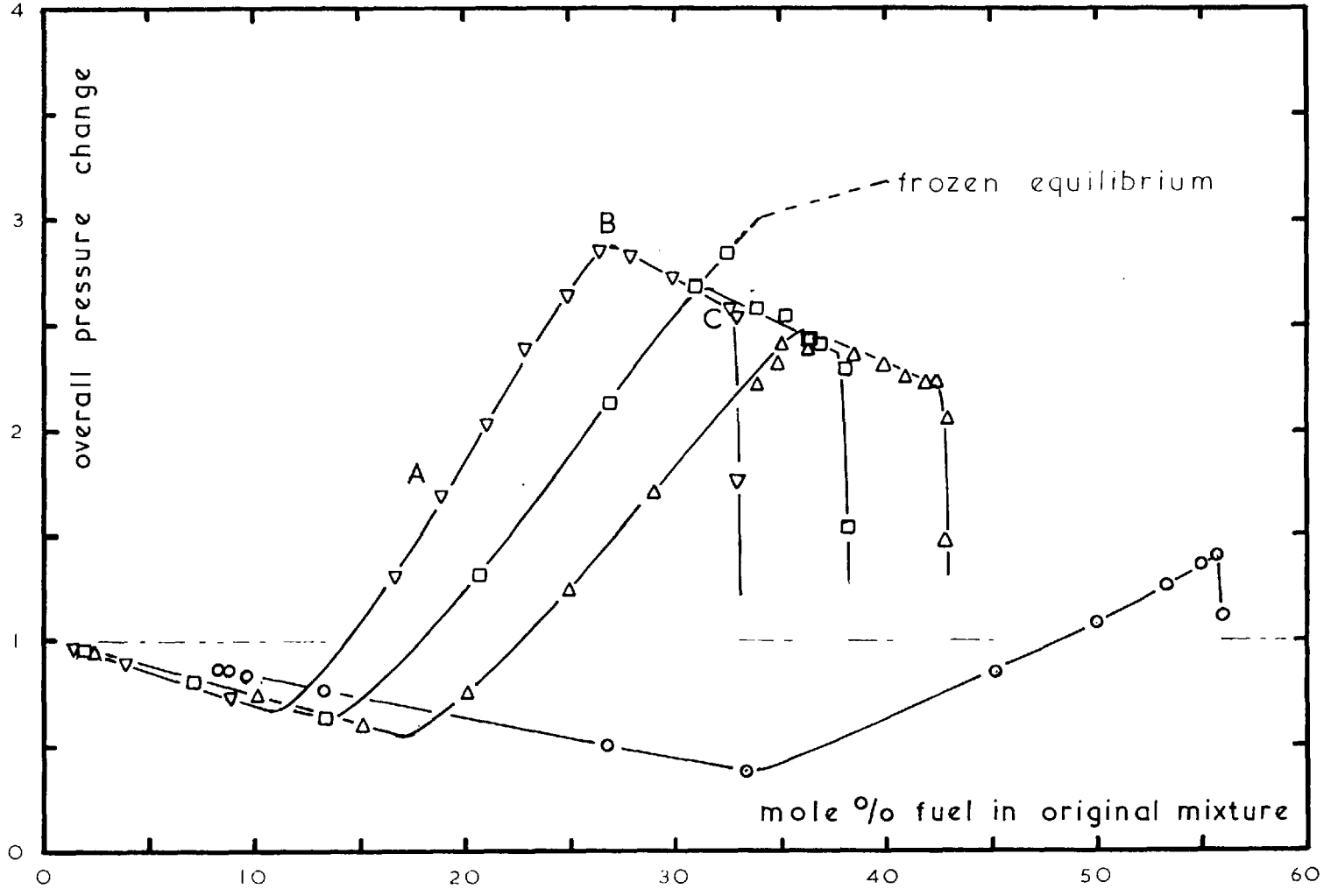



Fig. III.10. Overall pressure change in detonation of binary systems of oxygen with methane (o), n-propane (Δ), n-butane (□) and neo pentane (▽).

the detonation-limit compositions should be treated with great reserve. As for the latter, it should not be taken for granted that these rapid changes in final pressure coincide with the positions of the detonation limits. Overall pressure changes will almost certainly include other effects than those of reactions that take place between the detonation front and the C-J plane. By definition reactions taking place beyond this region cannot contribute to the sustentation of the detonation front, but will still affect the ultimate pressure.

Comparison of these results with notes made about soot-formation, shows that, in going from stoichiometric to fuel-rich mixture compositions, the first traces of soot deposits start to appear when the pressure change, due to the passage of the detonation front, becomes greater than 1.5 - 1.6. As can be seen from figure III.10, this empirical statement agrees with the fact that no soot was found in approaching the fuel-rich limit of methane. It should also be stated that throughout the solid-depositing composition regions, soot quantities were always found to be larger for the heavier fuel molecules.

In describing the general observations for the soot-depositing regimes, it will be useful to refer to the results for neo-pentane, as an example. At first, deposits

are a light, deep black powder, normally dry, but in the case of neo-pentane, slightly moist. Moving further away from the stoichiometric mixture ratio a point is reached on the pressure-change profiles where the slope of these curves increases still further. This point generally coincides more or less with the composition of maximum detonation velocity (point A in figure III.10 and figure III.7, respectively).

For the next percentages of rising fuel-content in the mixture, the amount of soot produced increases very slowly, until compositions are reached where the pressure change curve passes through its maximum, and the detonation-velocity curve normally has its first point of inflection (point B). From there on, soot-deposits become more bulky and greasy, the deep-black particles showing a snowflake-like structure. Initially an occasional deposit of the previous quality could be found; values calculated for the pressure-change would then lie close to the dotted extension of section A-B in figure III.10.

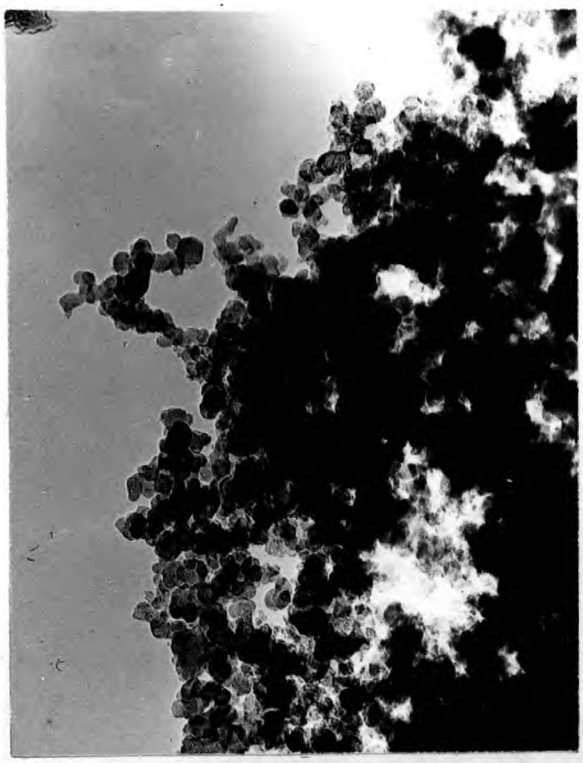
Beyond the limit at point C, and in a few other cases where, for reasons not well understood, the detonation failed to propagate through the test mixture, soot was only produced in very small quantities as a fine, pale black powder. In some experiments around limit compositions renewed ignition of the partly converted test mixture occurred

on reflection of the original shock front from the end plate of the tube. This would always result in final pressures and deposits comparable with those found well inside the limits.

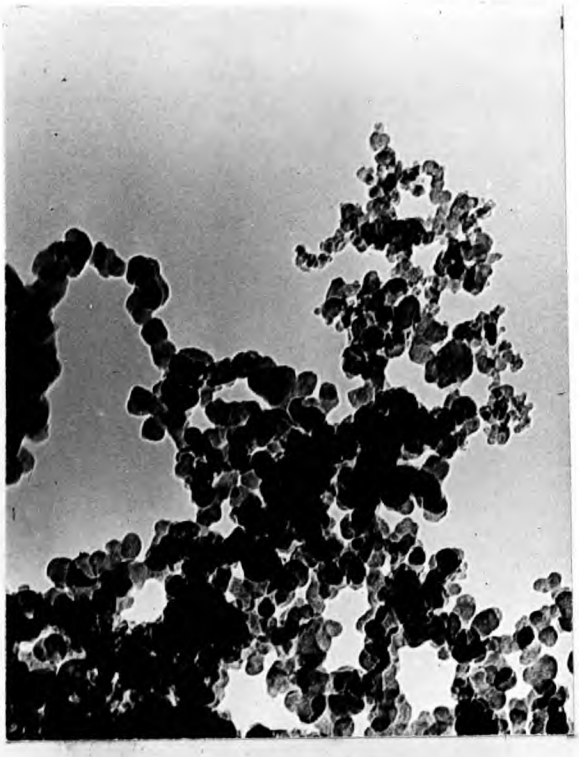
As has already been stated, no soot was found near the fuel-rich limit in experiments with methane-oxygen mixtures. However, a very fine grey dust could be seen on the swabs, used to clean the tube, after runs with extremely oxygen-rich mixtures, just inside the limits. Due to the very small quantities involved, it has, so far, not been possible to isolate this for further analysis.

Detailed study of the deposit, formed in a detonation wave, can sometimes throw light on the nature and sequence of the process, that has resulted in its formation. For this reason, samples were selected that could be representative for various phases of solid deposition. These were taken from the experiments on the n-butane-oxygen mixture at the following compositions: 32.64% butane, representing the first stages of soot formation; 37.75% butane, where the maximum amount of deposit was recorded for this system; and 38.68% butane, which is a composition outside the detonation limits.

From these samples electron micrographs and electron diffraction patterns have been made. The



(A)



(B)



(C)



(D)

Fig. III. II Electron micrographs ($x10^5$) and electron diffraction pattern from solid reaction products from n-$C_4H_{10}$-$O_2$ detonation; (A) : 32.64 % fuel; (B, D) : 37.75 % fuel; (C): 38.68 % fuel.

micrographs are shown in figure III.11, a,b and c, and for all three samples indicate particle sizes between 100-400 A. However, while particle size is predominantly around 250 A just inside the detonation limit (b), the deposits are of random size at the beginning of soot formation (a) and mostly between 100 - 200 A outside the limit (c). It should be mentioned that especially in the last case, contamination of the sample by larger particles, formed under the initiating impact from the priming mixture, might have occurred.

Due to the high density of these deposits it was difficult to prepare sufficiently thin specimens. As a result of this, the electron diffraction patterns are not very satisfactory, figure III.11.d. With less than the usual accuracy, the inter crystallite distance was found to be 3.52 A and 3.44 A for samples (a) and (b) respectively. Considering the possible error in these figures, the results correspond well with the same parameter for graphite, which has an inter crystallite distance of 3.40 A.

Gas chromatographic analysis has been carried out on the gaseous reaction products of two n-butane-oxygen mixtures. Selection of this system and of the initial composition values has been made after evaluation of the velocity data and will be explained in due course.

Table III.6. Reaction products from detonation of n-butane - oxygen mixtures in percentage of product gas.

| Reaction Products. | | Initial mixture in % $C_4H_{10}$ | |
|---|---|---|---|
| | | 13.3% | 35% |
| Gaseous Products : | $CO_2$ | 88 | 0.7 |
| | CO | - | 41.5 |
| | $CH_4$ | - | 4.1 |
| | $C_2H_2/C_2H_4$ | - | 0.8 |
| | $H_2$ | 3 | 51 |
| | $O_2$ | 8.5 | - |
| | total | 99.5 | 98.1 |
| Solid deposits | | - | + |
| Probable further products | | $H_2O$ | aromatics |

Data are presented in table III.6. Calculation of percentages has been performed on the basis of ad hoc calibration experiments. Information on additional, not analysed but probable reaction products is given.

## III. 5. Systems of ethylenic hydrocarbons and oxygen.

Detonation propagation in a mixture of an unsaturated hydrocarbon and oxygen has been investigated for propylene. Data are recorded in the usual way in table III.7.

Velocities have also been recorded in figure III.12. For information on aspects of homology, the results obtained by Schuller [1954] for ethylene - oxygen detonations are also shown. Numerical data for the latter experiments are recorded in appendix G , table 2.

Considering the general velocity pattern for marginal detonation of saturated hydrocarbons, the decline of detonation velocity near the fuel-lean limit of propylene-oxygen detonation is remarkably undisturbed. Mean detonation velocities for near-limit mixtures, only 0.1% of composition apart, are all situated on a smooth curve; fluctuations around mean velocity values are rarely above 50 m/sec and do not exceed 100 m/sec. At the fuel-rich limit, however, the velocity pattern resembles slightly more the usual behaviour found for the saturated hydrocarbons.

Table III.7 Detonation velocity and overall pressure change for the system propylene - oxygen.

| $\%C_3H_6$ | Mean velocity and fluctuations.(m/s) | Pressure change | Notes (see table III.1) |
|---|---|---|---|
| 2.40 | - | 0.983 | F |
| 2.45 | - | 0.966 | F |
| | 1340(+13, -18) | 0.957 | |
| 2.50 | - | 0.982 | F |
| | 1372(+19, -11) | 0.954 | |
| 2.55 | 1368(+19, -46) | 0.959 | |
| | 1379(+103, -86) | 0.957 | |
| 2.65 | 1401(+57, -49) | 0.948 | |
| 2.75 | 1417(+22, -9) | 0.950 | |
| 2.85 | 1451(±35) | 0.948 | |
| 3.00 | 1502(±37) | 0.948 | |
| 3.99 | 1658(+9, -22) | 0.927 | |
| 7.98 | 1955(± 0) | 0.839 | |
| 13.01 | 2178(± 0) | 0.717 | |
| 18.21 | 2359(± 14) | 0.614 | * |
| 23.19 | 2514(+7, -0) | 0.877 | * |
| 28.19 | 2622(± 0) | 1.319 | |
| 33.20 | 2682(+10, -0) | 1.772 | |
| 38.28 | 2592(± 0) | 2.277 | |
| 43.23 | 2294(± 17) | 2.322 | * |
| 45.72 | 2120(± 67) | 2.334 | ** |
| 48.19 | 2022(+40, -66) | 2.285 | **** |
| 49.02 | 1569(+200,-410) | 2.260 | **** |
| 49.57 | 1955(+36, -78) | 2.240 | **** |
| | 1920(+12, -50) | 2.252 | **** |
| 50.04 | - | 1.708 | ***; R.; F. |
| 50.51 | - | 1.304 | ** ; F |

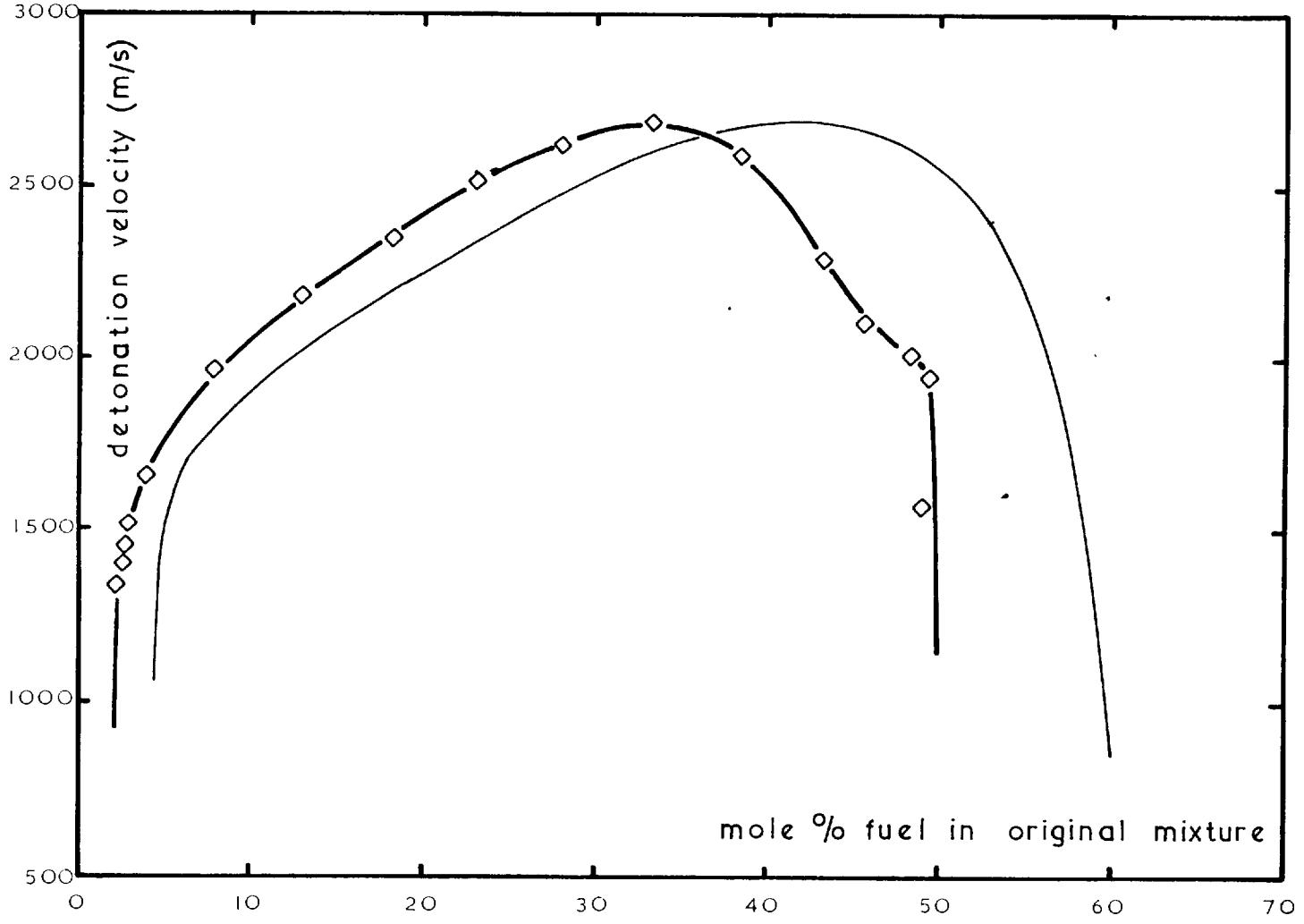



Fig.III.12. Detonation velocities for binary systems of oxygen with ethylene (SCHULLER, [1954]) and propylene (◇).

Overall pressure changes are also recorded in figure III.13. As can be observed, the maximum pressure reduction of the test mixture is again reached for the stoichiometric mixture. However, the actual value of the final pressure once more does not agree with the complete oxidation to carbon monoxide and water.

Soot formation over the propylene-oxygen system is rather different from the condensation phenomena as found for instance for propane detonation. In the latter case soot formation on the fuel-rich side of the detonation regime starts when, with increasing fuel content, the overall pressure change becomes greater than 1.5 and heavy deposits are formed in the marginal region beyond the composition of maximum overall pressure change, see figure III.10. For propylene-oxygen detonations, soot formation is first observed at the stoichiometric mixture composition, where a cloud of finely dispersed particles is formed. The amount of such deposits has been too small to permit collection in the usual way. However, with rising fuel concentration of the test mixture, the formation of condensation products does not increase any further. Instead it disappears again at a mixture composition of approximately 25 percent propylene, which corresponds to a fuel-oxygen ratio for complete conversion to carbon monoxide and water. In the

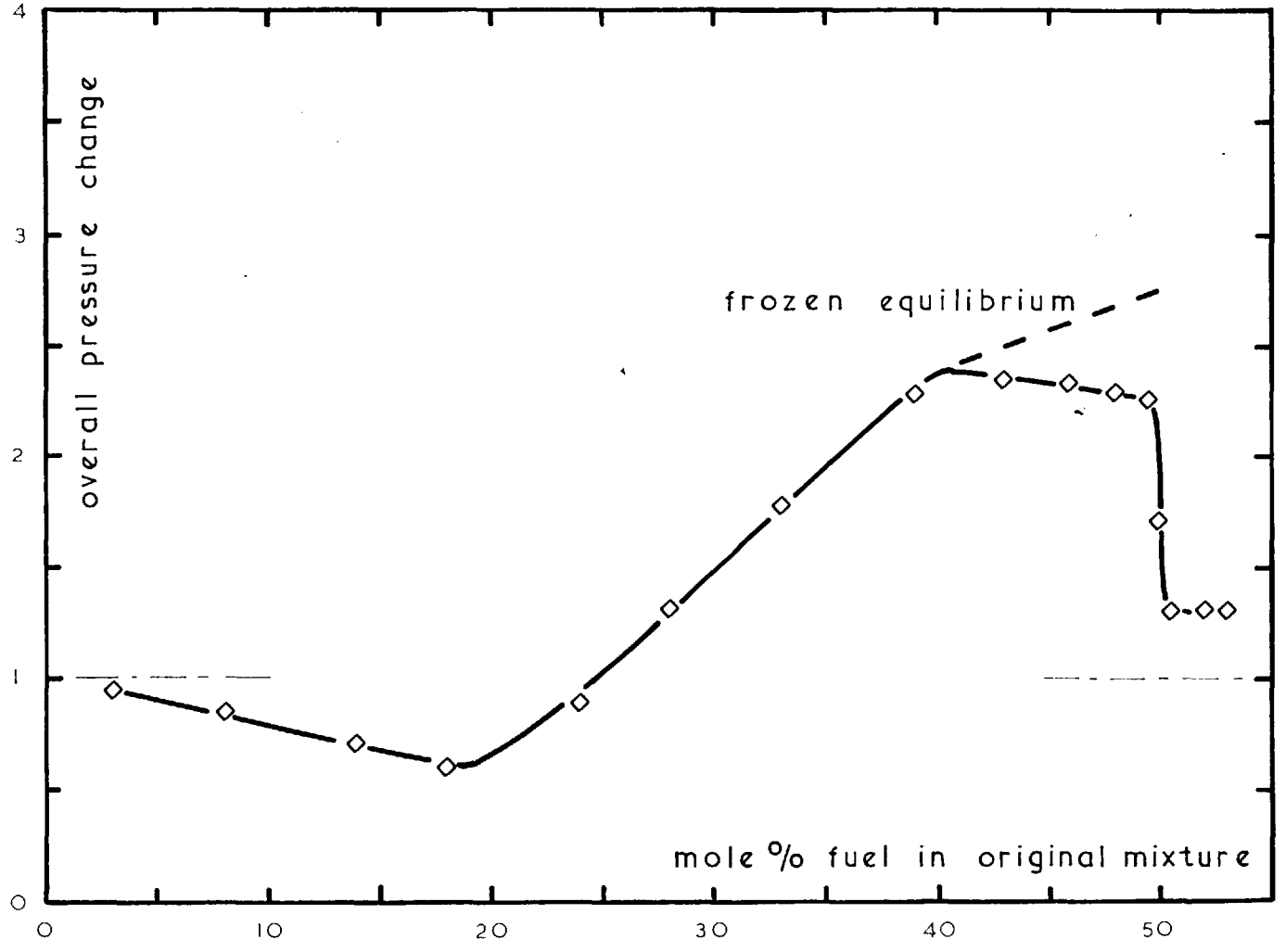



Fig. III.13. Overall pressure change in detonation of the system propylene oxygen.

composition regime between this mixture and the 40 percent propylene mixture, which holds only sufficient oxygen for complete oxidation of all carbon atoms to carbon monoxide, solid formation is not observed. However, it has been noted from the oscilloscope records that in this composition region the primary detonation wave appears to be followed closely by a second conductive front with comparable propagation velocity. With increase of propylene content above 40 percent, which represents also the mixture for which the overall pressure change reaches its maximum value (see figure III.13), condensation products are once more observed. Moderate to heavy soot formation is only found within 4 percent of composition difference from the propylene-rich detonation limit.

After detonating propylene-oxygen mixtures of 7, 13 and 18.2 (stoichiometric) percent fuel, a cloud of condensation products could be observed in the tube, which required about ten minutes to settle. However, amounts of these deposits were too small to permit collection of these in the usual way.

# Chapter IV. ELEMENTS OF DETONATION THEORY.

This chapter is not intended as a comprehensive treatment of the important aspects of detonation theory; such information can be found in one of the handbooks mentioned in section I. Detection and discussion of elements of detonation theory presented in this chapter is adapted to the requirements that arise from the evaluation of the experimental results.

## IV. 1. The detonation wave.

### a. The coordinate system.

As stated earlier, a detonation wave can be described as a shock front followed by a zone of chemical reaction. It has been accepted for some considerable time that for steady state detonation, the chemical reaction contributes fully to the sustentation of the detonation wave. An important confirmation of this opinion is the excellent agreement between measured propagation velocities of stable detonation and velocities calculated from the results of the hydrodynamic analysis of the state of completed reaction.

In dealing with aspects of the hydrodynamic treatment it is often useful to describe the various phases

of gas flow in a coordinate system fixed to the detonation wave. In laboratory coordinates, figure IV.1.a, the detonation wave propagates with velocity $W_d$ into the undisturbed test mixture, which has a flow velocity $w_1 = 0$. After passage of the detonation wave, pressure, density and temperature of the gas have changed from state 1 into state 2 and the gaseous reaction products will later be seen to follow the detonation front with velocity $w_2$.

In the case when the coordinate system is considered stationary in the wave front, see figure IV.1.b, the detonation front is at rest, while unreacted gas mixture enters it with velocity $u_1$ and reaction products leave the wave with velocity $u_2$ , $< u_1$. Consequently

(IV.1) $$u_1 = W_d$$

(IV.2) $$u_2 = W_d - w_2$$

As can be seen the "particle velocity" behind a detonation wave is :

$$w_2 = W_d - u_2$$

or,

(IV.3) $$w_2 = u_1 - u_2 \ .$$

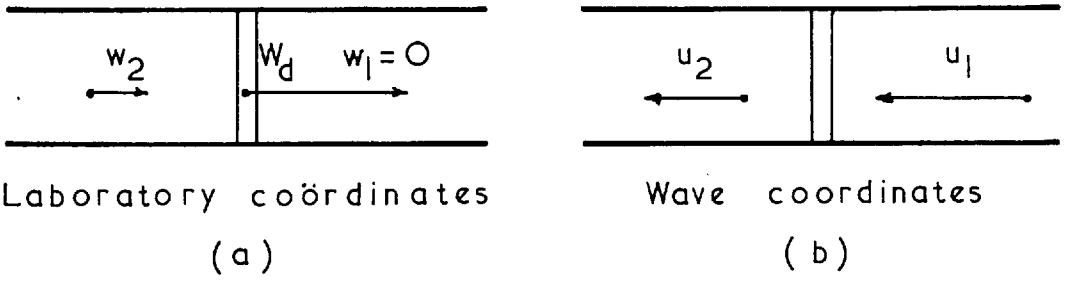



Fig. IV. 1. Detonation coordinates.

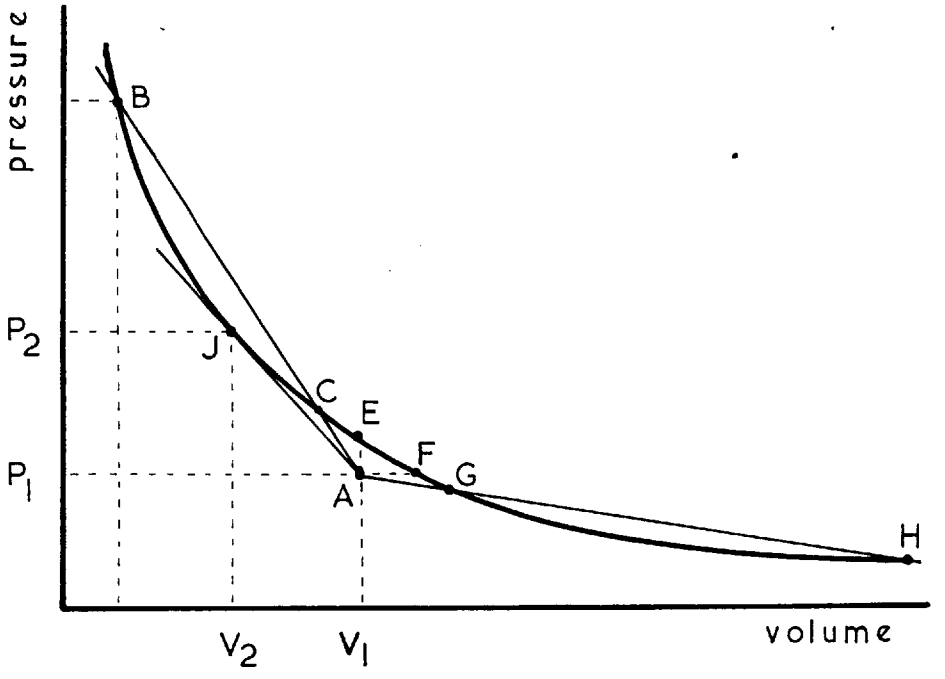



Fig. IV. 2. Hugoniot curve.

b. The conservation equations.

Whatever the nature of the reaction in a detonation wave, variations of state will be in accordance with the continuity principles for respectively mass, momentum and energy. For unit mass of gas mixture undergoing a chemical reaction with heat release Q, the conservation equations can respectively be written as

$$\frac{u_1}{V_1} = \frac{u_2}{V_2} \tag{IV.4}$$

$$P_1 + \frac{u_1^2}{V_1} = P_2 + \frac{u_2^2}{V_2} \tag{IV.5}$$

$$H_1 + \frac{u_1^2}{2} = H_2 + \frac{u_2^2}{2} - Q \tag{IV.6}$$

In this the enthalpy H is :

$$H = E + PV = (C_v + R)T = C_p T \tag{IV.7}$$

Evaluation of states in a detonation wave must be carried out on the basis of equations (IV.4), (IV.5) and (IV.6).

c. Detonation with infinite reaction rate.

If a detonation is considered as a shock front, followed by a chemical reaction of the gaseous mixture

components which goes to completion instantaneously, the Q in equation (IV.6) becomes the energy release of unit mass of gas mixture in complete combustion.

To obtain the general equation of state for such a process, first equations (IV.4) and (IV.5) are solved for $u_2$ ,

$$(IV.8) \qquad u_2^2 = V_2^2 \frac{P_2 - P_1}{V_1 - V_2}$$

and the result substituted in equation (IV.6)

$$(IV.9) \qquad H_1 - H_2 = \frac{(P_1 - P_2)(V_1 + V_2)}{2} - Q$$

Application of equation (IV.7) and division by $P_1V_1$

$$(IV.10) \qquad \frac{C_p(T_2 - T_1)}{P_1V_1} = \frac{1}{2}\left(\frac{P_2}{P_1} - 1\right)\left(\frac{V_2}{V_1} + 1\right) + \frac{Q}{P_1 V_1}$$

Substitute the equations of state for ideal gases

$$P_1V_1 = RT_1/m_1$$

with R = gas constant referred to unit mole of gas

m = molecular weight

and introduce the definitions :

$$c = 2C_p m_1/R \qquad q = 2Qm_1/RT_1$$

and

$$(IV.11) \qquad p = P/P_1 \qquad v = V/V_1$$

$$m = m_2/m_1 \qquad \theta = T/T_1 = pvm$$

in which c and q are state functions of the other variables. Equation (IV.10) will then change into the general equation of state, attainable on the basis of the conservation equations :

$$c(pvm - 1) = (v + 1)(p - 1) + q \qquad \text{(IV.12)}$$

This type of equation is called an Hugoniot and it has been derived for the burned gas.

For construction of the P - V plane a more useful form of equation (IV.12) is obtained by expressing c and the specific heat from equations (IV.11) and (IV.7) :

$$\frac{2m_1}{R}\left(\frac{H_2 - H_1}{T_2 - T_1}\right)(pvm - 1) = (v+1)(p-1) + q \qquad \text{(IV.13)}$$

d. The Chapman - Jouguet point.

If, instead of $u_2$, the detonation velocity $u_1$ is expressed from equations (IV.4) and (IV.5), the result is :

$$u_1^2 = V_1^2 \frac{P_2 - P_1}{V_1 - V_2} \qquad \text{(IV.14)}$$

or, if by definition :

$$D = u_1^2 / P_1 V_1 \qquad \text{(IV.15)}$$

$$D = (p - 1) / (1 - v) \qquad \text{(IV.16)}$$

This linear equation gives the slope of the so-called "Rayleigh line" which relates the initial state ($P_1V_1$) of the gas mixture (point A in figure IV.2) with the final state ($P_2V_2$), somewhere on the Hugoniot curve for the burned gas, which is also shown in figure IV.2. However, as the Rayleigh line is based on the mass and momentum equation only, it must be obeyed irrespective of the state of the burnt gas. In solving the two equations (IV.12) and (IV.16), there can be zero, one or two roots.

For solution given by point E, figure IV.2, the gas is burned without change of volume.

Between points E and F the right-hand term of equation (IV.14) is negative. This would correspond with an imaginary detonation velocity and consequently has no meaning. At F, the gas is burned at constant pressure, resulting only in expansion. Below F, the pressure decreases and the volume increases on combustion. Therefore the process is real. It follows from equations (IV.3) and (IV.4) that the particle velocity $w_2$ is negative for final volumes larger than $V_1$. Consequently the gas moves away from the wave, which is identical to rarefaction.

The only possible solutions must therefore be situated on the part of the curve above E. In principle, intersection with the Rayleigh line will produce two final

states. It can however be argued, as has been done by Jouguet [1905] and Becker [1922] that the true final state is the point of tangency, J, which was already suggested in the hypothesis put forward by Chapman [1899]. This point is called the Chapman-Jouguet point and it represents the final state of the normal processes of energy release that support the detonation front. As can be seen from equation (IV.14) it represents the detonation with the minimum velocity that satisfies the conservation principles included in the Rayleigh line and the Hugoniot curve.

e. Calculation of the parameters of state at the Chapman-Jouguet point.

The points of intersection of the Rayleigh line and the Hugoniot curve can be found by writing equation (IV.16) as

$$p = D(1 - v) + 1 \qquad \text{(IV.17)}$$

and substituting equation (IV.17) in equation (IV.12), leading to :

$$v^2 D(mc-1) - v(mc + Dmc) + (q + c + D) = 0 \qquad \text{(IV.18)}$$

As the C-J point is the point of tangency, the equation must have equal roots for the volume increase v, so

$$v = cm\,(D + 1) \,/\, 2D\,(cm - 1) \tag{IV.19}$$

with

$$(mc)^2\,(1 + D)^2 - 4D(mc-1)(q + c + D) = 0 \tag{IV.20}$$

The roots of equation (IV.20) are

$$D = X \pm (X^2 - Y)^{\frac{1}{2}}$$

$$X = \frac{2(mc - 1)\,(q + c) - m^2c^2}{(cm - 2)^2} \tag{IV.21}$$

$$Y = (cm)^2 \,/\, (cm - 2)^2$$

Evaluation of the thermodynamic data for the final state, from the data of the initial state starts with equation (IV.21).

(i) c,q and m vary with pressure and temperature;values for $P_2$ and $T_2$ are chosen and c,q and m are evaluated with equations (IV.11).

(ii) These are used to calculate D, equation (IV.21).

(iii) v follows from equation (IV.19).

(iv) p follows from equation (IV.17), and
$\theta$ follows from equation (IV.11).

The initial values chosen for $P_2$ and $T_2$ are corrected and the cycle of (i) to (iv) is repeated until satisfactory agreement is reached.

The final state parameters can be used to calculate the detonation velocity, by equation (IV.14). When experimental work is done this is often useful as a check on the validity of general assumptions.

f. The influence of turbulence on the C-J condition.

For conditions of laminar flow the velocity of sound in an ideal gas is :

$$a^2 = V^2 \frac{dP}{dV} = \gamma \frac{PV}{m_i} \qquad \text{(IV.22)}$$

If this is compared with equation (IV.8), $u_2$ can be seen to be equal to the velocity of sound in the burned gas and, according to equation (IV.2)

$$W_d = w_2 + u_2 = w_2 + a_2 \qquad \text{(IV.23)}$$

which means that, for assumed conditions of laminar flow, the detonation velocity is equal to the sum of the velocity of the gas particles and the speed of sound of the burned gas. Considering the situation at the C-J point, the combustion products would be moving away from the front at the local speed of sound.

Various investigations by White [1958, 1959, 1961] have shown that self sustaining detonations, apart from being

non-planar, have a turbulent reaction zone. Calculations of C-J conditions for this type of flow lead to a higher minimum detonation velocity than found when the correction for turbulence is neglected. Decay of turbulence after completion of reaction results in supersonic flow away from the C-J point.

Consequently there is no real justification for the assumption of equality between the propagation velocity of self sustaining detonations and the velocity of sound at the C-J point. The proper description for detonation velocity remains the minimum velocity for which the requirements of the conservation laws for (turbulent) flow at the C-J point can be met.

g. The Mach product.

A useful parameter to relate experimental detonation velocity data with theoretical considerations as discussed in this chapter is the Mach-product: $\gamma M^2$.

It follows from equation (IV.15) that

$$D = u_1^2 \, m_1 / R \, T_1$$

and from equation (IV.22) that

$$m_1 / R \, T_1 = \gamma / a_1^2 .$$

Consequently :

$$(IV.24) \qquad D = \gamma M^2 = u_1^2 m_1 / R T_1$$

in which $\gamma$ is the ratio of the specific heats : $C_p/C_v$ and M is the Mach number : $u_1/a$.

As can be seen from equation (IV.21), D is a function of q, the chemical reaction energy of the system. It follows therefore that values of $\gamma M^2$, obtained from experimental velocity data, give an indication of the energy transfer involved in the investigated detonation.

## IV. 2. The detonation front.

### a. Shock conditions.

Continuity principles, as considered in section IV.1.b, should apply equally well to the changes occurring in the shock front that precedes the reaction zone in detonation propagation. Similarly an equation of state can be derived from these principles, which describes the state of the test mixture after shock compression, but before the initiation of chemical reaction. In fact, the only difference in the basic equations used to derive the Hugoniot for the burned gas is that there is no energy release due to chemical reaction and that it seems safe to

assume that the average molecular weight has not changed in comparison. Consequently

$$q = 0$$

$$m = 1.$$

The Hugoniot equation of state for the shock-compressed gas can therefore be derived from equation (IV.13) as

$$\frac{2m_1}{R} \left( \frac{H_2 - H_1}{T_2 - T_1} \right) (pv - 1) = (v + 1)(p - 1) \qquad \text{(IV.25)}$$

and from equation (IV.11) :

$$pv = \theta \,, \qquad \text{(IV.26)}$$

while

$$D = (p - 1) / (1 - v) \qquad \text{(IV.16)}$$

remains valid.

For calculation of the parameters of the shock compressed gas, equations (IV.21) and (IV.19) can be used in adapted forms.

Proceedings starting from chosen values for the specific heats and temperature follow the same programme as for the C-J calculations, section IV.1.e. However, choice of the values for specific heats will depend on assumptions for the state of energy relaxation in the detonation front.

b. Energy relaxation in a shock front.

It follows from equation (IV.7) that the enthalpy change is generally described by

$$\Delta H = (C_v + R)\Delta T = C_p \Delta T \ . \tag{IV.27}$$

Values for $C_v$, $C_p$ and consequently for $\Delta H$ depend on $T_1$ and $T_2$ and on the state of equilibrium achieved at $T_2$.

The specific heat at constant volume, $C_v$, is $\frac{R}{2}$ or R for each degree of freedom, per mole, per degree $\Delta T$. The total number of degrees of freedom per molecule is 3n, if n is the number of atoms in the molecule.

Each molecule has three translational, three rotational and 3n-6 vibrational degrees of freedom. Linear molecules, including all diatomic molecules, have however only two rotational degrees of freedom, the third degree being degenerated into two vibrational degrees of freedom, of which therefore there will be 3n-5.

Excitation of the various degrees of freedom depends on the spacing of the energy levels for these modes. Differently described, this means that the absorption of energy by a molecule depends on the chance of a collision with an elementary particle of sufficiently high kinetic energy to effect the transfer to a higher mode of energy movement. This step requires $\frac{R}{2}$ cal. for translation and rotation and R cal. for vibration.

Translational energy level spacing is almost non-existent. The levels form a continuum and the relaxation time depends only on the collision frequency. Consequently $C_v$-translational = $\frac{3}{2}R$.

Rotational energy level spacing is usually small compared to (RT = NkT) and less than 10 collisions are sufficient for excitation. Only hydrogen has a relatively long "relaxation" time, requiring approximately 200 collisions. In practice this means that for temperatures involved in shock-front heating, the rotational relaxation can be considered to be instantaneous and to contribute R or $\frac{3}{2}R$ to the specific heat.

Spacing of vibrational energy levels is considerably higher, involving thousands of calories per mole. As a result of this, relaxation times at room temperature can be as much as a few milliseconds, and even at shock temperatures relaxation times of up to five microseconds do occur. Contributions to the specific heat are difficult to evaluate. For diatomic molecules the vibrational energy $E_{vibr.} = h\nu / (e^{h\nu/kT_{vibr}} - 1)$. For more complicated molecules calculations are accordingly much more difficult. Relatively long relaxation times are found for carbon monoxide and nitrogen. Generally, impurities tend to reduce vibrational relaxation times; hydrogen in particular has a marked effect.

In view of these differences in relaxation behaviour, calculation of specific heats involving translational and rotational excitation only, can be carried out according to the classical theory of $\frac{R}{2}$ per degree of freedom, per mole, per degree. For situations persisting for sufficient time to allow for reasonable attainment of vibrational energy relaxation, use can be made of the equilibrium data for $C_p$, which can be found in the literature.

c. Shock temperatures calculated from measured detonation velocities.

As has been shown in the previous sub-sections, parameters for the shock-compressed state of the detonation front can be calculated from the parameters for the initial state and selected values for the specific heat. Of particular interest for studies of marginal detonations is the shock temperature. Experimental investigation of detonation limits for various gaseous systems has suggested the requirement of a minimum temperature rise in the shock front for detonation . propagation.

Information on shock front temperatures at detonation limits can be evaluated from experimental results by adaption of the equations derived for the state parameters in the shock front. As has been shown in subsection

IV.1.g, values for D can be calculated from the velocity data; conditions for D apply equally to the shock-front and the C-J point. From these D values, shock temperatures can be calculated by trial and error as discussed in sub-section IV.2.a.

As there is no immediate interest in p and v-values, a direct calculation by elimination of these two parameters will be an advantage. Elimination of p, from equations (IV.26) and (IV.16) gives

$$(IV.28) \qquad Dv^2 - v(D + 1) + \theta = 0$$

A second equation in v is obtained by substituting equations (IV.26) and (IV.16) in equation (IV.25), which results in :

$$(IV.29) \qquad D(1 - v^2) = \frac{2m_1}{RT_1}(H_2 - H_1)$$

or

$$(IV.30) \qquad v^2 = 1 - \frac{Z}{D}$$

with

$$(IV.31) \qquad Z = \frac{2m_1}{RT_1}(H_2 - H_1)$$

Subsequent elimination of v from the two equations (IV.28) and (IV.30) gives

$$(IV.32) \qquad \frac{2D + 1}{D} = 2\theta - Z + \frac{\theta^2}{D - Z}$$

Calculation of $\theta$ now proceeds as follows.

(i) D is calculated from experimental data with equation (IV.24).

(ii) A value for $\theta$ is chosen.

(iii) Considering $\theta$, the energy relaxation in the shock front is estimated and Z is calculated with equation (IV.31) for the corresponding enthalpy values (see sub-section IV.2.b).

(iv) $\theta$ is calculated with equation (IV.32) and compared with the value assumed in (ii).

(v) Corrections to $\theta$, and possibly to the enthalpy values are made and (ii) to (iv) are repeated until acceptable agreement between estimated and calculated values for $\theta$ has been attained.

Ad (iii) With respect to the state of energy relaxation in the shock-front the following values will be found for $\Delta H$, equation (IV.27), see sub-section IV.2.b.

Translational relaxation only

$$\Delta H = \frac{5}{2} R \Delta T$$

Translational and rotational relaxation only :

- linear molecules $\Delta H = \frac{7}{2} R \Delta T.$

-non linear molecules $\Delta H = 4R \Delta T.$

For relaxation of all modes of energy absorption tabulated equilibrium data must be used.

Consequently the following values of Z can be used (equation IV.31) :

Translational relaxation only :

(IV.33) $$Z = 5\,(\theta - 1)$$

Translational and rotational relaxation only :

(IV.34) $$Z = 7(\theta - 1)$$ -linear molecules.

(IV.35) $$Z = 8(\theta - 1)$$ -non linear molecules.

For relaxation of all modes of energy absorption Z must be calculated with equation (IV.31).

## IV. 3. Detonations with finite reaction rate.

The description of section IV.1 is only concerned with the Chapman-Jouguet condition for the completed reaction, from which the detonation velocity can be derived. It does not consider in detail the structure of a detonation wave or of the reaction zone. In reality the reaction zone has a certain depth, in which the chemical reaction goes to completion with a finite rate.

The proper description of this phase of detonation propagation is due to the work of Zeldovich, Von Neumann and Doring, mentioned in chapter I. The description starts from the shock compressed state of the initial gas mixture that lies ahead of the reaction zone. The P - V relation,

which describes the sudden changes taking place in the shock front, is given by the Hugoniot equation (IV.25) and shown schematically in figure IV.3. The initial gas state is given by point A ($P_1 V_1$), the shock compressed state by point B($P_S$ $V_S$ ). The velocity of the wave is given by the slope of BA.

As the gas expands behind the shock front, reaction initiation follows. The conservation equations (IV.4), (IV.5) and (IV.6) will remain equally valid for any of the successive states of the system. The states are fixed in the system by taking Q in equation (IV.6) to be that fraction of the total chemical energy of the mixture which has been released at the state considered. Consequently a family of Hugoniot curves can be constructed for all states between Q = 0 and Q = 1. The last curve will correspond to the Hugoniot curve for the state of completed chemical reaction, discussed in section IV.1 and must therefore only have the point of tangency J in common with AB. J is again the C-J point, giving the minimum detonation velocity for self-sustained detonation, which will incidentally be somewhat turbulent (sub-section IV.1.f).

The attainment is achieved by way of ABCEJ. As can be seen, intermediate Hugoniot curves have two points of intersection with the Rayleigh line AB. However, the

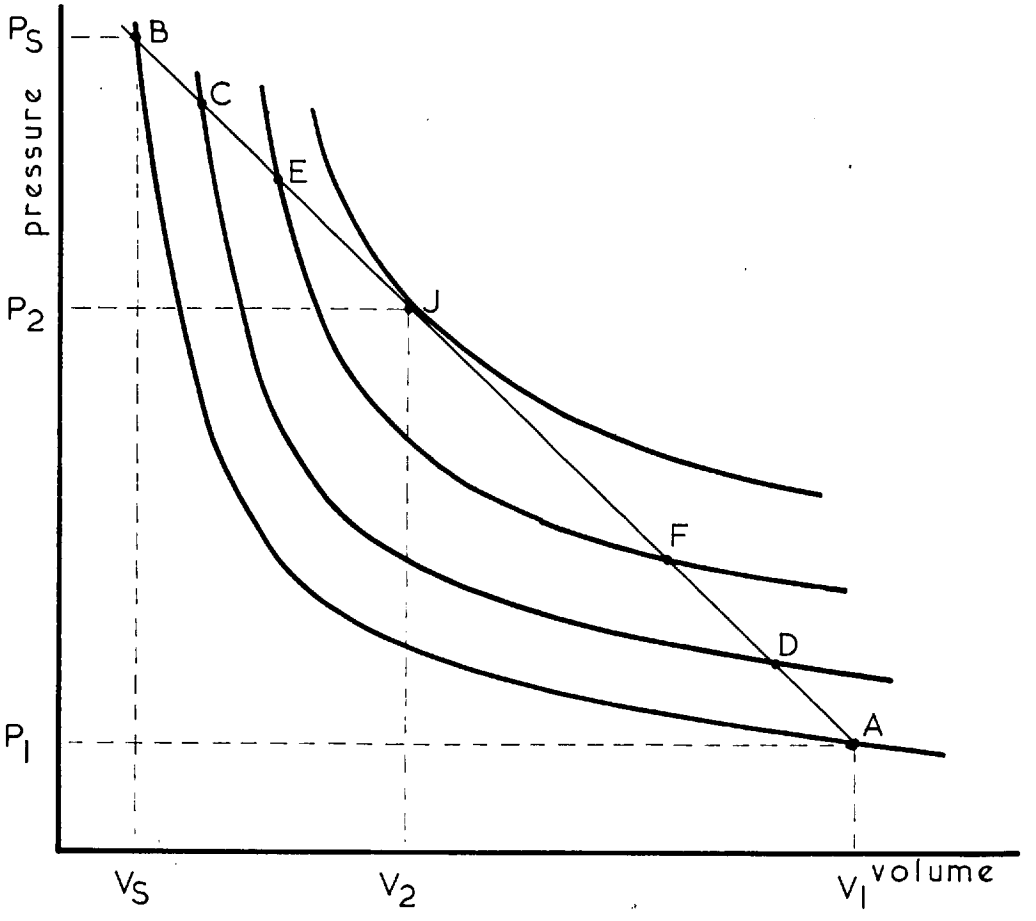



Fig. IV. 3. Family of Hugoniot curves, indicating gas state in detonation wave.

attainment of the C-J point J, directly over the intermediate stages D and F cannot be achieved as it implies spontaneous ignition of the unreacted gas mixture at $P_1V_1$, without the shock compression in the detonation front, indicated by $P_SV_S$.

As can be seen from figure IV.3, the pressure decreases along BJ, while V increases. Application of equation (IV.17) to this change of situation shows that the particle velocity will increase along this line.

To illustrate this description of a detonation wave, the following model can be of some use. Consider a steady state detonation, propagating with constant characteristic velocity into the unreacted gas mixture in a closed tube. In this model the gas, which has an initial mass-density equal to unity, is considered as being divided into a series of equal volumes; for convenience these volumes are supposed to be of such extension that each of the consecutive steps to be considered will apply to one of these units at the time. We will describe schematically the sequence of events undergone by one of the unit volumes as it is traversed by the detonation wave.

In figure IV.4.a, the detonation front is on the point of entering the gas volume considered, which is indicated as a traced section.

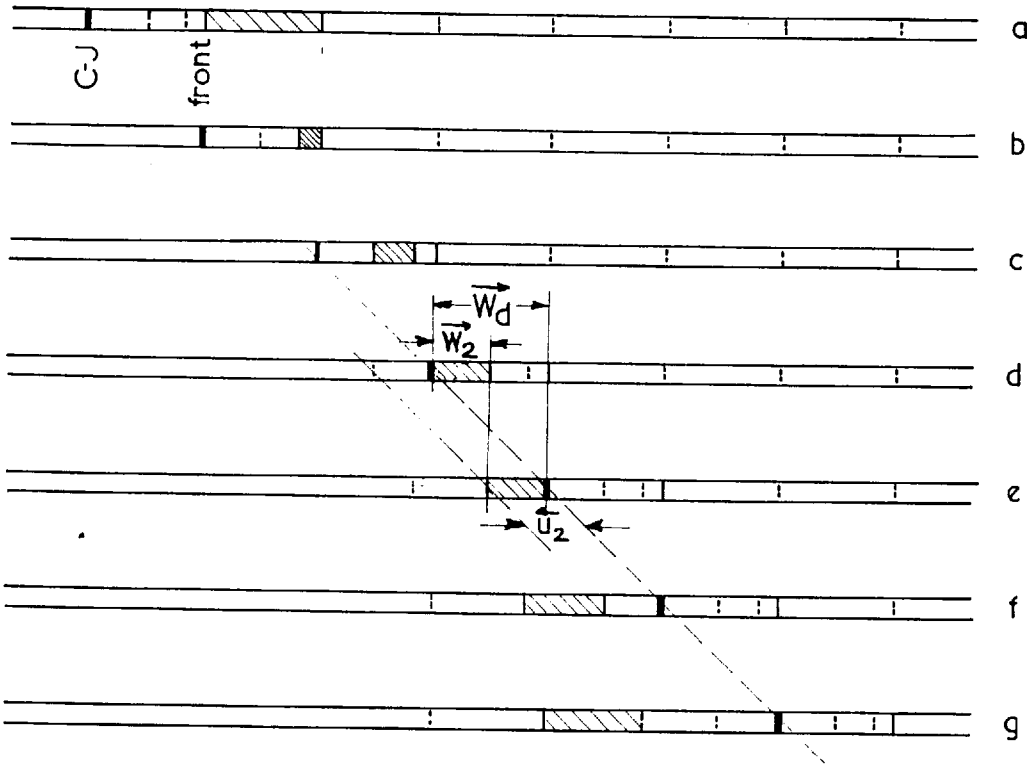



Fig. IV.4. Model of mass flow in a detonation wave.

To compress the unreacted gas to the mass density of the detonation front, the shock front has to proceed over the length of the unit volume to situation (b). As can be seen this implies that while the first particles, overtaken by the wave, have moved forward over almost the complete length of the original section, the particles at the other end of the volume undergo their first collision with excess translational energy in the direction of detonation propagation.

From situation (b) onwards, the mass-density will continuously decrease, as corresponds with the nature of the Rayleigh line in figure IV,3, section BJ. Situation (c) in figure IV.4 shows the limit of the induction period, which is followed by chemical reaction in situation (d). The chemical reaction is completed at the C-J plane, indicated by the bold vertical line.

According to equation (IV.2) conditions at the C-J plane imply that the detonation velocity ($W_d$) is equal to the sum of the velocity of the gas particles ($w_2$) in laboratory co-ordinates and the velocity of the reaction products ($u_2$) in wave co-ordinates. In vector notation the proper form of this equality becomes :

(IV.36) $$\vec{W}_d = \vec{w}_2 - \vec{u}_2$$

As can be seen from comparison of situation (d) and (e),

the identity is illustrated by this model. Figure IV.4 also shows that the passage of a detonation front is associated with forward movement of the gas undergoing combustion.

## IV. Conditions behind the Chapman-Jouguet plane.

Behind the C-J plane the conditions of the reaction products are governed by the existence of a rarefaction wave. As the detonation moves away from its initiation at one of the closed ends of the tube, it leaves behind a continuously increasing volume into which the hot gases of the C-J equilibrium composition must expand. This situation is illustrated by the sequence of expanding sections in the situations of figure IV.4.

The nature of the gas expansion behind the C-J plane can be considered in more detail from the continuously increasing separation between the detonation wave and the end of the tube. As this represents a reverse of normal compression, expansion waves must be propagating into the reaction products. The expansion pulses which constitute such waves propagate with the local speed of sound. As the gases into which these waves travel undergo expansion, the velocity of the expansion pulses diminishes continuously. The result will be that as the detonation travels further

away from the end of the tube, the reaction products emitted from the reaction zone will pass through an expansion wave of steadily increasing length and diminishing slope before they reach the tail of the wave, propagating at the local speed of sound.

In certain cases of marginal detonation, part of the chemical changes, resulting from the shock-compression in the detonation front, does not occur until some distance behind the C-J plane. Under such conditions this second phase in chemical change and energy release may lead to the build-up of another detonation front in the rarefaction wave. As this front will be propagating into hotter gas than the medium in which it has been formed, the new wave will accelerate until it enters the reaction zone of the primary wave. Usually such situations lead to acceleration of the primary wave which will consequently lose again the contribution of the secondary reaction. As a result an oscillating propagation velocity, related to alternating periods of unification and separation of the two reaction phases can often be observed.

# Chapter V. EVALUATION OF RESULTS.

## V. 1. Introduction.

Evaluation of experimental results should be in line with the initial justification and aims of the investigation. For the present studies, these considerations have been discussed in chapter I. Recapitulating in brief, investigation of detonation limits is intent on possible information on the structure and mechanism of detonation as obtainable from observed behaviour under marginal conditions. In the present research, homology of fuel molecules in a series of detonable systems has been added to the usual sources for information.

The evaluation of the experimental results on the detonation of hydrocarbon-oxygen mixtures has consequently been arranged in the following sections.

In section V.3, specification of detonation limits and determination of values for the systems investigated is considered.

In section V.4, the presence of any systematic information that could be attributed to homology is investigated. This is done for the results over the complete composition range of the detonation regime, as well as with particular interest to marginal conditions.

Possible conclusions that might follow from this investigation for the mechanism of hydrocarbon-oxygen detonations are discussed in section V.6.

Integral with this evaluation, attention is also paid to information related to the conclusions of previous work in the department [Miles et al., 1962, 1966]. As has been cited in section I.4, these conclusions concern the critical temperature rise and energy relaxation in the detonation front, and the contribution to detonation propagation from delayed energy liberation originating from the condensation of reaction products.

Prior to execution of this flexible programme , attention is paid to the results of the hydrogen-oxygen system. This is being dealt with in section V.2.

## V.2. The hydrogen-oxygen system.

### a. Velocity data.

In comparing the results for this system with the detonation velocities found by other investigators the agreement is on the whole satisfactory. In table V.1 some data from this work, derived from figure III.5, are compared with results obtained by other investigators. For most of the composition region concerned, differences are within

Table V. 1. Experimental detonation velocities (m/sec.) for mixtures of hydrogen and oxygen. (d = tube diameter in mm.).

| % $H_2$ | Dixon [1903] d = 9 | Berets et al. [1950) d = 10 | Schuller [1954] d = 15 | This work d = 25.4 |
|---|---|---|---|---|
| 20 | 1281 | - | 1511 | 1550 |
| 25 | 1707 | 1763 | 1730 | 1725 |
| 33.3 | 1927 | 1950 | - | 1930 |
| 50 | 2328 | 2328 | 2360 | 2320 |
| 66.7 | 2821 | 2825 | 2860 | 2845 |
| 80 | 3268 | 3390 | 3360 | 3350 |
| 89 | 3532 | - | - | 3707 |
| 90 | - | - | 3520 | 3721 |

the limits allowed for by the tube diameter effect, discussed in section II.1.a and the accuracy of velocity measurements (see appendix H ). Only near the hydrogen-rich limits do the new data rise above the other results mentioned.

The strong and reproducible fluctuations in propagation velocity, especially near the fuel-rich limit, are most intriguing and need further consideration. Possible explanations for this phenomenon are concerned with spin effects, spasmodic energy feedback from behind the C-J point, variation of reaction kinetics and with changes in energy relaxation in the detonation front.

A most striking aspect is the marked decrease in electrical conductivity of the detonation front at the first drop of the detonation velocity plot around 91% hydrogen. Within an alteration of mixture composition of 0.2%, probe output signals, as have been recorded on the oscilloscope screen, decrease in height by more than a factor of $10^3$ from 10 volts to less than 0.01 volts, although detonation like propagation velocities continue to exist for further increase of hydrogen concentration of almost two percent.

b. Detonation limits.

It is possible that the small extent of conductivity in hydrogen-oxygen detonations with more than

91% fuel explains why some investigators have found composition values for the hydrogen-rich detonation limit corresponding with such a mixture. From the present work values for respectively the oxygen-rich and the fuel-rich limit of the hydrogen-oxygen system seem to be

$$15.8\%\ H_2 \quad \text{and} \quad 92.9 - 93.0\%\ H_2 \ .$$

For the fuel-rich limit additional support can be derived from the corresponding discontinuity in the functional relation between mixture composition and overall pressure change, as displayed in figure III.6. Considering that such a step-wise change suggests a sharp difference between the overall reactions on the two sides of the critical mixture composition, it should be noticed that such a change does not seem to occur anywhere else in the same composition region. In choosing between the two values for the fuel-rich limit, the total correction to be applied to this composition for errors introduced in mixture preparation has been shown in section III.1.a to be of the order of -0.06% and could be incorporated in the result by selecting 92.9% hydrogen as the correct value.

Evaluation of the work of Pusch and Wagner [1965], who determined detonation limits for infinite tube diameters from experimental results, predicts hydrogen-oxygen limits in a 1-inch bore tube of respectively 14 and 92.8% hydrogen.

The same values can be obtained by correcting the limits found by Schuller [1954] as 15 and 91% for the difference in tube diameter, which is 15 mm as against 1-inch. Concluding, it seems that the value for the hydrogen-rich detonation limit at 92.9% hydrogen is acceptable, but that the oxygen-rich limit could be somewhat lower than 15.8% for detonations in a 1-inch tube.

c. Shock front temperatures for composition limits.

As has been explained, the temperature rise in the detonation front can be calculated from experimental velocity data. To this end, the front is considered as a pure shock, propagating at the same speed and through the same mixture as the detonation wave. In section IV.2.c, equation (IV.32) has been derived to express the temperature rise as a function of the Mach-product, $\gamma M^2$, which is proportional to the square of the propagation velocity; see equation (IV.24).

The method is in principle equally applicable to the experimental velocity data for all mixture compositions inside the detonation regime. However, under marginal and limiting conditions the spread in values for the Mach-products is even wider than for the velocities. Interpretation of the temperature rise calculated for

individual experiments in this composition region, is therefore not generally applicable. By comparison it is more useful to extrapolate the graphical representation of $\gamma M^2$-values as a function of mixtures with stable detonation to limit compositions. Limit values on such curves represent Mach-products that would have been found if detonation propagation had not failed. Assuming that shock temperatures are critical to detonation propagation [Gordon et al., 1959; Miles et al., 1962], temperature rises calculated from these limit values for the Mach-product will give the maximum temperature rise at which the detonation fails to propagate.

A selection of detonable hydrogen-oxygen mixtures has been made from table III.1, and Mach-products for these compositions have been calculated from the recorded detonation velocities. The new data are recorded in table V.2 and figure V.1. Extrapolation of the results to compositions of limit detonation gives a value for the Mach-product of 22.

Using equations (IV.24) and (IV.32), shock temperatures have been calculated for both limits, considering the various states of energy relaxation, discussed in section IV.2.b. The results are given in table V.3. Values for temperature rise, leading to breakdown of

Table V. 2. Mach-product numbers of detonation in mixtures of hydrogen and oxygen.

| % $H_2$ | $\gamma M^2$ | % $H_2$ | $\gamma M^2$ |
|---|---|---|---|
| 16.97 | 23.27 | 66.67 | 39.84 |
| 18.66 | 24.59 | 76.20 | 37.39 |
| 20.47 | 25.88 | 84.82 | 34.46 |
| 25.42 | 29.86 | 86.75 | 32.38 |
| 30.54 | 32.64 | 88.95 | 29.55 |
| 44.18 | 36.45 | 89.96 | 28.07 |
| 60.35 | 39.28 | 90.77 | 26.54 |

Table V. 3. Shock temperatures in degrees Kelvin of hydrogen-oxygen detonations at limit mixture compositions, calculated for various degrees of energy relaxation. (The underlined values are those for the most likely condition).

| Degree of energy relaxation. | Limit composition 16% $H_2$ | 93% $H_2$ |
|---|---|---|
| a. Translational only | 1590 | 1590 |
| b. $H_2$ : transl.<br>$O_2$ : transl. + rot. | 1280 | 1250 |
| c. transl. + rot. | 1230 | 1230 |
| d. $H_2$ : equipartition<br>$O_2$ : transl. + rot. | <u>1220</u> | <u>1205</u> |
| e. equipartition | 1135 | 1200 |

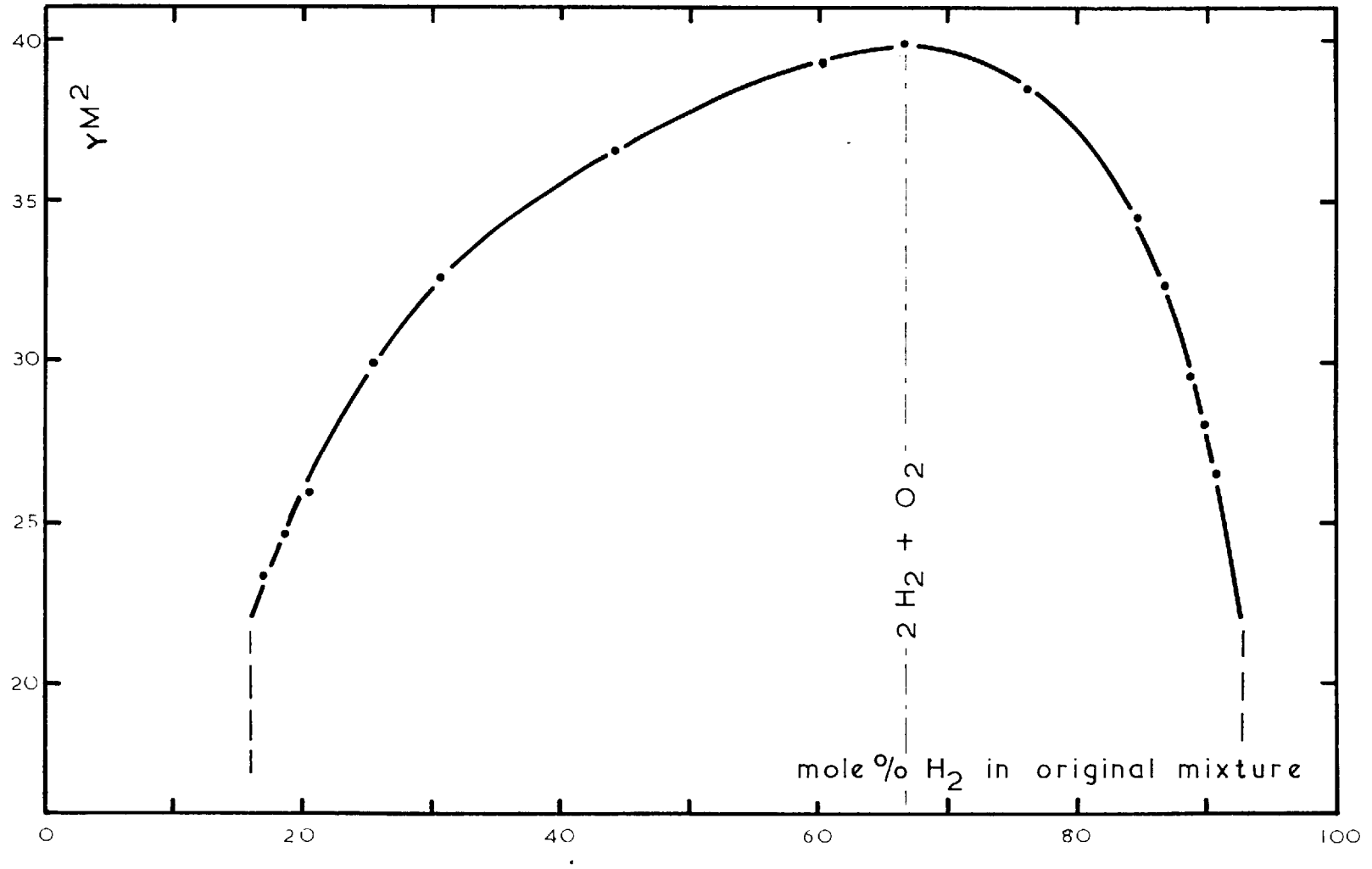



Fig. V. I. Mach product for the system hydrogen-oxygen.

detonation propagation, correspond well with the results of Gordon et al., [1959] and Miles et al., [1962], when equipartition of energy is assumed.

Wagner [1961] compared information from various authors on the length of induction periods for stoichiometric hydrogen-oxygen detonation and concluded that for initial pressures of one atmosphere, induction times are of the order of 1 $\mu$sec. This value can be considered as a minimum for limit conditions, where induction times will certainly not be shorter than for stable detonation.

In table V.4, some data have been collected for rotational and vibrational relaxation of hydrogen, oxygen and nitrogen at atmospheric pressure. As can be seen, rotational relaxation times for these gases under shock conditions must be negligible compared with the length of the detonation induction period.

Vibrational relaxation, however, needs more careful consideration. For a proper evaluation of the data in table V.4, relaxation times have to be multiplied with the ratio of the initial pressure over the mean pressure in the shock-front and the induction zone. For marginal detonation of 1 atmosphere hydrogen-oxygen mixtures this ratio is approximately 1/20. On this basis it seems unlikely that attainment of complete randomisation of energy

Table V. 4. Rotational and vibrational relaxation times in microseconds for hydrogen, oxygen and nitrogen at 1 atmosphere (compiled and evaluated from data by Cottrell and McCoubrey [1961] and Gaydon and Hurle [1963].

| | $H_2$ | $O_2$ | $N_2$ |
|---|---|---|---|
| Rotational relaxation | | | |
| 298°K | 0.023 | 0.002 | 0.002 |
| Vibrational relaxation | | | |
| 1200°K | | 20 | 660 |
| 1300°K | | 15 | 540 |
| 1400°K | | 12 | 440 |
| 1500°K | | 10 | 350 |
| 1600°K | | 9 | 280 |
| 2600°K | 0.8 | | |

distribution in hydrogen is not achieved before initiation of chemical reaction. However, a possible error, due to this assumption being false, will only have a negligible effect on the value of the calculated shock temperature, as can be seen from table V.3. For oxygen the chances seem to be in balance, as to whether vibrational relaxation does occur just before reaction initiation or not. Consequently the criterion for the calculation of a critical temperature for detonation propagation is somewhat in favour of the rotational temperature as this situation represents better the average condition throughout the induction zone. Shock temperatures for this most probable situation are given in table V.3, column d.

Data for the vibrational relaxation of nitrogen, which are also given in table V.4, support the opinion of Miles et al. [1962] that nitrogen additives in hydrogen-oxygen detonations do not participate appreciably in the energy exchange before the onset of chemical reaction. Even if induction periods in marginal detonation were 10 or 20 microseconds long, the vibrational relaxation of nitrogen would probably be too slow to influence the temperature of the induction zone.

d. The Mach-product as function of composition.

It has been explained briefly in section IV.1.g that the value of $\gamma M^2$ is effectively proportional to the extent to which the energy, released in the detonation wave, contributes to sustentation of the detonation front. This does not mean that detonation velocities are not indicative of the efficiency of the self supporting mechanism of detonation. For easy appreciation, Mach-product data are more convenient as can be explained as follows.

Considering equations, it is possible to write :

$$(V.1) \qquad \frac{u_1^2 m_1}{RT_1} = \gamma M^2 \propto q = \frac{2Q\, m_1}{RT}$$

Consequently the detonation velocity is proportional to Q, which has been described as the heat release per unit of mass, which means, per gram. The Mach-product however is proportional to q, which is the heat release per mole of mixture.

Maxima in the velocity data will therefore be obtained for mixtures with the highest energy release per gram of mixture. This composition will depend on the difference between the molecular weights of the components in the system, and is not related in a simple way to the chemistry of the process. On the other hand, maxima for

Mach-product data are found for mixtures with the highest energy release per mole of mixture and the corresponding compositions are directly related to the stoichiometry. Hence, although velocity-compcsition curves have an implicit significance for the energy factor in detonation propagation, the relation is much clearer illustrated by the Mach-product -mixture composition relation.

Further study of the Mach-product curve, given in figure V.1, reveals that for the hydrogen-oxygen system the maximum value of $\gamma M^2$ is reached for the stoichiometric composition ratio. This indication agrees with the traditional interpretation of chemical stoichiometry and with the profile of the diagram in figure III.6, for the overall pressure change resulting from detonation. It also illustrates the above given argument that for consideration of energy release in detonation processes, the Mach-product is generally a more useful parameter than the detonation velocity.

## V.3. Detonation limits for systems of saturated aliphatic hydrocarbon and oxygen.

Determination of the detonation limits for the systems investigated must follow from the experimental information collected in tables III.2 to III.5. In view of

the small variations between the combined marginal effects for the different systems, a standardised assessment is required for all charafacteristic phenomena that can be observed under marginal conditions.

True to the original macroscopic description by Berthelot and Veille [1881], a detonation will in principle continue to propagate at its characteristic velocity, irrespective of the length of the tube. On this basis the detonation regime for a system is the continuous range of all mixture compositions that will maintain combustion processes of this type. In the present research the potentiality for continuous detonation propagation is ascribed to all gaseous mixtures stored in a 1-inch bore tube of limited length, that will satisfy the following requirements.

In the first place the experiment must be carried out at ambient pressure and room temperature and be initiated by detonation impact from a mixture of stoichiometric hydrogen-oxygen. Secondly, it must lead to a "detonation-like" wave, propagating with an overall velocity at least orders of magnitude higher than normal combustion processes. Furthermore, under near-limit conditions, the overall pressure change and the nature of condensation products should be comparable with results obtained in adjacent regions with steady state detonation. Finally, re-ignition of the test mixture on reflection of the primary shock front from the

end plate of the detonation tube is not permitted; such phenomena must be considered as proof of insufficient energy liberation in the primary wave to guarantee continuation of sufficient energy support for the propagation of the detonation front.

By the gradual change of mixture composition towards a greater excess of one component, detonation limits are found as the intermediate between the composition of the most diluted mixture that satisfies all the four requirements and the least diluted mixture that fails to do so. It follows that the uncertainty of the limit composition depends on the accuracy and the reproducibility with which the test mixtures can be made. In section III.1.a this uncertainty has been shown to be less than 0.05%.

Results, given in tables III.2 to III.5 have been compared on the basis described above and detonation limits for the saturated hydrocarbon-oxygen systems were found to be those given in table V.5. For comparison, results for the system ethane-oxygen have again been taken from the experiments by Schuller [1954]. As those experiments were performed in a tube with an internal diameter of 15 mm., these limit data will indicate a narrower detonation regime than the composition values of limit detonation that will be obtained from ethane-oxygen detonations in a 1-inch bore tube.

Table V.5. Composition limits in percentage fuel for detonation in a one-inch bore tube of binary mixtures of oxygen and saturated aliphatic hydrocarbons, at ambient pressure and temperature. (Results for ethane-oxygen by Schuller in a 15 mm bore tube; between brackets evaluated limits for one-inch tube)

| Mixture $O_2$ + | Oxygen-rich limit ± 0.05 % | Fuel-rich limit ± 0.10% |
|---|---|---|
| Methane | 8.25 | 55.80 |
| Ethane | 4.0 [3.6] | 46.0 [46.4] |
| n-propane | 2.50 | 42.50 |
| n-butane | 2.05 | 37.95 |
| neo-pentane | 1.50 | 33.00 |

Results of the comparative study by Pusch and Wagner [1962, 1965], mentioned in section II.1.a, allows for an estimated correction of approximately one-third of a percent, to evaluate the limits for a 1-inch tube. As will be shown later, these corrected values fall in very well with the results of this work.

The fuel-rich limit for "Natural grade" propane of 96% purity, which is not given in table III.3, is approximately 41.1% propane, or about 1.4% inside the fuel-rich limit for 99.5% pure propane. The fluctuating marginal phenomena which are characteristic for all the near-limit mixtures of the high purity gases, have not been observed for mixtures of "Natural-grade" propane. The oxygen-rich limit for normal-pentane seems to be the same as for neo-pentane.

For some of the systems that are investigated in the present research, other authors report different results, some of which will be discussed here (see also table I.1).

Methane-oxygen detonations have been investigated by Pusch and Wagner [1965]. For a 16 mm. bore tube, the detonation limits are claimed by them to be respectively 8.5 and 51.5% methane. Extrapolation of these results by their own method to values for a one inch tube gives limit values of 8.1 - 52.0% methane. For the oxygen-rich limit the

agreement is quite satisfactory, but the fuel-rich limit is almost 4% lower than the result given in table V.5. However, Pusch and Wagner used 20 metres long test sections and detonation initiation was achieved in two steps. The first step involved spark ignition of stoichiometric methane-oxygen, the second step stabilisation of detonation propagation in a 10 cm. bore tube. The impact of this detonation on the test mixture in the narrow tube will probably not be identical to the impact from a detonating mixture of stoichiometric hydrogen and oxygen.

The methane-oxygen system has also been investigated by Payman and Walls [1923], who reported limits of 11.1 and 53.3% methane in a 1-inch tube.

Limits, as found by Laffitte and Breton [1936] for mixtures of oxygen and respectively propane and n-butane, are given as 3.1 - 37.0% propane and 2.8 - 31.4% butane. These limits are once more, well inside the detonation regimes, determined by the results in table V.5. However, Laffitte and Breton used a 14 mm bore tube, a low purity gas and a solid detonator of mercury fulminate for detonation initiation. Evaluation of results for the difference in tube diameter explains most of the difference in composition for the oxygen-rich limits.

Considering in general the different results and

the corrections that have to be applied to reach the limit compositions found in the present experiments, it seems that the values for the oxygen-rich limits can be correlated by evaluation of the influence of the tube diameter [Pusch and Wagner, 1965]. For the fuel-rich limits, other factors like strength of initiation impact seem to play an important role. This seems to agree with the fact that the critical temperature-rise required for detonation at the limit mixture composition is probably higher for all hydrocarbon-rich limits than for the oxygen-rich limits, as will be shown in section V.3.c.

## V.4. Homologous aspects of hydrocarbon-oxygen detonation.

### a. The detonation velocity data.

At this stage, the main results of this investigation comprise the detonation velocity data, displayed in figure III.7 and the variation with composition of the overall pressure change, shown in figure III.10. Actual values for these data and for the related mixture compositions can be found in tables III.2 to III.5, and the table for the compositions of the detonation limits, table V . 5. As has been explained, the experiments have been undertaken to find out whether the similarities and differences in the detonation of mixtures

of oxygen and various homologous fuel molecules, would reveal anything about the mechanism of stable or marginal detonation. Consequently the results must now be studied for such information. However the evaluated data for the overall pressure change may in part depend on reactions that do not contribute to detonation propagation. The comparative study of homologous effects must therefore be restricted to the velocity data, until some idea has been obtained on the reaction mechanism that leads to the recorded values for the change in pressure.

First observation of the profiles in figure III.7 shows a series of curves, similar in shape and height. As can be expected on the basis of classical reaction chemistry, the curves lie in the regions of higher oxygen contents for fuel molecules of relatively high molecular weight. Also, the narrowing of the detonation regime as the weight of the fuel molecule is increased is to be expected. Limits seem to contract around the stoichiometric mixture composition with increase of the molecular weight of the fuel molecule and to tend towards 100% oxygen as the number of carbon atoms in the hydrocarbon goes to infinity, see figure V.2.

More careful investigation shows that the detonation velocities are almost identical for the stoichiometric mixtures and for mixtures of optimum conversion to carbon monoxide and water. This is also demonstrated in

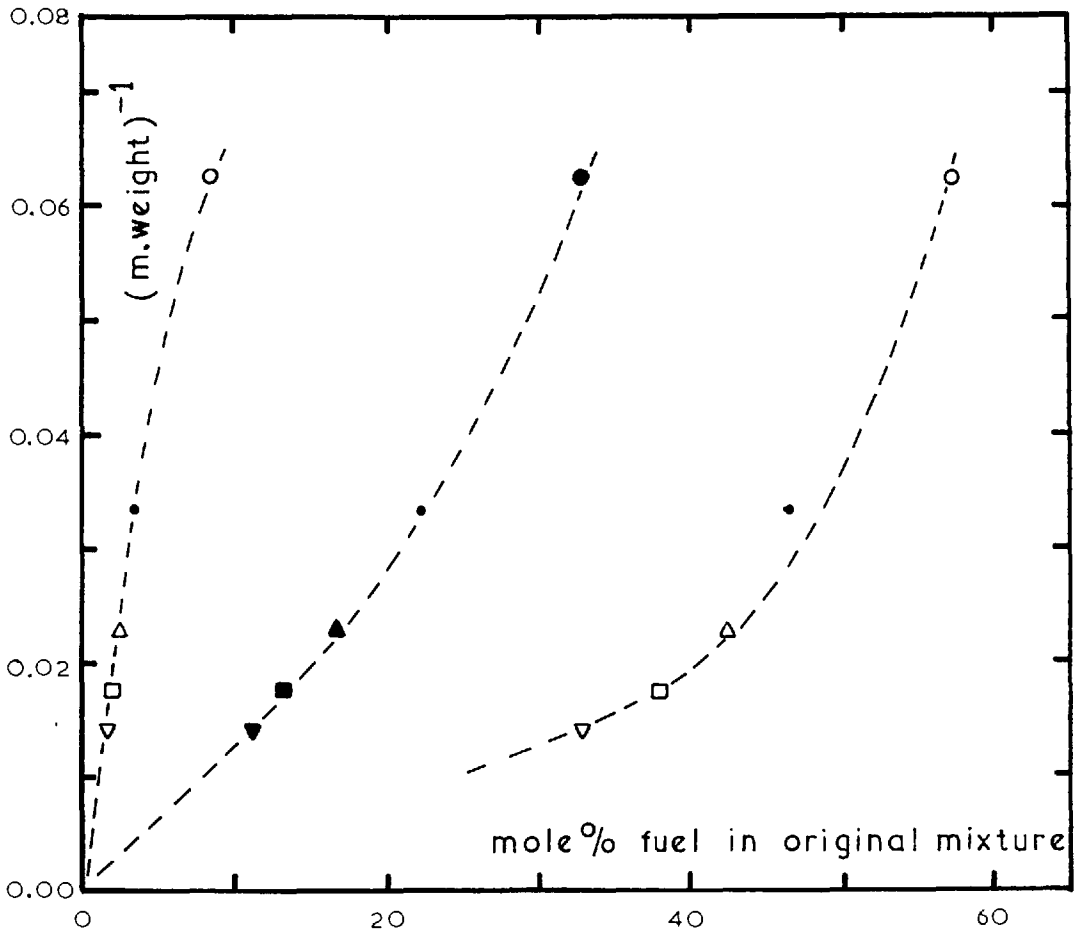



Fig. V.2. Stochiometric mixture ratios (closed symbols) and detonation limits (open symbols) for binary systems of oxygen with methane (o), ethane (•), n-propane (Δ), n-butane (□) and neo-pentane (▽).

table V.6. Apparently there is a slight, systematic decrease in velocity for both the stoichiometric mixture and the maximum velocity peak, but between the methane and pentane system, the difference is only -1.6%.

This, however, is where the general agreement ends. In fact, there is no accurate correspondence in the stoichiometry of the mixtures of maximum detonation velocity. If normalisation of the curves is attempted on this composition fair agreement will be obtained for mixtures on the oxygen-rich side, but towards the fuel-rich side curves will fan out. Normalisation on compositions for stoichiometric and carbon monoxide producing reactions leads only to uniformity for propagation velocities higher than 2300 metres/sec. Limit compositions failed to be normalised to a single value for all methods investigated.

Detonation propagation and detonation limits depend at least in part on the extent of energy release and energy feed-back to the shock front of the wave. This energy factor is taken into account in the equation for the conservation of energy, which is used to derive the Hugoniot relation. The success of the Hugoniot equation in evaluation of detonation velocities, confirms the energy assumption. In section IV.1.g, the energy factor has been shown to be proportional to the square of the detonation velocity and to

Table V.6. Experimental detonation velocities in metres per second for comparable binary mixtures of oxygen and saturated aliphatic hydrocarbons.

| | $C_nH_{2n+2} \rightarrow CO_2+H_2O$ | | $C_nH_{2n+2} \rightarrow CO + H_2O$ | | Maximum velocity |
|---|---|---|---|---|---|
| | %fuel | Veloc. | %fuel | veloc. | |
| Methane | 33.3 | 2395 | 40.0 | 2535 | 2640 |
| Ethane | 22.2 | 2370 | 28.6 | 2550 | 2630 |
| n-propane | 16.7 | 2385 | 22.2 | 2550 | 2620 |
| n-butane | 13.3 | 2365 | 18.2 | 2535 | 2610 |
| neo-pentane | 11.1 | 2355 | 15.4 | 2535 | 2600 |

depend furthermore on the ratio of the specific heats and the square of the sonic speed of the gas. In section V.2.d. it has been pointed out that the energy factor, directly related to the square of the detonation velocity is the energy release per gram of detonable mixture. It has been shown why it is more useful to convert the velocity results into Mach-product values, which are proportional to the energy release per mole of mixture.

As for aspects of homology of fuel molecules in comparative studies, the similarities and systematic changes in molecular structures are related to differences in bond-energies and reaction energies. Hence, although similarities in the velocity-composition curves, for the homologous series, such as given in table V.6, are significant, the chemistry is better illustrated by a comparison between the various curves for the relation of Mach-product and mixture composition in mole ratios.

b. Mach-product data.

Mixture compositions have been selected from tables III.2 to III.5 and Mach-products have been derived from the corresponding velocity-data. Recorded temperature values around ambient conditions have been used in these calculations. The results are given in tables V.7 to V.10, columns 1 and 2.

Table V. 7. Mach-product numbers and values for relative Mach-products and related mixture composition expressed as function of the co-ordinates with maximum Mach-product, for the system methane - oxygen (see also table V.11).

| % $CH_4$ | $\gamma M^2$ | $\frac{\text{composition}}{\text{comp. } \gamma M^2 \text{ max}}$ | $\frac{\gamma M^2}{\gamma M^2 \text{ max}}$ |
|---|---|---|---|
| 8.20 | 23.001 | 0.186 | 0.335 |
| 8.25 | 31.231 | 0.188 | 0.455 |
| | 26.087 | | 0.380 |
| 8.34 | 41.271 | 0.190 | 0.601 |
| | 34.382 | | 0.500 |
| 8.65 | 36.562 | 0.197 | 0.532 |
| | 32.337 | | 0.471 |
| 9.72 | 34.908 | 0.221 | 0.508 |
| 13.31 | 40.868 | 0.303 | 0.595 |
| 16.81 | 45.751 | 0.382 | 0.666 |
| 26.77 | 55.826 | 0.608 | 0.813 |
| 33.31 | 62.136 | 0.757 | 0.904 |
| 45.12 | 68.624 | 1.025 | 0.999 |
| 50.00 | 67.613 | 1.136 | 0.984 |
| 53.31 | 64.152 | 1.212 | 0.934 |
| 54.92 | 60.506 | 1.248 | 0.881 |
| 55.64 | 58.504 | 1.265 | 0.852 |

Table V. 8. Mach-product numbers and values for relative Mach-products and related mixture composition expressed as function of the co-ordinates with maximum Mach-product, for the system n-propane - oxygen (see also table V.11).

| $\%C_3H_8$ | $\gamma M^2$ | composition / comp. $\gamma M^2_{max}$ | $\gamma M^2 / \gamma M^2_{max}$ |
|---|---|---|---|
| 2.56 | 27.764 | 0.088 | 0.279 |
| 3.03 | 33.629 | 0.104 | 0.338 |
| 3.61 | 35.927 | 0.124 | 0.361 |
| 4.16 | 39.541 | 0.142 | 0.397 |
| 5.17 | 43.892 | 0.177 | 0.441 |
| 10.14 | 60.483 | 0.347 | 0.608 |
| 15.14 | 75.288 | 0.518 | 0.757 |
| 20.21 | 87.377 | 0.692 | 0.878 |
| 25.00 | 96.609 | 0.856 | 0.971 |
| 29.07 | 99.343 | 0.996 | 0.998 |
| 30.97 | 99.485 | 1.061 | 1.000 |
| 33.97 | 94.827 | 1.163 | 0.953 |
| 35.03 | 90.586 | 1.200 | 0.910 |
| 36.55 | 84.773 | 1.252 | 0.852 |
| 37.96 | 76.583 | 1.300 | 0.770 |
| 38.89 | 71.834 | 1.332 | 0.722 |
| 40.02 | 66.795 | 1.371 | 0.671 |
| 41.03 | 63.403 | 1.405 | 0.637 |
| 42.07 | 58.664 | 1.441 | 0.590 |
| 42.49 | 52.178 | 1.455 | 0.524 |

Table V.9. Mach-product numbers and values for relative Mach-products and related mixture composition expressed as function of the co-ordinates with maximum Mach-product, for the system n-butane - oxygen (see also table V.11).

| $\%C_4H_{10}$ | $\gamma M^2$ | composition / comp. $\gamma M^2_{max}$ | $\gamma M^2 / \gamma M^2_{max}$ |
|---|---|---|---|
| 2.10 | 27.890 | 0.083 | 0.259 |
| 2.39 | 32.814 | 0.094 | 0.305 |
| 3.01 | 37.105 | 0.119 | 0.345 |
| 3.61 | 39.803 | 0.143 | 0.370 |
| 7.20 | 57.940 | 0.285 | 0.539 |
| 13.43 | 81.013 | 0.531 | 0.754 |
| 20.85 | 102.780 | 0.824 | 0.956 |
| 27.01 | 106.006 | 1.068 | 0.986 |
| 31.04 | 93.075 | 1.227 | 0.866 |
| 34.07 | 75.133 | 1.347 | 0.699 |
| 35.34 | 67.036 | 1.397 | 0.624 |
| 36.47 | 65.374 | 1.442 | 0.608 |
| 36.95 | 64.881 | 1.460 | 0.604 |
| 37.01 | 60.173 | 1.463 | 0.560 |
| 37.18 | 60.237 | 1.470 | 0.560 |
| 37.35 | 59.665 | 1.476 | 0.555 |
| 37.54 | 63.233 | 1.484 | 0.588 |
| 37.75 | 80.312 | 1.492 | 0.747 |
| 37.93 | 54.335 | 1.499 | 0.505 |
| 38.17 | 15.563 | 1.509 | 0.145 |

Table V.10. Mach-product numbers and values for relative Mach-products and related mixture composition expressed as function of the co-ordinates with maximum Mach-product, for the system neo-pentane - oxygen (see also table V.11)

| % $neoC_5H_{12}$ | $\gamma M^2$ | composition / comp. $\gamma M^2_{max}$ | $\gamma M^2 / \gamma M^2_{max}$ |
|---|---|---|---|
| 1.50 | 25.348 | 0.070 | 0.228 |
| 1.65 | 27.771 | 0.077 | 0.249 |
| 1.75 | 29.490 | 0.081 | 0.265 |
| 2.20 | 34.642 | 0.102 | 0.311 |
| 4.00 | 48.218 | 0.186 | 0.433 |
| 8.00 | 67.957 | 0.372 | 0.610 |
| 12.39 | 87.831 | 0.576 | 0.788 |
| 16.75 | 103.824 | 0.779 | 0.932 |
| 18.99 | 108.547 | 0.883 | 0.974 |
| 21.19 | 111.383 | 0.986 | 1.000 |
| 23.04 | 108.078 | 1.072 | 0.970 |
| 25.04 | 101.562 | 1.165 | 0.912 |
| 26.48 | 96.006 | 1.232 | 0.862 |
| 27.99 | 82.878 | 1.302 | 0.744 |
| 29.99 | 74.816 | 1.395 | 0.672 |
| 30.96 | 72.236 | 1.440 | 0.648 |
| 32.20 | 85.432 | 1.498 | 0.767 |
| 32.60 | 87.640 | 1.516 | 0.787 |
| 32.90 | 68.839 | 1.530 | 0.618 |
| 33.04 | 59.978 | 1.537 | 0.538 |

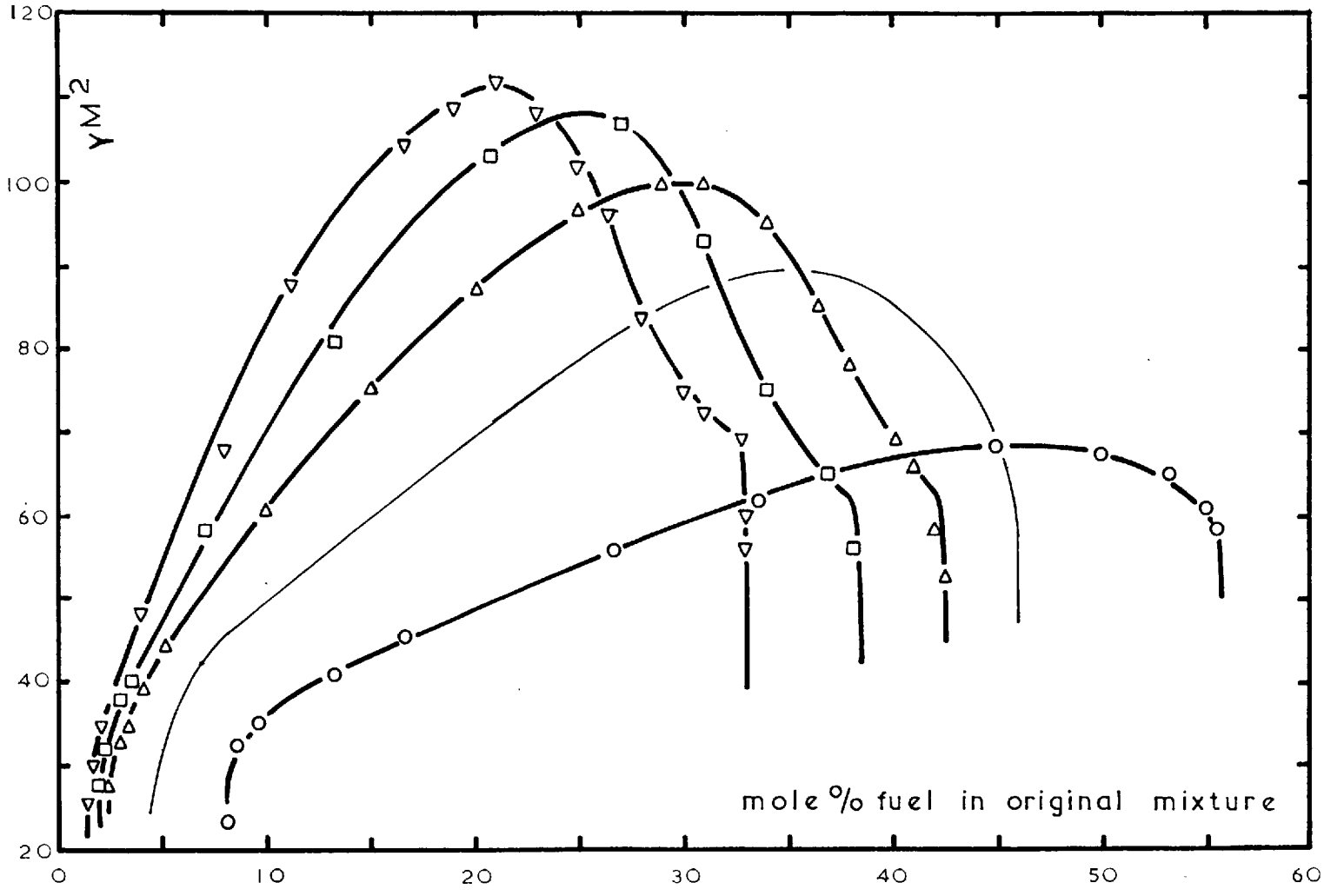



Fig. V. 3. Mach product for binary systems of oxygen with methane (o), ethane, n-propane(△), n-butane(□) and neo-pentane(▽).

Similar data for the ethane-oxygen mixture have again been obtained from Schuller's work [1954] and are given in appendix G, table 1. This applies also to all further calculations, on ethane, to be discussed in this study.

All data are also recorded in figure V.3. Compared with the pattern of the velocity curves, all comments related to mixture compositions only, still remain valid and aspects of the homology of the fuel molecules related to composition have not changed. The ordinate values, however, which represent the Mach-products, have changed the pattern considerably. Compositions for maximum $\gamma M^2$ differ from those for maximum velocity. The maximum values of the Mach-product all lie on a straight line, rising towards the systems with heavier hydrocarbons. The peak value for the neo-pentane -oxygen mixture seems however approximately 5% lower than the value given by the straight line for the same composition. On different straight lines can respectively be found all stoichiometric mixture compositions and all mixture ratios corresponding to complete conversion to carbon monoxide and water.

Another noticeable difference with the situation for the velocity curves is the similarity in the values of the curves for the compositions of the detonation limits. At the oxygen-rich limits, $\gamma M^2$ values are all around 30,

at the fuel-rich limits, breakdown values for the Mach-product are all approximately equal to 60. This similarity and the consequences of it for the shock-temperatures at limit conditions will be discussed in more detail in the next section

Graphical representation of the Mach-product data for each of the different systems, as realised in figure V.3, does not take any more advantage of the homology of the fuel molecules as the records of the detonation velocities, shown in figure III.7. However, unlike the maxima in the velocity-profiles, peak values for the Mach-product data of each system are fundamentally significant. On the basis of previously discussed considerations, the $\gamma M^2$-maxima must be obtained for such mixture ratios of each system as will produce the maximum degree of output and internal transfer of energy.

It is this common property of the maxima for the Mach-products, evaluated as experimental function of mixture composition, which permits incorporation of the homology of fuel molecules into a meaningful comparative investigation. For this purpose it is provisionally postulated that the reaction mechanism in the detonation of saturated aliphatic nydrocarbons with oxygen is similar at the maximum values for the Mach-product of each system. Depending on the validity of the assumption it can be expected to be more successful for comparative study of detonation properties of the higher

members of the homologous series, which have relatively small structural differences compared with methane and ethane.

Assuming that the explained similarity does exist, the homology of the fuel molecules can be taken into account by normalisation of the results on the coordinates of the points for which $\gamma M^2$ reaches its maximum value. From the individual curves in figure V.3, these maxima have been determined graphically. Coordinate values for this state in each system are given in table V.11. Normalisation of the data is subsequently achieved by expressing the coordinates for points on the various Mach-product curves as fraction of the coordinates given in table V.11 for each system. The new, dimensionless coordinates, derived in this way, are given in tables V.7 to V.10, columns 3 and 4, and are all recorded in figure V.4

The uniformity of results in the new representation is noteworthy. Although variations of a few percent around the mean value of $\gamma M^2 / \gamma M^2_{max}$ occur in some places, general correspondence in the data for different systems appears reasonable enough to construct a "master-curve" for detonation of saturated aliphatic hydrocarbons on this basis. Such a master curve will be satisfactory for all mixture compositions containing not more than 1.35 times the amount of hydrocarbon for which the Mach-product is maximal. For marginal detonation with excess of oxygen the master curve

Table V. 11. Co-ordinates for points of maximum $\gamma M^2$ for Mach-products as function of mixture composition; results for detonation of binary systems of oxygen and saturated aliphatic hydrocarbons.

| Fuel | $\gamma M^2_{max}$ | % Fuel |
|---|---|---|
| Methane | 68.7 | 44.0 |
| Ethane | 89.0 | 36.0 |
| n-propane | 99.5 | 29.2 |
| n-butane | 107.5 | 25.3 |
| neo-pentane | 111.4 | 21.5 |

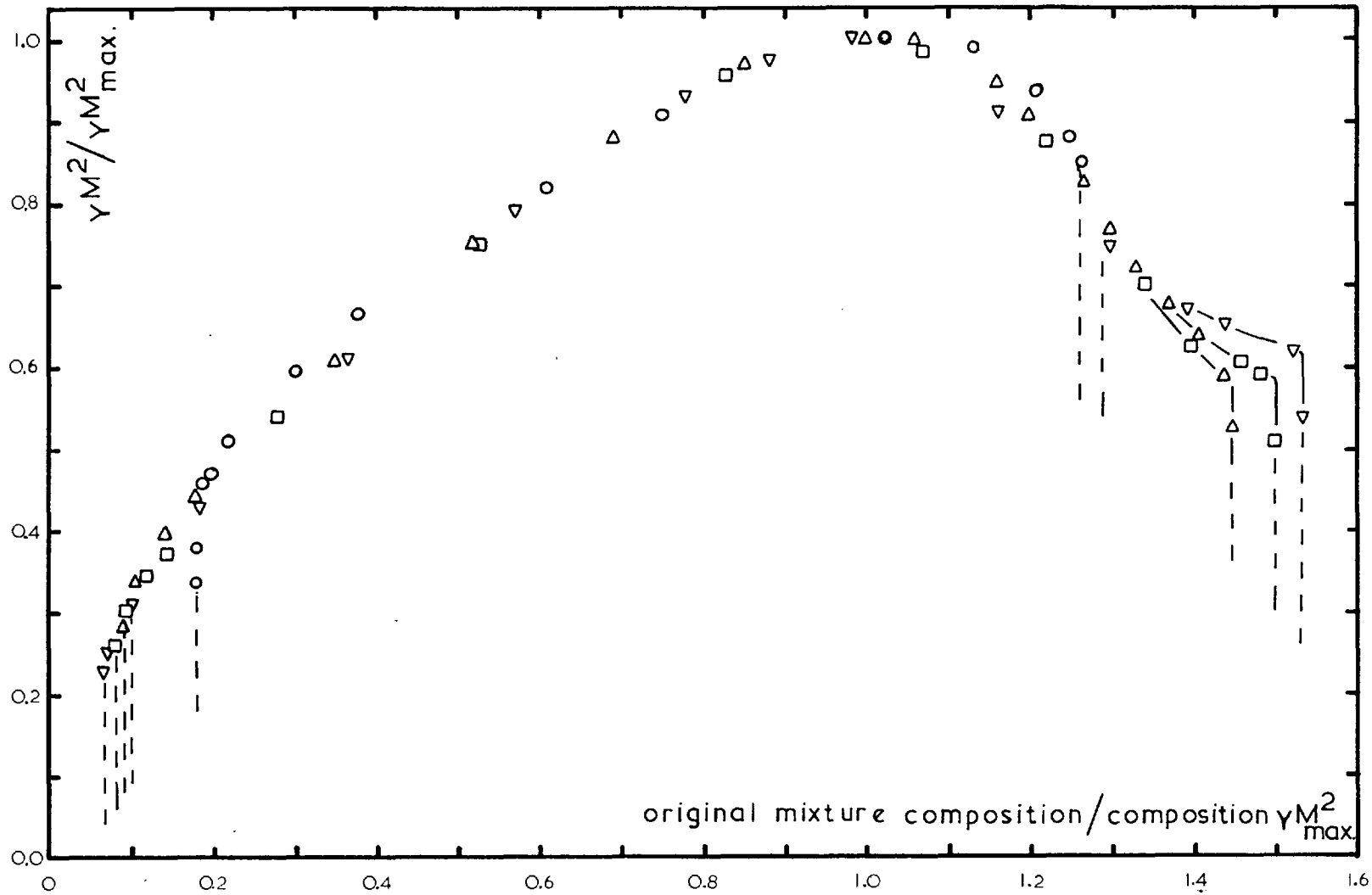





Fig. V.4. Relative Mach product vs. compositions as fraction of mixtures with maximum $\gamma M^2$; systems: oxygen with methane(o), n-propane(Δ), n-butane(□) and neo-pentane(▽).

is to be extrapolated on its existing trend to composition values somewhat beyond the oxygen-rich detonation limit for (neo)-pentane.

The master curve fails to represent two aspects of the experimental results. In the first place uniformity breaks down for compositions with higher hydrocarbon content than 1.35 times the amount for $\gamma M^2_{max}$. As can be derived from the notes on the formation of solid condensation products, the failure of this master-curve applies to the composition regions in which heavy soot formation has been observed; evaluation of data of figure III.10 indicates excessive deposits for composition ratios higher than 1.25 times $c\,\gamma M^2_{max}$.

The second failure of uniformity applies to the limit-compositions. However, by changing composition ratios towards excess concentration of either oxygen or fuel, limit compositions are reacned successively for all systems, starting with methane and followed by the other hydrocarbons in the sequence of the homologous series.

c. Shock front temperatures for composition limits.

The master curve for Mach-product values of alkanes-oxygen detonations has a special application for the calculation of critical shock temperatures for composition

limits to detonation propagation. The use of the Mach-product for this purpose has been explained in section IV.2.c and has further been illustrated by calculations for the detonation limits of the hydrogen-oxygen system, see section V.2.c.

In the representation of the master curve, the reliability of Mach-product values for individual systems is increased by the correlation to the values obtained for mixtures of other hydrocarbons and oxygen. This applies in particular to the limit values, which for each system are given accurately by the Mach-product data of the higher members of the homologous series. In view of the breakdown of uniformity near the fuel-rich limits, the advantage does not exist for temperature calculations on shock-fronts with excess hydrocarbon. For those limits and for the oxygen-rich limit of the pentane system, the usual extrapolation of the existing curves should again be used.

For the determination of limit values of $\gamma M^2$, the composition limits given in table V.5 must first be expressed as fraction of the compositions with maximum $\gamma M^2$, given in table V.11. Values for the Mach-product ratio can then be found from figure V.4. Actual limit values for $\gamma M^2$ are subsequently calculated with the maxima data in table V.11. With the use of equation IV.24, critical requirements for the temperature rise in the detonation front, to permit

detonation propagation under marginal conditions, can then be calculated. On the basis of the discussion in section IV.2.b, various degrees of internal energy relaxation can be considered.

Calculations of this type have been carried out for both limits of all systems investigated. Limit values for $\gamma M^2$ and critical shock temperatures are given in table V.12. With respect to the shock-temperature, various combinations of incomplete relaxation and equipartition of energy have been considered. Enthalpy data for the equilibrium state have been obtained from data for the ideal gas state, published in the Tables of the American Petroleum Institute, Research Project 44, 31 December 1952; tables Ou and 1u. For calculations at the fuel-rich limits of the methane and ethane system, the enthalpy data have been extrapolated to temperatures above 1500°K, according to the existing trend.

There seems to be little information in literature on induction times for hydrocarbon-oxygen detonation at 1 atm. However, it seems unlikely that the difference with hydrogen-oxygen detonations will be of orders of magnitude. The minimum time required for initiation of chemical reaction for the time being, is assumed to be approximately one microsecond.

Table V. 12. Mach-product numbers and shock-temperatures in degrees Kelvin for composition limits in detonation of binary systems of oxygen and saturated aliphatic hydrocarbons, assuming various degrees of relaxation of internal energy. (The most likely conditions are underlined ; temperatures rounded off to $5^{\circ}$).

| Limit, $\gamma M^2$ and degree of relaxation. | Mach product and shock-temperature | | | | |
|---|---|---|---|---|---|
| | $CH_4$ | $C_2H_6$ | $C_3H_8$ | $C_4H_{10}$ | $C_5H_{12}$ |
| 1. $O_2$-rich limit | | | | | |
| $\gamma M^2$ | 29.54 | 27.59 | 26.87 | 27.95 | 25.62 |
| a.translation. | 2035 | 1910 | 1865 | 1930 | 1795 |
| b.transl.+rot. | 1530 | 1455 | 1425 | 1470 | 1375 |
| c.$C_nH_m$ : equip. $O_2$: trans.+rot. | <u>1430</u> | <u>1360</u> | <u>1325</u> | <u>1355</u> | <u>1270</u> |
| d.equipartition. | 1315 | 1250 | 1220 | 1245 | 1175 |
| 2. Fuel-rich limit | | | | | |
| $\gamma M^2$ | 57.36 | 70.31 | 58.21 | 62.35 | 69.07 |
| a.translation. | 3660 | 4420 | 3710 | 3950 | 4345 |
| b.transl.+rot. | 2545 | 3085 | 2615 | 2795 | 3085 |
| c.$C_nH_m$:equip, $O_2$:trans.+rot. | <u>1690</u> | <u>1580</u> | <u>1220</u> | <u>1175</u> | <u>1185</u> |
| d.equipartition | 1640 | 1540 | 1200 | 1155 | 1165 |

As a first consequence, translational and rotational relaxation of the oxygen molecules must be considered to be complete within a fraction of the total induction period (see discussion of hydrogen-oxygen results, section V.2.c). Relaxation times for poly-atomic molecules are, as a rule, much shorter than for di-atomic molecules, which means that the hydrocarbons must at least be translationally and rotationally relaxed too.

Data for the vibrational relaxation of saturated aliphatic hydrocarbons have been compiled and evaluated from the work by Cottrell and McCoubrey [1961] and are given in table V.13. For application to the results of this work, the relaxation times quoted for ambient conditions have to be reduced on account of three factors. In the first place, temperature conditions in the shock-front and the induction zone will reduce the given values 3 to 10 times. Secondly, pressure conditions require another reduction by at least a factor of 10. Finally, induction times of mixtures are known to be generally shorter than those for pure components. Consequently it is unlikely that even methane or ethane molecules will not reach a state of equipartition of internal energy, long before the onset of chemical reaction.

As for the oxygen molecules in the limit mixtures, the same considerations as for the hydrogen-oxygen system

Table V.13. Vibrational relaxation times in $\mu$ sec. at ambient pressure for aliphatic hydrocarbons, compiled and evaluated from data by Cottrell and McCoubrey [1961].

| Substance | 298°K | 473°K | 573°K | 1300°K (estim.) |
|---|---|---|---|---|
| Methane | 1.86 | 0.67 | 0.58 | 0.30 |
| Ethane | 0.018 | | | |
| n-propane | 0.0041 | | | |
| n-butane | $<$ 0.0015 | | | |
| neo-pentane | $<$ 0.0015 | | | |
| Ethylene | 0.2 | 0.149 | 0.126 | 0.08 |
| Propylene | $<$ 0.006 | | | |

Table V.14. Mixture composition for maximum Mach-product and compositions of classical stoichiometry in binary mixtures of oxygen and saturated aliphatic hydrocarbons.

| Fuel | $C_nH_{2n+2} \rightarrow CO_2+H_2O$ | $C_nH_{2n+2} \rightarrow CO+H_2O$ | $\gamma M^2_{max}$ |
|---|---|---|---|
| Methane | 33.3 | 40.0 | 44.0 |
| Ethane | 22.2 | 28.6 | 36.0 |
| n-propane | 16.7 | 22.2 | 29.2 |
| n-butane | 13.3 | 18.2 | 25.3 |
| neo-pentane | 11.1 | 15.4 | 21.5 |

suggest the possibility that throughout the induction period oxygen molecules do not achieve complete randomisation of internal energy. However, as can be observed from the data in table V.12, this does not greatly influence the actual value of the critical temperature for detonation propagation in mixtures of limit composition.

Comparison of the most probable limit temperatures evaluated indicate a critical temperature rise for the higher members of the homologous series to approximately 1300°K for the oxygen-rich limit and about 1200°K for the fuel-rich limit. Results for butane detonations with excess oxygen seem to be somewhat higher than for the other gases.

Critical temperatures for ethane and even more so for methane are considerably higher. As this is particularly true for the fuel-rich limit, the effect seems to be inherent to the nature and properties of these hydrocarbons. Aspects of this will be discussed further at a later stage.

d. Homologous correlation of initial mixture compositions and Mach-product data.

So far, no attention has been paid to a common peculiarity of the Mach-product curves, derived from the

measured detonation velocities of the systems of oxygen and saturated aliphatic hydrocarbons. This characteristic property has been hidden in the normalised representation of the master curve. For discussion it will be required to return to the data for the individual systems, recorded in figure V.3 and in the values given in table V.11.

In sub-section V.2.d. the agreement between the mixture composition of maximum energy support, indicated for the hydrogen-oxygen system by the maximum Mach-product, and the classical stoichiometry, was discussed. Investigation into these aspects from the results of figure V.3, reveals that such correspondence does not exist for data obtained from detonations in hydrocarbon-oxygen systems. For comparison, some relevant data have been collected in table V.14. Apparently, the most favourable conditions for the propagation of these hydrocarbon-oxygen detonations are to be found for a stoichiometry which has a higher fuel concentration than required for the classical reaction of complete conversion into carbon monoxide and water.

The assumption of similarity in reaction mechanism for detonation of mixtures giving maximum energy support in each system, has resulted in the construction of the master curve. This curve justifies the assumption of similarity, by extending the agreement to almost the complete range of the detonation regime for these hydrocarbon-oxygen systems.

The assumed similarity in mechanism has led to a correlation of the experimental results which depends on the state of the gas mixture at the C-J point. Consequently such similarity, resulting from the homology of the fuel molecules, would in some way also be expected from initial conditions such as the composition of those mixtures of different systems which produce comparable results.

Before making this comparison of initial conditions, two points must be emphasized. Firstly, as in the derivation of the master curve and the calculation of shock temperatures, similarity on the basis of homology can be expected to increase for comparison between higher members of the homologous series, as these have relatively small differences in physical and chemical properties. In the second place, it must be remembered that comparison of initial mixture compositions is not intended to arrange the "left-hand" terms of reaction equations. Aspects of this nature will be considered later. The present interest is only concerned with similarities between initial conditions.

Considering the fuel percentage data, given in table V.14, the mixture compositions for maximum energy production in the various systems are approximately as follows :

$$
\begin{array}{lrcl}
 & 44.0 & CH_4 & + \quad 56.0\ O_2 \\
 & 36.0 & C_2H_6 & + \quad 64.0\ O_2 \\
(V.2) & 29.2 & C_3H_8 & + \quad 70.8\ O_2 \\
 & 25.3 & C_4H_{10} & + \quad 74.7\ O_2 \\
 & 21.5 & C_5H_{12} & + \quad 78.5\ O_2
\end{array}
$$

Although a fixed trend in the changes of the hydrocarbon-oxygen ratio can be observed with increase in the molecular weight of the fuel molecule, there is no distinct similarity between these composition ratios.

The homology of normal saturated aliphatic hydrocarbons is described by the fact that each member of the series consists of a chain of characteristic length of $CH_2$ groups, which is terminated at each end by a hydrogen atom. This common property can be introduced into the arrangement (V.2), by splitting up all fuel molecules into such homologous components. If the hydrogen atoms are then combined into molecules and the various $CH_2$-values are for convenience normalised to one-hundred, (V.2) changes into :

$$
\begin{array}{lrcl}
 & 100\ CH_2 & + \quad 100\ H_2 & + \quad 127.3\ O_2 \\
 & 100\ CH_2 & + \quad 50\ H_2 & + \quad 88.9\ O_2 \\
(V.3) & 100\ CH_2 & + \quad 33.3 H_2 & + \quad 80.8\ O_2 \\
 & 100\ CH_2 & + \quad 25\ H_2 & + \quad 73.8\ O_2 \\
 & 100\ CH_2 & + \quad 20\ H_2 & + \quad 73.0\ O_2
\end{array}
$$

If, from the mixture compositions given in (V.3) the sum of the fuel elements in each mixture is expressed as a percentage of the sum of all fuel and oxygen elements in that mixture, the following fuel percentages are obtained in the given sequence

(V.4)

| | | |
|---|---|---|
| methane | $(1CH_2 + H_2)$ | : 61.11% |
| ethane | $(2CH_2 + H_2)$ | : 62.79% |
| propane | $(3CH_2 + H_2)$ | : 62.26% |
| butane | $(4CH_2 + H_2)$ | : 62.87% |
| pentane | $(5CH_2 + H_2)$ | : 62.17% |

Considering the spread in these percentage values, it must be remembered that the mixture compositions for maximum $\gamma M^2$ have been determined by a graphical method from data which have a systematical error. As furthermore, the ratios have been normalised for the $CH_2$ groups and the related hydrogen contents, all errors in(V.3) have been accumulated in the factors for the oxygen content. It can for instance be shown that an error of half a percent in the composition for $\gamma M^2$ gives an error of up to one percent in the fuel percentages given in V.4.

It appears therefore that representation of the fuel molecules in the investigated hydrocarbon-oxygen detonations by the appropriate number of $CH_2$ groups and one hydrogen molecule allows satisfactory correlation of the

compositions for which the Mach-product reaches its maximum value in the various systems.

In view of the success achieved by the construction of the master-curve for normalised Mach-product data, the present results lead readily to the next step. Representation of the mixture compositions for maximum Mach-products on the basis of the ratio between oxygen and the homology-elements of the fuels has led to satisfactory agreement between the different systems. Consequently it seems useful to investigate next what degree of similarity will be achieved when over the complete detonation regime mixture compositions for relative Mach-products $\gamma M^2 / \gamma M^2_{max}$ are represented on the basis :

$$C_nH_{2n+2} + xO_2 = nCH_2 + H_2 + xO_2$$

This implies that normalisation on compositions with maximum Mach-product values will be dropped completely. The investigation has been carried out for all mixture compositions that have also been used for the calculation of the master curve and for which data are given in tables V.7 to V.10. All composition values have been recalculated in this way and are given, together with the corresponding relative Mach-products, in tables V.15 to V.18, columns 2 and 3. These results are also recorded in figure V.5. Ethane data can again be found in appendix G, table 2.

Table V. 15. Relative Mach products, compositions on homology-element basis and reduced overall pressure changes for detonation of the system methane - oxygen.

| % $CH_4$ | $\frac{\gamma M^2}{\gamma M^2_{max}}$ | % $CH_4$ as $CH_2 + H_2$ | $p_{u_{red}} \times 10^2$ |
|---|---|---|---|
| 8.20 | 0.335 | 15.15 | 2.822 |
| 8.25 | 0.455 | 15.24 | 2.809 |
| 8.34 | 0.500 | 15.40 | 2.801 |
| 8.65 | 0.532 | 15.92 | 2.786 |
| 9.72 | 0.508 | 17.72 | 2.755 |
| 13.31 | 0.595 | 23.49 | 2.557 |
| 16.81 | 0.666 | 28.78 | 2.398 |
| 26.77 | 0.813 | 42.23 | 1.836 |
| 33.31 | 0.904 | 49.97 | 1.450 |
| 45.12 | 0.999 | 62.18 | 3.395 |
| 50.00 | 0.984 | 66.67 | 4.492 |
| 53.31 | 0.934 | 69.55 | 5.406 |
| 54.92 | 0.881 | 70.90 | 5.845 |
| 55.64 | 0.852 | 71.50 | 6.042 |

Table V. 16. Relative Mach-products, compositions on homology-element basis and reduced overall pressure changes for detonation of the system n-propane - oxygen.

| % $C_3H_8$ | $\frac{\gamma M^2}{\gamma M^2_{max}}$ | $\%C_3H_8$ as $3CH_2 + H_2$ | $p_{u_{red}} \times 10^2$ |
|---|---|---|---|
| 2.56 | 0.279 | 9.51 | 2.878 |
| 3.03 | 0.388 | 11.11 | 2.867 |
| 3.61 | 0.361 | 13.03 | 2.799 |
| 4.16 | 0.397 | 14.79 | 2.737 |
| 5.17 | 0.441 | 17.90 | 2.654 |
| 10.14 | 0.608 | 31.09 | 2.179 |
| 15.14 | 0.757 | 41.64 | 1.720 |
| 20.21 | 0.878 | 50.33 | 2.183 |
| 25.00 | 0.971 | 57.14 | 3.483 |
| 29.07 | 0.998 | 62.11 | 4.708 |
| 30.97 | 1.000 | 64.22 | 5.271 |
| 33.97 | 0.953 | 67.30 | 6.063 |
| 35.03 | 0.910 | 68.32 | 6.267 |
| 36.55 | 0.852 | 69.74 | 6.466 |
| 37.96 | 0.770 | 70.99 | 6.368 |
| 38.89 | 0.772 | 71.80 | 6.476 |
| 40.02 | 0.671 | 72.74 | 6.300 |
| 41.03 | 0.637 | 73.57 | 6.093 |
| 42.07 | 0.590 | 74.39 | 6.018 |
| 42.49 | 0.524 | 74.72 | 6.026 |

Table V.17. Relative Mach-products, compositions on homology-element basis and reduced overall pressure changes for detonation of the system n-butane - oxygen.

| % $C_4H_{10}$ | $\gamma M^2 / \gamma M^2_{max}$ | $\%C_4H_{10}$ as $4CH_2 + H_2$ | $p_{u_{red}} \times 10^2$ |
|---|---|---|---|
| 2.10 | 0.259 | 9.69 | 2.903 |
| 2.39 | 0.305 | 10.91 | 2.866 |
| 3.01 | 0.345 | 13.43 | 2.803 |
| 3.61 | 0.370 | 15.77 | 2.753 |
| 7.20 | 0.539 | 17.95 | 2.311 |
| 13.43 | 0.754 | 43.68 | 1.735 |
| 20.85 | 0.956 | 56.84 | 3.480 |
| 27.01 | 0.986 | 64.88 | 5.479 |
| 31.04 | 0.866 | 69.24 | 6.635 |
| 34.07 | 0.699 | 72.10 | 6.303 |
| 35.34 | 0.624 | 73.21 | 6.236 |
| 36.47 | 0.608 | 74.16 | 5.813 |
| 36.95 | 0.604 | 74.56 | 5.875 |
| 37.01 | 0.560 | 74.60 | 5.777 |
| 37.18 | 0.560 | 74.74 | 5.713 |
| 37.35 | 0.555 | 74.88 | 5.786 |
| 37.54 | 0.588 | 75.03 | 5.719 |
| 37.75 | 0.747 | 75.20 | 5.760 |
| 37.93 | 0.505 | 75.34 | 5.896 |
| 38.17 | 0.145 | 75.53 | 5.690 |

Table V. 18. Relative Mach-products, compositions on homology--element basis and reduced overall pressure changes for detonation of the system neo-pentane - oxygen.

| % $C_5H_{12}$ | $\frac{\gamma M^2}{\gamma M^2_{max}}$ | $\%C_5H_{12}$ as $5CH_2 + H_2$ | $p_{u_{red}} \times 10^2$ |
|---|---|---|---|
| 1.50 | 0.228 | 8.37 | 2.972 |
| 1.65 | 0.249 | 9.15 | 2.961 |
| 1.75 | 0.265 | 9.66 | 2.951 |
| 2.20 | 0.311 | 11.89 | 2.874 |
| 4.00 | 0.433 | 20.00 | 2.595 |
| 8.00 | 0.610 | 34.29 | 2.067 |
| 12.39 | 0.788 | 45.90 | 2.047 |
| 16.75 | 0.932 | 54.69 | 3.347 |
| 18.99 | 0.974 | 58.45 | 4.230 |
| 21.19 | 1.000 | 61.73 | 4.974 |
| 23.04 | 0.970 | 64.24 | 5.733 |
| 25.04 | 0.912 | 66.71 | 6.256 |
| 26.48 | 0.862 | 68.36 | 6.664 |
| 27.99 | 0.744 | 69.99 | 6.515 |
| 29.99 | 0.672 | 71.99 | 6.165 |
| 30.96 | 0.648 | 72.90 | 5.955 |
| 32.20 | 0.767 | 74.02 | 5.840 |
| 32.60 | 0.787 | 74.37 | 5.751 |
| 32.90 | 0.618 | 74.63 | 5.669 |
| 33.04 | 0.538 | 74.75 | 5.589 |

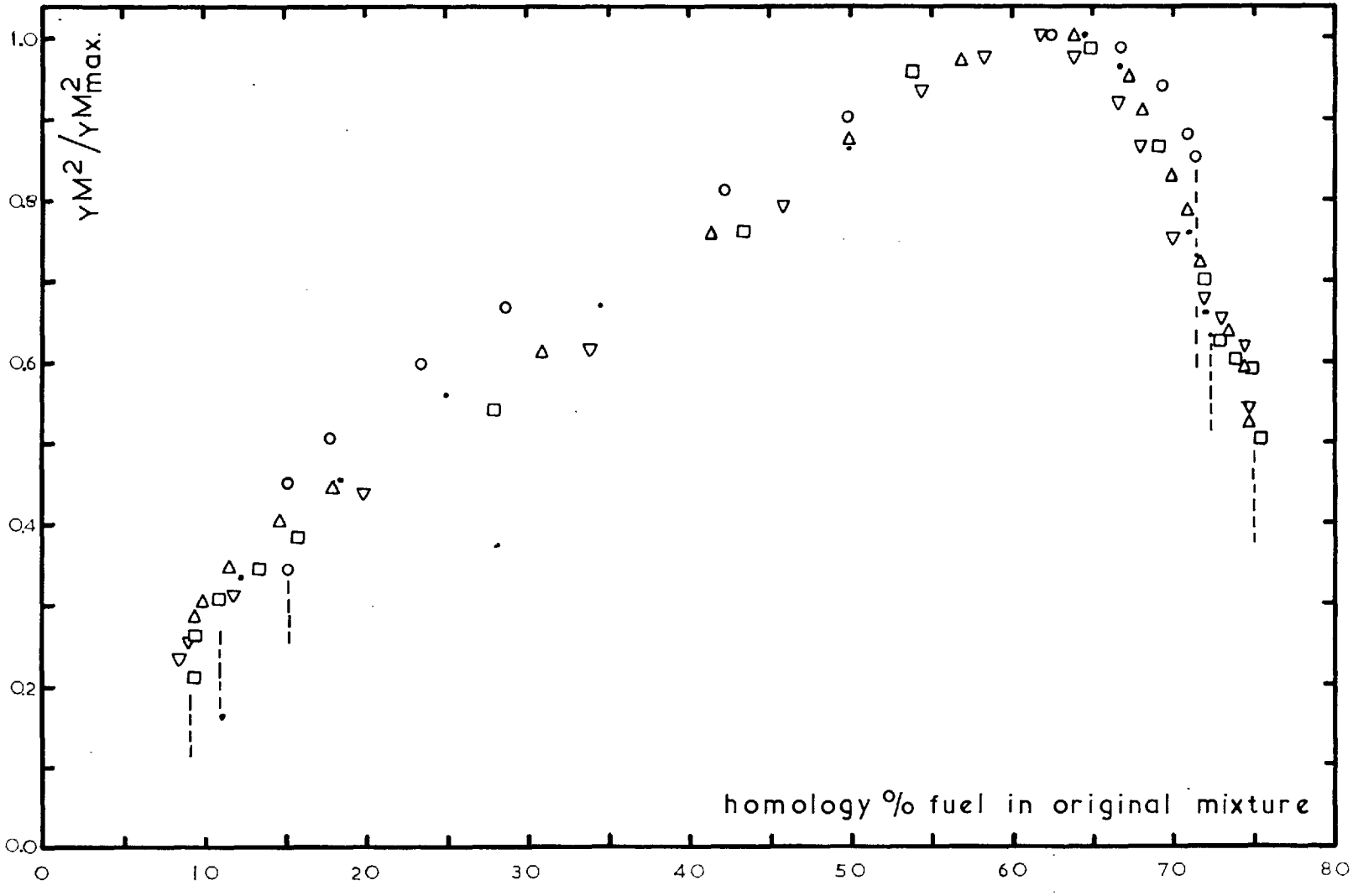



Fig.V.5. Relative Mach product vs. composition on homology element basis for binary systems of oxygen with methane(o), ethane(•), propane(△), butane(□) and neo-pentane(▽).

As can be observed the new representation gives a most satisfactory agreement for the results of propane, butane and (neo-) pentane. One further improvement on the merits of the master curve for normalised composition data is the extension of similarity between the results for these hydrocarbon-oxygen systems to the full range of the detonation regime, including the mixture compositions with heavy condensation of reaction products.

Another most important improvement, especially in view of the interest in marginal and limit effects, is the correlation of limit compositions for the systems with higher elements of the homologous series. Numerical values for the limits, expressed by the fuel percentage in mole ratio and by the fuel percentage as ratio of the sum of the oxygen molecules and the homology elements of the fuel, are given in table V.19. As can be seen, the correlation of limit values is particularly good for the fuel-rich limits.

With respect to the small variations between values for limit compositions of different systems it must be realised that the experimental errors in the determination of composition limits for detonation become enlarged in the new composition representation. It is however more likely that the differences are significant as they might well be related to small deviations of the various properties of the individual fuel molecules from the generalised pattern based

Table V. 19. Mixture composition with fuel percentage calculated on homology-elements basis for detonation limits and composition with maximum Mach-product; results for detonation of binary systems of oxygen and saturated aliphatic hydrocarbons (between brackets : mole percentages).

| Fuel | Fuel-lean limit [%] | $\gamma M^2$ maximum [%] | Fuel-rich limit [%] |
|---|---|---|---|
| methane | 15.20 (8.25) | 61.11 (44.0) | 71.63 (55.8) |
| ethane | 10.07 (3.60) | 62.79 (36.0) | 72.20 (46.4) |
| propane | 9.30 (2.50) | 62.26 (29.2) | 74.73 (42.5) |
| n-butane | 9.26 (2.05) | 62.87 (25.3) | 75.36 (37.95) |
| neo-pentane | 8.37 (1.50) | 62.17 (21.5) | 74.72 (33.0) |

on homology. This applies to the composition variations at the fuel-rich and at the oxygen-rich limits. Aspects of this will be discussed later.

Results for the methane-oxygen system are not similar to those from the systems containing higher saturated aliphatic hydrocarbons and oxygen. This applies to both the steady-state and the marginal condition. Limits are inside the composition values discussed above.

Limits for ethane-oxygen detonation are also inside these values, although the difference is less than for the fuel-rich limit. Steady state results for ethane-oxygen Mach-products agree quite well with behaviour of higher homologues, but in view of the nature of the methane results, similar deviations on a smaller scale can be observed at the oxygen-rich side of the steady-state regime between the ethane data and the results for heavier fuel molecules of the homologous series.

In all, the results clearly justify the construction of a new master curve for relative Mach-products as function of the composition expressed in homology elements. Agreement between results for higher homologues is excellent, but deviations are observed for methane-oxygen and ethane-oxygen systems. These differences have not been found to the same extent for the steady-state region of the original master curve, based on normalisation of composition on mixtures

with maximum Mach-product. However, as the new representation is based on fundamental properties, rather than on a mathematical technique, the new master curve must be considered to be more significant. This opinion is supported by the deviating behaviour of methane and, to a lesser degree, of ethane, which is in agreement with previous experience such as obtained from the calculation of shock-temperatures.

One of the noticeable differences between the detonation properties of the hydrogen-oxygen system and of the systems containing a saturated aliphatic hydrocarbon and oxygen, has been shown to be the mixture composition of maximum energy support to detonation propagation. Now that the similarity in stable detonation of these hydrocarbon-oxygen systems has been evaluated and related to the homologous relation of the fuel molecules, the question once more arises as to what information can be derived from these results on the mechanism of a stable detonation wave in a hydrocarbon-oxygen mixture.

As has been discussed in section I.2 propagation velocities for steady-state detonation have been calculated with great precision for a long time. The original theory by Chapman and Jouguet does not require the postulation of a reaction-mechanism or a structure of that part of a

detonation wave, which lies between the initial condition of the gas mixture and the assumed state of high-temperature chemical equilibrium at the C-J plane. This means that in all cases where agreement is found between calculated and measured detonation velocities, the propagation of the wave depends only on the difference between the initial and final, C-J, condition of the gas, which are related to each other by the principles of hydrodynamics and thermodynamics. Consequently the mechanism by which the final state is reached should not be relevant to detonation velocities or, for that matter, to Mach-product data derived from velocity measurements.

The significance of this for the results of the present investigation is that it supplies a means of testing whether the mechanism or structure of the detonation induction and reaction zone in hydrocarbon detonation has any influence on the relation between mixture composition and velocity or Mach-product for these related systems. If detonation velocities calculated from equilibrium conditions at the C-J plane for various compositions and systems do agree with the experimental results of this work, then the data cannot contain any information on how the C-J condition is attained. If, however, the present results differ from theoretical predictions, then the position of maximum Mach-product and the similarity observed for all investigated systems of

saturated aliphatic hydrocarbons and oxygen depends on a critical mechanism of energy liberation which reaches its optimum performance for the related compositions of maximum $\gamma_0 M^2$.

Detonation velocities, calculated from thermodynamical data, have been evaluated by other investigators. For the present purpose, use is made of their results. In table V.20 calculated and experimental velocities given by Döring and Schön [1950] and Manson, Brochet, Brossard and Pujol [1963] for respectively methane-oxygen and propane-oxygen are recorded, together with the experimental data obtained in the present study for the same mixtures. As can be observed, the difference between the calculated data and the experimental results is always within the error of measurement, which is for these velocities approximately one percent. It must therefore be concluded that neither for the mixtures of higher members of the homologous series, nor for the methane- or ethane-oxygen mixtures, has the mechanism of energy liberation and energy transfer any influence on the detonation velocity. The propagation of the detonation wave must depend entirely on the thermodynamic equilibrium at the C-J plane and can be accurately predicted from evaluation of that condition.

Two restrictive remarks must be made at this point. The first is that the statement of insignificance of the

Table V. 20. Comparison of theoretical detonation velocities [m/sec] calculated from the assumption of thermal equilibrium at the C-J plane, with experimental results (deviations as percentage of the calculated velocities).

| Mixture | Detonation velocity | | | | |
|---|---|---|---|---|---|
| | Calculated | Experimental | | | |
| | | See reference | | This work | |
| 1. Döring [1950] | | | | | |
| $CH_4 + O_2$ | 2637 | 2528 | -4.3% | 2640 | +0.1% |
| $CH_4 + 3/2\ O_2$ | 2531 | 2470 | -2.4% | 2535 | +0.2% |
| $CH_4 + 2\ O_2$ | 2389 | 2322 | -2.8% | 2402 | +0.5% |
| 2. Manson [1963] | | | | | |
| $C_3H_8 + 2\ O_2$ | 2587 | 2598* | +0.4% | 2602 | +0.6% |
| $C_3H_8 + 4\ O_2$ | 2470 | 2480* | +0.4% | 2486 | +0.6% |
| $C_3H_8 + 5\ O_2$ | 2362 | 2375* | +0.5% | 2380 | +0.8% |
| $C_3H_8 + 7\ O_2$ | 2201 | 2213* | +0.5% | 2213 | +0.5% |

* infinite tube diameter.

detonation mechanism does not at present apply to the limit conditions. This will be discussed later. The second restriction is that further consideration must be given to the region of heavy condensation of reaction products, as this situation is not covered by the data of table V.20.

c. Homologous correlation of C-J conditions.

The satisfactory agreement between relative Mach-products for different hydrocarbon-oxygen systems, as found when the fuel components of the mixtures are expressed as the sum of their homologous elements, supports the assumption of similarity in detail aspects of the detonation wave in mixtures with comparable composition. In the previous sub-section it has been shown that the only factor of influence on detonation propagation is the state of thermal equilibrium which exists at the C-J point. The combination of these two facts suggests that for all the hydrocarbon-oxygen mixtures with similar values for the relative Mach-product and composition on the basis of homology elements, the composition of the hot gas at the C-J point would be alike, especially for systems with larger fuel molecules.

It is possible to investigate this point of interest by execution of equilibrium calculations for various compositions of the different systems. The parameters for the burnt state, which follow from an evaluated equilibrium

composition, must lead to satisfactory values for the Mach-product. Calculation of the equilibrium compositions considers the various species that might be present. For the present hydrocarbon-oxygen detonations, possible species at the C-J point are given by the products in the following overall-reaction :

$$x\ C_nH_{2n+2} + (1-x)\ O_2 =$$

$$(V.5) \qquad a_1C + a_2CO + a_3CO_2 + a_4H_2 + a_5H + a_6O_2 + a_7O + a_8H_2O + a_9OH.$$

Calculations of this type for the systems propane - oxygen and n-hexane - oxygen have been carried out by Weir and Morrison [1954]. Equilibrium-composition percentages derived from their graphs have been collected in tables V.21, a and b. Also given are the percentage values, converted to the homology-elements representation. Graphical records of the percentages as function of the new composition basis are also shown in figures V.6, a and b. These data show the variation of equilibrium concentration with change of initial mixture composition for eight species; carbon was not present in significant quantities for the composition range considered. As can be observed, the similarity in equilibrium composition for comparable mixtures of oxygen and propane or n-hexane is remarkable. Difference in concentration for any of the species in the two systems is

Table V. 21. Calculated equilibrium composition in mole percent of the C-J phase for various mixtures of the system oxygen - propane and oxygen - hexane. (Compositions between brackets are for fuel percentages on the basis of homology elements).

| a $C_3H_8$% → | 5.0 (17.39) | 10.0 (30.77) | 15.0 (41.38) | 20.0 (50.00) | 25.0 (57.14) |
|---|---|---|---|---|---|
| $CO_2$ | 13.5 | 14.5 | 11.5 | 7.5 | 4.2 |
| CO | 1.2 | 9.5 | 19.5 | 30 | 39 |
| $H_2O$ | 17.5 | 25 | 30 | 33 | 34 |
| $O_2$ | 68 | 36 | 13.5 | 4.0 | 0.33 |
| $H_2$ | 0.09 | 0.95 | 3.7 | 8.5 | 17 |
| OH | 4.0 | 12 | 14 | 12 | 4.3 |
| H | 0.12 | 1.5 | 4.6 | 6.8 | 6.8 |
| O | 2.2 | 7.5 | 7.8 | 4.7 | 0.85 |
| C | -.- | -.- | -.- | -.- | -.- |

| b $C_6H_{14}$% → | 5.0 (26.92) | 10.0 (43.75) | 12.5 (50.00) |
|---|---|---|---|
| $CO_2$ | 23 | 13 | 5.5 |
| CO | 4.7 | 27 | 37.5 |
| $H_2O$ | 29 | 34 | 29 |
| $O_2$ | 41 | 8.0 | 1.5 |
| $H_2$ | 0.33 | 4.5 | 12.8 |
| OH | 5.8 | 10.8 | 8.7 |
| H | 0.31 | 3.6 | 8.7 |
| O | 2.6 | 4.7 | 3.2 |
| C | -.- | -.- | -.- |

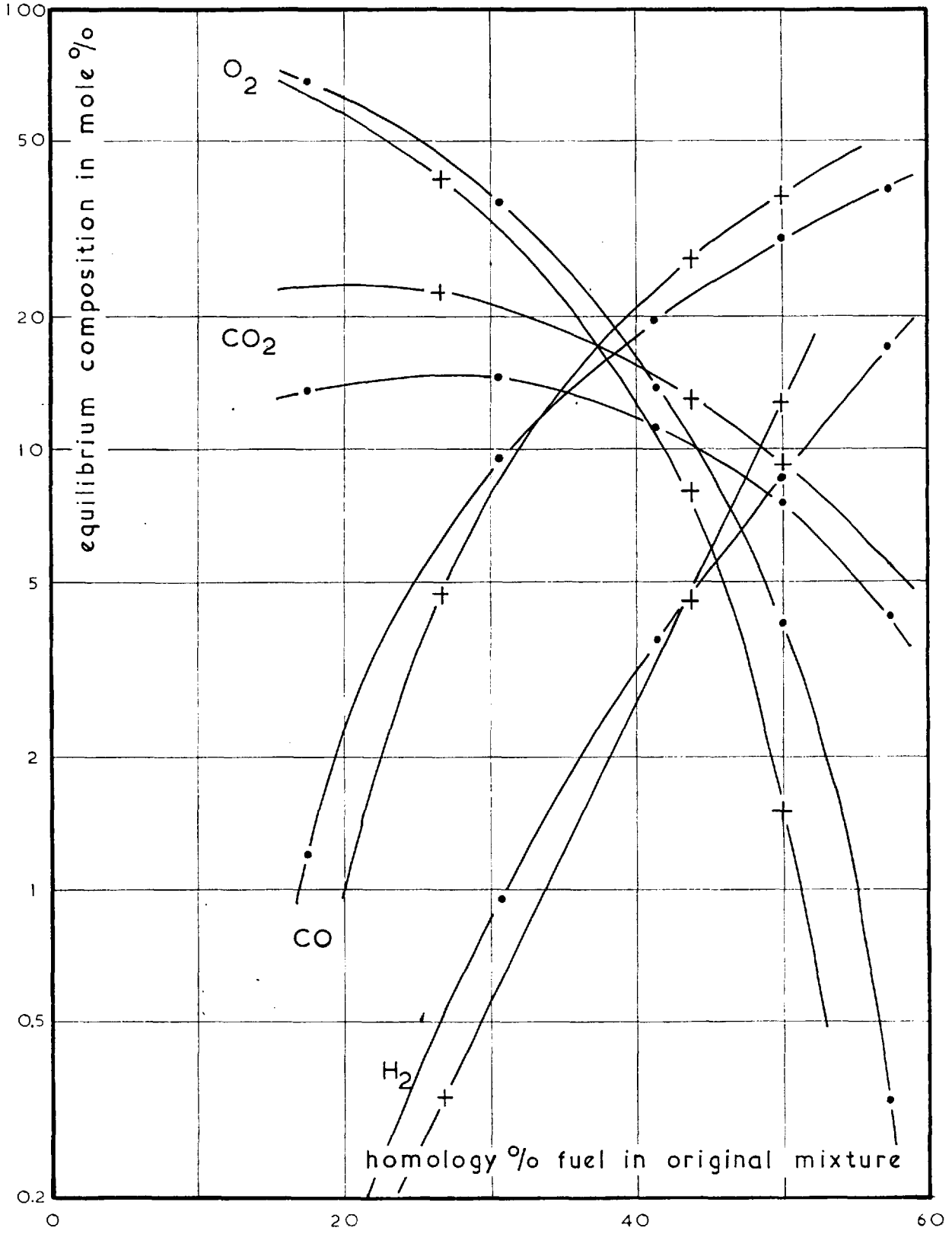



Fig.V.6.a. Computed C-J composition for $C_3H_8$-$O_2$(•) and $C_6H_{14}$-$O_2$(+)

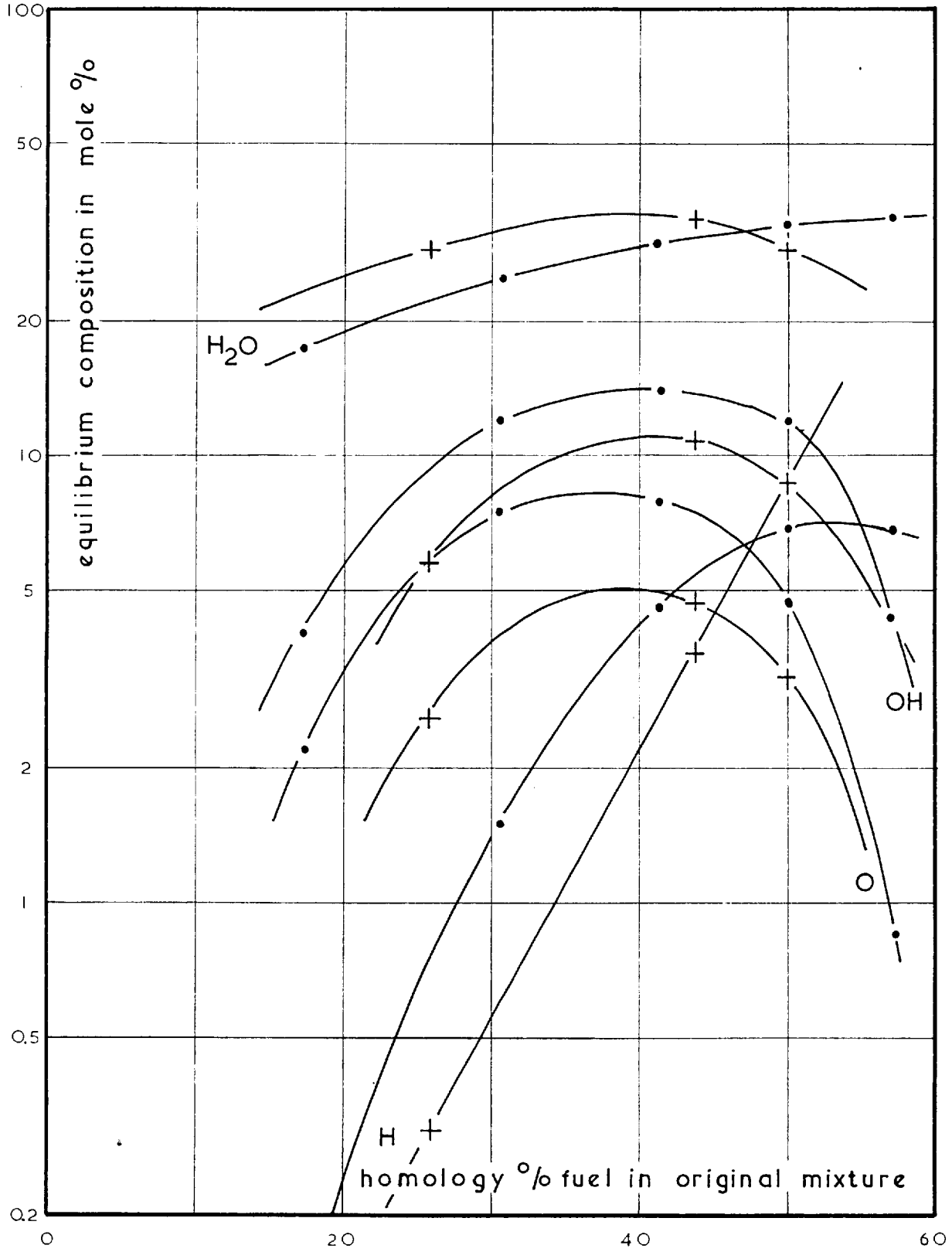



Fig.V.6.b. Computed C-J composition for $C_3H_8$-$O_2$(•) and $C_6H_{14}$-$O_2$(+)

never more than ten mole-percent and usually between two and three mole-percent. Percentages for systems, containing initially butane or pentane, can be assumed to have intermediate values.

From the equilibrium data, Weir and Morrison calculated values for the ratio of mean molecular weights $m_2/m_1$ (see equation IV,11). In the present research these data have been evaluated to give the mean molecular weight of the burned products of propane and hexane detonation. C-J values are given in table V.22. Recorded on the composition basis of homology-elements, as shown in figure V.7, the similarity in mean molecular weight of the reaction products can be observed.

As can be seen from figure V.5, the maximum energy support for detonation propagation in oxygen mixtures of the higher homologues occurs around 62.5% of fuel, considered on the homology basis. This situation is just outside the range of the analysis given by Weir and Morrison for the C-J condition and shown in figures V.6, a and b. Extrapolation of the observed trend of this analysis suggests that this composition coincides with maximum water vapour content. For higher fuel contents a gradual decrease of energy output must be understood on the basis of the observed fall in relative Mach-product values. This must be associated with a further decrease in

Table V. 22. Mean molecular weight of the unreacted phase and the reaction products for various mixtures of the systems oxygen - n-propane and oxygen - n-hexane.

| $C_3H_8$ % | Homology % | $m_2/m_1$ | $m_1$ | $m_2$ |
|---|---|---|---|---|
| 5.0 | 17.4 | 0.92 | 32.6 | 30.0 |
| 10.0 | 30.8 | 0.79 | 33.2 | 26.2 |
| 15.0 | 41.4 | 0.68 | 33.8 | 23.0 |
| 20.0 | 50.0 | 0.60 | 34.4 | 20.6 |
| 25.0 | 57.1 | 0.53 | 35.0 | 18.6 |

| $C_6H_{14}$ % | Homology % | $m_2/m_1$ | $m_1$ | $m_2$ |
|---|---|---|---|---|
| 5.0 | 26.9 | 0.76 | 34.7 | 26.4 |
| 10.0 | 43.8 | 0.63 | 37.4 | 23.6 |
| 12.5 | 50.0 | 0.51 | 38.8 | 19.8 |

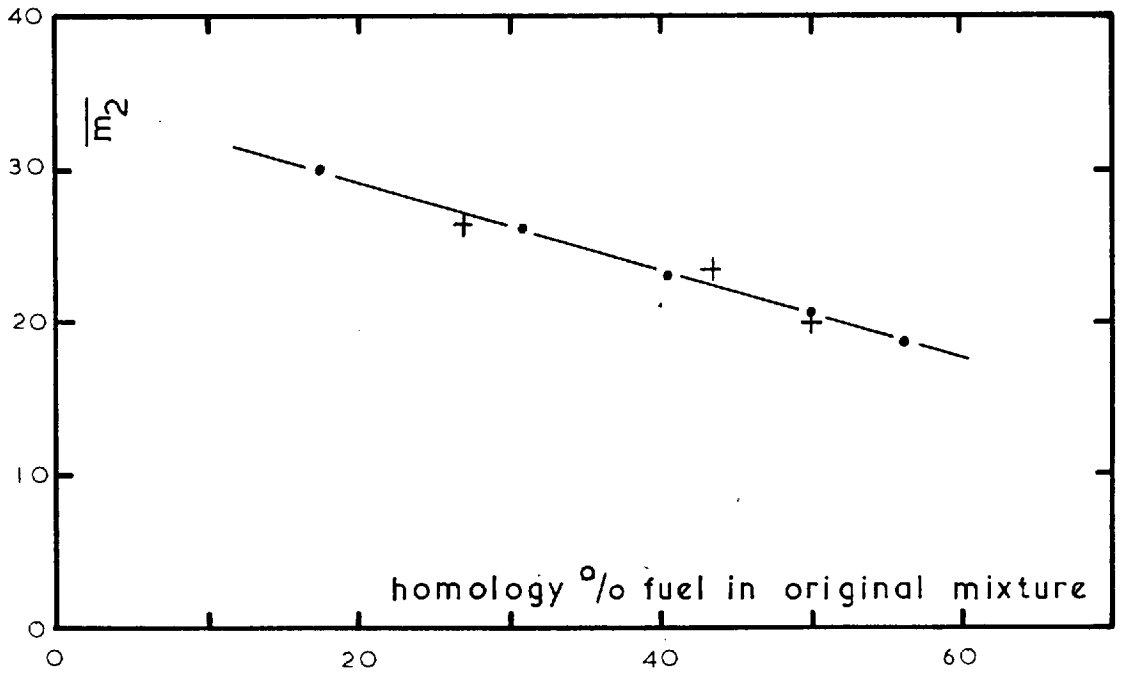



Fig. V.7. Mean molecular weight of reaction products at C-J plane for systems n-propane–oxygen (•) and n-hexane–oxygen (+), calculated from results by WEIR and MORRISON [1954]

oxygenated species and an increase of fuel components at the C-J plane.

The Mach-product curve indicates that from the homologous composition associated with the onset of heavy deposit formation, the further decline of energy release continues at a reduced rate. This appears to be caused by the presence of unoxidised carbon in the C-J equilibrium, which must occur when it is no longer converted to carbon monoxide through lack of oxygen. Calculation shows that feed-back of energy released in the condensation to graphitic carbon, which is likely to occur in the rarefaction wave, can replace a considerable part but not all of the energy lost by the decline of oxidation. Consequently the attainment of critical compositions to detonation propagation through fuel-dilution is only delayed.

f. Homologous correlation of final states.

The hot reaction products which are at thermal equilibrium at the C-J point, subsequently pass through the rarefaction wave to reach their final state. The wave is in effect a simple expansion process. Consequently there is no reason to assume that its effect will be different on comparable mixtures of different hydrocarbon systems,

related through homology. As it has been shown that the average molecular weight and the mixture composition of the species present at the C-J point differ very little for comparable mixtures of oxygen and paraffinic hydrocarbons, there is reason to assume that all final compositions are also similar. If this could be shown it would, in the first place give additional support to the opinion on the aspects of similarity at the C-J point.

In principle it is possible to investigate similarity between final states of comparable mixtures by studying the overall pressure changes which have been determined after each detonation experiment. These data have been recorded in table III, 2 to 5, and figure III.10. To correlate these values for the different systems, account must be made for the fact that the observed pressure changes depend on the change of mean molecular weight, due to the passage of the detonation front. The relation is given by :

$$P_1 \, V_1 \, m_1 = P_2 \, V_2 \, m_2 \qquad (V.6)$$

As $V_1 = V_2$, this can be written as

$$\frac{1}{m_1} \, \frac{P_2}{P_1} = \frac{1}{m_2} \qquad (V.7)$$

If it will be found that overall pressure changes, normalised according to equation (V.7) give similar values

for comparable mixtures of different homologous systems, then the mean molecular weight of the cooled reaction products is similar.

Normalised data for the overall pressure change have been included in tables V.15 to V.18, columns No.4. Recorded on the basis of composition expressed in homology elements, these data are also shown in figure V.8. Values for no reaction, outside the detonation regime, are indicated by broken lines. As can be observed the agreement is satisfactory, especially for the mixtures of oxygen and higher members of the homologous series. For those cases in which the rarefaction zone can be treated as a simple expansion wave, the similarity of molecular weight of the final reaction products supports the previously accepted opinion of such similarity at the C-J plane.

With respect to the influence of the rarefaction wave on the hot reaction products of the C-J plane, it is of interest to consider whether the C-J equilibrium is frozen in by the rarefaction wave or whether the temperature decline proceeds slowly enough to allow maximum shift of the equilibria to the exothermic side. To this end results of gas chromatographic analysis of reaction products from butane-oxygen mixtures, as given in table III.6, have been compared with final compositions estimated for both

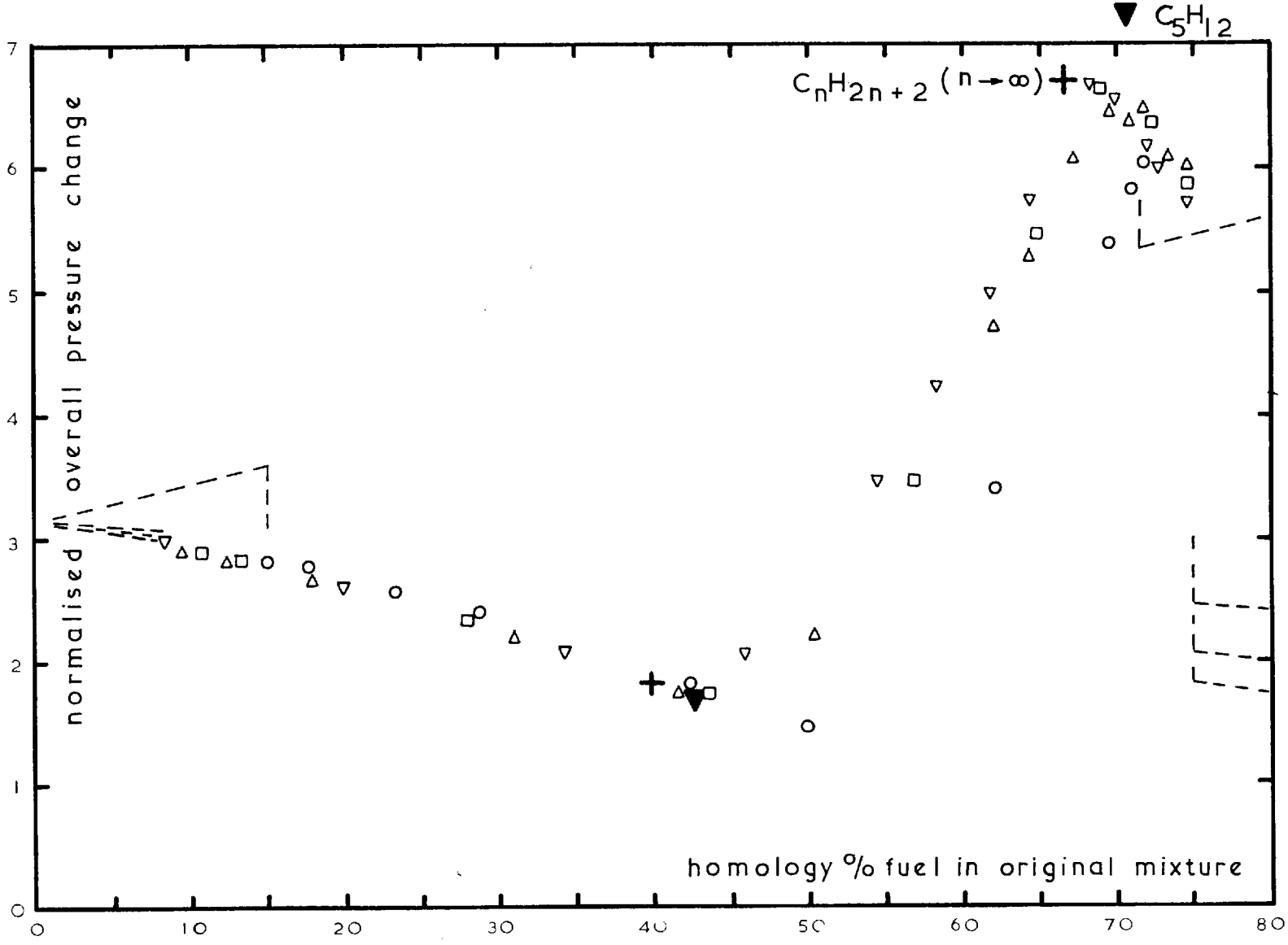





Fig.V.8. Normalised overall pressure change for binary systems of oxygen with methane(o), n-propane(Δ), n-butane(□) and neo-pentane(▽); calculated values: ▼, +.

the extreme possibilities from the C-J data given by Weir and Morrison. Data for the stoichiometric mixture are recorded in table V.23. As can be seen the experimental results agree extremely well with compositions evaluated for thermal equilibrium. This is particularly true when it is accepted that the measured hydrogen content is rather unreliable due to the insensitivity of the chromatograph detector for this gas, when helium is used as the carrier stream. Thermal equilibrium also follows from the analysis of the 35% butane-oxygen mixture, in which the presence of methane can be explained as one of the exothermic products of the equilibrium with carbon monoxide and hydrogen.

On this understanding the normalised plot for the overall pressure change can be seen to consist of three regions. For homologous fuel contents below approximately 40% the result is the oxygen diluted overall change of the stoichiometric system, which consequently goes to the reciprocal of the molecular weight of oxygen for zero percent fuel. Between 40 and approximately 67% the result reflects the change in amount of water formation, above 68% the volume reduction due to the increasing formation of methane. The slope in the curves tends to be slightly different according to the value of the molecular weight of the initial mixture. Theoretical values calculated for the

Table V. 23. Comparison of final composition of reaction products, calculated from the C-J composition for respectively frozen equilibrium and thermal equilibrium, with the results of gas chromatographic analysis, for detonation of stoichiometric n-butane - oxygen (compositions in mole percent).

| Compound | C-J comp. | Final composition | | | |
|---|---|---|---|---|---|
| | Calc. (±4000°K.) | Calculated Frozen eq. | Calculated Therm. eq. | Experimental Analysis | Experimental $[H_2]=9.8$ |
| $CO_2$ | 10.5 | 22.9 | 82.4 | 88.0 | 82.3 |
| CO | 23.8 | 52.0 | | | |
| $O_2$ | 8.0 | 24.0 | 7.8 | 8.5 | 7.9 |
| O | 6.0 | -.- | | | |
| $H_2$ | 4.2 | 1.1 | 9.8 | 3.0 | (9.8) |
| H | 4.5 | -.- | | | |
| OH | 12.0 | -.- | | | |
| $H_2O$ | 31.0 | (negl.) | (negl.) | (negl.) | (negl. |
| Total | 100.0 | 100.0 | 100.0 | 99.5 | 100.0 |

overall pressure change from detonation of oxygen with pentane and with $C_nH_{2n+2}$, $n \rightarrow \infty$ are indicated in figure V.8 for the boundary case between the three regimes mentioned above.

g. Homologous correlation of composition limits and aspects of the formation of condensation products.

In sub-section V.4.d the correspondence of the composition limits for mixtures of oxygen and normal saturated aliphatic hydrocarbons has been discussed. Investigating the composition in terms of homology-elements, a satisfactory agreement is observed between the compositions for maximum Mach-products and the detonation limits of binary systems containing oxygen and respectively n-propane, n-butane and neo-pentane (see Table V.19). Such correspondence might for instance suggest the requirement of a comparable dilution by excess of either of the two initial mixture components to attain the limiting condition for these three systems. To allow for more detailed discussion of such possibilities and their implications, some aspects of these limit compositions are investigated in detail.

Oxygen-rich limits.

With respect to the actual composition on homology-elements basis for the oxygen-rich detonation

limits, the result for the neo-pentane - oxygen system appears to have a somewhat higher oxygen content than the limits for n-propane and n-butane - oxygen systems. Several tentative explanations may be considered.

As far as the consequences of composition representation on homology-element basis are concerned, it can be pointed out that analysis of the neo-pentane molecule as $(5CH_2 + H_2)$ is not a realistic proposition in any way. Due to the structure of this molecule a more acceptable analysis would for instance be : $(C + 4CH_2 + 2H_2)$. When represented on this basis the newly calculated oxygen-rich limit for neo-pentane oxygen detonations would be 9.60% fuel.

The value of this consideration could be tested by comparable experiments with n-pentane-oxygen mixtures. However the additional investigations with n-pentane vapour have not been extensive enough to give a decisive answer to this question. The composition of the most diluted n-pentane mixture corresponds to a homology-elements concentration of 9.20% n-pentane. Consequently the possibility exists that a proper evaluation for the difference between normal and branched structure of the fuel-molecules could lead to a further improved agreement between the oxygen-rich limits.

Fuel-rich limits.

The introduction of composition representation involving homology-analysis of the fuel molecules has resulted in excellent agreement of the fuel-rich detonation limits for the higher saturated aliphatic hydrocarbons. As can be noticed, these hydrocarbons all produce considerable amounts of solid reaction products at the fuel-rich end of their detonation regime for mixtures with oxygen.

There are various reasons why the existence and correlation of the fuel-rich limits of these systems is likely to be connected with aspects of the formation of solid reaction products. It must for instance be difficult to understand how limiting factors to energy requirements for bond rearrangements taking place between the shock front and the normal C-J condition could give identical results for normal and branched fuel molecules. Furthermore, if the energy balance near the fuel-rich limit is considered, the dependence of detonation propagation on the condensation energy of carbon atoms can easily be appreciated. (Section V.4.

As shown in Appendix F, the ratio of the sublimation energy released in the formation of graphitic carbon and the net energy produced in the oxidation reaction

(V.8) $$x\ C_nH_{2n+2} + (1-x)\ O_2 \longrightarrow$$

$$2(1-x)\ CO + (nx + 2x - 2)\ C_{gr} + x(n+1)H_2 + Q$$

is equal to

$$(V.9) \qquad \frac{Q_C}{Q} = \frac{[x(n+2) - 2] \cdot 170}{-(4.8n + 65.2)x + 54.4}$$

In this equation x is the mole fraction of fuel and n the number of carbon atoms in a fuel molecule. Comparison with experimental data (see appendix) shows that for branched molecules, such as neo-pentane, n should be taken one integer higher.

Equation (V.9) can be used to calculate the ratio of $Q_C/Q$ for various mixture compositions inside the region of solid formation. If this is done for the compositions of detonation limits, values are obtained as given in table V.24. From these it appears that for the propane-oxygen system the sublimation energy of the graphitic carbon just about represents the net energy production of the overall reaction. However, for the binary systems n-butane-oxygen and neo-pentane-oxygen, the condensation energy of the carbon is more than twice the overall reaction energy produced. Consequently, detonation propagation at the fuel-rich limit of the propane system and over some range of composition near the limits of the other two systems must be entirely dependent on the condensation energy. Composition values for which $Q_C$ is equal to Q are also shown in table V.24.

Table V. 24. Calculated ratios between the energy released in condensation of graphitic carbon and the overall energy produced in the incomplete oxidation of detonated saturated aliphatic hydrocarbons at the fuel-rich limits and composition-values for $Q_C = Q$.

| | $C_3H_8$ | $C_4H_{10}$ | $C_5H_{12}$ |
|---|---|---|---|
| a. Fuel-rich limit. | | | |
| $Q_C/Q$ | 1.042 | 2.132 | 2.111 |
| Composition (mole %) | 42.50 | 37.95 | 33.00 |
| Composition (homology %) | 74.73 | 75.36 | 74.72 |
| b. $Q_C = Q$ | | | |
| Composition (mole %) | 42.43 | 34.41 | 30.71 |
| Composition (homology %) | 74.67 | 72.40 | 72.67 |

It is useful to point out a few assumptions that are implicit in this discussion. The first is, that the reaction of (V.8) goes to completion and represents the equilibrium condition at the C-J point. This implies that the calculated composition for which $Q_C$ is zero corresponds to the composition where solid formation starts. As can be seen from sub-section V.4.e and f and from figures III.10 or V.8, this is more or less true. A second assumption is that the condensation product is indeed graphitic carbon. The electron diffraction patterns (see section III.4) seem to confirm this assumption, but at the same time it is also possible that some hydrogen atoms are included in the structure. Finally it appears from the results for n-butane and neo-pentane detonations that most of the sublimation energy contributes to detonation propagation. An assumption that all sublimation energy takes part in the sustentation of detonation has however not been made.

Further reflection on aspects of the detonation limits at the fuel-rich end of the detonation regimes with solid formation, leads to the impression that some connection exists between the extent of oscillating propagation velocity and detonation limits. This is in itself not a new idea as spin effects near detonation limits have been known and studied for almost as long as detonation processes. In

the present case the scale and nature of the oscillations suggests that these phenomena are at least in part related to the formation of condensation products.

For a revealing investigation of this problem, further theoretical and experimental developments will be required. With the available methods and results, calculations and evaluations aimed at comparing possible modes of solid formation with observed instabilities fail through lack of information. However, it is possible to discuss tentatively the mechanisms for the condensation of reaction products that might explain some of the experimental observations and allow for the possibility of a uniform fuel-rich detonation limit for all condensating systems.

Oscillations in detonation velocity in the region of solid formation have been evaluated as relative variations of the mean Mach-product. Such values for $\Delta\gamma M^2 / \gamma M^2$ are recorded in figure V.9 as function of the composition on homology-elements basis for the systems concerned. As can be observed, for a given mixture composition the extent of relative oscillation in the Mach-product appears to be higher for mixtures with larger fuel-molecules. Near the composition of the detonation limit oscillations seem to increase very rapidly towards a peak value which could well be of the order of the mean Mach-product of each system.

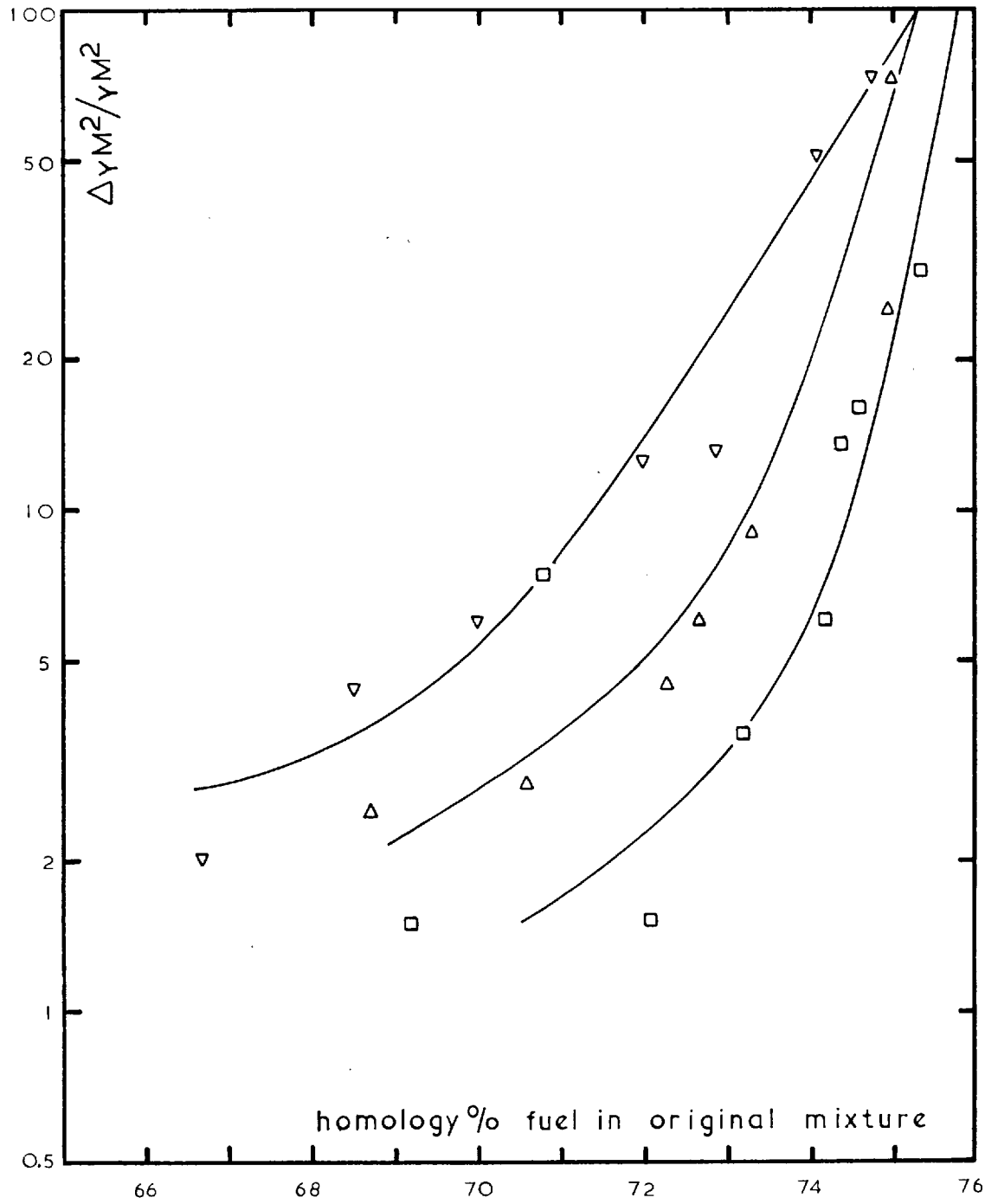



Fig.V.9. Variation of the mean Mach product for formation of solid condensation products from systems of oxygen with n-propane(△), n-butane(□) and neo-pentane(▽).

It has already been shown that participation of the condensation energy of carbon in the propagation of detonation near the fuel-rich limits is required to obtain a satisfactory energy balance. The calculations of Weir and Morrison have shown that for the system propane-oxygen the C-J temperature at the experimentally observed onset of carbon condensation is at least one hundred degrees below the sublimation temperature of graphitic carbon which is around 3960°K at 1 atmosphere. Considering that the increased pressure in the detonation wave further favours condensation, it seems likely that for this system graphitic carbon is already formed in the reaction zone.

Condensation within the boundaries of the reaction zone reduces the mean molecular weight of the remaining products. The extra energy, available from this process, will consequently assist to heat the remnant gas to higher temperatures and thus effectively increase the temperature at the C-J plane. If this new temperature level would approach the sublimation temperature of carbon, the solid formation in the reaction zone could become considerably reduced. This would imply a decrease in energy release and subsequently result in a return to lower reaction temperatures, where, possibly with some retardation, carbon sublimation would start again. The occurrence of such a reaction cycle would cause oscillations in the propagation

velocity of the detonation concerned.

Evaluation of the results of the calculations by Weir and Morrison for the n-propane-oxygen and n-hexane-oxygen systems indicates that, for a given composition, the systems with the larger fuel molecules have a higher C-J temperature. In the above suggested mechanism, this would mean that the likelihood of temperature fluctuations across and above the sublimation temperature of graphitic carbon is greater for pentane-oxygen systems than for propane-oxygen. Consequently, the possibilities for the occurrence of a metastable, undercooled carbon-gas phase before return of graphite formation would be larger for the heavier fuel molecules and this would correspond with the larger oscillations observed for the neo-pentane system.

More careful consideration of the implications of this possibility requires further extensive investigation. This also applies therefore to the consequences of such aspects of formation of condensation products on the occurrence and position of the fuel-rich detonation limits. The present information allows for the possibility that for a critical concentration of carbon in the reaction mechanism, instabilities in energy production will always become too large to allow for continuation of detonation propagation.

## V. 5. Results for systems of ethylenic hydrocarbons and oxygen.

In the context of the present study, interest in detonation propagation through mixtures of binary systems containing oxygen and ethylenic hydrocarbons can be two-fold. In the first place, investigation into such properties will be an independent source of information on such aspects of the homologous relations as are of influence on detonation propagation in these related systems. On this basis, the equipment and methods of this study would have been reapplied to produce a new series of results. On the other hand there is the second possibility of using these results for a comparative study of detonation in oxygen-containing systems of paraffinic and ethylenic hydrocarbons and to evaluate the influence of the small and systematic differences in structure of these fuel molecules on the detonation properties.

For this study the second possibility is of more interest than the first. As a consequence, the number of systems with double-bonded fuel molecules can be limited and the comparison can in principle be made between the results for a representative ethylenic system and the greatly similar information for systems of higher saturated hydrocarbons and oxygen.

Results for the binary system of oxygen and propylene have already been given in chapter III, table III.7 and figure III.12 and III.13. Results and evaluated data for the ethylene-oxygen system can be found in appendix G, table 2.

a. Steady-state conditions.

Some aspects of the velocity data, the overall pressure change and the formation of condensation products have also been discussed in section III.5. Comparison of the velocity curves in figure III.12 reveals the same similarities as found for the saturated hydrocarbons : peak velocities and detonation velocities for chemically related mixtures of the different systems are again comparable.

Conversion of the detonation velocities to Mach-product data gives results similar to those shown in figure V.3 for the saturated hydrocarbons. Values of maximum $\gamma M^2$ increase again with rise of the molecular weight of the fuel molecule. Mach-product data and graphically determined values for coordinates of $\gamma M^2_{max}$ are respectively given in tables V.25 and V.26. Values for the ethylene system can be found in appendix G , table 2. As can be observed Mach-product numbers for olefinic

Table V.25. Mach-product data, detonation limits and shock temperatures for detonation propagation in binary systems of unsaturated aliphatic hydrocarbons and oxygen. (Note : composition values between parentheses are for homology-elements representation.)

| | Ethylene | Propylene |
|---|---|---|
| a. Mach-product data | | |
| $\gamma M^2$ maximum | 91.7 | 103.2 |
| composition $\gamma M^2$ max. | 43.5 % | 34.0 % |
| | (60.63)% | (60.71)% |
| $\gamma M^2$ fuel-lean limit | 29.50 | 23.54 |
| $\gamma M^2$ fuel-rich limit | - | 54.50 |
| b. Limits | | |
| Fuel-lean limit | 4.1 % | 2.5% ±0.05% |
| | (7.9)% | (7.01)% |
| Fuel-rich limit | ±60 % | 50.0% ±0.1% |
| | ±(75) % | (75.0)% |
| c. Shock-temperatures * | | |
| Fuel-lean limit | ±1450°K | 1215°K |
| Fuel-rich limit | - | 1250°K |

* Shock temperatures, rounded off to 5°, calculated under the assumption of complete randomisation of internal energy for hydrocarbons and rotational temperature for oxygen.

Table V.26. Mach-product data, compositions on homology-elements basis and reduced overall pressure changes for detonation of the system propylene-oxygen.

| $\%C_3H_6$ | $\gamma M^2$ | $\gamma M^2/\gamma M^2_{max}$ | %fuel as $3\,CH_2$ | $p_{u_{Norm}}$ x$10^2$ |
|---|---|---|---|---|
| 2.45 | 23.536 | 0.228 | 7.01 | 2.968 |
| 2.50 | 24.635 | 0.239 | 7.14 | 2.958 |
| 2.55 | 25.103 | 0.243 | 7.28 | 2.967 |
| 2.65 | 25.665 | 0.249 | 7.55 | 2.938 |
| 2.75 | 26.468 | 0.256 | 7.82 | 2.943 |
| 2.85 | 27.612 | 0.267 | 8.09 | 2.936 |
| 3.00 | 29.520 | 0.286 | 8.49 | 2.935 |
| 3.99 | 36.132 | 0.350 | 11.99 | 2.861 |
| 7.98 | 50.706 | 0.491 | 20.65 | 2.558 |
| 13.01 | 64.601 | 0.626 | 30.97 | 2.152 |
| 18.21 | 76.277 | 0.739 | 40.05 | 1.815 |
| 23.19 | 87.915 | 0.851 | 47.53 | 2.554 |
| 28.19 | 96.872 | 0.938 | 54.08 | 3.786 |
| 33.20 | 102.894 | 0.997 | 59.86 | 5.013 |
| 38.28 | 97.267 | 0.942 | 65.04 | 6.350 |
| 43.23 | 77.744 | 0.753 | 69.55 | 6.387 |
| 45.72 | 66.586 | 0.645 | 71.65 | 6.376 |
| 48.19 | 60.963 | 0.590 | 73.62 | 6.200 |
| 49.02 | 36.915 | 0.358 | 74.26 | 6.119 |
| 49.57 | 56.757 | 0.550 | 74.68 | 6.055 |
|  | 55.093 | 0.534 |  | 6.087 |

hydrocarbons are higher than those for comparable mixtures of oxygen and saturated hydrocarbons with the same number of carbon atoms.

The Mach-product data have again been normalised as fraction of the maximum values. Compositions have been recalculated on the basis of oxygen and number of homology elements in the fuel molecule in a manner similar to that for the saturated aliphatic hydrocarbons; for the olefinic hydrocarbons this analysis considers the fuel-molecule as a number of $CH_2$-groups, with no additional $H_2$-groups. Values for these can be found in the above mentioned tables and are also recorded in figure V.10.

As can be observed from figure V.10, the correlation between the results for ethylene and propylene detonations, achieved by evaluation as relative Mach-products and composition on the basis of homology-element representation, is at least as good as between the results for ethane and propane detonations. The possibility for construction of a master-curve for detonation properties of olefinic hydrocarbons with oxygen does therefore exist.

To compare these results with those obtained for the saturated aliphatic hydrocarbons, the general pattern of comparable data for propane-oxygen and neo-pentane-oxygen systems has been added to figure V.10. As can be seen the

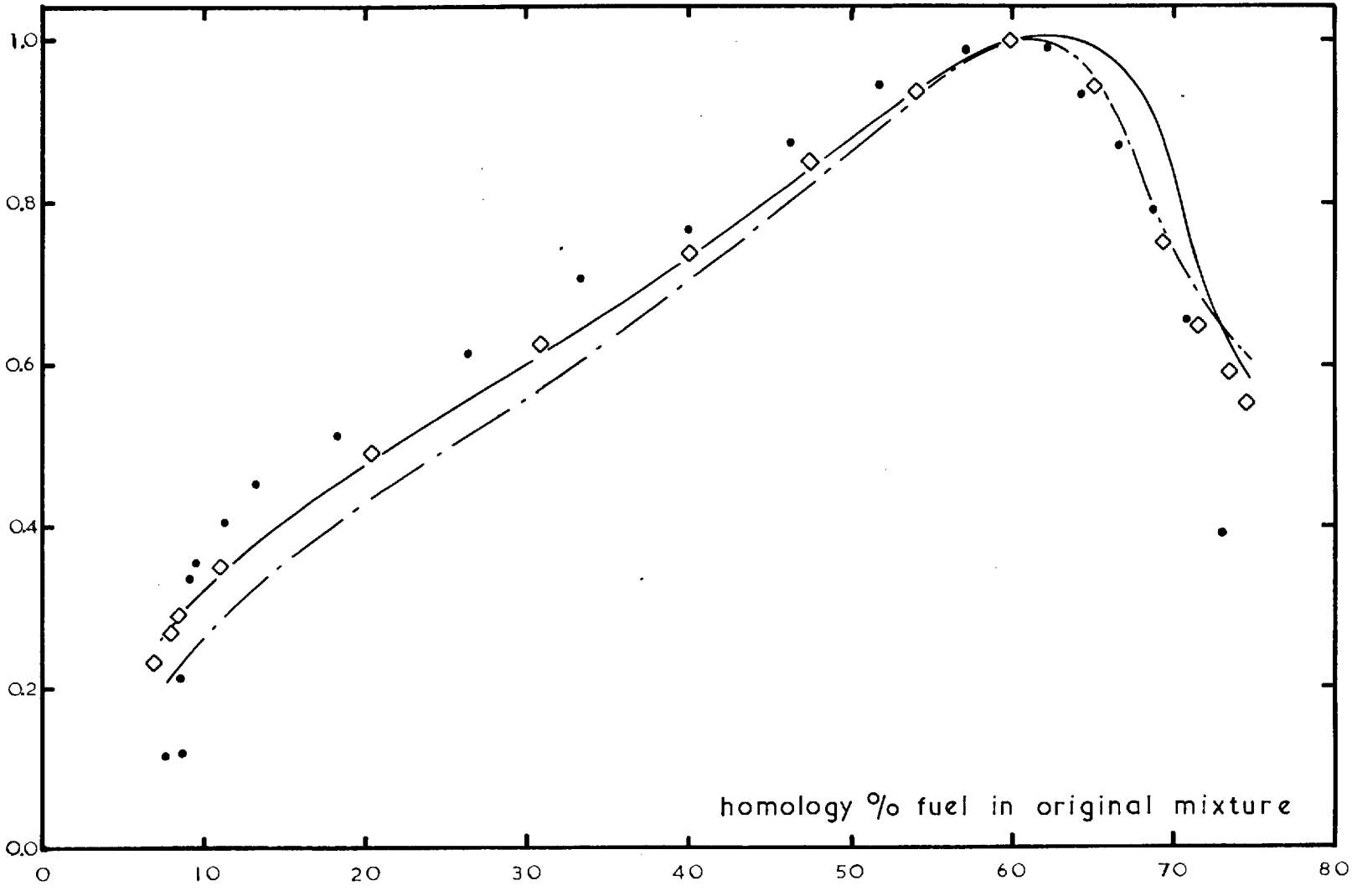



Fig.V.10. Relative Mach product vs. composition on homology basis for binary systems of oxygen with ethylene (•) and propylene (◇); $C_3H_8$-$O_2$ (——); neo-$C_5H_{12}$-$O_2$ (– – –)

overall agreement between the master-curve for the saturated and the olefinic aliphatic hydrocarbons is quite satisfactory.

Considering the similarities and differences between systems with saturated and olefinic aliphatic hydrocarbons in more detail it can in the first place be observed that the composition with maximum Mach-product expressed on the basis of homology-elements for the fuel-molecules, appears to be of somewhat lower fuel-content for the olefinic hydrocarbons. (cf. table V.19 and table V.25a). For mixtures with higher oxygen content, the correspondence between the relative Mach-products of comparable mixtures of propane-oxygen and propylene-oxygen in figure V.10 is as good as can be achieved for identical mixtures with the existing experimental error. However at the fuel-rich side of the composition with maximum Mach-product, the results for propylene-oxygen detonations seem to agree better with the values obtained for neo-pentane - oxygen mixtures. As a possible reason for this, it can be suggested that the differences between the various saturated hydrocarbons in the mixtures which are comparable on the basis of homology, are largest at the high fuel concentrations, where the influence of $H_2$-groups is large. Olefinic hydrocarbons have no spare $H_2$-groups, when analysed on this basis. Assuming that similarity between

detonation of saturated and unsaturated hydrocarbons, as appears from figure V.10,does exist, the results for propylene could possibly be considered comparable with those of large saturated aliphatic hydrocarbon molecules for which the possible influence of the additional $H_2$-group is relatively small.

b. Composition limits.

Composition limits to detonation propagation in the system propylene-oxygen have been determined from the combined information on velocity, overall pressure change and such information as given in the last column of table III,7. The same criterion has been used as in selecting composition limits for detonation of saturated aliphatic hydrocarbons (see section V.3). Values are given in mole percentage of fuel concentration in table V.25,b. Numbers between parentheses are the corresponding values on the basis of homologous representation as $(nCH_2 + O_2)$. The fuel-rich limit has not been located as accurately as for most saturated hydrocarbons, but the result for 50.04 percent propylene suggests that the true limit composition has only fractionally more oxygen. Limits for ethylene have been derived from the results by Schuller [1954], see appendix G,table 2. The value for the fuel-lean limit has again been corrected on the basis of the work by Pusch

and Wagner [1965] for the difference in tube diameter. The value for the fuel-rich limit is rather uncertain, as the composition values for the test mixtures appear to be two and a half percent of mole concentration apart.

The composition limits to detonation given for the olefinic hydrocarbons ethylene and propylene in table V.25.b can be compared with the limits for saturated aliphatic hydrocarbons given in table V.19. Such comparison shows that the compositions of the oxygen-rich detonation limits for propane and propylene correspond very well on the basis of mole-percentage fuel and oxygen. To a lesser extent this applies also to the more uncertain values for ethane and ethylene systems. For the fuel-rich limits correlation of all higher saturated aliphatic hydrocarbons and the two investigated olefinic systems is obtained around 75 percent of composition, evaluated with fuel concentration analysed in homology elements. It must be repeated that all these fuel-rich limits are situated in a region of considerable condensation of reaction products. By comparison, the correlation of the fuel-rich limits is better than of the oxygen-rich limits, in the latter case the differences between the results for different systems are of the order of two percent of composition on homology elements basis.

c. Shock-front temperatures at the detonation limits.

Shock temperatures at the composition limits have again been calculated in the usual way.

Values for $\gamma M^2$ have been obtained from extrapolation to limit composition of the results given in table V.26 and in appendix G, table 2. These data are recorded in table V.25.a. Due to the mentioned inaccuracy in the fuel-rich limit for the ethylene-oxygen system, a reliable value for the corresponding Mach-product could not be evaluated.

As can be observed from table V.13, vibrational relaxation times for ethylene are well below those for methane and still shorter for the higher olefines. Consequently it is again justified to assume complete relaxation of internal degrees of freedom of the fuel molecules and unrelaxed vibrational modes for oxygen. Shock-temperatures calculated for this most probable situation are given in table V.25.c. Comparison of these shock temperatures with the values given in table V.12 generally reveals satisfactory agreement.

d. The final state.

Little can be said about the conditions at the C-J plane and in the final state for detonation of mixtures

of olefinic hydrocarbons and oxygen. The correspondence between the master-curves for paraffinic and olefinic hydrocarbons and the similarity between the values for the reduced overall pressure change, given in table V.26 and those recorded in figure V.8, suggests that the analogy in behaviour of these different groups of homologous related systems extends also to aspects related to the reaction products. To check this supposition further experimental and/or theoretical investigation will be required.

## V. 6. Conclusions.

The evaluation of the experimental data collected in the investigation described in this thesis, has produced a variety of information of general applicability as well as of more special interest to detonation propagation. Some of this information is concerned with aspects of detonation that have only an indirect significance for the field of immediate interest of this study. Such is for instance the possibility of extensive correlation of properties of stable detonation in different binary gas mixtures, when a homologous relation exists between the different fuel components. Within the limitations set by the scope of this study, aspects of this property have not required investigation beyond the experimental proof of mere potentiality. Further research into the implications

and fundamental details of the method as well as of the conclusions that can be drawn from its results, may well be favoured in future.

However it must be realised that such investigation offers only limited prospects for revelations of the mechanism of steady-state detonations. While the understanding of such fundamental properties is the ultimate aim of detonation research, the present study has also shown for hydrocarbon-oxygen mixtures that propagation of steady state detonation depends only on the thermodynamic and hydrodynamic properties of the system. Consequently, observations such as also made by Dixon [1894, 1903] or Miles et al. [1962] on the optimal conditions of energy release for oxidation to carbon monoxide must in the first place be understood on the basis of thermal equilibrium properties at the C-J plane. The conclusion must therefore once more be that investigation of properties of stable detonation by the methods used in this work is not suitable to obtain detailed information on the mechanism of energy supply under those conditions.

As has been discussed in the first chapter, measurement of detonation velocities might only lead to significant information on the physics and chemistry of processes in the detonation front for experiments under

marginal conditions for detonation propagation. The present investigation has in fact primarily been undertaken to study such aspects against the background of the homologous relation of the fuel components; as an additional source of information the condensation of reaction products was to be studied. In as much as the homologous correlation of properties of stable detonation has furthered the evaluation of detonation behaviour under these special conditions, the results obtained for the steady-state detonation regime are of value to the aim of the present research. This is best demonstrated by referring to the achieved correlation of detonation limits for binary systems with aliphatic hydrocarbons by composition representation on the basis of homology elements.

One of the first aims of this research has been explained to be further investigation of the experimental experience (Wendlandt, [1925]; Gordon et al. [1959]; Miles et al. [1962]) of a common minimum shock front temperature of about 1200°K. This temperature, which has been calculated under the assumption of complete internal energy relaxation of the molecules in the detonation front, would be the minimum required to guarantee continuation of detonation propagation at the composition limits. By the introduction of homology-elements representation all detonation limits for the investigated hydrocarbon-oxygen

mixtures have become comparable and sometimes almost identical. Therefore, a comparison of the required temperature rise for each system and limit has become still more interesting.

Comparing the order of magnitude for the induction time before oxidation with fairly well established values for the various relaxation times of the mixture components, it has appeared unlikely that all vibrational degrees of freedom are excited before the onset of chemical reaction. While disagreeing with the assumptions made by the other investigators, this opinion gives some support to the impression obtained from experimental observation by Miles et al [1962] that internal degrees of freedom of diluent molecules, like nitrogen, to binary mixtures fail to equilibriate in the detonation front, even under limit conditions.

As discussed in chapter I, opinion is divided as to what extent the apparent limiting temperature rise is or is not a purely hydrodynamic condition, depending only on such parameters as the diameter of the tube. While not contesting the experimental proof that such conditions have a critical influence on detonation propagation under marginal conditions, we must refer to the critical temperature rises for the systems containing methane, ethane and ethylene, which have been evaluated as well above the usually required 1000$^{o}$K. As it is difficult to

understand how these differences are to be explained on hydrodynamic principles, other critical factors related to temperature requirements should at least be considered.

A possible explanation for this anomalous behaviour might follow from general experience for pyrolysis and oxidation of hydrocarbons. From this it is known that when at atmospheric pressure the initial temperature of the mixture is raised above $\pm$ 600°C dehydrogenation will be replaced by a cracking process as the initial reaction. Under the favourable conditions of high temperature and increased pressure of the detonation front such processes would certainly involve complete rupture of all carbon-carbon bonds. Further investigation will be required to consider whether such fragmentation of fuel molecules could occur at a sufficiently high rate to propose this step as the critical phase under conditions of marginal detonation. Assuming that this is acceptable it is worth considering the bond energies involved in this mechanism. As can be seen from table V.27, the strength of the carbon-carbon bond decreases considerably with increase of chain length and branching of the molecular structure. Consequently the existence of a cracking mechanism which becomes critical to detonation propagation under marginal conditions would agree very well with the temperature requirements given in table V.12. In addition it would explain qualitatively,

Table V.27. Bond energies in kcal/mole for primary fission of various aliphatic hydrocarbons (from Landolt-Börnstein, Band I, Teil 3,II [1951]).

| | $CH_3$ | $C_2H_5$ | $C_3H_7$ |
|---|---|---|---|
| H | 101* | 98 | 95 |
| $CH_3$ | 83 | 82 | 79 |
| $C_2H_5$ | 82 | 82 | 79 |
| n-$C_3H_7$ | 79 | 79 | 76 |
| i-$C_3H_7$ | 74.5 | 75 | 72 |
| n-$C_4H_9$ | 78 | 78 | 75 |
| T-$C_4H_9$ | 74 | 73 | 70 |

* The underlined values apply to the primary cracking of methane, ethane, propane, n-butane and neo-pentane.

even for composition representation on the basis of homology-elements, why detonation limits tend to shift towards higher dilutions with increase of the molecular weight of the fuel molecule. It also suggests that the fuel-lean detonation limit for the neo-pentane system could have a somewhat higher oxygen content than the same limit for the system n-pentane-oxygen. This interpretation of the slight exception in the oxygen-rich limit for neo-pentane is similar to the tentative suggestion made on grounds of its homology-elements, in as much as it relates the observed anomaly to the structure of the molecules.

On the basis of the data given in table V.27, the implications of the described cracking mechanism would suggest a small difference in homology-element composition for the detonation limits of the systems of oxygen and propane, butane and pentane. Such differences might well be close to the limits of the experimental accuracy. However, considering all aspects of the agreement between the fuel-rich limits for these systems and the correspondence with the composition values obtained for the fuel-rich limits of the ethylene and propylene system, the possibility of a decisive role for the formation of condensation products on the location of these limits, cannot be excluded. Aspects of this have been discussed in sub-section V.g, but

detailed evaluation does not appear possible on the basis of the presently available information.

With respect to the energy feed-back from reaction or condensation, the possibility of various other mechanisms must be considered. As has been suggested before (Miles et al. [1966]) radiation would in some ways appear to be a reasonable alternative to the hydrodynamic processes suggested. However, it seems unlikely that such a mode of energy transmission would play a predominant role in the propagation of detonation under marginal conditions, as it does not easily account for the oscillatory nature of the observed phenomena.

## V.7. Suggestions for further investigations.

One of the most urgent requirements for continuation and advance of the present research along the existing lines is the programming of calculations for evaluation of C-J equilibrium conditions and the detonation parameters. Computerisation of these operations will not represent a contribution of the first order to science. However, the availability of this mathematical tool will at least allow the investigator to consider the various theoretical possibilities with relative ease and without the fear of wasting valuable time; at best it will encourage him to

undertake careful examination of critical conditions to detonation propagation.

With respect to the details of the present study, the existence of an efficient programme would in the first place allow for an accurate evaluation of the C-J conditions for the systems with propane, butane and pentane. This will be useful, not only to improve on the approximations allowed by the results from Weir and Morrison, but also to extend the composition range considered to the regimes of solid formation and the detonation limits. Evaluation of C-J conditions with sublimation of gaseous carbon to graphite might reveal details of the extent and rate of condensation and assist in the correlation of comparable mixture compositions of different systems. For the fuel-rich limits it will be possible to evaluate theoretical values for Mach-products, considering various degrees of participation of sublimation-energy in detonation propagation. Considering the suggested mechanism of oscillating energy contribution from this source, the Mach-product values evaluated for steady-state conditions can be compared with the experimental observations and the existence of the limits might possibly be shown to be related to the extent of these oscillations. For the fuel-lean limits, possible evaluation of C-J temperatures will facilitate investigation of the purely diluting effect of

the excess oxygen, by allowing for accurate calculation of theoretical Mach-products from the supposed energy liberated at the C-J plane. As for the fuel-rich limits, evaluated detonation parameters assuming steady-state conditions, do not represent the actual limit situation, but they indicate the circumstances which the real detonation process just fails to maintain.

Another way to investigate limit conditions appears to be further experimental investigation of the critical temperature requirements, evaluated for the oxygen-rich detonation limits. Additional information might be obtained by replacing a small part of the excess of oxygen by an inert gas, which has only translational degrees of freedom. Alternatively other techniques can be considered, but the choice is rather restricted as interference with the front is likely to change the relaxation times. As a possibility optical investigation by means of the absorption spectrum can be suggested, but in order to be successful, the application will require some careful experimental design as even the fastest light sources have a discharge time of about 5 $\mu$sec. to half maximum intensity.

The use of an absorption spectrum method may have a better chance for success in the investigation of the proposed initial cracking mechanism. It would be

interesting to study not only the composition of the pre-oxidation zone but also its temperature, as the dissociation of the unreacted fuel molecules is an endothermic phase in the overall exothermic conversion to reaction products. Confirmation of the supposed cracking mechanism without getting involved in extensive instrumental development might possibly be obtainable from isotopic labelling of the fuel molecule. If, for instance, the carbon atom in the $CH_3$- group of propylene is replaced by the $^{14}C$-isotope, normal oxidation of the fuel-rich limit mixture would produce mainly non-radioactive carbon monoxide due to the extremely high oxygen affinity of the double bond. However, if the cracking precedes oxidation in the detonation front, close to one out of three carbon monoxide molecules would be radioactive. This ratio could probably be further increased by detonation of the true limit composition. As under such conditions the energy failure can be expected to start to influence the cracking mechanism, rupture of the single carbon-carbon bond ($\pm$ 80 kcal/mole) will be more likely than for the double bond ($\pm$ 150 kcal/mole). Consequently there will be a better chance that oxygen will attack the methyl radical, preferentially to association with the larger double bonded group.

As a next step in dealing with aspects of the

formation of solid reaction products and the contribution of the detonation wave, investigation of detonation propagation in fuel-rich hydrocarbon-oxygen mixtures, diluted with considerable excess of inert gas, should be considered. This possibility has been suggested earlier by Miles et al [1966]. The aim would be to decrease the volume reduction due to condensation to such an extent that the continuation of detonation propagation becomes only dependent on the energy of the chemical reaction and some of the factors involved in the conversion of undiluted mixture can be independently evaluated.

With reference to the suggested alternative of total or partial energy feed-back by radiation, experimental investigation could be attempted either by observation or interference. Whereas the former approach would probably require optical means of measuring any radiation of sufficient intensity to be of significance, the latter techniques could attempt to reveal the influence of high - power photon input on the propagation velocity of a detonation wave.

It would be of both scientific and technical interest to investigate further the significance and possibilities of the observed correlation of steady state and limit conditions for detonation of organic fuel

molecules. As the correlation has made use of the Mach-product, which depends only on the initial conditions and the detonation velocity, there is no reason why the agreement should in principle not be extended to include other pressures, temperatures and molecular weights for the fuel molecule. As for the last possibility it would appear from this work that detonation of a trace of hydrocarbon of high molecular weight or of solid carbon-hydrogen structures in near one hundred percent oxygen can in principle be realised.

Appendix A. The non-additivity of partial pressures in mixing two gases with dissimilar molecules.

Part 1. Estimating the correction for the first admitted component by comparison of similar experimental data.

a. Principle.

The extent of non-additivity of partial properties on mixing two gases with dissimilar molecules is given by :

$$(A.1) \qquad \frac{\Delta PV}{PV} = x_1 x_2 (2B_{12} - B_{11} - B_{22}) = x_1 x_2 X$$

PV is the pressure-volume product for a mole of gas mixture, evaluated from the component properties under the assumption of ideal gas behaviour; $x_1$ and $x_2$ are the mole fractions of the two gases and the B-values are the second virial coefficients for the gas mixture and its components. Equation (A.1) is derived in part 2 of this appendix.

Experimental values of $\Delta PV/PV$ are not available for the binary gas mixtures used in the investigations of this thesis. By studying such data as are available an estimate can be made for the systems of present interest. A conversion curve is used to evaluate corrections for other compositions than those of equimolar ratios, such as mixtures corresponding to detonation limits. The appropriate value for $\Delta PV/PV$ is then converted into a

correction for the concentration of the mixture component first admitted to the storage vessel. This correction is used to evaluate the accuracy and correction for the mixture compositions quoted in this thesis. This is done in Appendix B.

b. Correction evaluation.

Values of $\Delta PV/PV$ for equimolar mixtures of some binary gaseous systems have been determined experimentally by Michels and Boerboom [1953]. Few of the components used correspond to those of the systems investigated in the work of this thesis. By comparison $\Delta PV/PV$-values for equimolar mixtures of oxygen and hydrogen or hydrocarbons can only be estimated on a tentative basis. As a first approximation the contributions for oxygen and nitrogen are assumed to be of the same order of magnitude. The experimental information to be used is given in table A.1.

Considering the information available for the hydrogen-nitrogen system, the deviation from the pressure-volume product calculated by addition for equimolar hydrogen-oxygen will probably not be larger than $2 \times 10^{-4}$. Estimation of corresponding figures for a hydrocarbon-oxygen system is more difficult, as various factors, influencing the results of table A.1 have to be considered.

As can be seen by comparing data for binary systems containing carbon dioxide, the extent of non-additivity is smaller with nitrogen than with hydrogen. In addition, increase of size of the hydrocarbon molecule appears to support deviation from ideal gas behaviour.

Taking into account these considerations, the extent of non-additivity in the pressure-volume product of equimolar methane-oxygen is estimated to be of the order of $10 \times 10^{-4}$. For larger fuel-molecules this value is likely to increase.

The estimated values are equal to :

(A.2) $$\Delta PV/PV = x_1 x_2 X = X/4 .$$

To evaluate data for limit compositions these figures have to be multiplied by 4 and by the appropriate mole fraction product. For convenience a curve has been constructed to give the conversion factor for calculation of $\Delta PV/PV$ for any mixture ratio from the value for the equimolar mixture, see figure A.1. Values for equimolar and limit mixtures of the systems hydrogen-oxygen and methane-oxygen obtained in this way are given in table A.2.

Considering values of $\Delta PV/PV$ for the most important mixture-ratios of limit-detonation in systems of higher aliphatic hydrocarbons and oxygen, two opposing influences can be named. As has already been said, the

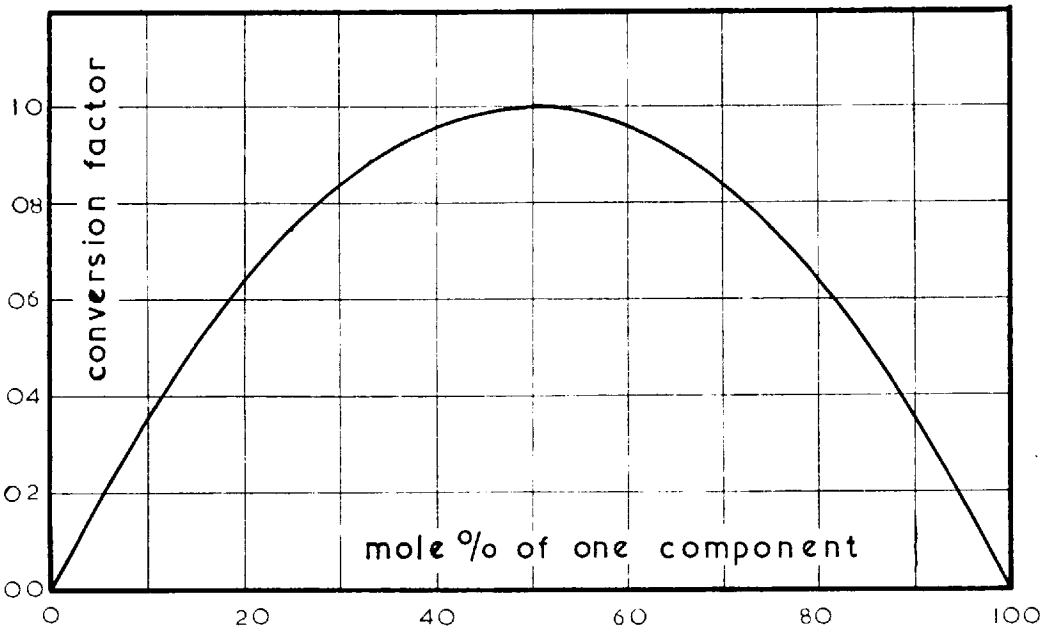



Fig.A.1. Conversion curve for evaluation of non-additivity of partial properties in binary mixtures from data for the equimolar mixture.

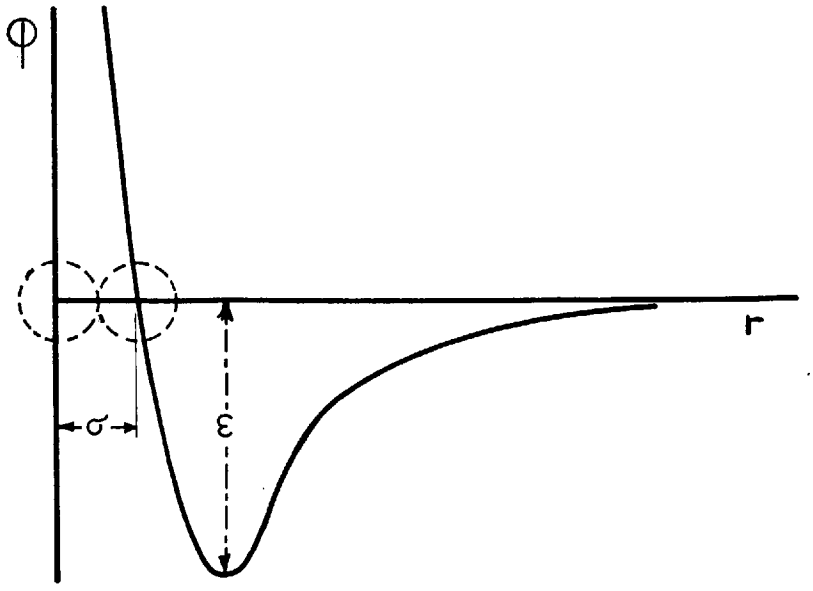



Fig.A.2. Force parameters of the inter-molecular potential field.

increase of the molecular weight of the fuel molecule appears to extend the non-additivity. On the other hand, as limit mixtures for higher homologues are further away from the equimolar ratio than methane-oxygen limits, the mole fraction product will be smaller. For the present it will be assumed that these opposing tendencies more or less cancel out and that $\triangle PV/PV$ values for limit-compositions of the hydrocarbon-oxygen systems investigated are comparable to the values estimated for the methane-oxygen system.

For the practice of this work it is more useful to convert the estimated non-additivity into a composition percentage correction for the mixture component first admitted to the storage vessel. As the mixtures have a higher pressure than the sum of the pressures of the individual components ($\triangle PV/PV$ is positive) the correction on the measured pressure of the first admitted component is positive. As mixture compositions have been calculated from measured pressure-ratios, the composition percentage of this component requires the same relative correction, which can be evaluated as a correction expressed in percentages of the total mixture. Consequently the magnitude of this correction will be related to mixture composition in the same way as given by figure A.1 for the value of $\triangle PV/PV$. Corrections calculated in this way for the systems hydrogen-oxygen and methane-oxygen are shown in figure III.1.

Table A.1. Some experimental values for $\triangle PV/PV$ for equimolar mixtures of binary gaseous systems (Michels and Boerboom [1953]).

| Mixture | $(\triangle PV/PV) \times 10^4$ |
|---|---|
| $H_2 - N_2$ | $+ 1.7 \pm 0.2$ |
| $CO_2 - N_2$ | $+ 4.6 \pm 0.2$ |
| $CO_2 - H_2$ | $+ 11.0 \pm 0.2$ |
| $C_2H_4 - H_2$ | $+ 13.5 \pm 0.2$ |
| $C_3H_6 - H_2$ | $+ 43.0 \pm 0.2$ |

Table A.2. Estimated values for $\triangle PV/PV$ for equimolar and detonation-limit compositions of binary systems of oxygen with hydrogen and methane.

| Composition | $H_2 - O_2$ | $CH_4 - O_2$ |
|---|---|---|
| 50% - 50% | $2.0 \times 10^{-4}$ | $10 \times 10^{-4}$ |
| fuel-lean detonation limit | $1.0 \times 10^{-4}$ | $3 \times 10^{-4}$ |
| fuel-rich detonation limit | $0.5 \times 10^{-4}$ | $10 \times 10^{-4}$ |

Part 2. The principle of calculating the correction for the first admitted component from the force constants of the pure gases.

In part 1 of this appendix the extent of non-additivity of partial properties in mixing oxygen with an aliphatic hydrocarbon has been estimated to be approximately the maximum permissible for quoting detonation limits to within one-tenth of a percent of composition. It could be argued that a more accurate evaluation of the influence of this factor is desirable. Alternatively future research with fuel molecules causing larger deviations from ideal gas behaviour in mixing with oxygen, will require an appropriate calculation of the correction to be applied in such conditions. Part 2 of the appendix will therefore consider the principles of the cause for deviatory behaviour and outline a method to calculate the corrections required.

## I. The virial equation of state and the parameters of the intermolecular potential field for pure gases.

### a. The virial equation of state.

Behaviour of gases is generally described by the equation of state, which has the form :

$$pV = RT\,(A + B\rho + C\rho^2 + \ldots) \qquad (A.3)$$

A,B,C, etc. are the virial coefficients, $\rho$ is the molar density.

The first term on the right-hand side represents the ideal gas state, which assumes no other forces operative than external; for one mole of gas, A equals unity. B is the second virial coefficient; the product $RTB\rho$ represents the contribution of internal forces in the system due to two-body interaction; C is the third virial coefficient, related to contributions from three-body interaction. For the pressure range involved in detonation research, with initial pressures of 1 atmosphere, three-body interaction will have little influence on the gaseous behaviour and only the first two right-hand terms in equation (A.3) are of interest.

By examining the virial of external and internal forces in more detail, the special form of equation (A.3) for two-body interaction only can be derived as :

$$pV = RT\,(1 + B\rho) \qquad (A.4)$$

with

$$B = 2\pi N \int (1 - e^{-\varphi/kT}) r^2 dr \,.$$

In this expression N is the Avogadro number, $\varphi = \varphi(r)$, the intermolecular potential and r is the distance between two molecules; $\exp(-\varphi/kT)$ is the Boltzmann factor. For further reference see e.g. : Taylor and Glasstone, II, 313-316 [1951].

b. The intermolecular potential field.

According to Lennard-Jones, the intermolecular potential field for two-body interaction to be found in the

second virial coefficient (equation A.4) can be described by

$$\varphi(r) = \frac{\alpha}{r^{12}} - \frac{\beta}{r^{6}} \tag{A.5}$$

The equation generally satisfies the experimental results from compressibility measurements; the shape of the potential field is as shown in figure A.2.

For $r = \sigma$, $\varphi = 0$. For $\varphi = -\varepsilon$,

$$\left(\frac{\partial \varphi}{\partial r}\right) = 0 = -\frac{12\alpha}{r^{13}} + \frac{6\beta}{r^{7}} \tag{A.6}$$

If equations (A.5) and (A.6) are solved for $\alpha$ and $\beta$,

$$\varphi = -4\varepsilon\left[\left(\frac{\sigma}{r}\right)^{12} - \left(\frac{\sigma}{r}\right)^{6}\right] \tag{A.7}$$

In this way the intermolecular potential field has been expressed as function of two characteristic parameters, $\sigma$ and $\varepsilon$, also called the "force constants". As can be seen from figure A.2, $\sigma$ can be considered as the collision diameter of the gas, while $\varepsilon$ is the depth of the potential well, related to the point of maximum attraction.

c. The principle of the corresponding states applied to the intermolecular potential field.

As the Lennard-Jones potential is essentially a mathematical description, which satisfies the experimental facts, it is possible to apply the principle of the corresponding states to the potential representation as

function of the characteristic parameters (equation A.7). Normalisation of r-values on the collision diameter $\sigma$ and of the potential $\varphi$ on its minimum value $-\varepsilon$ is introduced by :

$$\text{(A.8)} \qquad \begin{aligned} r &= r^* \sigma \\ \varphi &= \varphi^* \varepsilon \quad , \quad \text{while} \\ kT &= T^* \varepsilon \end{aligned}$$

will later be needed. Substitution in equation (A.7) gives the reduced Lennard-Jones potential

$$\text{(A.9)} \qquad \varphi^* = -4 \left( \frac{1}{r^{*12}} - \frac{1}{r^{*6}} \right) = f \left( \frac{r}{\sigma} \right)$$

When equations (A.8) and (A.9) are substituted in the expression for the second virial coefficient, equation (A.4), its reduced form becomes

$$\text{(A.10)} \qquad B^* = \int (1 - e^{-\varphi^*/kT^*}) \, r^{*2} \, dr^*$$

with, supplementary to equation (A.7)

$$\text{(A.11)} \qquad B^* = \frac{B}{\frac{2}{3}\pi N \sigma^3} \quad \text{and} \quad T^* = \frac{kT}{\varepsilon}$$

As the reduced Lennard-Jones potential is in principle applicable to all (non-polar) gases, the relations of equation (A.11) are generally valid.

d. Calculation of force constants for pure gases.

Values of $B^*$ and $T^*$ can be calculated from theory and have been tabulated in literature (Hirschfelder et al.

[1954], page 114, table I.B). They can be used to obtain values for $\sigma$ and $\varepsilon$.

Second virial coefficients can be calculated from isotherm measurements. A graphical method to determine the force constants then proceeds as follows. For equation (A.11) can be written :

$$\text{(A.12)} \qquad \begin{aligned} \ln B^* &= \ln B - \ln \tfrac{2}{3}\pi N\sigma^3 , \quad \text{and} \\ \ln T^* &= \ln T + \ln \frac{k}{\varepsilon} \end{aligned}$$

Graphs of theoretical values of ln B* vs ln T* can be made to coincide with graphs of ln B vs. ln T. The differences in the coordinates of the two curves are equal to the second terms on the right hand side of both of equation (A.12). From these $\sigma$ and $\varepsilon$, (usually given as $\varepsilon/k$) can be obtained.

e. Force constants for oxygen and aliphatic hydrocarbons.

Hirschfelder et al [1954], give force constants, which have been calculated either from transport properties or from second virial coefficients and temperatures. For calculations involved with state properties, only the latter should be used. Data, related to the gases, studied in the investigation of this thesis, are given in table A.3.

Table A.3. Force constants for the intermolecular potential field, calculated from experimental compressibility data (from Hirschfelder et al. [1954], page 114, table I.B).

| Gas | $\varepsilon/k$ [°K] | $\sigma$ [Å] |
|---|---|---|
| $O_2$ | 117.5-118 | 3.46-3.58 |
| $CH_4$ | 148.2 | 3.817 |
| $C_2H_6$ | 243 | 3.954 |
| $C_3H_8$ | 242 | 5.637 |
| $n\text{-}C_4H_{10}$ | 297 | 4.971 |
| $C_2H_4$ | 199.2 | 4.523 |

## II. The non-additivity of partial state parameters on mixing two gases with dissimilar molecules.

### a. The non-additivity in mixing real gases.

In the present treatment, the non-additivity of partial pressures on mixing two different gases in a fixed volume is discussed. As can be shown the result will apply equally to mixing two volumes of gas at constant pressure.

Consider $n_1$ moles of gas at pressure $p_1$ in a volume V. These are to be mixed with $n_2$ moles of a different gas, which would on its own have had a pressure $p_2$ in the same

volume V. According to equation (A.4), the equation of state for each of these components is given by

$$p_i V = n_i RT + n_i B_{ii} p_i , \qquad i = 1,2 \tag{A.13}$$

and the equation for the final mixture is :

$$PV = (n_1+n_2)RT + (n_1+n_2)B_m P \tag{A.14}$$

in which $B_m$ is a second virial coefficient for the actual mixture of $n_1$ moles of component (1) with $n_2$ moles of component (2). Due to the difference in molecular interaction forces of the two gases, the sum of the partial pressures of the components is not equal to the final pressure, but, in the fixed volume V :

$$p_1 + p_2 = P - \Delta P \tag{A.15}$$

It follows from equations (A.13), (A.14) and A.15) that

$$V\Delta P = (n_1+n_2)\, B_m P - n_1 B_{11} p_1 - n_2 B_{22} p_2$$

As V = constant and, with second order of error :

$$\frac{p_1}{P} \approx \frac{n_1}{n_1+n_2}$$

$$\Delta PV = (n_1+n_2)B_m P - \frac{n_1}{n_1+n_2} B_{11} P - \frac{n_2}{n_1+n_2} B_{22} P$$

To express this in mole ratios, the equation has to be divided by V; divide also by P :

$$\frac{\Delta PV}{PV} = \frac{n_1+n_2}{V} B_m - \frac{n_1}{(n_1+n_2)V} B_{11} - \frac{n_2}{(n_1+n_2)V} B_{22}$$

or

$$(A.16) \qquad \frac{\Delta PV}{PV} = B_m - xB_{11} - x_2B_{22}$$

b. The non-additivity expressed in virial coefficients for interaction of similar and dissimilar molecules.

To replace the coefficient $B_m$ in equation (A.16) by the virial coefficient $B_{12}$, for the exchange of forces between a molecule (1) and a molecule (2), the possibilities for interaction of internal forces, as described in I.c, must be reconsidered. For sufficiently large numbers of both species in the system, this can be done in the following way.

Assume one mole of mixture with mole fractions of each species : $x_1$ and $x_2$. For a molecule of species (1), the interaction with all other molecules is given by

$$x_1B_{11} + x_2B_{12}$$

For the whole mole fraction $x_1$ the interaction will therefore be :

$$(A.17) \qquad x_1^2B_{11} + x_1x_2B_{12}$$

Similarly, the interaction concerning all molecules in fraction $x_2$ is :

$$(A.18) \qquad x_1x_2B_{12} + x_2^2B_{22} .$$

Consequently, from equations (A.17) and (A.18),

$$(A.19) \qquad B_m = x_1^2B_{11} + 2x_1x_2B_{12} + x_2^2B_{22}$$

which, by substitution in equation (A.16) gives :

$$(A.20) \qquad \frac{\Delta PV}{PV} = x_1 x_2 (2B_{12} - B_{11} - B_{22}) .$$

c. Calculation of second virial coefficients for interaction between non-polar, dissimilar molecules.

As force constants can be derived from experimentally determined second virial coefficients, the reversed operation is in principle also possible. For this, force-constants must be available.

For the intermolecular potential field between two dissimilar molecules, values of $\sigma$ and $\varepsilon/k$ from compressibility measurements are rare. To overcome this problem until such times that sufficient experimental data will be available, Hirschfelder and Rosevaere [1939] have suggested the use of empirical mixing rules, which have been proved to give satisfactory results in various applications. According to these :

$$(A.21) \qquad \begin{aligned} \varepsilon^2_{12} &= \varepsilon_{11} \cdot \varepsilon_{22} \\ \sigma_{12} &= \tfrac{1}{2}(\sigma_{11} + \sigma_{22}) \end{aligned}$$

The second virial coefficient $B_{12}$ can now be evaluated as follows :

(i) select force constants $\varepsilon$ and $\sigma$ for the pure components from literature (see table A.3)

(ii) calculate $\varepsilon_{12}$ with equation (A.21).

(iii) calculate T* for the required T, with equation (A.8) or (A.11).

(iv) select the corresponding value for B* from literature tables (Hirschfelder et al. [1954], page 114, table I.B).

(v) calculate $\sigma_{12}$ with equation (A.21).

(vi) calculate $B_{12}$ with equation (A.11).

d. Summary.

The correction for the non-additivity of partial state properties can be evaluated as follows : For known values of the mole fractions $x_1$ and $x_2$ and temperature :

(i) values for $B_{11}$ and $B_{22}$ can be found in literature.

(ii) values for $B_{12}$ can be calculated as explained in section III.c.

(iii) the correction is then given by equation (A.20)

For comparison of some calculated values with experimental data, see : Michels and Boerboom [1953].

## Appendix B. The accuracy of calculated mixture compositions.

Compositions of gas mixtures, quoted in this thesis, have been calculated from the individual pressure increases, indicated by the manometers on the storage vessels after admission of each mixture component. It has been assumed that the ratio of these pressure increases is identical to the mole fraction ratio of the components in the mixture. This appendix is concerned with considering the nature and extent of deviations from the assumed linearity of measured pressure increases and mixture percentage. The discussion is applied to both the test mixture and the primer preparation.

### Part I. The accuracy of test mixture compositions.

To discuss the various factors that influence the accuracy of test mixtures, the dimensions of the storage vessel and of the manometer connected to it, will be needed repeatedly. The following dimensions apply :

| | | | |
|---|---|---|---|
| V | = | vessel volume, including connections and volume manometer at vacuum : | : 11.8 litres |
| r | = | vessel radius | : 14 cm. |
| | | manometer radius | : 0.35 cm. |

a. The first factor, affecting the accuracy of mixture compositions calculated from manometer readings, is the non-additivity of partial pressures on mixing two dissimilar gases in a basically constant volume. Aspects of this are discussed in detail in appendix A. As can be found there, the correction for the percentage of the first admitted component, which as a rule has been the fuel, is for equimolar mixtures of oxygen and respectively hydrogen and methane, $10^{-2}$ and $5 \times 10^{-2}$ of total mixture percentage (see also figure III.1). The values fall off towards zero and 100% of fuel.

b. A second systematical error results from the volume increase of the system due to the displacement of mercury in the manometer. As gas enters the evacuated storage vessel, the mercury in the differential manometer moves away from the gas until at a final pressure of approximately two atmospheres, the volume of about 76 centimetres of manometer tube has been added to the storage space of the vessel. The total increment can be calculated as 30 cc.

For an equimolar mixture of fuel and oxygen, the first admitted component will attain 1 atmosphere. The amount of gas will then be :

$$(11800 + \frac{50}{100} \times 30) \text{ cc} = 11815 \text{ cc gas}$$

or

11..815 x 1 litres.atmospheres of component 1.

With the second component added, there is :

$$(11.800 + 30 \times 10^{-3}) \times 2 = 23.660 \text{ litres. atm. gas.}$$

The percentage of the first component in this mixture is therefore :

$$\frac{11.815}{23.660} \times 10^2 = \underline{49.937\ \%}$$

or 0.063% lower than calculated without this correction.

This is the maximum deviation possible as a result of this volume change. For 25% (75%) and 4%(96%) mixtures of the first admitted component the deficiency is respectively -0.048% and -0.010%.

c. Another systematical error in mixture ratios calculated from pressure readings is caused by the <u>expansion of the storage vessel with increase of internal pressure</u>. The stress on the cross-section of the spherical vessel, exerted by the pressure on the two opposing halves, is :

$$F = \frac{\pi r^2 . P}{2\pi r . dr}$$

dr being the wall-thickness, which is approximately 0.5 cm. For P = 2 atm. :

$$F = 28 \text{ kg/cm}^2$$

The elongation of the vessel diameter, normal to the cross-section plane is :

$$\triangle d = \frac{F \cdot d}{M}$$

M is the elasticity modulus, which for materials like glass must be of the order of $10^6$ kg/cm$^2$. Thus :

$$\Delta d = 28^2 \times 10^{-6} \approx 8 \cdot 10^{-4} \text{ cm.}$$
$$\Delta r \approx 4 \times 10^{-4} \text{ cm.}$$

The volume change of the vessel due to a change of internal pressure from vacuum to two atmospheres is :

$$(V + \Delta V) - V = \tfrac{4}{3}\pi (r^3 + 3r^2 \Delta r + \ldots) - \tfrac{4}{3}\pi r^3$$
$$\approx 4\pi r^2 \Delta r$$
$$V = 4\pi \times (1.4)^2 \times 10^2 \times 4 \times 10^{-4}$$
$$\approx 1 \text{ cc} = + 0.0084\%$$

The true volume change is likely to be somewhat smaller as up to ambient filling pressures the vessel is compressed by atmospheric overpressure from the outside. However the correction to the total pressure is certainly not larger than $+ 8.10^{-5} = + 1.6 \times 10^{-4}$ atmospheres and the partial pressure of the first admitted component should therefore be corrected with

$$\underline{\underline{- 8 \times 10^{-5} P_1}}$$

d. Vessel conditions leading to non-systematic errors in the evaluated mixture compositions are those of <u>temperature fluctuations</u> during mixing operations, as can for instance be caused by changes in room temperature. Usually mixing procedures require up to half an hour. Over such lengths of

time mean room temperatures did not change more than two tenths of a degree centigrade.

More important are temporary increases of temperature inside the vessel, due to the incomplete dissipation of the heat of compression as is generated when the second mixture component is added to the first gas, already inside the vessel. In practice, pressure readings after admission of the second component have always been postponed until the temperature inside the vessel had returned to within $0.3^{\circ}C$ of its previous stable value or $0.2^{\circ}C$ of the room temperature. The influence of an overall temperature rise of $0.3^{\circ}C$, occurring between reading the pressure for respectively the first admitted component and the mixture of the two gases, has therefore to be evaluated.

The thermal expansion of gases is given by :

$$V_{T+\Delta T} = V_T \left( 1 + \frac{\Delta T}{273.15} \right)$$

As the expansion of the vessel will be small compared to the volume change of the gas,

$$P_{T+\Delta T} \approx P_T \left(1 + \frac{\Delta T}{273.15} \right)$$

or :

$$P_T \approx P_{T+\Delta T} \left(1 - \frac{\Delta T}{273.15} \right)$$

If the pressure of the first admitted component is $P_{1,T}$ and the temperature corrected pressure of the mixture is $P_{tot,T}$,

the true percentage of the first admitted component is given by :

$$\frac{P_{1,T} \times 10^2}{P_{tot,T}} = \frac{P_{1,T} \times 10^2}{P_{tot,T+\triangle T}\left(1 - \frac{\triangle T}{273.15}\right)}$$

As : $P_{tot,T} + \triangle T = 2$ atmospheres

$\triangle T = 0.3^{\circ}$ centigrade

it follows that :

$$\frac{P_{1,T} \times 10^2}{P_{tot,T}} = \frac{P_{1,T} \times 10^2}{1.9978} \quad \%$$

Therefore : $P_{tot,T}$ is $(2.2 \times 10^{-3})/2$ too low, or the correction for the measured pressure of the first admitted mixture component is about :

$$\underline{\underline{+ \ 1 \times 10^{-3} \ P_1}}$$

The coefficient for linear thermal expansion of glass is approximately $8.4 \times 10^{-6}$. The increase of the vessel volume for a temperature change of + 0.3°C is therefore:

$$\triangle V_{0.3^{\circ}} = 2.52 \times 10^{-5} \times 3 \times 10^{-1} \times 11.8 \times 10^{3} \text{ cc.}$$

$$= 8.92 \times 10^{-2} \text{ cc.}$$

Thus : $\left(\frac{\triangle V}{V}\right)_{0.3^{\circ}} = \frac{8.92 \times 10^{-2}}{11.8 \times 10^{3}} \approx 8 \times 10^{-6}$

Consequently the true final pressure is $8 \times 10^{-6}$ higher or the correction to $P_1$ is

$$\underline{\underline{- \ 8 \times 10^{-6} \ P_1}}$$

For the influence of temperature changes on the mercury level in the manometer, only the length of mercury column which counterbalances the pressure of gas in the other arm of the manometer is to be considered. For a temperature increase $\triangle T$ the new volume of mercury is :

$$(B.2) \qquad (V + \triangle V)_{Hg} = \pi r_m^2 \, l_{Hg} \, (1 + \alpha_{Hg} . \triangle T)$$

if : $r_m$ = radius of manometer

$l_{Hg}$ = length of mercury column at $T^o$.

The new volume of mercury is also equal to :

$$(B.3) \qquad (V + \triangle V)_{Hg} = \pi \, (r_m + \triangle r_m) \, . \, l'_{Hg}$$

if : $r_m$ = increase of radius due to $\triangle T$

$l'_{Hg}$ = length of mercury column at $T + \triangle T$.

Consequently, for :

$\alpha_l$ - glass = $8.4 \times 10^{-6}$

$\alpha_{cub}$ - Hg = $1.8 \times 10^{-4}$

equation (B.2) = $38.4846 \times l_{Hg} \, (1 + 1.8 \times 10^{-4} \, . \triangle T)$

= $38.4915 \times l_{Hg}$ for $\triangle T = 1^oC$

equation (B.3) = $38.4853 \times l'_{Hg}$

while eq. (B.2) = eq. (B.3).

The elongation of the mercury column per $^oC$ is therefore given by :

$$\frac{l'_{Hg}}{l_{Hg}} = \frac{38.4915}{38.4853} = 1.00016$$

or : $$\triangle l_{Hg} = 1.6 \times 10^{-4}$$

For a temperature change of 0.3°C the elongation of the difference in height between the two mercury levels of the manometer is thus of the order of $5 \times 10^{-5}$. The correction applies only to the final manometer reading, when the vessel is filled with the two components to a total pressure of two atmospheres. As this pressure is calculated from the sum of the final reading and the vacuum reading, which is of the same although opposed order of magnitude, the correction to the total pressure for a temperature increase of + 0.3°C is $-2.5 \times 10^{-5} \times P_{tot}$. Thus the correction to the measured pressure of the first admitted component is

$$\underline{\underline{+ 2.5 \times 10^{-5} P_1}}$$

e. The final correction to be considered is again for a systematic uncertainty. In practice the variation in manometer readings, obtained with the kathetometer (see sub-section II.2.c) is $4 \times 10^{-2}$ mm. Mean values for at least three readings are therefore taken as $\pm 2 \times 10^{-2}$ mm. Pressures have been evaluated by subtraction or addition of two differences in mercury levels of the manometer and are therefore accurate to $\pm 8 \times 10^{-2}$ mm mercury.

As a pressure of two atmospheres equals approximately 1500 mm of mercury column, the absolute uncertainty in any component is :

$$\pm \frac{8 \times 10^{-2}}{1.5 \times 10^{3}} \approx 5 \times 10^{-5}$$

or $\pm \underline{\underline{5 \times 10^{-3} \%}}$ of mixture composition.

f. Review of all these corrections, either in percentage of mixture composition or as correction to the measured pressure of the first admitted component, indicates that the only important factors are the non-additivity of partial pressures, the volume increase of the vessel due to the displacement of mercury in the manometer and the thermal expansion of the gas mixture, which has been assumed not to exceed 0.3°C. By calculating these corrections for a number of compositions, expressed as percentage of the total mixture for the first admitted component, graphical representation of the individual corrections and their sum has been realised as shown in figure III.1.

As the highest fuel-ratio for hydrocarbon-oxygen detonations is 56% methane and fuel has been the first admitted component for these systems, the total correction for the hydrocarbon-oxygen systems, assuming all assumptions are correct, is less than +0.06% fuel. In preparation of hydrogen-oxygen mixtures, oxygen has always been admitted as the first component. The maximum correction applies therefore to the oxygen-rich limit, which is at 84% oxygen. As can be seen the correction is of the same order as for hydrocarbons but of opposite sign with respect to fuel : - 0.06% hydrogen (see figure III.1).

Part II. The accuracy of priming mixtures.

As the spherical storage vessel for the primer mixture has an internal diameter of 21 cm and is connected to the mercury manometer by 50 cm glass tubing of 0.7 cm internal diameter, the vacuum volume of this part of the system has been calculated as 4.866 litres.

It is assumed that only those factors will be important to the accuracy of the stoichiometric mixture of hydrogen and oxygen, that are also significant for the test-mixture compositions. Corrections will be evaluated for an exact case of a mixture, composed by admitting 1 atmosphere of oxygen and supplementing this to an absolute pressure of 3 atmospheres with hydrogen. On measuring the final pressure, the temperature is $0.3^{\circ}$ centigrade above its previous stable level. The theoretical composition is 33.33% oxygen, this being the first admitted component.

a. The non-additivity of partial pressures.

As this correction is independent from the mixing equipment, its value can immediately be found from figure III.1, as $\underline{\underline{+ 0.9 \times 10^{-2}\ \%}}$ oxygen.

b. The mercury displacement in the manometer.

For an absolute pressure change of 3 atmospheres, the displaced volume in the manometer is

$$1.5 \times 76 \times \pi.(0.35)^2 = 45 \text{ cm}^3$$

For 1 atmosphere oxygen the total amount of gas in the system is :

$$(4.866 + \tfrac{1}{3} \times 0.045) \times 1 = 4.881 \text{ litr.atm.}$$

After adding hydrogen to 3 atmospheres :

$$(4.866 + 0.045) \times 3 = 14.733 \text{ litr.atm.}$$

The true composition percentage of oxygen is therefore :

$$\frac{4.881}{14.733} \times 10^2 = 33.13\%$$

and the correction is : $\underline{\underline{- 20 \times 10^{-2}\%}}$ oxygen.

c. The thermal expansion of the gas mixture.

A thermal expansion of the gas mixture, due to a temperature rise on addition of hydrogen, will affect the final pressure in the system according to equation (B.1) (Part 1, sub-section d). For :

$$P_{tot,T + \Delta T} = 3 \text{ atmospheres}$$
$$\Delta T = 0.3^{\circ}C$$

the equation becomes :

$$\frac{P_{1,T} \times 10^2}{P_{tot,T}} = \frac{P_{1,T} \times 10^2}{2.9967} \quad \%$$

Thus : $P_{tot,T}$ is $(3.3 \times 10^{-3})/3$ too low and the correction to $P_1$ is therefore $+ 1.1 \times 10^{-3}$. $P_1$. In percentage :

$$\underline{\underline{+ 3.7 \times 10^{-2} \%}} \text{ oxygen.}$$

d. The overall correction for the primer.

This can now be evaluated from addition of the three corrections calculated above. The correction is $-15.6 \times 10^{-2}\%$ oxygen. The true composition of priming mixtures used in the experiments is therefore around 66.82% hydrogen and 33.18% oxygen.

## Appendix C. The time dependence of detonation initiation by spark ignition.

### Object.

The investigation discussed in this section has been undertaken for two reasons. The first and main purpose has been to determine for detonation propagation in a 1-inch tube the relative positions of precursing disturbances and of the accelerating or stabilised detonation front. In addition information has been sought about the length of tube required for establishing stable detonation in the priming section of the tube.

### Experimental.

To carry out such investigations, the two end plates of the detonation train used in the velocity measurements described in this thesis (figure II.2) have been interchanged, the sparking plug with attachments now being mounted on the free end of the timing section of the train. During the experiments the plate valve has been kept open. The probe circuits have all been connected to separate inputs of Dual-beam Tektronix oscilloscopes to facilitate identification and sequence of individual output signals. The electronic equipment is triggered by a signal obtained from the firing operation of the sparking plug in the way described in sub-section II.2.b of this thesis.

With this arrangement measurements have initially been carried out on detonation initiation in three mixtures of stoichiometric hydrogen-oxygen. Time intervals measured between firing the sparking plug and subsequent signals from the different probe-circuits are given in table C.1. As can be observed there is a considerable time lag between the primary signals of the first couple of probes and those of the other two. This fact does not appear to correspond with the idea of a combustion front, steadily accelerating away from the closed end of the tube.

In a fourth experiment the detonation train has been rearranged into its usual alignment. For this run the train has also been filled completely with stoichiometric hydrogen-oxygen at ambient pressure and the time interval has been measured between firing the sparking plug and the primary signal from the first timing probe. The information has also been entered in table and figure C.1. To indicate the propagation of a stable detonation wave leading to the last result, a characteristic has been drawn in figure C.1 for the appropriate velocity of approximately 2845 metres per second (see table III.1). While its position agrees with an interpretation of the primary signals of the first two probes as representing the passage of the accelerating flame-front, the signals from probe 3 and 4 appear to be caused by much later conductivity variations.

Table C.1. Time intervals in milliseconds between firing the sparking plug and subsequent output signals from the various probe-circuits.

| | Probe number and distance from spark | | | | |
|---|---|---|---|---|---|
| | 1 | 2 | 3 | 4 | 1* |
| | 4.0 cm. | 34.5 cm. | 65 cm. | 95.5 cm. | 463 cm. |
| Run 1 | 3.374 | 4.679 | | | |
| | | 7.155 | 9.269 | 9.589 | |
| | | | 9.685 | 9.835 | |
| | 9.809 | 10.165 | 10.485 | 10.692 | |
| | | | 11.263 | 12.198 | |
| | | 12.406 | | | |
| Run 2. | 3.756 | 5.417 | | | |
| | | 9.491 | 9.748 | 9.907 | |
| | | | 10.311 | 10.311 | |
| | | | 10.800 | 11.167 | |
| | | | 11.699 | 12.523 | |
| | 12.705 | 12.800 | | | |
| | | 13.405 | | | |
| Run 3 | 4.348 | 5.983 | | | |
| | | 8.084 | 11.461 | 12.087 | |
| | | | 12.278 | 12.413 | |
| | | | 12.888 | 13.055 | |
| | 13.062 | 13.354 | | | |
| Run 4 | | | | | ± 7.0 |

* This number 1 refers to the usual arrangement (figure II.2 of this thesis).

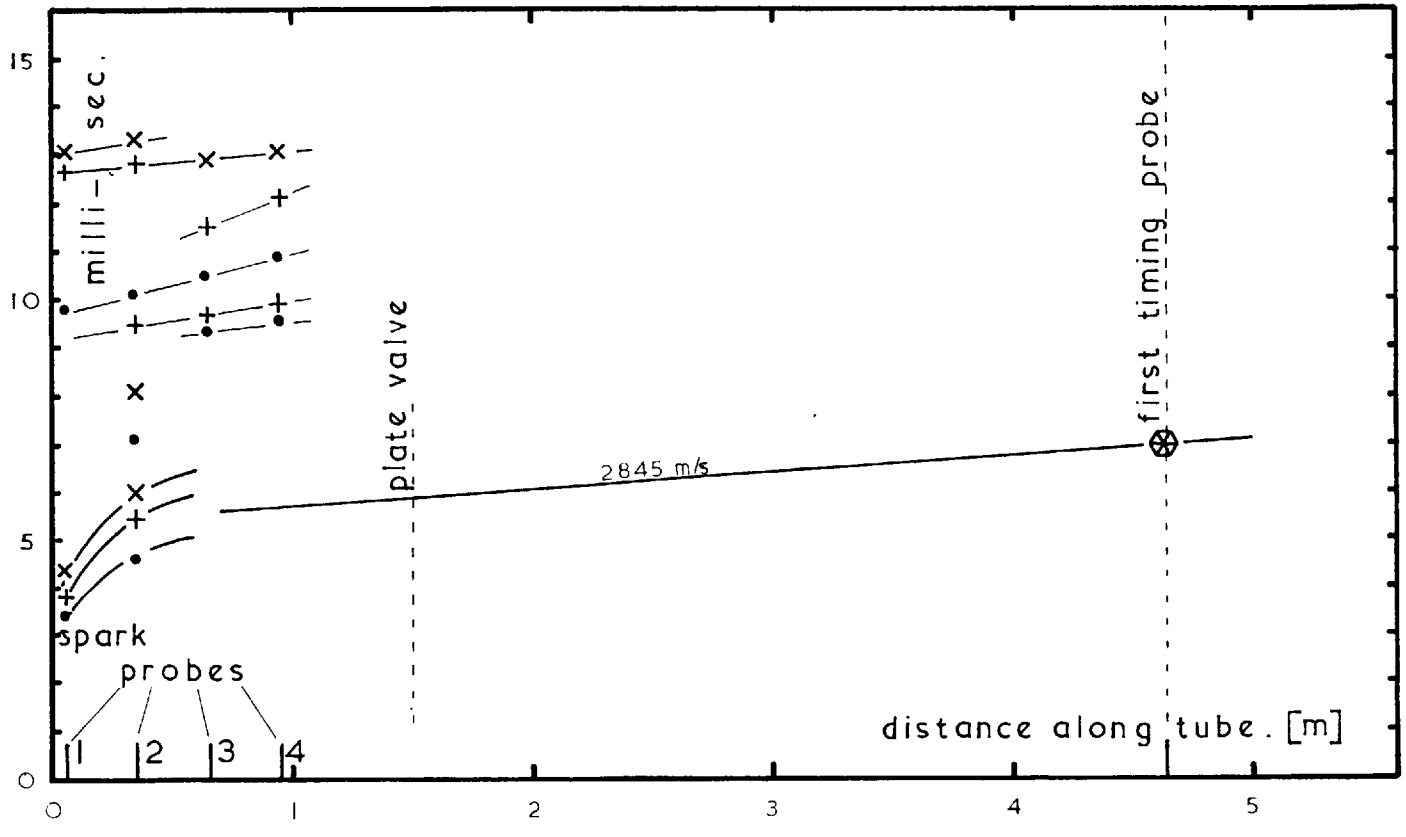



Fig. C.I. Time dependance of propagation of spark ignited detonation in $2H_2 + O_2$; consecutive experiments 1-4 : (•, +, ×, ⊛), see table C.I.

Further study of this observation has been attempted by photographic investigation of flame development in stoichiometric hydrogen-oxygen. To this end a pyrex glass tube, 30 centimetres long and with a 1-inch bore, has been mounted vertically and fitted at its lower end with a brass sealing plate holding the sparking plug. The upper end has been clamped in a brass collar, incorporating a gas inlet. To prevent damage to the tube, it has been sealed on top by a loose thin brass plate, resting on an O-ring, which is blown off by the impact of the upward propagating, accelerating flame initiated in the tube by firing the sparking plug. The outside of the tube has been covered with black sticky tape leaving only free a 3/32-inch slit, parallel with the axis of the tube. Flame propagation in stoichiometric hydrogen-oxygen has been recorded with a rotating drum camera, the film moving at right angles to the slit.

An example of these photographic records is shown in figure C.2. The picture indicates that a few milli-seconds after the primary flame movement starts to accelerate along the tube (A) a zone of intense combustion moves backwards towards the end plate (B). Comparison of the time-calibration with figure C.1 shows that the later signals of probe 1 and 2, and all signals from probe 3 and 4 are caused by the increased conductivity in this wave. It is

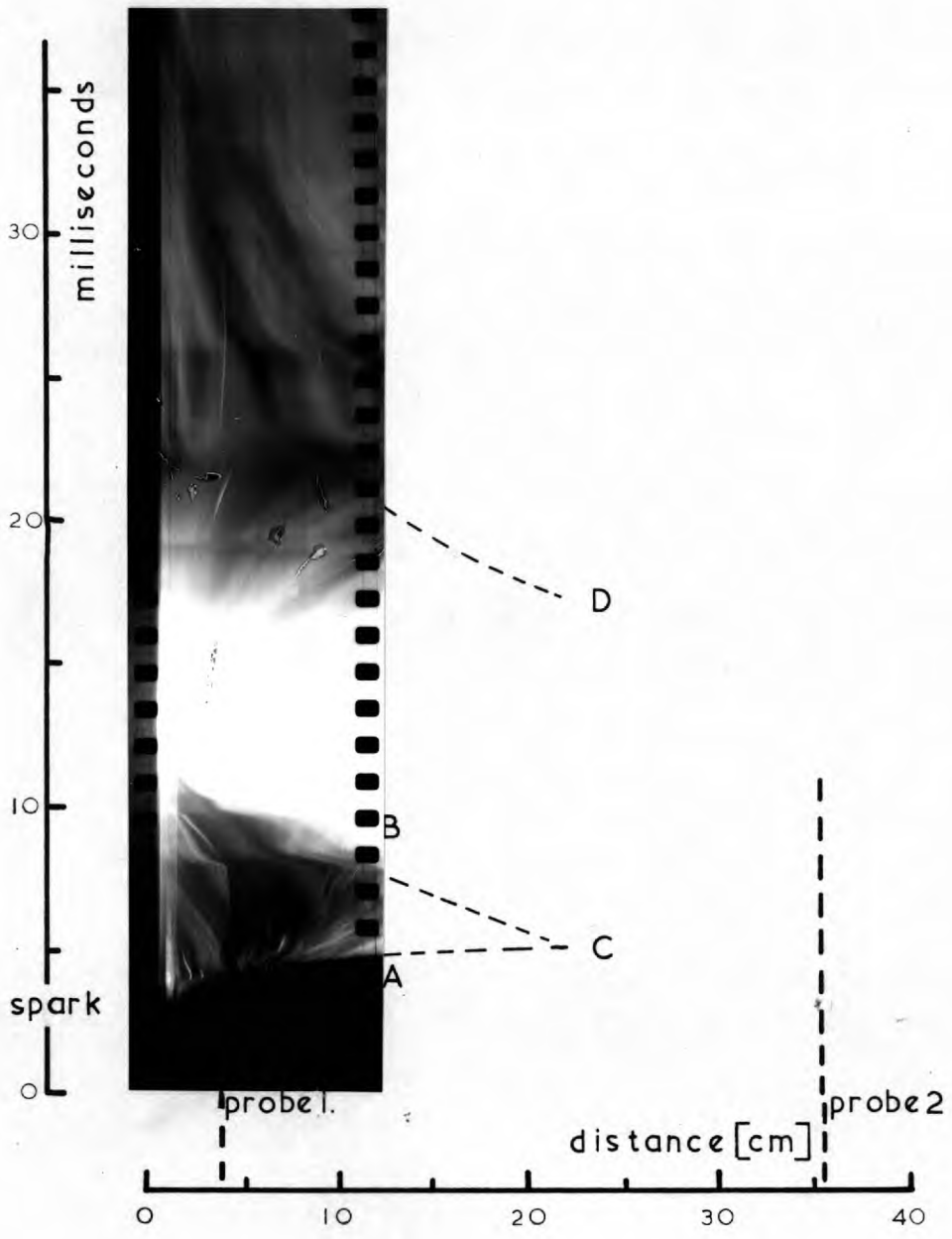



Fig.C.2. Initiation of spark ignited detonation in stochiometric hydrogen-oxygen

possible that the returning wave originates from the shock initiation of the real detonation which is caused by compression waves generated by the accelerating flame front in the way described by Bone et al. [1936]. The initiation would occur at a point outside the range of the picture in figure C.2, e.g. point C in figure C.2. In the photographic investigation flash-back of the gases appears also to occur after the primary wave has opened the end of the tube (D). This is probably represented by the much cooler region more than 20 Msec. after initiation. Alternatively secondary signals in figure C.1 could refer to flow back of hot gases in the wave, returning after reflection of the primary detonation wave from the end of the tube. Clarification of this problem requires further investigation. As yet, all suggestions do not explain clearly why probes 3 and 4 have not reacted to the passage of a primary wave.

However, at present the only point of direct interest in this photographic observation is the indication that stable detonation starts beyond the range of 12 cm from the spark and approximately 5 Msec. after firing the sparking plug. This would correspond with the relative positions of the primary signals of probe 1 and 2 and of the characteristic of 2845 metres per second, drawn in figure C.1 through the result of run no 4 (see table C.1). From these it appears that stable detonation must be established

approximately 60 centimetres from the sparking plug. Further support for this opinion is obtained from inspecting the inside of the priming section of the detonation train. About two feet from the end the wall bears the beginning of a clear erosion pattern, which continues down the tube. A similar result has also been reported by Laffitte[1928].

To indicate accurately on these photographic records the moment of firing the sparking plug, some films have been marked by a very short duration light flash at time zero. This has been achieved in the following way: The trigger line operating in the normal detonation velocity measurements from the solenoid placed around the high tension line to the sparking plug (see sub-section II.2.b of this thesis), has been used in the same way to trigger a very fast sweep from an oscilloscope set at high trace intensity. With a mirror-and-lens arrangement an image of a small section of the trace was projected on the rotating film. It is regretted that such a record is no longer available for reproduction in this discussion.

Apart from allowing the accurate registration of the time zero-point, the further study of such records has shown that there is an average time lag of approximately three milliseconds between the charging of the sparking plug and the first photographic observation of the following

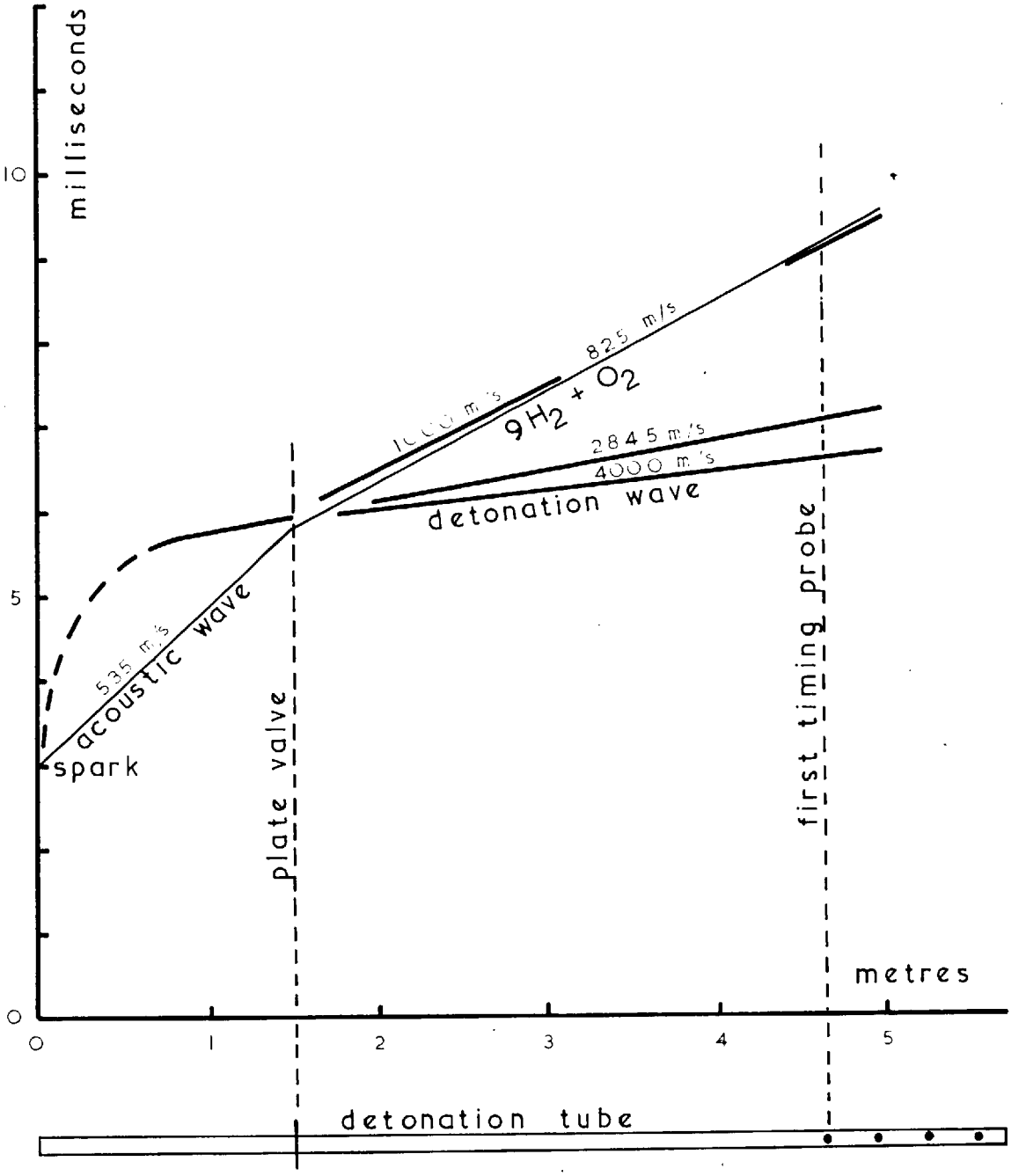



Fig. C.3. Relative positions of the detonation front and possible acoustic precursors.

spark discharge. The important conclusion to be drawn from this for the current points of interest is that the acoustic precursors to detonation in the detonation train cannot be generated less than three milliseconds after the firing operation.

Conclusions.

The above mentioned results indicate in the first place that steady-state conditions in the priming section of the detonation train will be attained approximately two feet from the spark and six milliseconds after firing.

As for the relative positions of the detonation front and possible precursor effects, characteristics for detonation propagation and acoustic precursors in mixtures of various mean molecular weights can be compared in figure C.3. From these it follows that even for detonating mixtures with very high sound velocities, acoustic precursors are overtaken by the detonation wave several feet away from the first timing probe in the detonation train.

Appendix D. Calculation of the final pressure of the test mixture from the measured final pressure in the detonation train.

1. Principle.

With propagation of combustion down the 1-inch detonation tube the following conversions of gaseous components take place. In the priming section stoichiometric hydrogen-oxygen is assumed to change into water vapour at saturation pressure over liquid water; from the small amount of air, introduced into the system by operating the plate valve, the oxygen is consumed in combustion, leaving behind the nitrogen; the test mixture is changed into its own reaction products at pressure $P_u$. However, reaction products from all sections spread over the volume of the complete detonation train and of the mercury manometer which, after having been evacuated, is used to read the overall final pressure $P'_u$. The various steps in reaching this situation are listed in table D.1.

Using the notation introduced in table D.1, it follows that

$$P'_u \ (V_p + V_v + V_t + V_m) =$$

$$(P_{H_2O})_{T_i} \cdot V_p + (P_{N_2})_{1 \text{ at}} \cdot V_v + P_u \cdot V_t + 0 \cdot V_m$$

Therefore, the final pressure of the test mixture is

$$(D.1) \qquad P_u = \frac{P'_u(V_p+V_v+V_t+V_m) - (P_{H_2O})_{T_i}.V_p - (P_{N_2})_{1\ at}.V_v}{V_t}$$

2. Correction evaluation.

To be able to use equation (D.1) for the calculation of the final pressure of a test mixture, the various volumes, referred to in the formula, have to be determined. This is done from measured dimensions of the system, as given in figure D.1.

Calculated volumes of parts of sections are given in table D.2. The characters refer to those used in figure D.1. The calculated errors are in fact too conservative, as they are evaluated from simple addition of possible errors in the individual dimensions. The true errors in the data of table D.2 and in values later to be derived are therefore smaller.

From the data of table D.2 the volumes of all sections are calculated as given in table D.3. Substitution of these values in equation (D.1) gives

$$P_u = (1.3167 + 1.742\ x10^{-4}.1)P'_u - 0.30888(P_{H_2O})_{T_i} - 0.26 \pm 1.8\%$$

For practical use the equation is more conveniently written as :

(D.2) $$P_u = A.P'_u - B \quad [\text{mm Hg}]$$

in which : $A = 1.3167 + 1.742 \times 10^{-4}.\, l$ ,

$l$ being the distance in centimetres between the 100 mark on the manometer scale and the mercury level and

$B$ = values, calculated for different temperatures and tabulated in table D.4.

3. Calibration experiments.

To test the accuracy of equation (D.2) for calculation of the final pressure of the test mixture, a series of calibration experiments has been performed. In these, the detonation train has first been evacuated as in preparation for a normal test run. The tube sections were then filled with nitrogen at such pressures as would represent the pressures of local reaction products after a detonation experiment. The plate valve was subsequently opened and the overall pressure in the tube was measured in the usual way.

The results of these calibration experiments are given in table D.5. As can be observed the mean practical error over all experiments is $\pm$ 1.4 mm of mercury pressure difference. It follows from comparison with the calculated error of $\pm$ 1.8% that for final test mixture pressures above 8 cm of mercury, the accuracy of equation (D.2) is much better than predicted. In practice this applies to all experiments but those with near-stoichiometric hydrogen-oxygen mixtures.

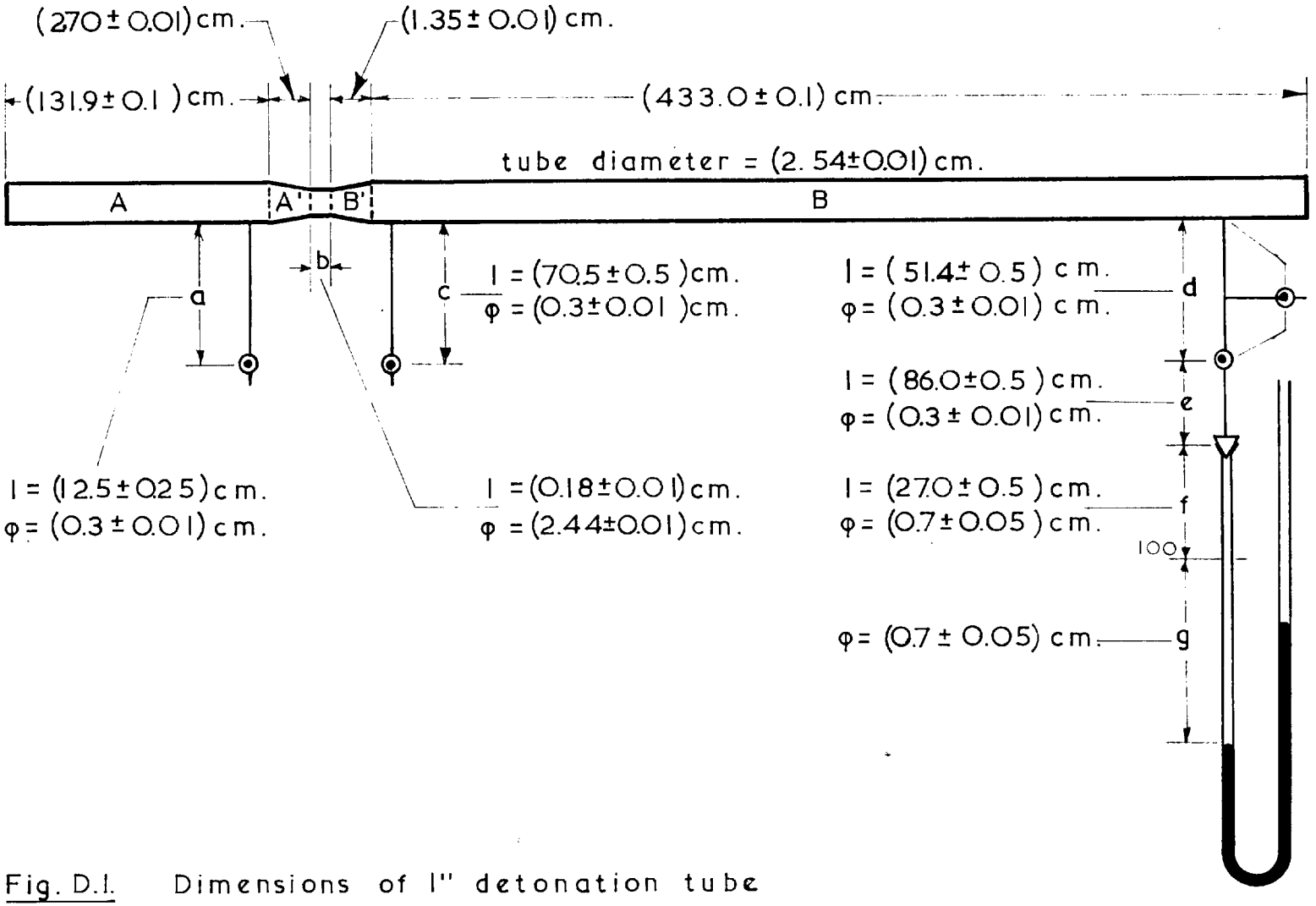



Fig. D.1. Dimensions of 1" detonation tube

Table D.1. Analysis of pressure development in detonation train.

| Section | Volume notation | Initial pressure | Final pressure local | Final pressure overall |
|---|---|---|---|---|
| Priming section | $V_p$ | $P_i$= 1 atm. | $(P_{H_2O})_{T_i}$ | $P'_u$ |
| Plate valve | $V_v$ | 1 atm. | 4/5 atm.$N_2$ | $P'_u$ |
| Test section | $V_t$ | $P_i$= 1 atm. | $P_u$ | $P'_u$ |
| Manometer | $V_m$ | vac. | vac. | $P'_u$ |

Table D.3. Volumes of sections of 1-inch detonation train.

Priming section : $V_p = (682.38 \pm 5.94)\ [cm^3]$
$= 682.38[cm^3] \pm 0.87\%$

Plate valve : $V_v = (0.842 \pm 0.053)\ [cm^3]$
$= 0.842\ [cm^3] \pm 6.3\%$

Test section : $V_t = (2209.20 \pm 18.34)\ [cm^3]$
$= 2209.20\ [cm^3] \pm 0.83\%$

Manometer : $V_m = (16.47 \pm 2.10)\ [cm^3]$
$+ ((0.3848.1)[cm^3] \pm 2.8\%)$
$= 16.47\ [cm^3] \pm 0.83\% +$
$((0.3848.1)[cm^3] \pm 2.8\%)$ *

* l in cm.

Table D.2. Volumes of parts of 1-inch detonation train. (Note: the characters refer to those used in figure D.1).

Priming section : $A = (850.97 \pm 7.32) \times \pi/4\ [cm^3]$ *
$= 850.97 \times \pi/4\ [cm^3] \pm 0.86\%$ **

$A' = (16.74 \pm 0.20) \times \pi/4\ [cm^3]$
$= 16.74 \times \pi/4\ [cm^3] \pm 1.2\%$

$a = (1.125 \pm 0.097) \times \pi/4\ [cm^3]$
$= 1.125 \times \pi/4\ [cm^3] \pm 8.6\%$

Plate valve : $b = (1.072 \pm 0.068) \times \pi/4\ [cm^3]$
$= 1.072 \times \pi/4\ [cm^3] \pm 6.3\%$

Test section : $B = (2793.54 \pm 22.35) \times \pi/4\ [cm^3]$
$= 2793.54 \times \pi/4\ [cm^3] \pm 0.80\%$

$B' = (8.37 \pm 0.13) \times \pi/4\ [cm^3]$
$= 8.37 \times \pi/4\ [cm^3] \pm 1.6\%$

$c = (6.35 \pm 0.46) \times \pi/4\ [cm^3]$
$= 6.35 \times \pi/4\ [cm^3] \pm 7.3\%$

$d = (4.59 \pm 0.35) \times \pi/4\ [cm^3]$
$= 4.59 \times \pi/4\ [cm^3] \pm 7.6\%$

Manometer : $e = (7.74 \pm 0.56) \times \pi/4\ [cm^3]$
$= 7.74 \times \pi/4\ [cm^3] \pm 7.2\%$

$f = (13.23 \pm 2.12) \times \pi/4\ [cm^3]$
$= 13.23 \times \pi/4\ [cm^3] \pm 16\%$

$g = 0.49 \times l \times \pi/4\ [cm^3] \pm (2.8 + \triangle l)\%$ ***

* $\pi/4 = 0.785397$

** Errors are too conservative (see text)

*** $l$ = length of volume in cm.

$\triangle l$ = relative error in $l$.

Table D.4. Values for B as function of temperature, for the calculation of the final pressure of the test mixture (equation (D.2)).

| Degrees C | Tenth of degree Centigrade | | | | | | | | | |
|---|---|---|---|---|---|---|---|---|---|---|
| | $^{o}.0$ | $^{o}.1$ | $^{o}.2$ | $^{o}.3$ | $^{o}.4$ | $^{o}.5$ | $^{o}.6$ | $^{o}.7$ | $^{o}.8$ | $^{o}.9$ |
| 15° | 4.21 | 4.24 | 4.26 | 4.29 | 4.31 | 4.34 | 4.37 | 4.39 | 4.42 | 4.44 |
| 16° | 4.47 | 4.50 | 4.53 | 4.55 | 4.58 | 4.61 | 4.64 | 4.66 | 4.69 | 4.72 |
| 17° | 4.75 | 4.78 | 4.81 | 4.83 | 4.86 | 4.89 | 4.92 | 4.95 | 4.98 | 5.01 |
| 18° | 5.04 | 5.07 | 5.10 | 5.13 | 5.16 | 5.19 | 5.22 | 5.26 | 5.29 | 5.32 |
| 19° | 5.35 | 5.38 | 5.41 | 5.45 | 5.48 | 5.51 | 5.54 | 5.58 | 5.61 | 5.64 |
| 20° | 5.68 | 5.71 | 5.74 | 5.78 | 5.81 | 5.85 | 5.88 | 5.92 | 5.95 | 5.99 |
| 21° | 6.02 | 6.06 | 6.09 | 6.13 | 6.16 | 6.20 | 6.24 | 6.27 | 6.31 | 6.35 |
| 22° | 6.38 | 6.42 | 6.46 | 6.50 | 6.54 | 6.57 | 6.61 | 6.65 | 6.69 | 6.73 |
| 23° | 6.77 | 6.81 | 6.85 | 6.89 | 6.93 | 6.97 | 7.01 | 7.05 | 7.09 | 7.13 |
| 24° | 7.17 | 7.21 | 7.26 | 7.30 | 7.34 | 7.38 | 7.43 | 7.47 | 7.51 | 7.55 |
| 25° | 7.60 | 7.64 | 7.69 | 7.73 | 7.77 | 7.82 | 7.86 | 7.91 | 7.96 | 8.00 |
| 26° | 8.05 | 8.09 | 8.14 | 8.19 | 8.23 | 8.28 | 8.33 | 8.37 | 8.42 | 8.47 |
| 27° | 8.52 | 8.57 | 8.62 | 8.67 | 8.72 | 8.76 | 8.81 | 8.86 | 8.92 | 8.97 |

Table D.5. Difference between the calculated and true final pressure of the test mixture as found from calibration experiments with nitrogen.

| $P_{H_2O}$ [mm.Hg] | $P_{u_{exp}}$ [mm.Hg] | $P_{u_{calc}}$ [mm.Hg] | $P_{u_{exp}} - P_{u_{calc}}$ [mm.Hg] |
|---|---|---|---|
| 12.0 | 0.0 | 1.3 | + 1.3 |
| | 763.7 | 762.5 | - 1.2 |
| | 1476.7 | 1472.8 | - 3.9 |
| 18.0 | 0.0 | 0.9 | + 0.9 |
| | 763.7 | 762.6 | - 1.1 |
| 24.0 | 0.0 | 0.5 | + 0.5 |
| | 763.7 | 762.6 | - 1.1 |
| | 1482.2 | 1480.9 | - 1.3 |

## Appendix E. Condensation products from detonation of fuel-rich n-butane - oxygen mixtures.

Electron micrographs and electron diffraction patterns have been made from samples formed at three different mixture compositions. The plate reference numbers correspond to those under which the records are stored in the Department file.

The quality of the diffraction patterns is not good enough to allow determination of the crystallite size; only the inter-crystallite layer distance was measured.

Some of the plates are in part shown in figure III.11.

Table E.1.

| % $C_4H_{10}$ | Plate reference number. | Micrograph Particle size. | Diffraction pattern Interlayer distance. |
|---|---|---|---|
| 32.64 | 5864- 5866<br>5867 | (100-300) A | (3.44 - 3.44) A |
| 37.75 | 5859-5862<br>5863 | (200-300) A | (3.51 - 3.52) A |
| 38.68 | 5856-5858 | (100-300) A | |

Appendix F. Calculation of the ratio between the energy from carbon sublimation and the net reaction energy for detonation of fuel-rich hydrocarbon-oxygen mixtures.

The overall reaction for incomplete oxidation of a saturated aliphatic hydrocarbon to carbon monoxide, graphitic carbon and molecular hydrogen is given by the equation :

$$x\ C_nH_{2n+2} + (1-x)\ O_2 = 2(1-x)CO + (nx+2x-2)C_{gr} + x(n+1)H_2 + Q \qquad (F.1)$$

Oxygen, hydrogen and graphitic carbon represent the ground state of these species at room temperature and have zero heat of formation. The value of Q consequently depends on the heat of formation of respectively a mole of hydrocarbon and a mole of carbon monoxide from the elements. The latter is given in literature (e.g.: Lewis and Von Elbe, [1963], page 680) as :

$$C_{gr} + 1/2\ O_2 = CO + 27.2\ \text{kcal.}$$

The heat of formation of saturated aliphatic hydrocarbons has been calculated as follows. The heat of combustion of normal saturated aliphatic hydrocarbons for conversion to carbon dioxide and water is given by :

$$C_nH_{2n+2} + (3n+1)/2\ O_2 =$$

$$n\ CO_2 + (n+1)H_2O_{liq} + (158n + 58)\ \text{kcal},$$

As it furthermore can be found that

$$H_2O_{liq} + 10\ \text{kcal} = H_2O_{gas}$$

$$C_{graph.} + O_2 = CO_2 + 94\ \text{kcal, and}$$

$$H_2 + 1/2\ O_2 = H_2O_{gas} + 57.8\ \text{kcal.}$$

it can be shown that :

$$nC_{graph.} + (n+1)H_2 = C_nH_{2n+2} + (4.8n + 10.8)\ \text{kcal.}$$

Experience has shown that heats of formation for branched saturated aliphatic hydrocarbons are quite accurately calculated by increasing the proper value for n by one integer. For instance, the heat of formation for pentane molecules is, (see Perry [1963], table 3-135);

n-pentane : calculated: -34.8 kcal;
experimental: - 35.00 kcal.

neo-pentane : calculated : -39.6 kcal;
experimental: -39.67 kcal.

The value of Q in equation (F.1) can now be calculated. The energy released in oxidation is :

| | | |
|---|---|---|
| "Atomisation" $C_nH_{2n+2}$ | : $-4.8nx + 10.8x$ | kcal. |
| Formation CO | : $- 54.4x + 54.4$ | kcal. |
| | $Q = -(+4.8n + 65.2)x + 54.4$ | kcal |

The sublimation energy for carbon is given by :

$$C_{gas} = C_{graphite} + 170 \text{ kcal.}$$

Consequently, for the reaction of equation (F.1), the ratio between the energy supplied by condensation of gaseous carbon and the net energy produced in the oxidation reaction is given by :

$$\frac{Q_C}{Q} = \frac{[x\ (n + 2) - 2]\ .\ 170}{-(4.8n + 65.2)x + 54.4}$$

Appendix G. Measured detonation velocities and evaluated data for binary systems of oxygen with ethane and ethylene.

Data for the binary systems of oxygen with ethane and ethylene have been obtained from the detonation velocity measurements by Schuller [1954]. The experiments were performed in a 15 mm bore tube. Detonation was initiated with a stoichiometric hydrogen-oxygen primer. The test section of the tube consisted of a 10 metres long coiled section, followed by a straight length of tube, 1 metre long, which was used to measure the propagation velocity by a method comparable to the one used in our own research.

Values for the Mach-product, the relative Mach-product and the composition on the basis of homology elements have been evaluated as described in chapter V of this thesis.

Table G.1. Detonation velocities, Mach-product data and compositions on homology-elements basis for the system ethane-oxygen.

| % $C_2H_6$ | Mean velocity [m/sec] | $\gamma M^2$ | $\frac{\gamma M^2}{\gamma M^2_{max}}$ | $\%C_2H_6$ as $2CH_2 + H_2$ |
|---|---|---|---|---|
| 3.8 | - | - | - | 10.59 |
| 4.0 | 1130 | 16.733 | 0.188 | 11.11 |
| 4.5 | 1505 | 29.672 | 0.333 | 12.39 |
| | 1520 | 30.267 | 0.340 | |
| 5.0 | 1545 | 31.261 | 0.351 | 13.64 |
| 6.0 | 1660 | 36.066 | 0.405 | 16.07 |
| 7.0 | 1760 | 40.518 | 0.455 | 18.42 |
| 10.0 | 1960 | 50.158 | 0.564 | 25.00 |
| 15.0 | 2140 | 59.612 | 0.670 | 34.62 |
| 20.0 | 2290 | 68.055 | 0.765 | 42.86 |
| 25.0 | 2440 | 77.026 | 0.865 | 50.00 |
| 30.0 | 2560 | 84.529 | 0.950 | 56.25 |
| 31.8 | 2610 | 87.766 | 0.986 | 58.31 |
| 35.0 | 2630 | 88.941 | 0.999 | 61.18 |
| 38.0 | 2630 | 88.777 | 0.997 | 64.77 |
| 40.0 | 2585 | 85.659 | 0.962 | 66.67 |
| 43.0 | 2480 | 78.695 | 0.884 | 69.35 |
| 45.0 | 2300 | 67.602 | 0.760 | 71.05 |
| 45.5 | 2250 | 65.340 | 0.734 | 71.47 |
| 46.0 | 2140 | 58.488 | 0.657 | 71.88 |
| 46.25 | 2100 | 56.313 | 0.633 | 72.08 |
| 46.5 | - | - | - | 72.28 |

* $\gamma M^2_{maximum} = 89.0$

composition $\gamma M^2_{max}$ = 36.0 mole% $C_2H_6$ = 62.79 hom.%

Table G.2. Detonation velocities, Mach-product data and compositions on homology-elements basis for the system ethylene-oxygen.

| $\%C_2H_4$ | Mean velocity [m/sec] | $\gamma M^2$ | $\frac{\gamma M^2}{\gamma M^2_{max}}$ * | % $C_2H_4$ as $2CH_2$ |
|---|---|---|---|---|
| 3.75 | - | - | - | 7.23 |
| 4.0 | 901 | 10.611 | 0.116 | 7.69 |
| 4.5 | 940 | 10.806 | 0.118 | 8.61 |
| | 1225 | 19.602 | 0.214 | |
| 4.75 | 1535 | 30.769 | 0.336 | 9.07 |
| 5.0 | 1580 | 32.590 | 0.355 | 9.52 |
| 6.0 | 1680 | 36.800 | 0.401 | 11.32 |
| | 1685 | 37.019 | 0.404 | |
| 7.0 | 1775 | 41.028 | 0.447 | 13.08 |
| 10.0 | 1902 | 46.934 | 0.512 | 18.18 |
| 15.0 | 2090 | 56.316 | 0.614 | 26.09 |
| | 2110 | 57.399 | 0.626 | |
| 20.0 | 2250 | 64.858 | 0.707 | 33.33 |
| 25.0 | 2350 | 70.304 | 0.767 | 40.00 |
| 30.0 | 2520 | 80.329 | 0.876 | 46.15 |
| 35.0 | 2620 | 86.274 | 0.941 | 51.85 |
| 40.0 | 2690 | 90.339 | 0.985 | 57.14 |
| 45.0 | 2700 | 90.441 | 0.986 | 62.07 |
| 50.0 | 2540 | 79.516 | 0.867 | 66.67 |
| 52.5 | 2430 | 72.539 | 0.791 | 68.89 |
| 55.0 | 2200 | 59.261 | 0.646 | 70.97 |
| 57.5 | 1710 | 35.684 | 0.389 | 73.02 |
| 60.0 | 855 | 8.891 | 0.097 | 75.00 |
| 62.5 | 870 | 9.175 | 0.100 | 76.92 |

* $\gamma M^2_{maximum} = 91.7$

composition $\gamma M^2_{max}$ = 43.5 mole % $C_2H_4$ = 60.63 hom.%

## Appendix H. Determination of detonation velocities with the electronic counter.

### I. The equipment.

Although the timing equipment, described in this appendix, was designed before the present work was started, it is included in this appendix for a matter of record.

#### 1. General description.

The timer is a multi-channel system, consisting of five units of three decade counters. A 1-MHz clock pulse train is fed through gating circuits to each of the counters. The system is arranged in such a way that a single pulse us capable of operating all the gates and thus starting all the counters, while serial pulses will close the gates and thus stop the individual counters sequentially. Gating circuits are arranged in such a way that they operate once only. The system logic is schematically illustrated in figure H.1. The timer is thus capable of measuring time intervals between a unique signal from the first station and each one of the subsequent signals from a further five stations; intervals of time between these subsequent signals are obtained by difference. The basic timing unit is a microsecond but readings on the counters represent intervals of two microseconds, the presence or absence of odd digits being indicated on a meter. The capacity is thus 1999 microseconds.

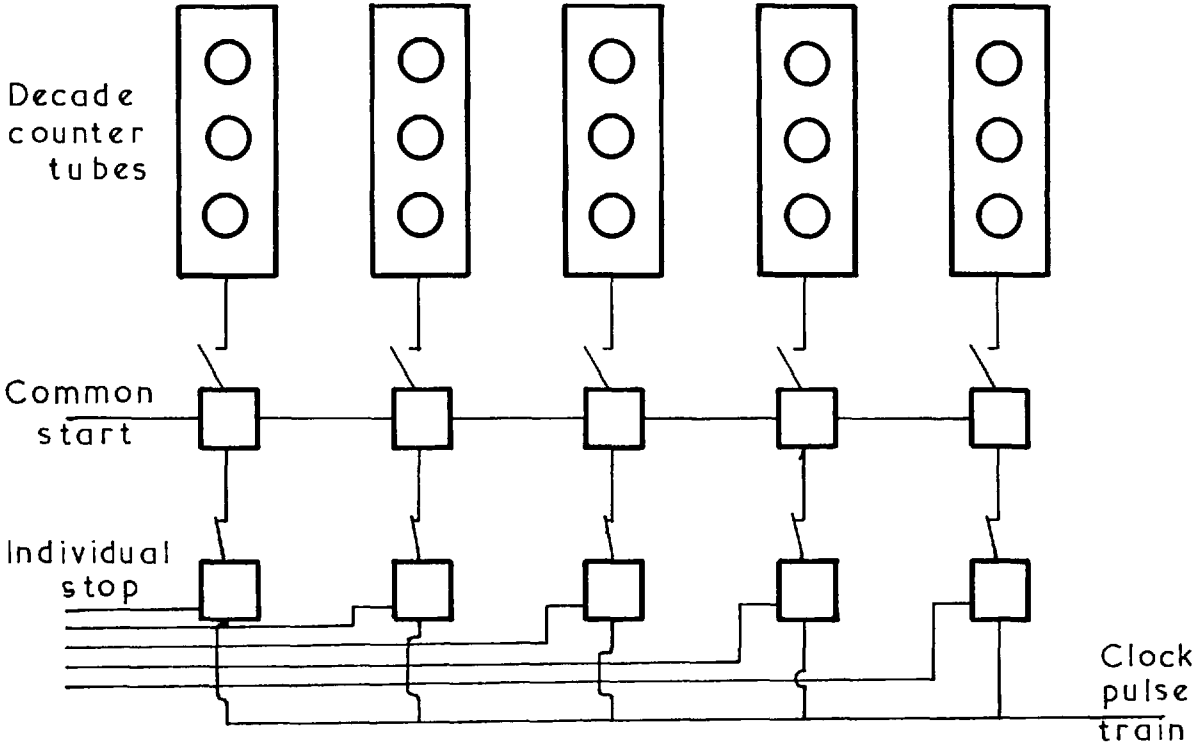



Fig. H.I. System logic for counter operation

The counter is constructed in the following units, shown in the diagram, figure H.2: a "580V Power supply" and a"Power supply and Control"unit; Sub-units I and II; the Timing unit; and the 1-MHz oscillator. The power supply and the pulse generator are housed in the first pair of units; the timing unit contains the counters and gating sections in two subdivisions. The start unit and the five stop units are contained in the two subsidiary units, each of which is associated with three timing stations.

The 1-MHz clock pulse train is obtained from an AIRMEC oscillator, type 213 (frequency controlled by crystal contained in a temperature controlled oven).

2. Channel circuit description.

In figure H.2 a circuit for one channel of the timer is shown schematically in block-diagram form.

Signals from the external 1 MHz source A are shaped and fed through the gating circuit C. Following amplification, the signals actuate a 1 MHz binary E, which forms the basic counting unit. The state of the binary (i.e. the condition of the two halves of the circuit representing zero or unity in the binary scale) is indicated on a meter.

The series of pulses produced by the binary, each time it returns to the zero position, is fed via a cathode follower to three decade counter tubes in series, H, L and N,

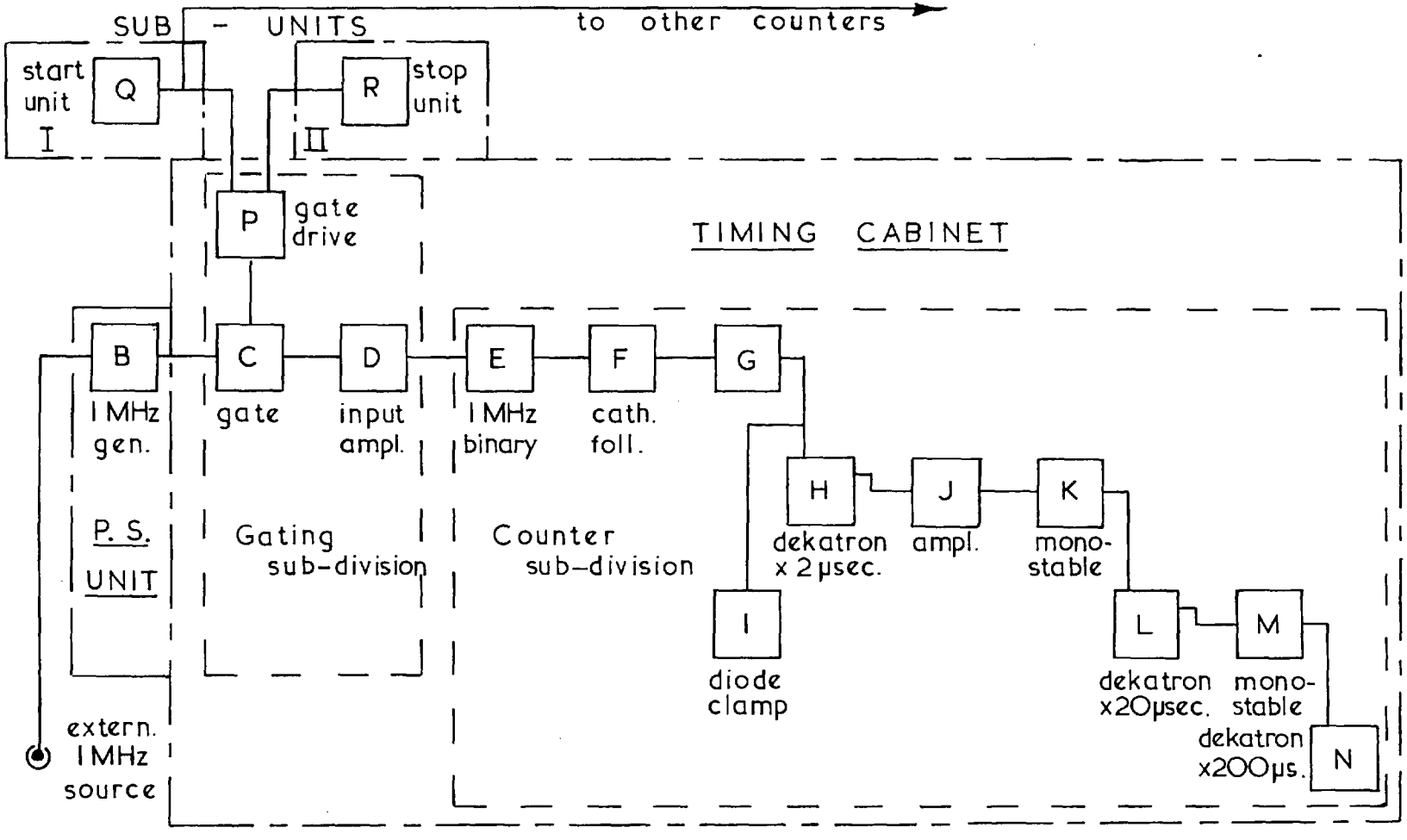



Fig.H.2. Block schematic of 1-channel counter.

which record units of 2 microseconds, 20 microseconds and 200 microseconds respectively. The amplifier J, monostables K and M, and various ancillary circuits are required to maintain the clock-pulse train at an acceptable signal level.

The gate in each channel has an associated gate drive P, fed by a 'start' (or 'open'), and a 'stop' (or 'close') command. The former command is derived from a start unit Q, common to all five channels. The stop command is derived from a stop unit R, attached to the individual channels.

After operation the timing units and the start and stop sub-units are reset by a press button switch, located on the "Power Supply and Control" unit.

Power supplies, -150V, +250V, +250V -stabilized and +280V, all fused and switched, are located in the "Power supply and Control" unit; the +580V power supply is also switched and fused in this unit.

## 3. Construction.

### Arrangement.

The pulse generator is common to all the channels and is located in the "Power supply and Control unit"; the start unit is also common to all channels and is contained in sub-unit I; operation of the start unit is indicated by a neon ~~lamp~~. Stop units are located in their appropriate sub-units I or II.

The timing unit is divided into the five individual channels; each channel is further sub-divided into two parts, one containing gating facilities, the other the 1-MHz bistable and its meter indicator, and the three decade counters. Certain common facilities such as reset and valve heater supplies are also housed in the main body of this unit.

All these divisions are shown in figure H.2 by dotted lines.

Connections.

The 1-MHz output from the AIRMEC oscillator is fed into the pulse generator at socket S.K.3. Output from the pulse generator to the side entry of the timing unit is realised by way of the cable assembly PL.2.C.U. from SK 2.

Internal connections to the gating sub-sections are by 8-way plug and socket and from gating sub-sections to timing sub-sections by red and black 'mini'-plug and sockets. Connections from timing sub-sections to the micro-ammeter are by two mini-sockets, fixed on the panel which carries the counter tubes.

Signals from stations are fed into two of three mini-plugs on the start-unit and stop-units; the bottom black mini-socket is an earth connection; the top red and black mini-sockets are for positive and negative signals respectively.

The start unit is connected from exit (1.o) by coaxial cable to the side entrance (1.i) on the timing unit; stop-units are connected by similar cables from exits (2.o - 6.o) to entries (2.i - 6.i). Internal connections within the timing unit from the start sub-unit socket (1.i) is by a looped coaxial connector to all the gating sub-section sockets (A). Individual internal connections from 'stop'-sockets to sockets (B) on gating sub-sections are also by coaxial lead.

Other connections, including power supply and reset -pulses carriers, are all by multi-way cable assemblies; multi-way plugs and sockets are designated by a code consisting of two letters, followed by a number, followed by two letters. The first two letters PL or SK refer to plug and socket respectively; the last two letters refer to the unit, and the number to a particular connection on that unit.

Circuit description.

Circuits are not given, but a functional description is presented. Block diagrams are shown in figures H.3, a, b and c.

a. Pulse-generator.

Signals from the AIRMEC 1-MHz oscillator are fed through a cathode follower to a tuned amplifier, followed by an amplifier with adjustable bias, which allows the passage

of required positive signal-peaks. The resultant signal train is then fed via another cathode follower to the gating sub-section of the timing unit *.

b. Gating sub-section.

A bistable operating on the 'start' and 'stop' commands from the start and stop sub-units, controls the gate-drive amplifier, which sets the voltage level on the screen of a second amplifier to either of two levels. The signal train from the pulse generator is fed to the grid of this second amplifier and appears on the anode when the screen voltage is at the appropriate set level; at the other set level the valve is cut off and no signal appears at the output. The two set levels can be adjusted by a pre-set variable resistor. The bistable is re-set by a pulse derived from a relay operated by the press button switch.

c. Timing sub-section.

The gated pulse train is fed into a high frequency bistable which divides the pulse train by two. This was necessary since, despite the claims by the manufacturer, the decade counter tubes were not capable of reliable operation at 1 MHz. A micro-ammeter is used to indicate the state of

---

* For constructional convenience half of a E182cc valve in the timing sub-section is used as a pulse amplifier to modify the pulse train between the pulse generator and the gating sub-section; the output from this amplifier is by the black mini-plug.

the bistable at the end of the gated pulse train. The 500 K-Hz pulse train from the bistable is counted by an Eleska, EZ 10B decade counter tube after suitable shaping by an anode tuned amplifier circuit in which forward conduction of the diode prevents all but the first negative going excursion appearing at the auxiliary cathode of the counter tube. The correct D.C. level at this cathode is maintained by the clamping action of the diode. With this arrangement the counter tube records intervals of 2 microseconds and every ten counts a read-out voltage is developed across the last cathode resistor. Each pulse, derived from such a voltage change, is amplified and fed to a monostable, which produces a pulse of the required width to operate a second decade counter tube; this tube thus records intervals of 20 micro-seconds. A modification has been introduced in the first decade counter circuit to reduce the unwanted 500 K Hz negative signals which appears on the last cathode of the counter tube: the positive 500 K Hz signal from the cathode of the tuned amplifier is fed forward to the last cathode of the counter tube and is amplitude-adjusted to just balance out the negative pulses. A similar process, without the amplifier, allows for the registration of 200$\mu$sec. intervals on a third decade counter tube.

Two wire-wound linear pre-set resistors are provided in the timing sub-section to allow for the adjustment of the

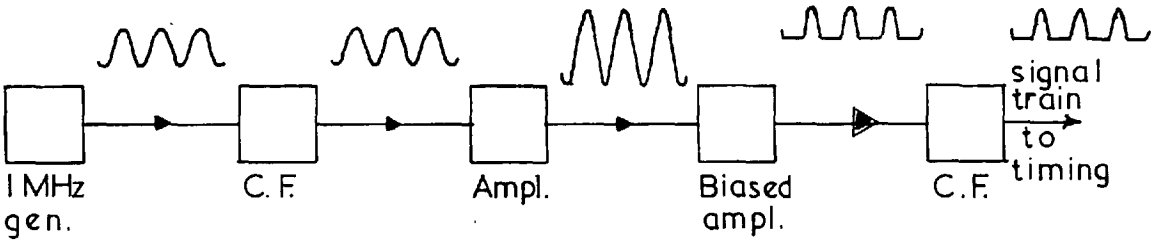
voltage levels at the ammeter terminals, in order that the meter may read zero or full scale, when the bistable is in the initial or second state respectively. A third carbon linear pre-set resistor is provided to adjust the amplitude of the feed forward signals from the amplifier to the last cathode of the first counter tube. The bistable and the counter tubes are reset by a pulse derived from a relay operated by the press button switch.

d. Start sub-unit.

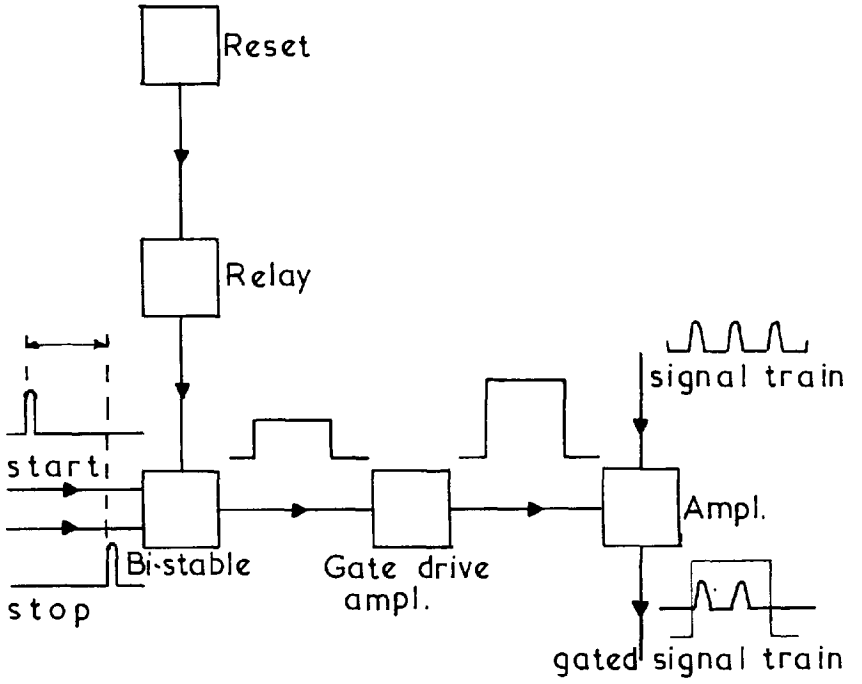
Positive or negative signals from the timing station are fed respectively to the grids of the first or second valves in a difference amplifier. Irrespective of the input grid used, a positive signal appears on the anode of the second valve, and this signal is used to fire a thyratron, which is held at cut-off by a negative bias, adjustable by a variable resistor. When the thyratron conducts, a neon indicates the current flow in the anode load. The thyratron is reset by an interruption of the power supply to the anode. The output signal to the timing unit is derived across a small value cathode resistor.

e. Stop sub-units.

These are identical to the start sub-unit in all but two respects: the thyratron is automatically reset when the voltage on the capacitor from which the current is derived, falls below the cut-off level; as a result a neon indicator is not required.

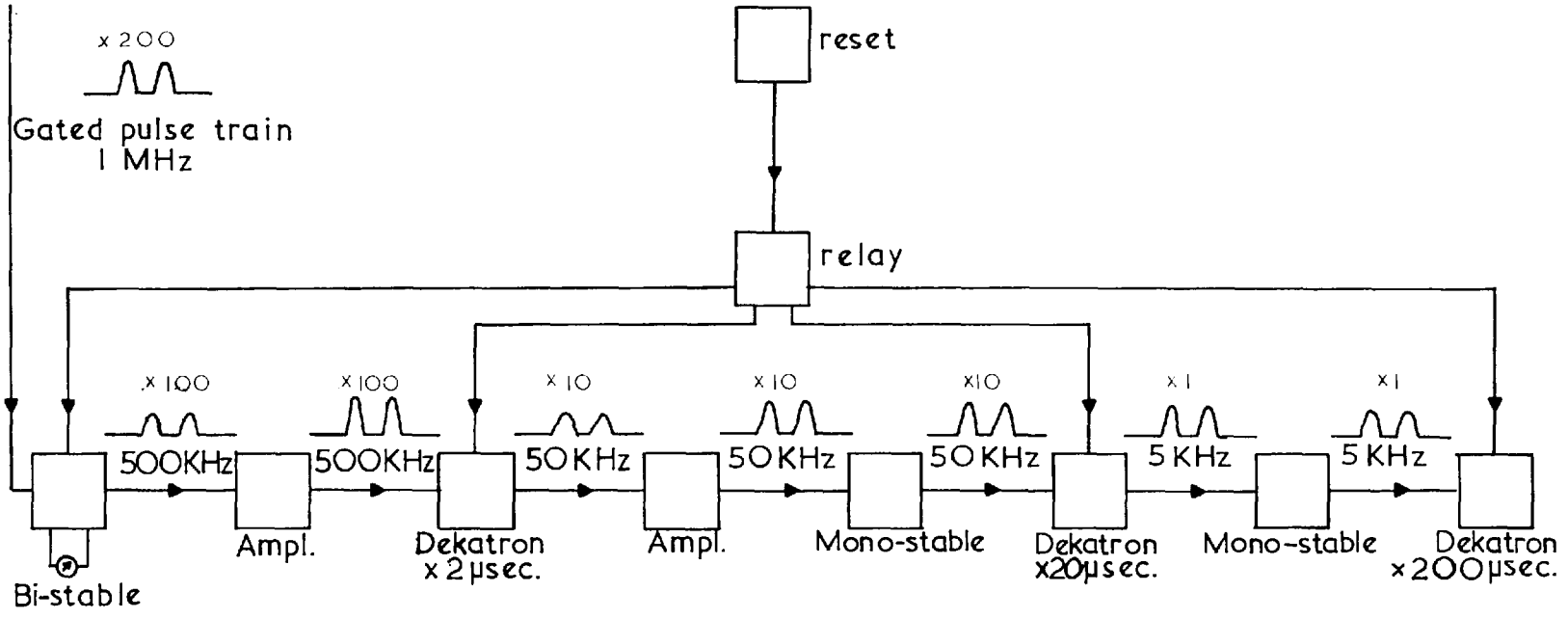



PULSE GENERATOR



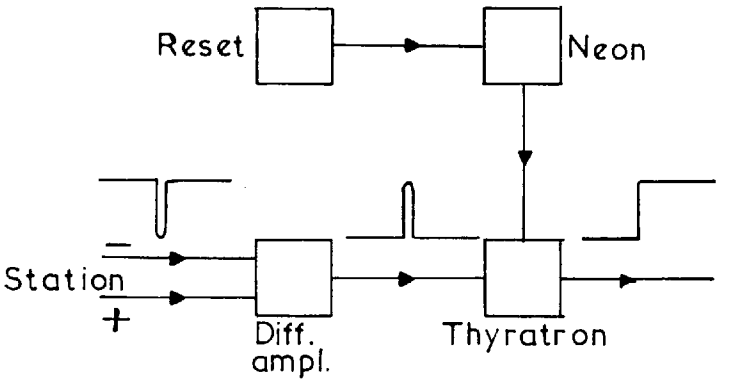

GATING SUBSECTION

Fig. H. 3. a. Counter circuits block diagrams

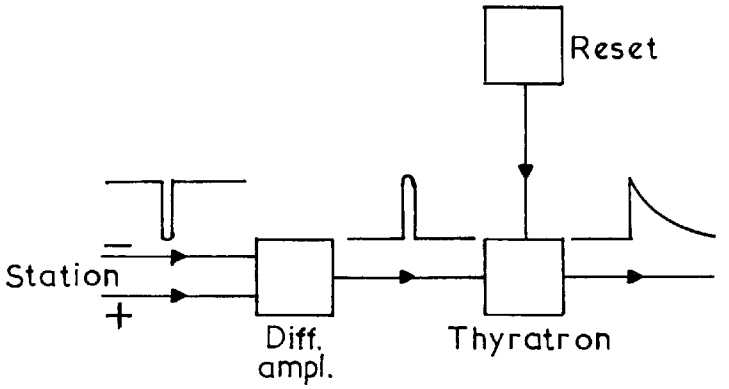



TIMING SUB SECTION

Fig. H.3.b. Counter circuits block diagrams.




START SUB-UNIT




STOP SUB-UNIT

Fig.H.3.c. Counter circuits block diagrams.

## II. The uncertainty in counter measurements.

This section contains considerations on the operation of the counter which resulted from the work described in this thesis.

### a. Possible errors in registered time-intervals.

Two types of error must be considered.

If it is supposed that there is no inaccuracy about the trigger point on the microsecond cycle, the gate will always come either before or after the trigger signal.

At the start, the gate pulse can come at most 1 microsecond too early, so that there is a wait of 1 microsecond before the first pulse is counted. This will give the correct start to the count. If the gate comes immediately before the pulse, it counts this as 1 microsecond although hardly any time has elapsed; this gives an error of + 1 microsecond.

At the stop, the gate pulse can come a microsecond too late, so that there is a wait of 1 microsecond after the last pulse has been counted. This will give an error of -1 microsecond in the count.

Hence the timing of this single sequence can be : correct, short by 1 microsecond due to a stop error or 1 microsecond too long due to a start error.

In the difference between two counts started by the gate pulse, the start error is the same for either record: both correct or both + 1 microsecond. The stop for the first count may be correct or -1 microsecond out and the same applies for the second count. Therefore, the error on the difference may be : correct, when both counts are correct or both out by -1 microsecond; -1 microsecond out when the first count is correct and the second out by -1 microsecond; or +1 microsecond out when the first count is -1 microsecond out and the second count is correct. The error is therefore $\pm$ 1 microsecond.

The second form of error is that, due to the uncertainty about the trigger point. As a result of this the start could occur 1 microsecond early in one count and correct in the second, in which case there will be an additional error of -1 microsecond in the difference. If, on the other hand, the first count was correct and the second count started 1 microsecond early, this would give an additional error of +1 microsecond in the difference. Hence the overall error could possibly be $\pm$ 2 microseconds.

Two factors mitigate against this. Firstly, it is unlikely that there will be a fluctuation from channel to channel as to which starts early. Hence, although the

error will still be ± 2 microseconds, fluctuations would extend from either +1 to -2 microseconds or from +2 to -1 microseconds consistently. Secondly, the chance of a difference at the start of the two counts is small. Hence the majority of fluctuations of the magnitude ± 2 microsecond are real effects and should be included in calculations of fluctuations.

Summarising, it will be necessary to differentiate between maximum possible errors, and fluctuations. The former are the greater and must be quoted as ± 2 microseconds. For evaluations of fluctuations a systematic error of ± 1 microsecond is a more realistic figure.

b. The error in detonation velocity measurements.

For convenience, the systematic error of ± 1 microsecond has been evaluated as an uncertainty in detonation velocities measured with the equipment from signals, generated by probes at 1 foot intervals along the timing section of a detonation tube. The figures are given for the complete range of propagation velocities that can be observed for any system under ambient conditions, see table H.1.

Table H.1. The uncertainty in detonation velocity measurements with the 5-channel counter for inter probe distances of 1 foot.

| Velocity range [m/sec.] | Error [m/sec] | Velocity range [m/sec.] | Error [m/sec] |
|---|---|---|---|
| 0 - 390 | 0 | 2734 - 2788 | 25 |
| 391 - 676 | 1 | 2789 - 2842 | 26 |
| 677 - 873 | 2 | 2843 - 2896 | 27 |
| 874 - 1033 | 3 | 2897 - 2948 | 28 |
| 1034 - 1171 | 4 | 2949 - 2999 | 29 |
| 1172 - 1295 | 5 | 3000 - 3049 | 30 |
| 1296 - 1408 | 6 | 3050 - 3099 | 31 |
| 1409 - 1512 | 7 | 3100 - 3148 | 32 |
| 1513 - 1610 | 8 | 3149 - 3196 | 33 |
| 1611 - 1702 | 9 | 3197 - 3243 | 34 |
| 1703 - 1789 | 10 | 3244 - 3290 | 35 |
| 1790 - 1872 | 11 | 3291 - 3336 | 36 |
| 1873 - 1952 | 12 | 3337 - 3381 | 37 |
| 1953 - 2029 | 13 | 3382 - 3426 | 38 |
| 2030 - 2102 | 14 | 3427 - 3470 | 39 |
| 2103 - 2174 | 15 | 3471 - 3514 | 40 |
| 2175 - 2243 | 16 | 3515 - 3557 | 41 |
| 2244 - 2310 | 17 | 3558 - 3600 | 42 |
| 2311 - 2375 | 18 | 3601 - 3642 | 43 |
| 2376 - 2438 | 19 | 3643 - 3684 | 44 |
| 2439 - 2500 | 20 | 3685 - 3725 | 45 |
| 2501 - 2560 | 21 | 3726 - 3765 | 46 |
| 2561 - 2619 | 22 | 3766 - 3806 | 47 |
| 2620 - 2677 | 23 | 3807 - 3846 | 48 |
| 2678 - 2733 | 24 | 3847 - 3885 | 49 |

## REFERENCES.


Becker, R.; Zeits. für Physik, 8, 321 [1922].

Belles, F.; VIIth Symp.(Int.) on Combustion. 745 [1959]. Butterworths, London.

Berets, D., Greene, E. and Kistiakowsky, G.; Journ.Amer.Chem.Soc., 72, 8100 [1950].

Berthelot, M. and Vieille, P.; Comp.Rend.Acad.Sci., 93, 18 [1881].

Bone, W. and Fraser.R.; Phil.Trans.Roy.Soc., A228, 197 [1929]; id., A230, 363 [1931]; Proc.Roy.Soc., A130, 542 [1931].

Bone,W., Fraser,R. and Wheeler, W.; Phil.Trans.Roy.Soc., A235, 29 [1936].

Brinkley, S.Jr. and Richardson, J.; IVth Symp.(Int.) on Combustion, 450 [1953].Williams & Wilkins.

Chapman, D.; Phil.Mag., 5. 47, 90 [1899].

Cottrell.T. and McCoubrey, J.; 'Molecular energy transfer in gases'. Butterworths, London [1961].

Dixon, H.; Phil.Trans.Roy.Soc., A184, 97 [1894]; id, A200, 315 [1903].

Döring, W.; Ann.der Physik, 43, 421 [1943].

Döring, W. and Schön, H.; Zeits. für Elektrochemie 54, 231 [1950].

Fay, J.; Journ.Chem.Phys. 20, 942 [1952].

Garner, W.; Trans.Far.Soc., 22, 253 [1926].

Gaydon, A. and Hurle, I.; 'The shock tube in high-temperature chemical physics'. Chapman & Hall, London [1963].

Gordon, W., Mooradian, A. and Harper, S.; VIIth Symp.(Int.) on Combustion, 752 [1959] Butterworths, London.

Harper, S. and Gordon. W.; 'Advances in Chemistry', 21, 38, [1959].

Hirschfelder, J., Curtiss, C. and Bird, R.; 'Molecular Theory of Gases and Liquids', 2nd Ed. [1964]. John Wiley & Sons, Inc. New York-London.

Hirschfelder, J. and Rosevaere, W.; Journ.Phys.Chem., 43, 15 [1939].

Hugoniot, R.; Journ.Ecole Polytech. 38, 3, [1887]; id. 39, 3, [1888].

Jost, W. and Schuller, W.; [1953], see Schuller, W.

Jouguet, E.; Journ.Math., 7, 347, [1905]; id. 8, 6, [1906].

Kistiakowsky, G., Knight, H. and Malin, M.; Journ.Chem.Phys., 20, 884 [1952].

Kistiakowsky, G. and Zinmann, W.; Journ.Chem.Phys., 23, 1889 [1955].

Laffitte, P.; Comp.Rend.Acad.Sci. 186, 951 [1928].

Laffitte, P. and Breton, J.; Comp.Rend.Acad.Sci., 202, 316, [1936].

Lewis, B. and Friauf, J.; Journ.Amer.Chem.Soc., 52, 3905 [1930].

Lewis, B. and Von Elbe, G.; 'Combustion, Flames and Explosions of Gases', Academic Press Inc. [1963]

Mallard, E. and Le Chatelier, H.; Comp.Rend.Acad.Sci., 93, 145 [1881].

Manson, N.; Zeits.für Elektrochemie, 61, 586 [1957].

Manson, N., Brochet, Ch., Brossard, J. and Pujol, Y.; IXth Symp.(Int.) on Combustion, 461, [1963] Academic Press, New York and London.

Manson, N. and Ferrié, F.; IVth Symp.(Int.) on Combustion, 486 [1953]; Williams & Wilkins, Baltimore.

Manson, N. and Guénoche, H.; Comp.Rend.Acad.Sci., 240, 1318 [1955].

Michels, A. and Boerboom, A.; Bull.Soc.Chim.Belg. 62, 119, [1953]. (Comm."Van der Waals Fund" 134).

Mikhelson, V.; Uch.Zap.Imperatorsk, Moskovsk Univ. Otdel Fiziko-Mat., 10, 1 [1893].

Miles, J., Munday, G. and Ubbelohde, A.; Proc.Roy.Soc., A269, 165 [1962]; id. A291, 167 [1966].

Munday, G.; Journ.Sci.Instr., 40, 603 [1963].

Neumann, J.von.; O.S.R.D. Report 549, [1942].

Payman, W. and Walls, J.; Journ.Chem.Soc., 123, 420 [1923].

Peck, M. and Thrap, R.; Journ.Chem.Phys., 26, 740 [1957].

Perry, J.; 'Chemical Engineers Handbook, Ed.IV. [1963] McGraw Hill, New York, Toronto, London.

Pusch, W. and Wagner, H.; Comb. and Flame, 6, 157, [1962]; Zeits. für Elektrochemie 69, 503 [1965].

Schuller, W.; Thesis, Darmstadt, [1954].

Shchelkin, K. and Troshin, Ya.; 'Gasdynamics of Combustion' Mono Book Corporation, Baltimore [1965].

Taylor, H. and Glasstone, S.; 'Treatise on Physical Chemistry', II, 313-316 [1951]; Van Nostrand Co.Inc.

Vieille, P.; Comp.Rend.Acad.Sci., 129, 1228 [1889].

Wagner, H.; Zeits.für Elektrochemie, 59, 906 [1955]; id. 'Fundamental Data obtained from Shock Tube Experiments' Chapt.IX, 320, [1961]. Ed. A.Ferri, AGARDograph, Pergamon Press.

Weir, A. and Morrison, R.; Ind.Eng.Chem., 46, 1056 [1954].

Wendlandt, R.; Zeits.Phys.Chem., 110, 637 [1924];
id. 116, 227 [1925].

White, D.; Abstr.Bull.Am.Phys.Soc., 3, 290 [1958]; id.
Phys.Fluids, 4, 40 [1961].

White, D. and Martin F.; VIIth Symp.(Int.) on Combustion, 856
[1959]. Butterworths, London.

Zeldovich, Ya.; Journ.Exptl.Theoret.Phys. (U.S.S.R.)
10, 542 [1940].

Zeldovich, Ya. and Kompaneets, A.; 'Theory of Detonation'
[1960]. Academic Press: New York -
London.